Analysis of land use changes and water resources in lowland catchments of Northern Germany

Dissertation

Zur Erlangung des Doktorgrades der

Mathematisch-Naturwissenschaftlichen Fakultät

der Christian-Albrechts-Universität zu Kiel

vorgelegt von

M.Sc. Chaogui Lei

Kiel, 2021

Analysis of land use changes and water resources in lowland catchments of Northern Germany

Dissertation

Zur Erlangung des Doktorgrades von

der Mathematisch-Naturwissenschaftlich Fakultät

der Christian-Albrechts-Universität zu Kiel

Vorgelegt von

M.Sc. Chaogui Lei

geboren in Hunan, China

Kiel, 2021

Erste Gutachterin: Prof. Dr. Nicola Fohrer

Zweite Gutachterin: Prof. Dr. Eileen Eckmeier

Tag der mündlichen Prüfung: 9 December 2021

Abstract

Rivers provide one of the most valuable and accessible fresh water resource. Water resources conditions of river catchments are affected by catchment characteristics and human activities. With increasing pressures from natural disturbances and anthropogenic activities, water quality is degraded and sustainable management becomes more challenging. A better understanding of hydrological process and water quality dynamics under the changing environment is thus critical for river health as well as human well-being.

There are different influences of land use and other catchment characteristics on water quality and quantity. The effects vary in time and space. A good understanding of the key influential factors will help to develop effective catchment management plans for addressing water resources issues. However, a systematic assessment of cause-effect relationships between land use and water quality or quantity is still rare, particularly across different temporal and spatial scales. This study aims to explore the spatially distributed catchment variables controlling landscape patterns, and to identify the important catchment characteristics and spatial scales for explaining the water quality or quantity dynamics.

The rural lowland catchments (namely Kielstau and Stör) in Northern Germany were selected as study areas. Intensive field campaigns have been carried out in the two catchments: land use mapping in both catchments and a water quality campaign (2018-2019) in the Stör catchment that complements campaigns from 1992-1994 and 2009-2011. Different multivariate statistics and a hydrological modelling (SWAT) approach have been applied. The distribution patterns of each specific land use class were identified based on logistic regression analysis using spatially distributed variables. Furthermore, stepwise multiple linear regression (SMLR) and redundancy analyses (RA) were applied to investigate influences of main categories of catchment characteristics (incl. land use, soil, and topography) on water quality at multiple spatial and temporal scales. The SWAT model was calibrated and validated for modeling the dynamic processes of streamflow, sediment, total phosphorus (TP), and total nitrogen (TN). The variabilities in main water balance components and nutrients in response to varied

landscape patterns were investigated by applying the integrated approach of SWAT modeling and partial least squares regression model (PLSR).

Results of the prediction of land use patterns revealed that the logistic regression models using topography, soil properties, socioeconomic variables, and landscape indices were robust enough to accurately explain the distributions of each single land use class in space. The reasonable performance for temporal validation demonstrated that the models are robust in time. The predicted results confirmed that non-agriculture and agriculture were well separated, while cultivated areas showed wide suitability for main crops (incl. winter cereals, corn, and rapeseed). The inclusion frequency into best models indicated that the most important spatially explicit variables for predicting land use patterns were drained soil area, distance to protected areas, the fractal dimension index of land patches, and population density. These variables were influenced by the dominant land use (agriculture) and the river course of the Kielstau River.

To understand the key impacts on water quality, a combined approach of SMLR and RA was used to investigate the effects of different catchment characteristics on seasonal water quality at multiple spatial scales. Results from SMLR and RA analyses indicated that the water quality of streams situated in relatively steeper agriculture areas and two major peatlands was mostly poorer, particularly in winter compared to summer. The main attributes of soil, land use percent and landscape metrics were quantified to strongly affect stream water quality. The comparison of reach, riparian and sub-catchment scale effects revealed that catchment characteristics at the larger scales (riparian and sub-catchments) can better explain the variations of stream water quality concentrations when compared to the reach scale. The most influential variables differed with respect to the spatial scales and the individual water quality parameters. More forest area and a larger landscape shape index resulted in better water quality. This effect became stronger at the reach scale. Permeable or organic soil structures and steeper croplands would lead to an increase of NO_3-N at larger scales. These results provide insights on proposing novel and sustainable location specific land-water management of river catchments.

Results of SWAT models illustrated that daily streamflow between 1990 and 2019 was represented very well (NSE: 0.79, KGE: 0.87 - 0.88, PBIAS=0.3% - 7.2%), the

daily loads of sediment (NSE: 0.54 - 0.65, KGE: 0.58 - 0.59, PBIAS: -22.2% - 12%) and TP (NSE: 0.29 - 0.56, KGE: 0.22 - 0.65, PBIAS: -46.2% - -4.7%) achieved an acceptable model performance and TN achieved satisfactory to good performances (NSE: 0.64 - 0.86, KGE: 0.71 - 0.91, PBIAS: -11.5% - 5%), during a time span of three years (incl. 2009-2011, 2018-2019). Furthermore, the constructed SWAT models were applied to different land use scenarios (in 1987, 2010, and 2019, respectively) and thus modeled the variations of water quality and quantity in response to land use changes. According to PLSR results, the modeled variations in water quality and quantity variables can be largely explained (over 67% explained variation) by the changes in land use percent and structure indices at the subbasin scale. The subbasin-scale area percent, connectedness, and aggregation degree of arable land patches played important roles in positively affecting sediment, TP, TN, surface runoff while negatively affecting base flow. Increase of pasture was responsible for the reductions of nutrient loads. Expansion of urban areas was most explanatory for the increase of surface runoff. The major changes of water balance components and nutrients were attributed to the interactive transformations between arable land and pasture.

Investigating the long-term temporal and spatial changes of water quality and quantity under changing catchment characteristics enhances our understanding of the overall dynamics of catchment water resources. The research findings revealed that catchment characteristics underwent considerable spatial or temporal changes, thus resulting in variations in water quality and hydrological processes within the Stör catchment during the last thirty years. Consequently, the results of this PhD dissertation can contribute to develop sustainable, integrated, and spatially specific management plans for land and water resources in the region and beyond.

Zusammenfassung

Flüsse stellen eine sehr wertvolle und direkt zugängliche Süßwasserressource dar. Die Wasserressourcen von Flusseinzugsgebieten werden durch die Eigenschaften des Einzugsgebiets und die menschlichen Aktivitäten im Einzugsgebiet beeinflusst. Mit zunehmendem Druck durch natürliche Veränderungen und anthropogene Aktivitäten verschlechtert sich die Wasserqualität und eine nachhaltige Bewirtschaftung wird schwieriger. Ein besseres Verständnis der hydrologischen Prozesse und der Dynamik der Wasserqualität in einer sich verändernden Umwelt ist daher für das Flussökosystem und das menschliche Wohlbefinden von entscheidender Bedeutung.

Es gibt unterschiedliche Einflüsse der Landnutzung und anderer Einzugsgebietseigenschaften auf die Wasserqualität und quantität. Die Effekte variieren in Zeit und Raum. Ein besseeres Verständnis der wichtigsten Einflussfaktoren wird dazu beitragen, effiziente Managementpläne für Einzugsgebiete zu entwickeln, die dazu beitragen, die Wasserressourcen zu verbessern. Eine systematische Untersuchung von Ursache-Wirkungs-Beziehungen zwischen Landnutzung und Wasserqualität bzw. -quantität über verschiedene zeitliche und räumliche Skalen hinweg wurde bisher nur selten durchgeführt. Ziel dieser Doktorarbeit ist es deshalb, die räumlich verteilten Einzugsgebietsvariablen, welche die Landschaftsmuster beeinflussen, zu untersuchen und wichtige Einzugsgebietsmerkmale und räumliche Skalen zur Erklärung der Wasserqualitäts oder quantitätsdynamik zu identifizieren.

Als Untersuchungsgebiete wurden die ländlichen Tieflandeinzugsgebiete Kielstau und Stör in Norddeutschland ausgewählt. Diese Doktorarbeit umfasst Landnutzungs-untersuchungen in den beiden Einzugsgebieten und eine Gewässergütekampagnen (2018-2019) im Stör-Einzugsgebiet, die die Kampagnen aus den Jahren 1992-1994 und 2009-2011 ergänzt. Es wurden verschiedene multivariate statistische Verfahren und ein hydrologisches Modell (SWAT) verwendet. Die räumlichen Muster jeder einzelnen Landnutzungsklasse wurden unter Verwendung eines logistischen Regressionsansatzes und räumlich verteilten Variablen untersucht. Darüber hinaus wurden schrittweise multiple lineare Regressionsanalysen (SMLR) und Redundanzanalysen (RA) angewendet, um den Einfluss der Haupteinzugsgebietsmerkmale (einschließlich

Landnutzung, Boden und Topographie) auf die Wasserqualität auf mehreren räumlichen und zeitlichen Skalen zu untersuchen. Das SWAT-Modell wurde kalibriert und validiert, um die Dynamik von Abfluss, Sediment, Gesamtphosphor (TP) und Gesamtstickstoff (TN) zu modellieren. Die Auswirkungen der unterschiedlichen Landschaftsmuster auf die Wasserhaushaltskomponenten und die Nährstoffe wurden durch Anwendung eines integrierten Ansatzes aus SWAT-Modellierung und partieller Kleinste-Quadrate-Regression (PLSR) untersucht.

Die Ergebnisse der logistischen Regressionsmodelle für die Landnutzungsmuster zeigten, dass sie unter Verwendung von Topographie, Bodeneigenschaften, sozioökonomischen Variablen und Landschaftsindizes robust genug waren, um die räumliche Verteilung jeder einzelnen Landnutzungsklasse zu erklären. Die zeitliche Validierung zeigte, dass die Modelle zudem zeitlich robust sind. Die Ergebnisse bestätigten eine deutliche Trennung von landwirtschaftlichen und anderen Flächen, während die Anbauflächen für verschiedene Hauptackerkulturen (u. a. Wintergetreide, Mais und Raps) geeignet sind. Die Aufnahmehäufigkeit der erklärenden Variablen in die besten Regressionsmodelle zeigte, dass die wichtigsten räumlich expliziten Variablen für die Erklärung der Landnutzungsmuster die entwässerte Bodenfläche, die Entfernung zu Schutzgebieten, der fraktale Dimensionsindex der Landnutzungsflächen und die Bevölkerungsdichte waren. Diese Variablen werden stark durch die dominante Landnutzung (Landwirtschaft) sowie durch den Flusslaufder Kielstau beeinflusst.

Um die wichtigsten Auswirkungen auf die Wasserqualität zu verstehen, wurde ein kombinierter Ansatz von SMLR und RA verwendet, mit dem die Auswirkungen verschiedener Einzugsgebietseigenschaften auf die saisonale Wasserqualität auf mehreren räumlichen Skalen untersucht wurde. Ergebnisse der SMLR- und RA-Analysen zeigten, dass die Wasserqualität der Gewässer in vergleichsweise steilen landwirtschaftlichen Gebieten und Feuchtgebieten vor allem im Winter meist schlechter war. Insbesondere beeinflussten Bodenparameter, der Landnutzungsanteil sowie Landschaftsmetriken die Wasserqualität stark. Der Vergleich unterschiedlicher Skalen (Flussabschnitt-,, Ufer- und Teileinzugsgebietsskala) zeigte, dass Einzugsgebietsmerkmale auf den größeren Skalen (Ufer und Teileinzugsgebiete) die Variation der Wasserqualität im Vergleich zur Flussabschnittsskala besser erklären

können. Die einflussreichsten Variablen unterschieden sich hinsichtlich der räumlichen Skalen und der einzelnen Wasserqualitätsparameter. Größere Waldflächen und ein höherer Landschaftsformindex führten zu einer besseren Wasserqualität. Dieser Effekt wurde auf der Flussabschnittsskala stärker. Durchlässige oder organische Bodenstrukturen und steilere Ackerflächen würden zu einem Anstieg von NO_3-N auf größeren Skalen führen. Diese Ergebnisse liefern Erkenntnisse für ein neuartiges und nachhaltiges standortspezifisches Land-Wasser-Management in Flusseinzugsgebieten.

Die Ergebnisse der SWAT-Modelle zeigten, dass die täglichen Abflussmengen zwischen 1990 und 2019 sehr gut berechnet werden (NSE: 0,79, KGE: 0,87 - 0,88, PBIAS=0,3% - 7,2%). Die Modellgüte im Messzeitraum von drei Jahren (2009-2011, 2018-2019) für die täglichen Sedimentfrachten (NSE: 0,54 - 0,65, KGE: 0,58 - 0,59, PBIAS: -22,2% - 12%) und TP (NSE: 0,29 - 0,56, KGE: 0,22 - 0,65, PBIAS: -46,2% - -4,7%) sind akzeptabel und für TN befriedigend bis gut (NSE: 0,64 - 0,86, KGE: 0,71 - 0,91, PBIAS: -11,5% - 5%). Darüber hinaus wurden die SWAT-Modelle mit verschiedenen Landnutzungsszenarien (mit der Landnutzung der Jahre 1987, 2010 bzw. 2019) angetrieben und so die Variation der Wasserqualität und -quantität als Reaktion auf Landnutzungsänderungen modelliert. Nach den PLSR-Ergebnissen lassen sich die modellierten Schwankungen der Wasserqualitäts- und -quantitätsvariablen weitgehend (über 67% erklärte Varianz) durch die Veränderungen des Landnutzungsprozentsatzes und der Strukturindizes auf der Subeinzugsgebietsskala erklären. Der Flächenprozentsatz im Subeinzugsgebiet, die Konnektivität und der Aggregationsgrad von Ackerlandflächen hatten einen positiven Einfluss auf Sediment, TP, TN, Oberflächenabfluss, während sie den Basisabfluss negativ beeinflussten. Eine Zunahme von Grünland führte zu einer Reduzierung der Nährstoffbelastung. Die Ausdehnung von Siedlungsflächen war die Variable, die die Zunahme des Oberflächenabflusses am besten erklären konnte. Die wesentlichen Veränderungen der Wasserhaushaltskomponenten und Nährstoffe werden auf die Veränderungen des Anteils von Ackerland und Grünland zurückgeführt.

Diese Untersuchung der langfristigen zeitlichen und räumlichen Veränderungen der Wasserqualität und -quantität unter veränderten Einzugsgebietseigenschaften verbessert unser Verständnis der Dynamik von Wasserressourcen in Einzugsgebieten.

Die Forschungsergebnisse zeigen, dass sich die Eigenschaften des Einzugsgebietes räumlich oder zeitlich stark veränderten, was in den letzten dreißig Jahren zu Veränderungen der Wasserqualität und der hydrologischen Prozesse im Stör-Einzugsgebiets führte. Folglich können die Ergebnisse dieser Dissertation dazu beitragen, nachhaltige, integrierte sowie raumspezifische Bewirtschaftungspläne für Land- und Wasserressourcen in der Region und darüber hinaus zu entwickeln.

Contents

Abstract i
Zusammenfassung viii
Chapter 1 General introduction 1
1.1. Background 1
1.2. Characteristics of land use pattern 5
1.3. Water resources dynamics and land use change 8
1.4. Hydrological modeling 12
1.5. Research gaps and questions 14
1.5.1. Research gaps 14
1.5.2. Research questions 15
1.6. Thesis structure 16
Chapter 2 Water quality measurement campaigns 17
2.1. Monthly measurement campaign 17
2.2. Daily automatic monitoring 18
2.3. Lab analyses 19
Chapter 3 Identifying the most important spatially distributed variables for explaining land use patterns in a rural lowland catchment in Germany 21
Abstract 22
3.1. Introduction 23
3.2. Materials and methods 25
3.2.1. Study area 25
3.2.2. Land use data 26
3.2.3. Explanatory variables 28
3.2.4. Logistic regression approach 31
3.2.5. Validation and evaluation 33
3.3. Results 33
3.3.1. Model performance 33
3.3.2. Variable impact 34
3.3.3. Variable importance 36
3.3.4. Analysis of probability maps of land use patterns 37
3.4. Discussion 42
3.4.1. Most important explanatory variables 42
3.4.2. Model performance 43
3.4.3. Value of landscape metrics for explaining land use patterns 44

3.5. Conclusion 45

Chapter 4 Effects of land cover, topography, and soil on stream water quality at multiple spatial and seasonal scales in a German lowland catchment 47

Abstract 48

4.1. Introduction 49

4.2. Materials and methods 52

4.2.1. Study area 52

4.2.2. Water quality monitoring 54

4.2.3. Multi-scale environmental factors 55

4.2.4. Statistical analysis 56

4.3. Results 59

4.3.1. Spatial and seasonal variations in water quality 59

4.3.2. Differences of predictive capabilities and important predictors 60

4.3.3. The effects of catchment characteristics on water quality 62

4.4. Discussion 67

4.4.1. Water quality variations 67

4.4.2. Key variables for water quality prediction 68

4.4.3. Effects of spatial and temporal scales 70

4.4.4. Management insights 71

4.5. Conclusion 72

Chapter 5 Influences of land use changes on the dynamics of water quantity and quality in the German lowland catchment of the Stör 74

Abstract 75

5.1. Introduction 77

5.2. Materials and methods 80

5.2.1. Study area 80

5.2.2. Land use data and landscape metrics 81

5.2.3. Hydrologic and water quality modeling 84

5.2.4. Partial least squares regression 89

5.3. Results and discussion 90

5.3.1. Calibration and validation of streamflow and water quality 90

5.3.2. Characteristics of land use change 93

5.3.3. Differences of changes in water quantity and quality 96

5.3.4. Influences of changes in land use metrics on water quantity and quality 97

5.4. Conclusion 105

Chapter 6 General discussion and conclusion 107

6.1. General discussion of research questions 107
6.2. General conclusion 117
6.3. Outlook 118
References 120
Acknowledgments 141
Annex 143
Declaration 163

Chapter 1 General introduction

1.1. Background

Land use change is a significant part of global change with local as well as regional consequences (Chang et al., 2018). Globally increasing population and rapid socio-economic development have resulted in the expansion of areas used for residential, industrial, or agricultural purposes, giving rise to threats to water quality or ecological health of river systems (Gu et al., 2020; Pereda et al., 2019; Winsemius et al., 2016). Consequently, effects of land use change on water resources have been aggravated (Ren et al., 2003; Zou et al., 2018). The water crisis in terms of water scarcity and water quality deterioration becomes prominent and is one of the major challenges in 21st century (Tsani et al., 2020). Approximately 70% of freshwater on earth is used for crop irrigation and 20% for the industrial sector (Tibaijuka, 2003). Agriculture impacts hydrological process by controlling the partitions of precipitation into different water balance components, such as evapotranspiration, surface runoff, and groundwater recharge (Watts et al., 2015). Moreover, it is one major diffuse pollution source of water resources. Industrialization or urbanization considerably increase impervious areas and thus accelerate runoff and increase the loading of contaminants into water bodies (Astuti et al., 2019). The pollution risks of surface water and groundwater were markedly exacerbated in recent decades, due to intensive agricultural or urbanization activities (Parris, 2011). In Europe, rural development is important, as over half of the population in the 25 European Union member states live in rural areas covering 90% of the territory (Pašakarnis et al., 2013). During the second half of the 20th century, European land use has considerably changed due to numerous transformations in technology, socio-economy, and political management of land resources (Rounsevell et al., 2012). Agriculture was substantially intensified particularly during 1960s-1980s. However, arable land has been decreased in areas with low suitability for agriculture, e.g., due to a decreasing profitability of farming and rural emigration (Haberl et al., 2007; Mueller et al., 2012). This stimulated a thorough change of the traditional agricultural landscape (Fischer et al., 2012). Influenced by some of the most intensively managed croplands in the world (Mueller et al., 2012),

European standing or flowing waters show high incidence of eutrophication (EEA, 2005) due to the enrichment in nutrients (nitrogen and phosphorus) predominantly generated from agriculture activities. Quantification and management of the diffuse source pollution of water quality from rural land use has been regarded as one important challenge in environmental issues in Europe (Kay et al., 2006). In addition to studies on the direct impact of land use change on catchment hydrology (Siriwardena et al., 2006; Wagner et al., 2019), studies indicated that land use gradients on a large scale are likely to influence the local climate regime, which additionally alter hydrological process and water quality (Suh and Lee, 2004). Many international research programs relevant to land use effects on water resources were initiated, such as the International Geosphere-Biosphere (IGBP) and International Human Dimensions Program on Global Environmental Change (IHDP) (Ehlers, 2016; von Falkenhayn et al., 2011). So far, a number of studies using field observations or modeling approaches evaluated the impacts of changes of individual land use areas on hydrological variables (e.g., evapotranspiration and streamflow) (Getachew and Melesse, 2012; Siriwardena et al., 2006) or water quality components (e.g., sediment and nutrients) (Molina-Navarro et al., 2014; Wilson et al., 2014). However, the multifaceted influences of land use with respect to spatial aspects (including spatial structure or scales) on water resources have not been fully understood.

The quantitative exploration of dynamic mechanisms of land use influencing hydrological process and water quality within catchments becomes more of an important field in the forefront development of hydrology (Blöschl et al., 2019; Giri and Qiu, 2016). It is deemed as one of the essential goals of the 21 century to provide sufficient safe water resources to meet the demand for growing world's human population (Tarhule, 2017). Depletion of nutrient pollution in particular of freshwater resources on the global level is part of the United Nations' Sustainable Development Goals (SDG6) (Hakimdavar et al., 2020). Since 2000, the European Water Framework Directive has been implemented with the goal of achieving good water quality and ecological status of all water bodies in all European Union member states preliminarily by 2015 and in exceptional cases by 2027 (WFD, 2000).

In Europe, agriculture continues to be an important source of contaminants (Volk et al., 2009). Some freshwater is still subject to pollution. In general, nitrate pollution has been slightly improved since 2008, however, the deterioration of water quality still occurs in areas with relatively high N inputs to agricultural soils. For example, high N leaching and runoff losses are found in some regions in Netherlands, and Belgium (>50 kg N/ha/year) and northwestern Germany (20-50 kg N/ha/year) (Velthof et al., 2014). Although the agriculture sector constitutes a minor part of national economy in Germany, agriculture land use covers more than 50% of the country's land surface area, composed of a range of crop plants (e.g., winter wheat, barley, rye, corn, and winter rape) and pasture. The manure, fertilizers or pesticides are routinely applied in agricultural areas to enhance crop productivity. However, excessive application of them may produce chemical residues accumulated in soil or delivered to water bodies. Substances leached from agriculture into water commonly carry nitrogen (N) and phosphorus (P). The entry of N and P plays an important role in providing essential nutrients for phytoplankton (Wu et al., 2011) and macrophyte growth (Gao et al., 2009), but at excessive amount, they cause water eutrophication and threaten water quality, ecology stability, and human health. The complicated trade-offs of agriculture, food production, ecology, and water quality becomes an important issue worthy of more political and scientific attention in Germany. It has been reported that the main water pollution in Germany is the consistently high levels of nutrients of nitrogen (N) and phosphorus (P) (Hirt et al., 2008; Nguyen and Venohr, 2021). The Nitrate Directive (EEC, 1991a) and the Urban Waste Water Treatment Directive (EEC, 1991b) have been in effect in Germany since 1991, in order to facilitate the decreases of NO_3-N as well as N and P from domestic or industrial sewage. The input of P to water bodies declined to an extent but still presents a serious problem particularly in tributary rivers in the federal state of Schleswig-Holstein (Northern Gemany). Approximately two-thirds of the river water bodies in Schleswig-Holstein failed to achieve the orientation values of TP as stipulated in Annex 7, Ordinance on the Protection of Surface Waters 2016 (OGewV 2016), which indicates that the target of a good ecological status has not been reached (Ta et al., 2020). N pollution is a continuously serious problem, predominantly in forms of total nitrogen and nitrate nitrogen exceeding the thresholds suggested for

good water quality. Northwestern (e.g., Lower Saxony) or northern parts (Schleswig-Holstein) of Germany have a large proportion of agricultural areas and dense livestock, in which water bodies receive highest inputs of nitrogen surplus (Kirschke et al., 2019). This increases the possibility of failing the goal of achieving a good chemical and ecological status by 2027, as proposed by European Water Framework Directive. Moreover, many regions have failed the target of European Nitrate Directive (91/676/EEC) by exceeding the limit of 50 mg/L nitrate in groundwater. The critical contamination of surface water and groundwater in agriculture-intensified northern Germany calls for in-depth investigation of nutrient pollution to achieve sustainable land use and water management. Schleswig-Holstein, a lowland northern federal state of Germany, is dominated by cropland and rangeland. It has the largest percentage of agricultural area (68.8% of the federal state, in 2018) as well as the third highest livestock density (107 units/100 ha, in 2010) among all the federal states in Germany (Kirschke et al., 2019). Meanwhile, this region is characterized by the enduring and high N surplus and high coincidence of the magnitude of nitrate pollution with agriculture and grazing rate (Kirschke et al., 2019; Ta et al., 2020).

The rural lowland catchments of the Kielstau and the Stör located in northern Germany (Figure 1-1) , have been not only an important water supply area for human living, but also a research focus area in views of hydrology and water quality for many years (Ripl and Hildmann, 2000; Schmalz and Fohrer, 2009; Song et al., 2015; Venohr et al., 2005a). The flat topography, low flow velocity, shallow groundwater table, and resultant organic (moist and fertile) soils are typical for this lowland ecosystem (Hesse et al., 2008). Agricultural land use composed of different kinds of energy crops, row crops, and cereals is prevailing in the catchment. Tile drainages have been widely implemented to drain excessive soil water in order to facilitate machinery agriculture and improve crop productivity. Meanwhile, they alter the natural water cycle and accelerate transportation of nutrient substances to streams via directly connecting agriculture fields to streams (Schmalz et al., 2008). The hydrological cycle is highly affected by the intense interaction between surface water and shallow groundwater. The extent of interaction varies with riparian topography and seasons (Krause et al., 2007). Hydrological processes influence the occurrence of water quality problems in streams,

ponds and lakes, by changing the retention time of water and nutrients (Hesse et al., 2008). Thereby, N and P pollution in the lowland catchment become complicated because of the interaction between aquatic and terrestrial systems (Krause et al., 2007). In the past century, the natural river network and the landscape were artificially regulated to expand areas suitable for agriculture (Gessner et al., 2010), which resulted in potential water balance and water quality issues (Ripl et al., 1996; Schmalz and Fohrer, 2010). During recent years, the renaturation of riparian landscape was initiated and caused changes to land use patterns in the Stör catchment. N and P levels were reduced to an extent, however, in general, they did not achieve the values which indicate a good chemical and ecological status as pronounced as a goal of WFD 2027, particularly in winter. To help efficiently address water resources management, research on water quality and hydrology under varying catchment environments is necessary.

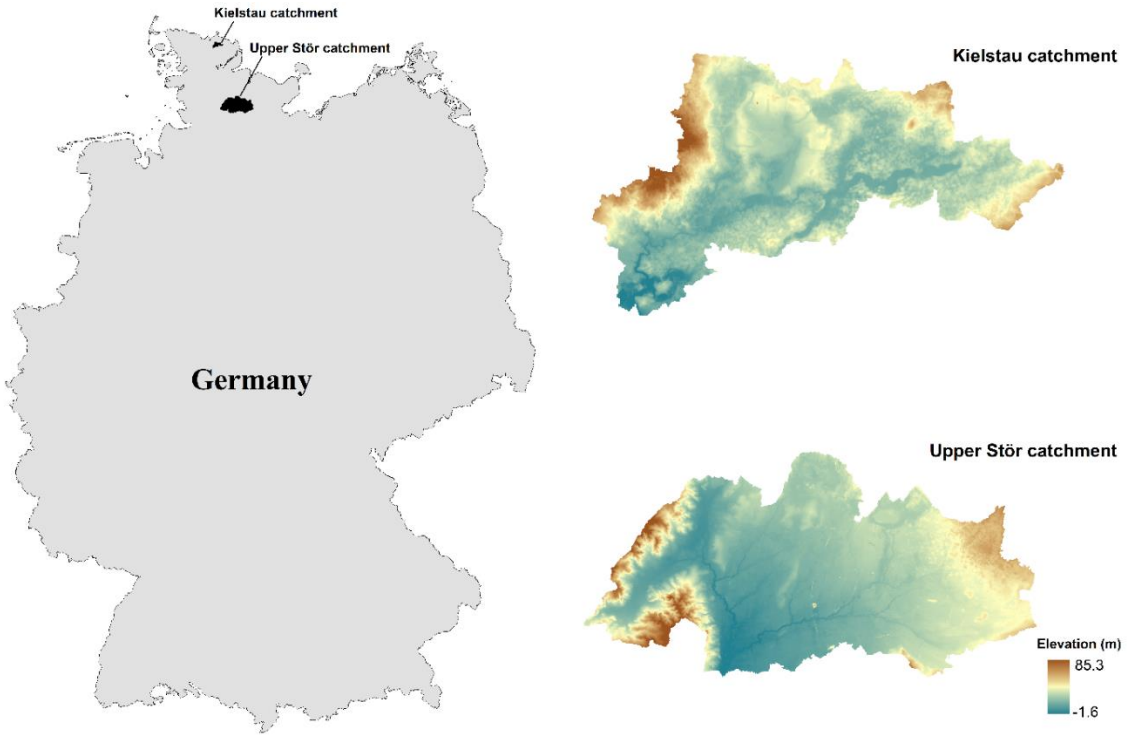

Figure 1-1. The catchments of the Kielstau and the Upper Stör in Germany and their topography.

1.2. Characteristics of land use pattern

Land use is the product of natural process interacting with anthropogenic activities. Land use patterns vary in space and time due to multiple drivers of climate, nature conservation, socio-economic and bio-physical conditions (Baumann et al., 2011; Yang

et al., 2014). Vice versa, the changes of land (LUCC) affect different aspects of the local climate (Betts et al., 2007; Searchinger et al., 2018), ecosystem functions (Von Schiller et al., 2008), hydrological and aquatic environment (DeFries and Eshleman, 2004), thus affecting the development of economy and society (Lambin and Meyfroidt, 2011). Land use change is on the forefront of scientific topics in the field of global change research. The European Union (EU) initiated the MARS (Monitoring Agricultural Resources) project in 1988 to monitor agriculture land use and its dynamics using remote sensing techniques. European agriculture was considerably changed in the extent and structure during the second half of the last century, due to the substantial changes in technology, socio-economy and policy (Rounsevell et al., 2003). Through history, land use patterns have become less traditional mainly under the influences of urban expansion and agriculture intensification (Deng et al., 2009; Lawrence et al., 2007; Mustard et al., 2012). The transformation of land use types or of the spatial structure of land use may cause water quality degradation, soil erosion, the loss of ecological diversity and other environmental threats (Allan, 2004; Meneses et al., 2015). Therefore, the evaluation of land use patterns and their changes has become an important multidisciplinary research topic that deserves attention (Galpern and Gavin, 2020; Ramachandran et al., 2018; Tong et al., 2012; Zhang et al., 2013; Zhao et al., 2020).

Land use pattern characteristics include not only the area percentage of each land use type (composition) but also the spatial relationships of these land use types (configuration). The land use percentage has been widely used in the study of influences on water quality and hydrology within different catchments (Carlson and Arthur, 2000; Risal et al., 2020; Xu et al., 2020b). The increase of urban area results in increased surface runoff (Weng, 2001). The expansion of agriculture area may lead to nutrient enrichment and water quality deterioration (Parris, 2011), while the increase of forest can improve water quality by filtering pollutants and soil particles (Yan et al., 2013). The spatial information of land use is complex and cannot be represented by the lumped indicator of land use area percentage. The composition and spatial distribution of land use simultaneously influence the energy and matter fluxes across the catchment. The spatial distribution of certain land use classes affects the pollution of water bodies,

for instance, more agriculture or urban area located near rivers may magnify the deliveries of pollutants to rivers (Li et al., 2018; Tanaka et al., 2016).

With the emergence and development of remote sensing and spatial analysis techniques, land use classifications can be readily achieved and landscape metrics can be efficiently assessed (Amiri et al., 2018; Kupfer, 2012). The shape, dominance, and diversity metrics of land use are able to characterize the main spatial structures of a landscape. These landscape metrics can characterize land use gradients (Fernandes et al., 2011), and have been used for land use modeling (Yang et al., 2014). Moreover, they have been recently applied to study landscape ecology, water quality as well as flood magnitudes (Amiri et al., 2018; Kupfer, 2012). Significant influences of landscape metrics on water quality and ecological conditions of streams have been revealed (Ding et al., 2016; Peterson et al., 2011). Landscape pattern metrics are commonly assessed either the entire landscape or single class level. It is worth mentioning that the utility of landscape metrics at the class level helps to distinguish the individual effects of the spatial pattern of each land use class. Consequently, the land use class in a specific spatial setting which is influential to catchment hydrology is identifiable and separable from multiple classes. Compared to the relationships measured using the lumped indicators at the landscape level, the results of relationships with water quality using the measures of landscape pattern at the class level are better understood and readily applied to guide land use planning and water management (Ding et al., 2016; Gémesi et al., 2011). Investigating landscape patterns with regard to composition and configuration of each land use class receives a growing attention (Chan and Vu, 2017; Ding et al., 2016; Urrutia et al., 2020).

The lowland catchments of Germany are dominated by rural landscapes which are affected by agriculture activities (Fig. 1-2). The spatial and temporal variability of specific land use classes and their relationships with catchment characteristics and water resources have not been fully investigated so far.

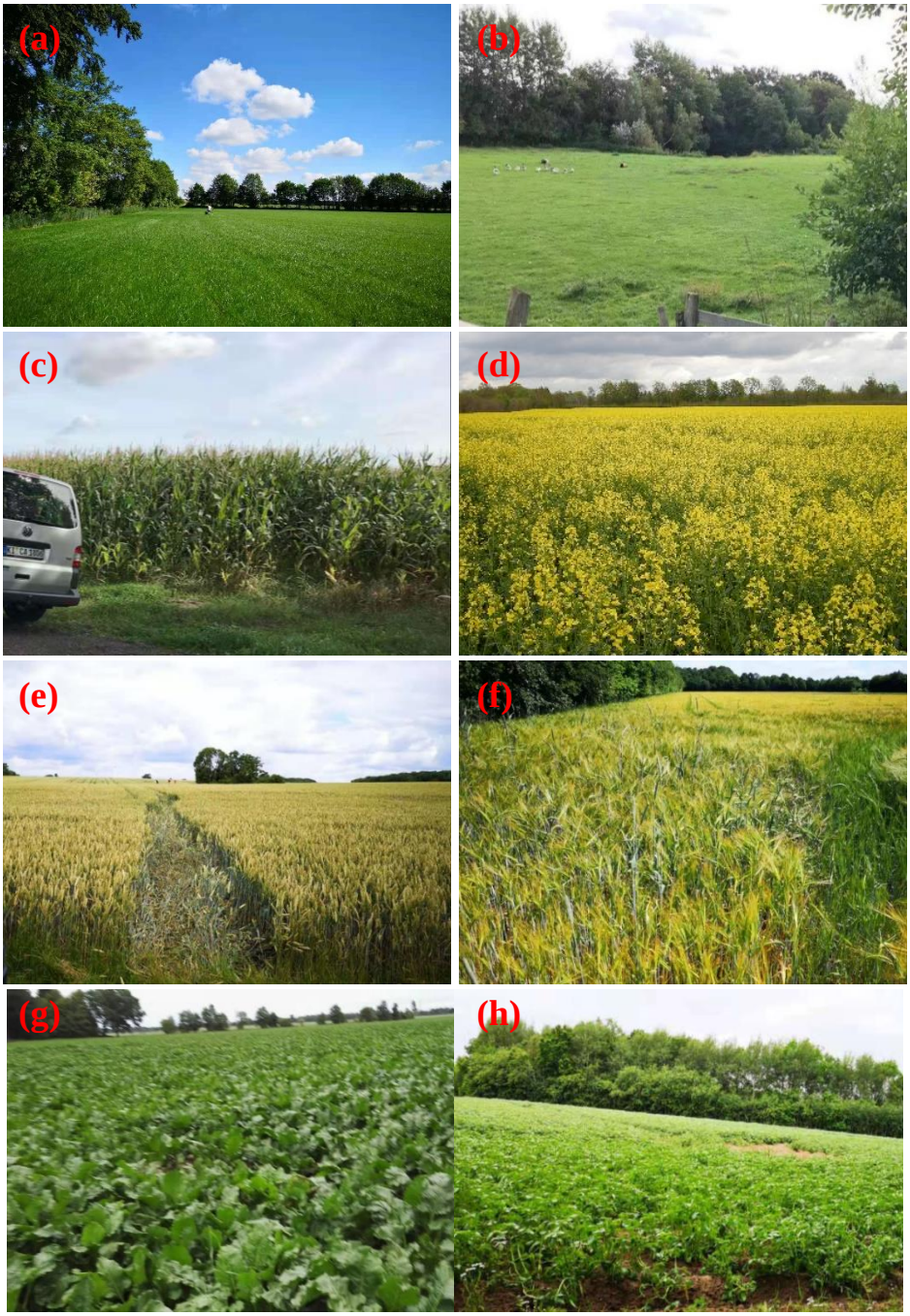

Figure 1-2. Common land uses in the upper Stör catchment (a) field grass; (b) pasture;(c) corn; (d) winter rape; (e) winter wheat; (f) winter barley; (g) sugar beet; (h) potato. (d) was photographed by Pott, others were by Lei.

1.3. Water resources dynamics and land use change

Water resources play a vital role in sustaining life as well as agricultural irrigation, fishing farming, industrial and economic development. About 2.5% of the water in earth's hydrosphere is stored as fresh water (Korzoun, 1978). Only a minor fraction (0.26%) of the total amount of fresh water is stored in lakes, reservoirs, and river

system as the most accessible forms for economic and human consumptions, and other important water sources (Shiklomanov, 1991). The river system is of great importance in regulating the local hydrological cycle and providing ecosystem services. Although river water can be more frequently and naturally replenished (16 days on average) compared to other fresh water resources (Pidwirny, 2006), it still faces diverse stressors. Rising human population, rapid economic development and land use changes have globally increased the consumption and regulation of river water resources (Sabater et al., 2018; Sabzi et al., 2019). Consequently, river water quantity changes due to over-exploitation and a varied flow regime and river water quality changes due to nutrient surplus (Werners and Ludwig, 2012), thus limiting the utility of water resources. Water pollution or water surplus or scarcity may compromise human health, induce disasters (e.g., flood or drought), and hinder economy development (Barceló and Sabater, 2010; Bhaduri et al., 2016; King-Okumu et al., 2018). According to Xu et al. (2020a), surface water runoff exhibits spatial variability under different gradients of urbanization across the city of Munich, Germany. Al-Awadhi and Mansour (2015) found distinct spatial variations in water drought severity and flood occurrence in the Omani provinces in the USA. Water quality deterioration is reported in the upper-middle part of the Llobregat River catchment in Spain (Mutlu, 2019). Water quality parameters (e.g., DO and nitrate) are often distinguished with different concentrations in dry and wet seasons (Alberto et al., 2001). The literature demonstrates that different components of water quantity or quality manifest spatial and temporal variations, likely due to the influences of environmental process or human activities.

In Germany, national water resources are currently assessed as sufficient, as only about 23% of the available resources are used (UBA, 2018). However, water shortages may still occur in regions suffering from unfavorable water balance, particularly in the federal state of Brandenburg (Zebisch et al., 2005). Groundwater and surface water in Germany is threatened by water quality pollution by nutrients and heavy metal (Becker, 2017; Fuchs et al., 2017). This is predominantly due to different inputs of fertilizer, manure and pesticide residues from widespread cultivated areas, as well as the industrial chemicals, pathogens, heavy metals from waste water plants and construction sites (e.g., mining region) into water bodies (UBA, 2018). The temporally varying

stream flow regime may aggravate the fluctuations of water quality conditions (Lam et al., 2012). High levels of nitrogen (N) and phosphorus (P) result in a major water quality problem particularly in agricultural areas (Guse et al., 2015b; Pott, 2014). Agriculture and shallow groundwater are characteristic for the lowland rural catchments in northern Germany. A variety of agriculture management practices of tillage, grazing, and the application of fertilizers and pesticides are routinely used. These activities may probably result in the residues of manure, fertilizer and pesticide carrying physicochemical and biochemical constituents of water quality as well as fragile soil, thus intensifying the risk of water quality pollution or soil erosion (Borrelli et al., 2017; Schoumans et al., 2014; Tu, 2011). In lowland river catchments with a high groundwater table, tile drainages are installed and tributaries are straightened or channelized to support agriculture, which change the natural water balance and accelerate agrochemicals transport (Schmalz et al., 2008; Smith et al., 2015). There is intense inter-connection between near-surface groundwater and surface water in the lowland catchments, resulting in plentiful groundwater recharge to streams. This complicates the runoff process, meanwhile changes the release and transportation of pollutants and increases the risk of nutrient pollutions in terms of both streams and groundwater (Hesse et al., 2008; Krause et al., 2007). So far, the complex catchment characteristics in lowlands and the main relationships between rural landscape and water quality and hydrology are rarely investigated in northern Germany (Guse et al., 2015a; Guse et al., 2015b; Haas et al., 2016). Therefore, the following issues are important and worth being further addressed, including: (1) analyzing land use patterns using spatially distributed factors; (2) understanding the scale effects of catchment characteristics on water quality; (3) investigating the influences of land use changes on both water quality and quantity.

So far, the relationships between land use/cover changes (LUCC) and surface water quality have been widely studied (Fan and Shibata, 2015; Fernandes et al., 2021; Mehdi et al., 2015; Shrestha et al., 2018; Wijesiri et al., 2018). They mainly include three waves, i.e., since the early 1960s, researchers explored the linkages between morphological characteristics and the physical indicators of water quality such as turbidity, dissolved oxygen and water temperature (Harrel and Dorris, 1968). The

second wave started to focus the analysis of this topic at the catchment scale since the 1970s (Bormann et al., 1969). Subsequently, the third wave of studies was dedicated to land use impacts on suspended sediment, nutrients and ecological condition of streams through GIS techniques and multivariate analysis (Fitzpatrick et al., 2007; Jones et al., 2001). Recently, with the advancement of GIS and remote sensing techniques, relevant studies investigated influences of both land use area and pattern on water chemistry components and sediment from multiple spatial scales, such as catchment, sub-catchment or riparian buffers (Bu et al., 2014; Pratt and Chang, 2012). Land use effects actually vary with the setting of spatial scales. Venohr et al. (2005b) and Zhou et al. (2012) found strongest correlations between land use and water quality at the sub-catchment scale, while Dodds and Oakes (2008) and Shi et al. (2017) indicated that land use pattern adjacent to streams are more related to water quality. These findings demonstrate that the topic of land use effects on water quality at different scales needs to be further investigated.

Despite the richness of literature studies, only few of them previously explored the associations between the landscape pattern of individual land use classes and hydrological (e.g., runoff and base flow) (Boongaling et al., 2018; Li et al., 2021b) or water quality components (e.g., sediment yield, nitrate and phosphate) (Motamedi et al., 2019; Peng and Li, 2021). However, the spatial information of land use, from the landscape ecology perspective, is also essential in determining hydrological connectivity, runoff routing, and the delivery of sediment and chemicals (Kuo and Brierley, 2013; Lane et al., 2009; Zhang et al., 2018). Recent studies started to relate stream water quality and quantity to landscape configuration, using the measures of the aggregation, diversity, or the interconnection of land patches. Roberts (2016) revealed the effects of the landscape configurational metric of contagion on streamflow. Zhou and Li (2015) found the significant correlations between the composite landscape index and soil erosion. Shi et al. (2017) illustrated that the aggregation index, largest patch index or shape indices were more useful than land use percent in explaining water quality dynamics. The influence of landscape also depends on location or distance to the streams (Ding et al., 2016; Peterson et al., 2011). Configuration or distance indices of the landscape can help to assess the supplementary effects of land use change on

water resources. A combined application of spatially explicit landscape measures and land use percent receives growing attention in the study of land use effects on water resources (Boongaling et al., 2018; Ding et al., 2016). Such a detailed study on the effects of composition and configuration of land use on water quality and quantity is necessary in lowland catchments in northern Germany, which is vulnerable to variability in water balance and nutrients due to a variety of influences from rural landscape characteristics (Elfert and Bormann, 2010; Krause et al., 2007; Lam et al., 2012).

1.4. Hydrological modeling

Hydrological models are useful tools for the prediction and management of water resources within catchments (Sood and Smakhtin, 2015). The application of hydrological models has been increasing, due to the increases of readily available spatial data and computational resources, and its wide applicability in areas lacking in observations of long-term series of hydrologic data (Karen and Patrick, 2021; Loliyana and Patel, 2020; Suliman et al., 2015). Models like MIKE-SHE (Refshaard and Storm, 1995), HSPF (Hydrological Simulation Program-Fortran) (Bicknell et al., 2001), SWAT (Soil and Water Assessment Tool) (Arnold et al., 1998), DHSVM (Distributed Hydrology-Soil Vegetation Model) (Wigmosta et al., 1994), TOPMODEL (topography-based hydrological model) (Kirkby and Beven, 1979), and VIC (Variable Infiltration capacity model) (Liang et al., 1994) have often been employed to assess the impacts of land use or vegetation changes on water resources on the catchment scale (Aredo et al., 2021; Bai et al., 2020; Gumindoga et al., 2014; Huang et al., 2019; Li et al., 2021a; Luo et al., 2020; Ni et al., 2021; Srivastava et al., 2020). The physically-based, semi-distributed or distributed hydrological models are efficient tools to evaluate the effects of LUCC on hydrology, since they consider the spatial heterogeneity and hydrological processes, SWAT, a semi-distributed model, has been applied in many catchments worldwide to investigate both water balance and water quality dynamics at different-sized catchments (Abbaspour et al., 2015; Donmez et al., 2020; Fohrer et al., 2005; Wu et al., 2012). SWAT becomes an increasingly important tool for assessing the responses of catchment hydrology to LUCC, due to its feasibility for an integrated modeling of

water and nutrients even under circumstance where data are limited (Strehmel et al., 2016; Wagner et al., 2015). Numerous applications of SWAT have been reported with respect to water quantity (e.g., river discharge, groundwater dynamics, and soil water) (Prusty et al., 2021; Tigabu et al., 2020; Xie et al., 2020), and water quality assessment (e.g., land use and management change, best management practices in agriculture) (Amin et al., 2020; Gong et al., 2019; Qi et al., 2018). Baker and Miller (2013) used SWAT to show that LUCC resulted in increases in surface runoff and decreases in base flow in River Njoro watershed, Kenya's Rift Valley. Yan et al. (2013) quantified the relative contribution of changes in individual land use types to the variations in streamflow and sediment yield with the application of SWAT model and multivariate analysis. Nguyen et al. (2019) demonstrated that SWAT model is more robust in predicting dynamics of sediment and nutrient loads under different land use scenarios compared to the simple model SOURCE. In northern German catchments, a few cases exemplify that SWAT was successfully applied as a modeling tool: Lam et al. (2012) evaluated the long-term impact of point and diffuse source pollution (dominated by agriculture) on nitrate load in the Kielstau catchment using SWAT. They illustrated that daily flow and nitrate load were satisfactorily modeled and diffuse sources contributed dominantly (95%) to nitrate load. Song et al. (2015) coupled SWAT with HEC-RAS to investigate the sediment dynamics in the Upper Stör catchment. They concluded that heterogonous land use conditions resulted in different sediment amounts among sub-catchments. Haas., et al (2017) used the SWAT model to investigate water quality variations in response to the implementation of different best management practices of buffer strips, fertilization reduction and alternative crops in the Treene catchment. They demonstrated that combined BMPs of fertilization reduction, buffer strips and soil coverage exhibited greater effectiveness than other BMPs in nitrate load reduction. Guse et al. (2015b) dynamically modeled the spatial distribution of agricultural crops and their impacts on nitrate load in the Treene catchment. The constructed model showed a good performance on the daily time scale and allowed for the assessment of nutrient dynamics in response to changes of land use. Overall, the application studies demonstrated that SWAT is a powerful tool for simulating hydrological process and

water quality components and is applicable in lowland catchments of Northern Germany.

Although the SWAT model has numerous applications worldwide, previous studies revealed that the original SWAT version sometimes performed relatively poorly for recession limbs and low flow periods (Guse et al., 2014; Koch et al., 2013; Pfannerstill et al., 2014). Strong groundwater interaction is an important characteristic in German lowlands, which considerably affects low flows. To enhance the process-oriented representation of low flow periods, Pfannerstill et al. (2014) developed SWAT3s in Kielstau catchment (a northern lowland catchment in Germany), by conceptually separating the shallow groundwater aquifer of the original SWAT into a fast and slow shallow aquifers. The adapted version of SWAT can enhance the representation of low flows and thereby improve the representation of hydrological process and water quality which are largely controlled by groundwater dynamics in lowlands (Haas et al., 2016; Pfannerstill et al., 2014). Therefore, the SWAT3s is suitable to accurately predict the influences of LUCC on hydrology and water quality in German lowland catchments with abundant groundwater recharge.

1.5. Research gaps and questions

1.5.1. Research gaps

River systems are strongly affected by landscape processes, and stream water resources interact intensively with the surrounding landscape. Water resources of a river basin vary with spatial and temporal scales, as they are easily influenced by heterogeneous land use and anthropologic activities. The consequences of the hydrological processes are not produced by the land use area alone. They are a result of the synergistic effects of the extent and spatial structure of land use (Boongaling et al., 2018; Van Nieuwenhuyse et al., 2011). To shed light on the contributions of changing land use pattern on the dynamics of water resources, the changes in the composition and spatial arrangement of landscape are important factors to be investigated. It is well known that the modification of land use strongly affects hydrological processes and water quality conditions (Fan and Shibata, 2015; Fohrer et al., 2005; Tong and Chen, 2002). The interplay often occurs in the main hydrologic components such as

evapotranspiration, groundwater flow, and surface runoff (Amiri et al., 2016; Bin et al., 2018). Water quality depends to a large extent on these hydrologic components. The "cause-effect" relationship of land use and water resources becomes more complicated due to diverse spatial-scale effects. Predicting the responses of catchment hydrology and water quality to changing land use is challenging. There is still potential for improvement based on the previous studies. Firstly, earlier studies explored the effects on water quality or hydrological elements using simple and lumped indicators of land use percent, neglecting the spatial structure and location information of land use patterns (Ahearn et al., 2005; Tong and Chen, 2002). Secondly, the spatial scale effect is not fully considered. Land use effects sometimes depends on the spatial resolution of data and the setting of spatial scales (Wu et al., 2002). The scale setting in most contemporary studies may not be sufficient to identify the most effective scale. Thirdly, the linking of landscape metrics to hydrology needs to be encouraged. Linking landscape process to hydrologic modeling will allow to better analyze the hydrological responses to changing environment. Such integrative research should be encouraged so as to assess the long-term interplay of land use and hydrology.

It is necessary to take landscape metrics into account when studying the effects of land use patterns on water resources. Meanwhile, the investigation of the key spatial extent controlling water quality can provide an important reference allowing catchment managers to make a more informed plan for improving water quality effectively. Moreover, a dynamic representation of water quality and quantity under long-term land use changes is helpful to achieve an integrated assessment of water and land resources.

1.5.2. Research questions

The thesis primarily aims to quantify the contributions of land use changes on catchment hydrology and water quality variations in space and time. The main research questions of this study include:

(1) Which variables typically affect land use patterns in rural lowland catchments of Northern Germany?

(2) How does water quality evolve seasonally and spatially and how do land use and other catchment characteristics influence water quality at different spatial and season scales?

(3) How can daily water quality dynamics be represented by a hydrological model and how do changes of areal percent and landscape indices of each land use class affect water quality and quantity at subbasin scale?

1.6. Thesis structure

The PhD thesis is sectioned of six chapters. The first chapter is a general introduction involving the background information, state of the art of the research topic and the research gap and research questions. The second chapter covers the main measurement campaigns by the author of this work. The third chapter investigates the pattern of each specific land use type associated with spatially distributed variables in a rural lowland catchment. In the fourth chapter, the influences of land use on multiple water quality parameters at different seasons and scales are quantified. The fifth chapter focuses on the dynamic modeling of the contributions of land use changes on the dynamics of water balance components and nutrients. The last chapter discusses and concludes the main findings of the thesis.

Chapter 2 Water quality measurement campaigns

Three different measurement campaigns of stream water quality were carried out in the Stör catchment. Two historic measurement campaigns were conducted during 1992-1994 (Ripl et al., 1996) and 2009-2011 (Pott, 2014), and a recent campaign was conducted as a part of this PhD project during 2018-2019. The latter includes monthly and daily measurements and is described in detail in this chapter.

2.1. Monthly measurement campaign

During the monthly campaign from Oct. 2018 - Nov.2019, water samples were collected from the central section of the stream at twenty-one sampling sites on a monthly basis (usually in the middle of the month). These sites gauge sub-basins of the catchment (Figure 2-1). These sites are consistent with those from the two former measurement campaigns and have been selected considering different land uses as well as accessibility of the sampling point. The water samples were taken from rivers with a sampling beaker (Figure 2-2), contained in clean plastic bottles, and transported to laboratory on the same day. In-situ parameters including pH, dissolved oxygen (DO), water temperature (WT), and electrical conductivity (EC) were measured using a multi-parameter monitoring instrument (WTW Multiline).

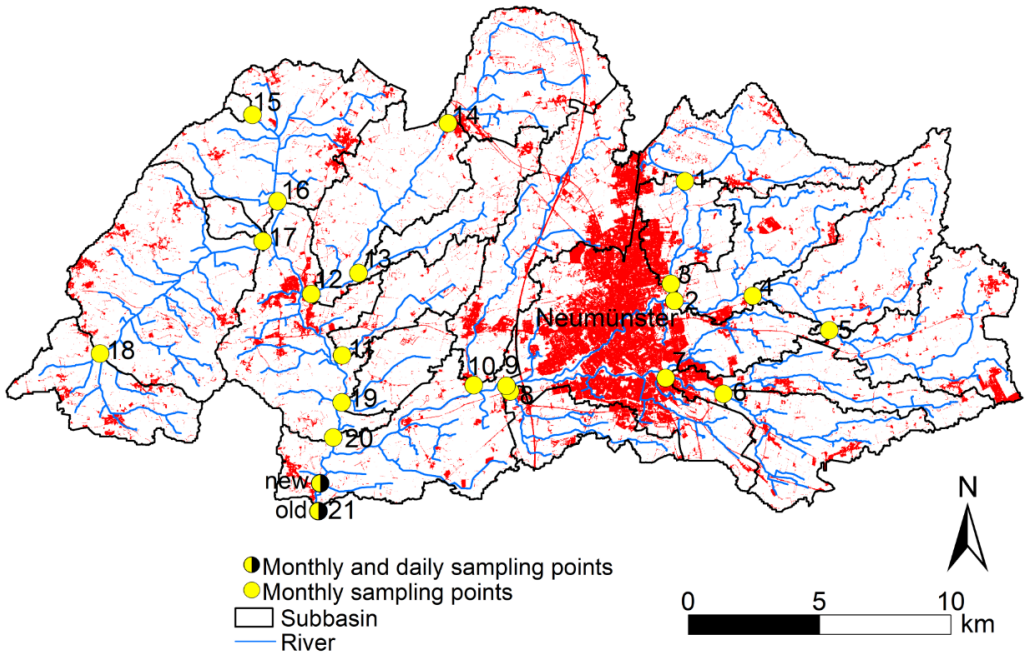

Figure 2-1. The distribution of twenty-one monthly sampling sites and the daily sampling site (new: sampler location in 2018-2019, old: sampler location in 2009-2011).

Figure 2-2. Monthly manual collection of water samples.

2.2. Daily automatic monitoring

Daily mixed samples were taken by an automatic and cooled ISCO 6172 sampler in Willenscharen near the outlet of the catchment (Figure 2-3. (a)). As electricity power supply was not available at the gauge Willenscharen, the sampler has been installed about 400 m upstream of the outlet gauge (Fig. 2-1). The sampler was installed in a flood-safe location, in a few meters distance from the river side. The water collector tube was installed in the central part of the river and at a depth of 0.3 m above the riverbed (Figure 2-3c). The sampler was programmed to collect water samples every 72 minutes, making 20 sub-samples for each day. However, the frequency was adjusted to collect 14 subsamples per day during a short testing phase (October-early November 2018). Each daily sample is composed of about 2 liters of stream water. The automatic sampler is equipped with 24 1-liter bottles (Figure 2-3a), so that it provides a storage capacity of twelve daily samples. The temperature inside the sampler was kept at around 3-5 °C. The water samples were taken to the laboratory and replaced with new bottles every ten to twelve days.

Figure 2-3. (a) ISCO sampler in Willenscharen, (b) sampling site of the river, (c) water tube collector installed in river, (c) view of the sampling probe.

2.3. Lab analyses

The monthly and daily water samples have been processed and analyzed in the laboratory of the Department of Hydrology and Water Resources Management at Kiel

University (Figure 2-4) using German standard procedure for water analysis (DEV) (Einheitsverfahren,1997). Eight water quality parameters were analyzed in the lab, which included total suspended sediment (TSS), total phosphorus (TP), soluble orthophosphate-phosphorus (PO_4-P), total nitrogen (TN), nitrate-nitrogen (NO_3-N) and ammonium-nitrogen (NH_4-N), Chloride (Cl^-), and Sulphate (SO_4^{2-}). To derive the concentration of TSS, 1 liter water sample was filtered through a 0.45 μm cellulose-acetate filter paper to obtain sediment particles. The concentration was determined by weight difference before and after drying (at 105 °C) and cooling for at least 1.5 hours, respectively. More details of lab analyses of other parameters and some results can be found in Chapter 4 of this thesis. The measurement values of nutrients are given in Annex.

Figure 2-4. Analysis of water quality parameters in laboratory (e.g., NH_4-H, PO_4-P, and TP by the author as shown in the photo).

Chapter 3 Identifying the most important spatially distributed variables for explaining land use patterns in a rural lowland catchment in Germany

Chaogui Lei *, Paul D. Wagner, Nicola Fohrer

Department of Hydrology and Water Resources Management, Institute for Natural Resource Conservation, Kiel University, Olshausenstr 75, 24118 Kiel, Germany

Correspondence author: Chaogui Lei (cglei@hydrology.uni-kiel.de)

J. Geogr. Sci. 2019, 29(11): 1788-1806, DOI: https://doi.org/10.1007/s11442-019-1690-2
Submitted: 2018-11-08 ─ Accepted: 2019-02-21 ─ Published: 2019-10-29

Abstract

Land use patterns arise from interactive processes between the physical environment and anthropogenic activities. While land use patterns and the associated explanatory variables have often been analyzed on the large scale, this study aims to determine the most important variables for explaining land use patterns in the 50 km² catchment of the Kielstau, Germany, which is dominated by agricultural land use. A set of spatially distributed variables including topography, soil properties, socioeconomic variables, and landscape indices are exploited to set up logistic regression models for the land use map of 2017 with detailed agricultural classes. Spatial validation indicates a reasonable performance as the relative operating characteristic (ROC) ranges between 0.73 and 0.97 for all land use classes except for corn (ROC = 0.68). The robustness of the models in time is confirmed by the temporal validation for which the ROC values are on the same level (maximum deviation 0.1). Non-agricultural land use is generally better explained than agricultural land use. The most important variables are the share of drained area, distance to protected areas, population density, and patch fractal dimension. These variables can either be linked to agriculture or the river course of the Kielstau.

Keywords: land use pattern; logistic regression model; rural lowland catchment; Germany

3.1. Introduction

Land use and land cover affect the climate (Foley et al., 2005; Bonan et al., 2012), ecosystem structure (Ramachandran et al., 2018), hydrology and aquatic environment (DeFries and Eshleman, 2004), and thus have an impact on the development of the economy and population (Lambin and Meyfroidt, 2011). Throughout history, land use and land cover patterns have been diversified by urbanization, farmland expansion, and agricultural intensification (Lambin et al., 2001; Lawrence et al., 2008; Mustard et al., 2012). European agricultural land use has experienced considerable changes in the second half of the last century due to transformation in technology, socio-economy, and political management (Rounsevell et al., 2003). This has brought about considerable discrepancies in land use patterns. Heterogeneity of land use patterns affects several environmental aspects, such as air quality (Vleeshouwers and Verhagen, 2002), the distribution of the main components in the hydrological cycle (Neupane and Kumar, 2015), and biological diversity and ecosystem services (Alberti, 2005). Moreover, the economic development can be affected (Dissart and Vollet, 2011). Consequently, land use patterns are a multidisciplinary research topic that receives growing attention (Kok and Veldkamp, 2001; Zhang et al., 2013; Long and Qu, 2018; Ramachandran et al., 2018).

Since land use results from properties of the physical environment and from socio-economic development, relationships to biophysical and socio-economic spatially distributed variables are used to analyze land use change patterns (Mas et al., 2014; Aquilué et al., 2017). Relevant variables haven been used in a large number of land use change studies (Mitsuda and Ito, 2011). Properties of the environment, accessibility, socio-economic development, and neighborhood and micro-policy variables are incorporated into statistical analyses like multiple linear regression or logistic regression, to study driving forces of urbanization (Deng et al., 2010; Shu et al., 2014). Among these variables, the relative importance of accessibility and socio-economic variables for urbanization has been shown (Liu et al., 2010). In contrast, spatial determinants that influence the location of agricultural land mostly relate to soil fertility, climatic patterns, or distance to markets (Mottet et al., 2006; Piquer-Rodriguez et al., 2018). These commonly used variables can be categorized as biophysical variables (e.g.,

topography, soil properties, climatic variables) and socio-economic variables (e.g., population density, distance to roads or villages, etc.), most of which have been used to predict spatial patterns of urban or agricultural land use change (Oñate-Valdivieso and Sendra, 2010; Baumann et al., 2011; Yang et al., 2014). Landscape metrics (like perimeter-area ratio) that quantify specific spatial characteristics of land patches represent land use heterogeneity in space (Inkoom et al., 2018). They manifest land use impact gradients (Fernandes et al., 2011), and are applied to land use modeling (Yang et al., 2014). Hence, landscape metrics have a potential to explain land use location, considering bidirectional connections between the land patch configuration and land use dynamics. In a particular region, the spatial pattern of one land use type is primarily shaped by a definite set of variables (van Meijl et al., 2006). The identification of important explanatory variables for spatial patterns of all land use classes facilitates a more efficient prediction of land use dynamics and allows for a better understanding of the land use system.

Studies about spatio-temporal characteristics and dynamics of agricultural land mostly focus on one lumped agricultural or cropland class (Li and Yeh, 2002; Piquer-Rodriguez et al., 2018). This is in part due to the accessibility of coarse agricultural classification data, e.g. from agencies (Feranec et al., 2010) or derived from remote sensing data (El-Kawy et al., 2011), as well as a predominant focus on the large scale (Etter et al., 2006). Several detailed classes are only rarely considered, e.g., in the study (Mehdi et al., 2018) which depicts separate spatio-temporal patterns of cereals, soybeans, corn, and oilseeds. The conservation of different spatial patterns of croplands enhances agricultural productivity (Semwal et al., 2004; Brandes et al., 2016). Cropland change is driven by a large number of influencing factors and differs from region to region (Mehdi et al., 2018). Müller et al. (2009) have examined the characteristics of cropland variation and cropland abandonment. However, in summary, the determinants of cropland patterns have not gained much attention, yet.

To address this research gap, we developed logistic regression models for 11 agricultural and three non-agricultural land use classes in the rural catchment of the Kielstau, Germany. We used biophysical and socioeconomic variables as well as landscape metrics to identify the most important determinants of land use patterns. In

particular, this study focuses on three objectives: 1) to find the best variables to explain the distribution of each land use class, 2) to identify the most important explanatory variables for the land use pattern, and 3) to analyze competition between land use classes in the catchment.

3.2. Materials and methods

3.2.1. Study area

The Kielstau catchment (Figure 3-1) is a small rural catchment in northern Germany covering an area of 50 km^2 (Fohrer et al., 2014; Wagner et al., 2018). It is a subbasin of the Treene river. The mean annual precipitation and temperature are 893 mm and 8.3°C (DWD, 2009), respectively. The topography is comparatively even, with an elevation ranging from approx. 27 m to 78 m a.s.l. (Figure 3-1). Soils of Gleysol, Podzol, and Luvisol (Figure 3-1) dominating this catchment are mainly used as arable land, and grassland or pasture. Kielstau is the main river with a total length of approximately 17 km, flowing through Lake Winderatt about 5 km downstream from the river source. The Lake Winderatt is surrounded by protected areas that are mainly used for moderate grazing (Fohrer and Schmalz, 2012). The Kielstau receives discharge from two main tributaries: the Moorau and the Hennebach. To secure agricultural productivity, subsurface tile drainages have been installed during land reallocation(Riedel and Polensky, 1987), which caused wide, drained areas that were estimated to cover 38% of the entire catchment (Fohrer et al., 2007).

Croplands constitute 63% of the study area and the majority is found in larger land patches as compared to the other land use classes. Among them, winter wheat, winter barley, winter rape, or corn take up a larger proportion, while winter rye, beans, oats, or row crops (sugar beet, potatoes, etc.) constitute a relatively smaller area. Crop rotations are commonly applied, resulting in constant changes within the croplands. Grassland or pasture (20%–21%) is mainly found in proximity to rivers and lakes or in protected areas. Urban, forest, water, and garden or orchard each occupy a smaller and persistent proportion.

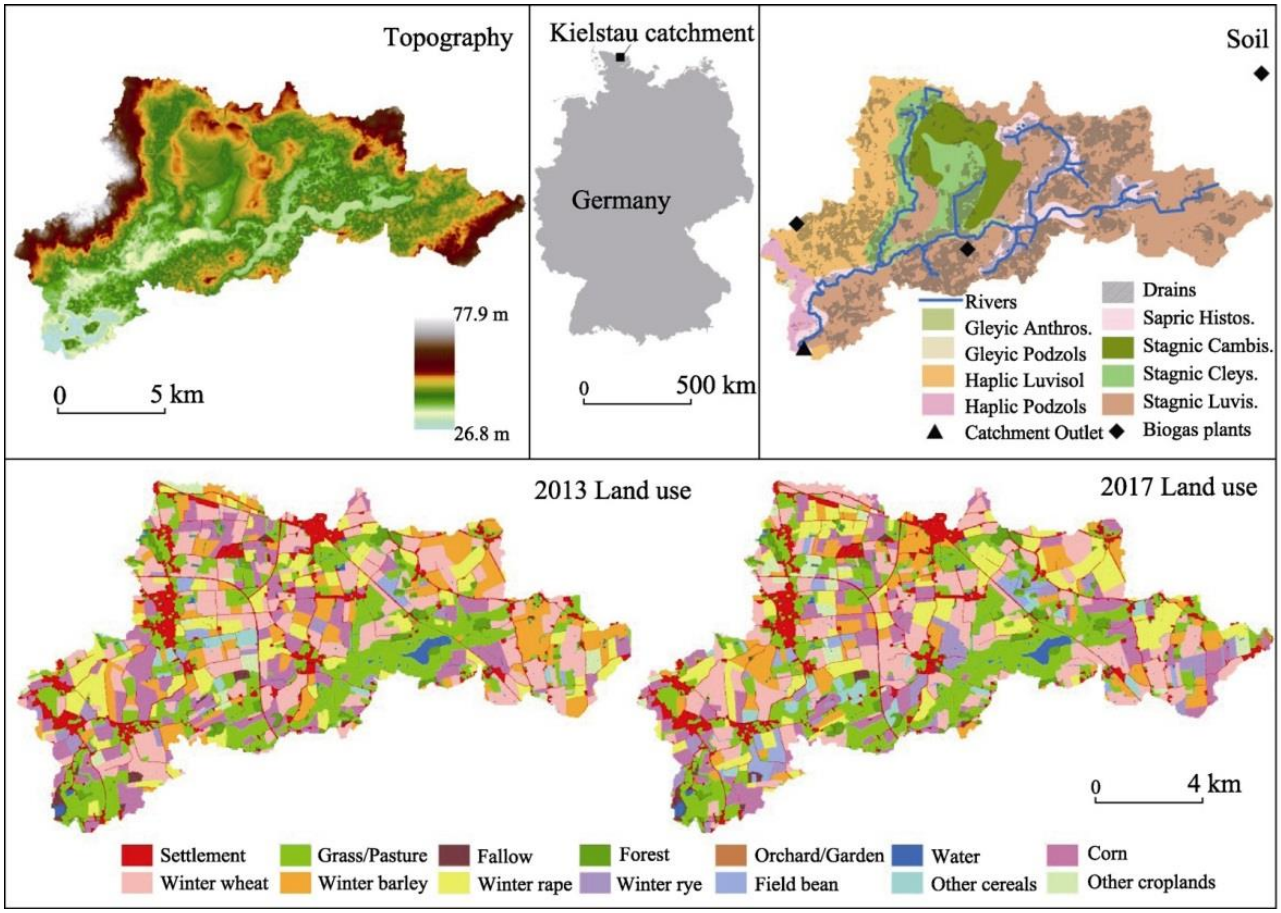

Figure 3-1. Location of the Kielstau catchment, spatial distribution of topography (LVA, 1992–2004), soil (BGR, 1999), main stream network (LANU, 2003), biogas plants, and land use in 2013 and 2017.

3.2.2. Land use data

Land use maps of the years 2013 and 2017 (Figure 3-1) are used for spatio-temporal pattern analysis. The maps were acquired through field surveys in spring and early summer of 2013 and 2017. The main base data for this mapping process was extracted from the automated landed property map (ALK–Automatisierte Liegenschaftskarte, 2004) released by the state survey office of Schleswig-Holstein (LVERMA-SH). This map provides the outlines of all land patches. The land use class of every patch was mapped in the field. Furthermore, the consistency of the derived land use data was checked with the help of 0.2 m-resolution orthophotos (LVA, 2013, 2016) that were taken on 01/03/2013 and 26/08/2016.

Croplands comprise 62.8% in 2013 and 63.1% in 2017 of the catchment (Table 3-1). They are mainly classified into (1) cereals, including winter wheat, winter barley, winter rye, oats, and a smaller fraction of summer wheat and summer barley, (2) energy

crops, like winter rape and corn silage, (3) row crops including potatoes and sugar beet, as well as (4) field bean, strawberries, and vegetables. With regard to semi-natural land use, grassland, meadow, mowing meadow, and pasture account for 20.8% in 2013 and 20.3% in 2017 (Table 3-1), respectively, and are primarily found along the rivers. The forest areas are nearly stable over time. Fallow areas are croplands that are not cultivated in the current year. It is mainly located in the southwestern region. Water areas cover approximately 1.8% including lakes, ponds, rivers and open creeks. Residential sites are located near main road intersections, with a slight increase from 10.5% in 2013 to 10.6% in 2017. Garden or orchard plots are scattered mostly near villages. To avoid very small land use classes and samples, the land use was divided into the following 14 main classes: settlement areas (residential, commercial, and industrial lands), fallow, grassland or pasture (field grass, meadow and pasture), corn, other croplands (strawberry, potato, sugar beet, etc.), forest, winter rye, winter rape, garden/orchard, winter wheat, other cereals (oats, summer wheat, summer barley), field beans, winter barley, and water.

Table 3-1. Areal percentages of land use classes in the Kielstau catchment in 2013 and 2017.

	Settlement area	Fallow	Grassland /Pasture	Corn	Other crops	Forest	Winter rye	Winter rape	Orchard /Garden	Winter wheat	Other cereals	Field bean	Winter barley	Water
2013	10.5	0.7	20.8	13.0	1.6	3.1	1.4	10.8	0.5	22.0	1.2	1.0	11.8	1.8
2017	10.6	0.6	20.3	10.7	2.1	3.1	3.5	11.8	0.5	21.4	2.0	2.4	9.2	1.8
Change	0.1	-0.1	-0.5	-2.3	0.5	0	2.1	1.0	0	-0.6	0.8	1.4	-2.6	0

3.2.3. Explanatory variables

Twenty-six spatially distributed variables have been used to explain the location of land use classes in space. Variables are depicted in Table 3-2, including topography variables, soil properties, distance and socioeconomic variables, and landscape metrics. All datasets are processed to a 10 m grid resolution. Spatial patterns of slope, silt content, drained soil share, distance to protected areas, population density, and fractal dimension are given as examples in Figure 3-2. Topography, soil properties, distance and socioeconomic variables are widely used to explain spatial patterns of land use and land use change (Verburg et al., 2004; Qasim et al., 2011). Landscape metrics have been previously used to quantify landscape structure and to assess land use and land cover change.

A 5 m digital elevation model (DEM) derived from topographic map of Schleswig-Holstein (LVA, 1992–2004) has been used to generate elevation, slope, and aspect data at a 10-m resolution. The distance to roads or villages has been calculated from polygon roads and villages shapefiles that were extracted from land use maps in 2013 and 2017. The distance to rivers has been calculated from the main rivers shapefile of the Kielstau catchment (LANU, 2003). The distance to protected areas was derived based on the distribution of protected areas surrounding the Lake Winderatt and the Kielstau river (StiftungNaturschutz, 2016). By combining the land patch map with tile drained areas estimated (Fohrer et al., 2007), the percentage of drained area per patch was calculated. With regard to population density, (i) every 50 m^2 settlement area is reclassified as one residential site based on a village map that was extracted from the land use map and from the digital basis landscape model (ATKIS-Basis-DLM) (LVA, 2016); (ii) residential sites are interpolated into a residence density raster using a Kernel algorithm (Silverman, 1981; Yan et al., 2011); (iii) the mean value of residents per site in each town is derived by dividing the number of inhabitants per town in June 2013 and December 2015 (Statistik Nord, 2013, 2015) by the amount of residential sites; (iv) the spatial population density is the product of the residence density raster with the mean value of residents per site. Soil properties are acquired from a combined application of soil type distribution derived from a Digital Soil Map (BGR, 1999) and

soil attributes generated for a modeling study (Fohrer et al., 2014). As German biogas plants take in cereals, weeds, corn, and sunflowers as feedstocks (Golon, 2009), their distribution potentially affects crop distribution. Distance to biogas plants has therefore been considered and calculated according to the locations of two biogas plants within the catchment and another one near the catchment. Explicit outlines of land patches were extracted from land use maps in 2013 and 2017. Landscape metrics of all patches have been calculated with the Patch Analyst 3.1 extension for ArcGIS 10.3 and all other calculations have been carried out in ArcGIS 10.3.

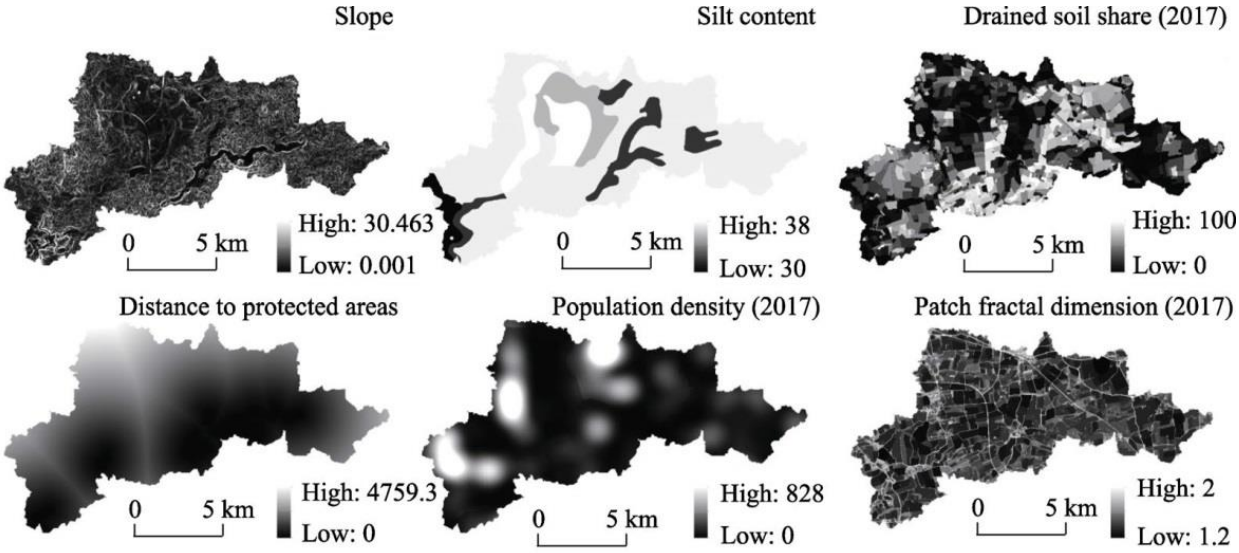

Figure 3-2. Examples of potentially important explanatory variables to land use distribution

Table 3-2. Spatially distributed explanatory variables used in this study

Variable	Unit	Source
Elevation	m	DEM for S.-H. (LVA, 1992-2004)
Aspect	Degree	Calculated from DEM
Slope	Degree	Calculated from DEM
Clay content	%	Digital soil map (BGR, 1999)
Silt content	%	
Sand content	%	
Rock content	%	
Organic carbon content	%	
Available water capacity	mm/mm	
Soil depth	mm	
Moist bulk density	mg/m^3	
Saturated hydraulic	mm/hr	
Moist soil albedo	-	
Usle_k factor	-	
Drained soil share	%	
Distance to rivers	m	Calculated from river network shapefile (LANU, 2003)
Distance to roads	m	Calculated from road distribution derived from 2013, 2017 land use
Distance to villages	m	Calculated from village distribution derived from 2013, 2017 land use
Distance to nature conservancy	m	Calculated from nature conservancy distribution (StiftungNaturschutz, 2016)
Distance to biogas plants	m	Calculated from biogas plants location
Population density	$Persons/km^2$	Calculated from community population and village distribution from 2013, 2017 land use maps
Patch size	m	Calculated from 2013 and 2017 land use maps
Patch Perimeter	m	
Shape index	-	
Perimeter-area ratio	m^{-1}	
Fractal dimension	-	

3.2.4. Logistic regression approach

Logistic regression models are used to analyze spatial patterns of all land use classes in the catchment with 26 explanatory variables (Table 3-2). Water areas are excluded from the analysis study as they occupy only a small proportion of the area. For each class C, a binary coding is employed, where 1 indicates the presence of class C; 0 indicates the presence of another class. The probability P_i for each pixel *i* (10 m × 10 m) for the appearance of this land use class is calculated using a function of explanatory variables $X_{n,i}$ as follows:

$$\mathrm{Log}\left(\frac{P_i}{1-P_i}\right) = \beta_0 + \beta_1 X_{1,i} + \beta_2 X_{2,i} + \beta_3 X_{3,i} + \beta_4 X_{4,i} + \beta_5 X_{5,i} \quad (3\text{-}1)$$

where βn is the regression coefficient for the variable $X_{n,i}$. To seek the most important explanatory variables and avoid over-fitting, the number of explanatory variables *n* is

limited to five. Previous studies also showed that five explanatory variables are sufficient to acquire reasonable results (Baumann et al., 2011; Wagner and Waske, 2016).

The relative operating characteristic (ROC) is used to assess model performance. The ROC statistic is the area under the curve of the rate of true positives versus the rate of false positives for a range of threshold values applied to the probabilities to achieve a binary classification. It ranges from 0.5 (random separation) to 1 (perfect discrimination) (Pearce and Ferrier, 2000). An ROC≥0.7 indicates that the independent variables have a strong capacity to model the dependent variable (Pontius and Schneider, 2001). In this study, the ROC value is used to select the model that is more suitable to explain land use patterns. To ensure that the selected variables are not collinear, Pearson's correlation (r) is calculated for each variable pair. When r exceeds 0.7, the variable that better explains the land use appearance is retained and the other one removed (Baumann et al., 2011; Wagner and Waske, 2016). The logistic regression models of all possible combinations of five explanatory variables from non-collinear variable datasets are set up, by removing non-significant variables that are unable to optimize model performance according to a stepwise approach. Among these combinations, the 13 best logistic regression models with the highest ROC, one for each land use class, are selected and used for the analysis. To avoid spatial autocorrelation, for each specific land use class a stratified random sample is extracted by taking 20% of all pixels from its binary land use raster in 2017, and by excluding adjacent pixels in this sample (Wagner and Waske, 2016). The derived sample is randomly divided into two equal parts: one for calibration and one for validation of the models.

To assess the relative importance of the explanatory variables, all possible models derived from the calibration process by the ROC values are sorted and the first 50 best models for each class are selected. Then, how often each variable is included into these 50 models is counted. The percentage of the inclusion of a variable into best regression models is regarded as variable importance. All calculations, model executions, and analyses are performed in R and with the help of the R packages ROCR (Sing et al., 2005) and raster (Hijmans et al., 2016).

3.2.5. Validation and evaluation

The derived logistic regression models are quantitatively and visually evaluated in space and time (Pontius Jr et al., 2004). First, the validation half of the stratified random samples from the 2017 binary raster are used for spatial validation using the ROC statistic. Second, the model applicability is tested in time. To this end, some of the explanatory variables are updated: landscape metrics in 2013 are updated due to reshaped land parcels. Distance to villages is updated using slightly changed settlement areas in the 2013 land use map. Population density is recalculated by using village residence map and population data for the year 2013. The probabilities for each specific land use class in the entire catchment in 2013 are calculated, by applying the best logistic regression models to the 2013 explanatory variables. The derived probabilities are compared against the observed 2013 land use map with the help of the ROC statistic.

To further assess the plausibility of modeled results, R-G-B composites are used to visualize the competition for land in space between three different land use classes. An R-G-B composite is built by overlaying any three probability maps. In R-G-B composite maps, dark areas indicate low probabilities for these three classes, whereas light colors (near white) correspond to high probabilities for all of them, i.e. strong competition for land. Water areas are masked in white.

3.3. Results

3.3.1. Model performance

All explanatory variables that are included in the best logistic regression models are significant ($p<0.05$, Table 3-3). The best models are well above random discrimination as ROCs are greater than 0.5 (Table 3-3). The ROC for calibration (ROC_cal) ranges from 0.68 for corn to 0.97 for settlement areas. With regard to the spatial validation ROC values (ROC_val_2017) between 0.73 and 0.97 (Table 3-3), except for a slightly lower ROC of 0.68 for corn, are within the range of reliable precision 0.7–0.9 (Wu et al., 2009) or nearly 100% accurate with ROC value close to 1 (Pontius Jr and Schneider, 2001), highlighting reasonable performances of the derived models. Slightly lower ROC values from temporal validation (ROC_val_2013) indicate

that the prediction of the 2013 land use pattern is a little worse (Table 3-3) Nevertheless, ROC_val_2013 values are greater than 0.71 with the exception of corn. The ROC for calibration differs from that for spatial validation and temporal validation by a maximum of 0.03 and 0.08, respectively. Hence, the derived regression models are reliable and robust both in space and in time. They can be used to accurately predict the spatial distribution of land use classes. Only corn is predicted with a slightly lower accuracy. Spatial patterns of croplands are often less accurately explained than non-croplands. For instance, ROCs for corn, winter wheat, and winter barley are equal to or smaller than 0.75, whereas ROCs for settlement areas, orchard/garden, fallow, and forest are equal to or larger than 0.84.

3.3.2. Variable impact

The majority of explanatory variables are included at least once in the best logistic regression models (Table 3-3) However, only few soil properties are used due to their higher collinearity, e.g. silt content has a positive correlation with soil organic carbon (r= 0.83) and clay content is negatively correlated with moist bulk density (r= –0.75). As only the variable that better explains land use appearance is included, soil organic carbon, available water capacity, and some other properties were not included in the best models (section 2.2.4).

The odds ratio, depicted as the value of exponent β_n for the n-th variable, represent the impact of this variable on the predictor. The probability for land use presence will increase upon an increase in the n-*th* variable with odds ratio being greater than 1, whereas probability decreases with an increase in the variable when odds ratio is below 1. Table 3-3 shows that topography variables tend to affect natural or semi-natural land uses. Specifically, with an increase in slope by 1 degree the probability for fallow, forest, or orchard/garden appear to increase by 35.7%, 34.7%, and 50.3% (odds ratios=1.35698, 1.34681, 1.50291). When terrain ascends by 1 m, the probabilities for fallow and field beans decrease by 17.4% and 15.2% (odds ratios= 0.82567, and 0.84845, respectively).

Soil content variables (clay, silt, sand, or rock content) are mainly used to explain the occurrence of agricultural lands, e.g., with an increase of silt by 1%, winter wheat

and winter barley become more probable by 8.9%, and 10.6%, respectively, and winter rye becomes less probable by 2.6%. Grassland or pasture is more probable on areas with a deeper first soil layer (0.2% increase per mm). The drained soil share affects seven land use classes. With an increase in the proportion of drained area by 1%, the probabilities for settlement, garden or orchard, and forest presence decrease by 3.4%, 2.4%, and 2.6%, respectively, while the probability for pasture increases 1.2%. Other crops (3.3%) and winter rye (1.3%) are less probable if the drained area share increases, whereas field beans are more probable (2.0%). The contrary effect on field beans is in agreement with the higher probability for field beans at low elevations, indicating that field beans are primarily found at lowland areas with a high drainage percentage in the catchment.

Distance variables and population density explain all land use classes. Particularly, distance to protected areas and population density are included in the best models for eight and five land use classes, respectively. As further away from protected areas, grassland or pasture becomes less probable (0.03% per meter, Table 3-3). In contrast, settlement areas and orchard or garden seem more probable (0.03%, 0.04% per meter, respectively) with increasing distance from protected area. There is no clear impact direction on croplands (Table 3-3). Population density has a clear effect on land use patterns; with an increase of one more person per square kilometer, settlement areas (0.4%) are more likely to be found, whereas fallow (0.9%), forest (0.8%), corn (0.3%), and other crops (0.3%) are less probable.

The influence of patch structure in particular of the fractal dimension is evidently different for croplands and non-croplands. An increase of fractal dimension indicating more complex patch shape (nearer 1 – simpler shape; 2 – irregular and complicated shape (Forman, 2014; Forman and Godron, 1981)) suggests that settlement area and forest (odds ratios > 1, Table 3-3) are more likely to be found on irregular patches, whereas croplands corn, winter rye, winter rape, winter wheat, other cereals, field beans, and winter barley all with odds ratios < 1 (Table 3-3) are more likely to be on simpler patches (e.g. large rectangles).

3.3.3. Variable importance

In addition to the best logistic regression model, the 50 best logistic regression models are derived for each land use class to evaluate the importance of explanatory variables. All models achieve a reliable performance with ROCs ranging from 0.72 to 0.97 except for corn (Table 3-4). Moreover, ROCs of the 50 best models only differ by a maximum of 0.03, indicating similar performance. The variables that are also included in the best model mostly have the greatest importance (percentages are marked in bold in Table 3-4). Some are even included in all of the 50 best models (100% inclusion). Overall, distance variables and population density are particularly important as they account for 31.7% of the variables that are used in these models, followed by soil properties (29.0%) and landscape metrics (28.7%), whereas topography (10.7%) is less important for rural land use patterns in this lowland region.

Distance to roads, distance to villages, distance to biogas plants, population density, and drained soil share are important for all land use classes, as they are at least included in two of the 50 best models (i.e. ≥ 4% inclusion, Table 3-4). Elevation, distance to protected areas, distance to villages, population density, drained soil share, perimeter-area ratio, and fractal dimension are of utmost importance as they are included at least one time in each 50 best models. Among them, patch fractal dimension (Pfd) is quite important for settlement areas (100% inclusion), mixed croplands (100% inclusion), field beans (96% inclusion), winter rye (88% inclusion), and forest (72% inclusion); distance to protected areas affects other croplands, winter rye, winter rape, and other cereals (inclusion ≥ 98%); drained soil share greatly explains the appearance of settlement areas, other croplands, forest, grassland, and field beans (inclusion ≥ 90%). Further important influences indicated by 100% inclusion are: elevation for fallow and field beans, distance to villages for orchard/garden, population density for forest, and patch perimeter-area ratio for other croplands.

In general, the variables distance to protected areas (mean inclusion 48%), population density (32%), drained soil share (51%), and patch shape complexity (fractal dimension, 66%) are largely important as they are more frequently included and used for 10 to 13 land use classes. Topography and soil properties contribute to fewer land use classes with a relatively low importance. The lower importance of topography is

largely related to smaller terrain variations and similar potentials for crops throughout the catchment. The low impact of soil properties mainly results from the exclusion due to collinearity between soil variables, e.g. organic carbon content and moist bulk density are highly correlated with available water capacity (r= 0.84 and r= –0.85, respectively) and are, therefore, excluded as available water capacity is preferred during variables selection (Table 3-4). Nevertheless, soil properties in-deed provide crucial information for the spatial distribution of cropland, e.g. silt content is an important explanatory variable for the spatial patterns of major cereals (winter rye 34%, winter wheat 98%, and winter barley 58%, respectively, Table 3-4) and part of the best model for these classes.

3.3.4. Analysis of probability maps of land use patterns

The probability maps for each land use class in 2013 are calculated using the best logistic regression model and the respective explanatory variables. For most of the land use classes, the spatial patterns of one or two defining explanatory variables show up clearly in their probability maps. For settlement areas, patterns of population density and drained area share are visible in the probability map: higher probability of settlement in areas of higher population density and lower percentages of drained area (Figure 3-2 and Figure 3-3). Soil depth is part of the best model for grassland or pasture, and its outline is prevalent along the Kielstau river and to the east of Winderatt lake in the probability map for grassland. As a component of the best models for fallow and forest, the slope pattern is particularly visible in the southwestern part of the probability maps. For winter rye and winter barley, silt content is a determinative variable and results in clearly silt-analogous pattern in the probability maps. The probability map for orchard/garden exhibits a pattern similar to the variable distance to villages with higher likelihood nearer to villages. Other cereals are clustered near biogas plants, which is generally consistent with the surveyed distribution of other cereals in 2013 (Figure 3-1). The probability for field beans depends to a great degree on drained soil share. Field borders are explicitly visible in probability maps for all croplands, underlining the great importance of incorporating patch parameters into the cropland models.

R-G-B composite maps have been produced by overlaying probability maps to visualize competition between land use classes. From the composite map of settlement (Red, R), grassland/pasture (Green, G), and forest (Blue, B) as shown in Figure 3-4a, a majority of areas are found in these colors without mixing, i.e. settlement areas, grassland/pasture, and forest are well separated and do not compete for similar lands. In proximity to water areas, especially near the Kielstau River, green colors dominate indicating the high suitability for grassland or pasture. If the blue channel forest is replaced with winter wheat in Figure 3-4b, blue colors indicate the suitability for winter wheat. They are mostly found in areas with low probabilities for settlement, grassland/pasture and forest that are depicted in black in Figure 3-4a. The non-mixing colors red, green, and blue in Figure 3-4b can imply that no competition exists between dominant agricultural (e.g. winter wheat) and non-agricultural land use classes. In the R-G-B composites of the main croplands in Figure 3-4c and Figure 3-4d, the probability maps of corn (R) or winter barley (R), winter rape (G), and winter wheat (B) are compared. An obvious feature is that mixed and light colors are prevailing in the two maps, suggesting that similar areas are simultaneously suitable for two or three crop types. Moreover, mixed colors present in the same patches in both composite maps represent the suitability of similar fields for these four main crops. Due to relatively high simulated probabilities for corn (depicted in red), more purple and magenta colors (mix of red and blue) are dominant in Figure 3-4c than in Figure 4d indicating higher probabilities for corn as compared to the competition of winter barley with winter wheat and winter rape. The cyan-blue colors dominating Figure 3-4d represent areas that are suitable for winter rape and winter wheat. The suitability of fields for different crop types is in agreement with crop rotations in the Kielstau catchment. The most common rotation is a mix of cereals and rapeseed, followed by a combination of corn and cereals, and of corn, cereals, and rapeseed (Kandziora et al., 2014).

Table 3-3. Best logistic regression models for appearance of each land use class: odds ratios and performances for calibration, spatial validation and temporal validation.

	Settlement Area	Fallow	Grassland /Pasture	Corn	Other crops	Forest	Winter rye	Winter rape	Orchard /Garden	Winter wheat	Other cereals	Field bean	Winter barley
Slope		1.35698				1.34681			1.50291				
Elevation		0.82567										0.84845	
Clay content													0.96506
Silt content							0.97395			1.08879			1.10590
Sand content				1.02167									
Rock content								0.96062	0.87759	1.03514			
Soil depth			1.00214										
Saturated hydraulic conductivity											0.97200		
Drained soil share	0.96589		1.01220		0.96738	0.97378	0.98724		0.97593			1.01979	
Distance to rivers							1.00193						1.00071
Distance to roads			1.00172					0.99680					
Distance to villages									0.97280	0.99925			
Distance to nature conservancy	1.00032		0.99972		1.00143		0.99883	1.00042	1.00038		0.99880	1.00034	
Distance to biogas plants					0.99963						0.99956	1.00041	
Population density	1.00445	0.99114		0.99719	0.99706	0.99203							
Patch size	0.99998			0.99999		0.99998							
Perimeter			0.99905	1.00040				1.00069		1.00040	0.99927		0.99940
Shape index		0.11730											
Perimeter-area ratio		1.2×10^{9}			5.5×10^{-18}								
Fractal dimension	8.8×10^{8}			9.8×10^{-8}		2.1×10^{2}	5.1×10^{-6}	9.6×10^{-14}		6.2×10^{-9}	1.1×10^{-8}	2.9×10^{-6}	7.8×10^{-9}
ROC_cal	0.97	0.87	0.78	0.68	0.86	0.85	0.76	0.78	0.92	0.72	0.80	0.78	0.74
ROC_val_2017	0.97	0.85	0.78	0.68	0.88	0.84	0.76	0.77	0.89	0.73	0.82	0.77	0.74
ROC_val_2013	0.97	0.88	0.76	0.65	0.78	0.84	0.71	0.71	0.89	0.75	0.84	0.76	0.71

Table 3-4. Percentages of inclusion of each explanatory variable into the best 50 logistic regression models for each land use class. The best combination is depicted in bold.

	Settlement area	Fallow	Grassland /Pasture	Corn	Other crops	Forest	Winter rye	Winter rape	Orchard /Garden	Winter wheat	Other cereals	Field bean	Winter barley	Mean value
Aspect	4%	2%	2%		20%	10%		6%	22%	12%		16%	6%	8%
Slope	22%	**72%**	20%	16%		**38%**	24%		**80%**	10%	8%		2%	22%
Elevation	30%	**100%**			8%			4%	26%	12%	6%	**100%**		22%
Clay content	22%	32%			16%								**50%**	9%
Silt content		6%	12%			8%	**34%**	8%		**98%**			**58%**	17%
Sand content			6%	**58%**		28%		8%			10%	16%		10%
Rock content	18%		12%	10%		8%	16%	**16%**	**68%**	**34%**	10%	8%	38%	18%
Available water capacity				12%			14%							2%
Soil depth			**94%**		18%									9%
Saturated hydraulic conductivity					16%						**34%**	26%		6%
Moist soil albedo				10%	14%	32%		18%	28%	8%	26%			10%
Usle_k factor	22%		4%	4%	4%	10%		14%		14%			48%	9%
Drained area share	**100%**	22%	**94%**	8%	**100%**	**100%**	**36%**	20%	**50%**	4%	32%	**90%**	6%	51%
Distance to rivers		20%	20%	8%		12%	**96%**					12%	**36%**	16%
Distance to roads		16%	**36%**	4%	16%	2%	18%	**38%**	26%	14%	22%	10%	10%	16%
Distance to villages		28%	4%	12%	22%	8%	8%	8%	**100%**	**54%**	12%	30%	16%	23%
Distance to nature conservancy	**30%**		**34%**	64%	**100%**	8%	**100%**	**100%**	**34%**	12%	**98%**	**24%**	18%	48%
Distance to biogas plants	20%	40%	6%	6%	**20%**	6%	22%	10%	36%	4%	**60%**	**26%**	6%	20%
Population density	**66%**	**50%**	6%	**58%**	**22%**	**100%**	12%	44%	4%	4%	10%	28%	8%	32%
Patch size	**48%**		42%	**82%**	8%	**48%**	12%	46%		66%		6%	36%	30%
Perimeter			**68%**	**42%**			8%	**60%**		**70%**	**58%**		**54%**	28%
Shape index		**54%**												4%
Perimeter-area ratio		**54%**			**100%**				6%					12%
Fractal dimension	**100%**		34%	**100%**		**72%**	**88%**	**100%**		**64%**	**100%**	**96%**	**100%**	66%
Min ROC_cal	0.97	0.85	0.77	0.66	0.85	0.83	0.73	0.78	0.90	0.72	0.77	0.76	0.72	
Max ROC_cal	0.97	0.87	0.78	0.68	0.86	0.85	0.76	0.78	0.92	0.72	0.80	0.78	0.74	

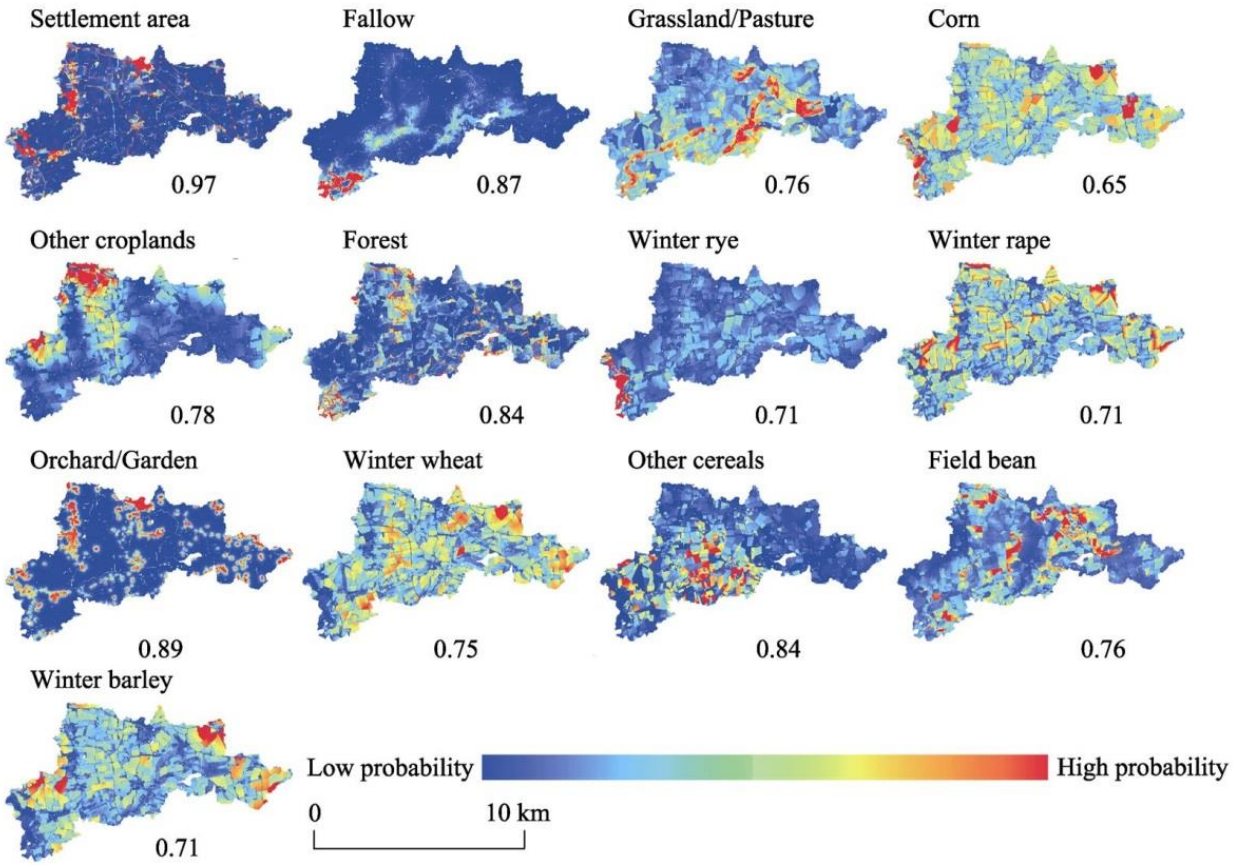

Figure 3-3. Probability maps for predicting each land use class pattern in 2013 using the best logistic regression models. The corresponding relative operating characteristic (ROC) statistic is provided.

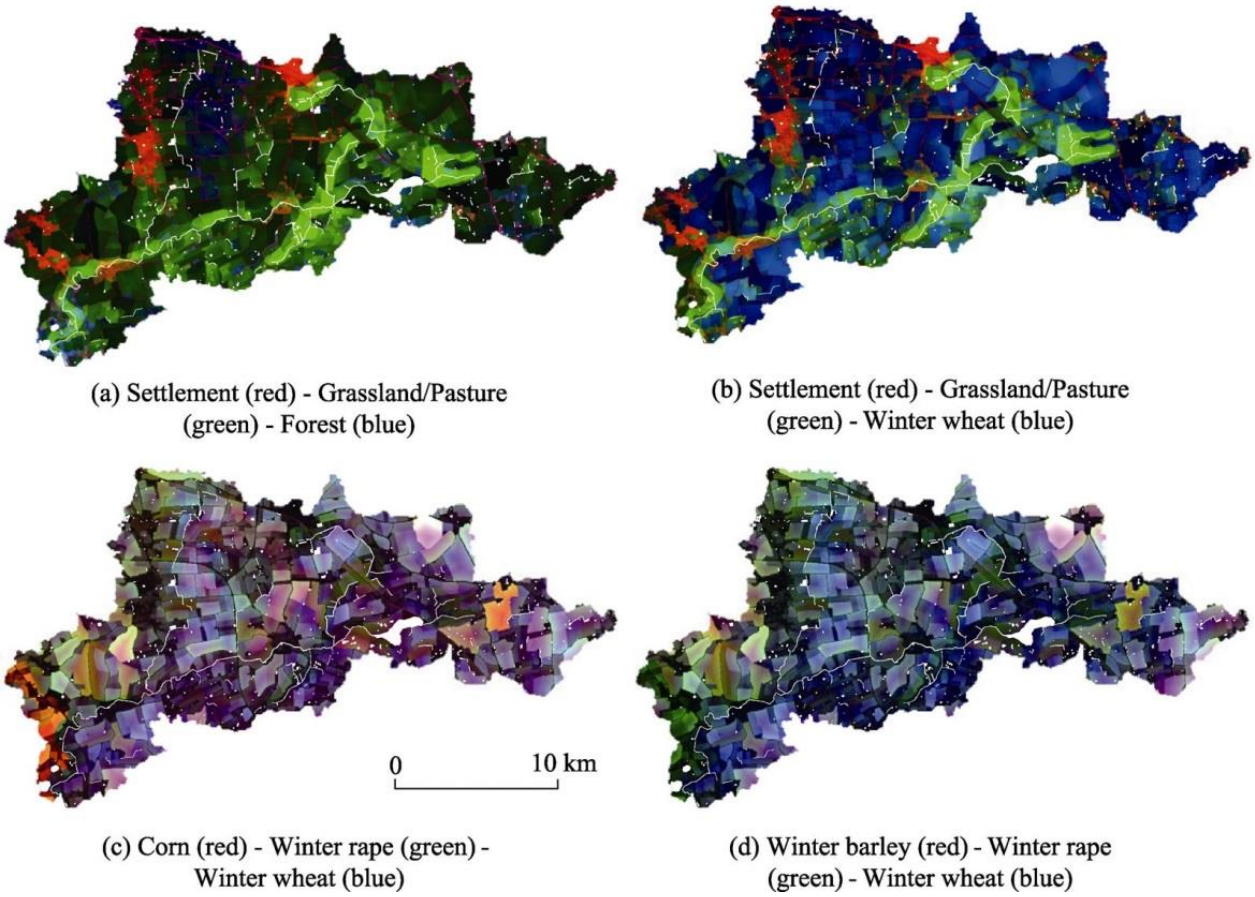

Figure 3-4. R-G-B composites indicating spatial competition among land use classes. Water areas are masked in white

3.4. Discussion

3.4.1. Most important explanatory variables

Our findings indicate which variables are important for the spatial distribution of land use classes in a small agricultural catchment in Germany. Most of these results are in agreement with our general understanding of the catchment. For instance, grassland or pasture have the highest probability near protected areas, the Kielstau river, and Lake Winderatt, which agrees with the principle that grassland or pasture instead of cropland is in direct vicinity to rivers to sustain water resource quality (Gerrish et al., 1995; Qureshi et al., 2013). Obviously, population density is a defining variable for settlement areas (Yue et al., 2013). Simpler patch shapes result in higher probability for croplands while more complex shapes are found in non-cropland areas. This is a reasonable result as crops are usually grown on larger and simpler fields as compared to other land use classes. The visual evaluation of the probability maps further confirms the plausibility

of using the logistic regression models to simulate land use competition. The R-G-B composites of probability maps (Figure 3-4) indicate no strong competition between settlement areas, grassland/pasture, and croplands, which is reasonable in a rural environment that is not exposed to strong population pressure. However, the different crops (winter wheat, winter rape, corn, and winter barley) compete for the same locations, as indicated by the mixing and light colors in the both R-G-B composites of the probability maps Figures 4c and 4d. This is in agreement with the fact that these crops can be grown on the same fields. Crop variations are related to farmer decisions as well as to crop rotation practices of around three years that occur in the study area (Kandziora et al., 2014).

Our analysis shows that the most important variables to explain land use patterns in the Kielstau catchment are distance to protected areas, fractal dimension, drained soil share, and population density. These variables underline the agricultural character of the rural catchment, as fractal dimension, drainage density, and (low) population density are linked to agriculture. Moreover, the course of the Kielstau River affects the land use pattern as the variables distance to protected areas (Figure 3-2) and distance to rivers are linked to the Kielstau River, and the soil map includes properties of the flood plain (Figure 3-2). However, this may in part be explained by the fact that our analysis is carried out at the catchment scale. The logistic regression models are based on a dataset with a spatial resolution of 10 m. On a coarser spatial scale the spatial structure of the explanatory variables will be different and also the land use pattern will change, when smaller fields are merged. Consequently, other variables may be more important on the large scale. Nevertheless, we are confident that the 10 m resolution is appropriate for our comparatively small study area.

3.4.2. Model performance

The quantitative model performance as well as the visual evaluation of the probability maps (Figure 3-3) indicates that the derived logistic regression models can reasonably explain land use patterns in the Kielstau catchment. The patterns are overall consistent with the land use maps for 2013 and 2017 (Figure 3-1) and the ROC values for both spatial validation and temporal validation are mostly greater than 0.7 indicating

a reasonable performance. The lowest ROC value for corn (0.65) may be attributed to the fact that corn cultivation is possibly more affected than other crops by non-spatial variables like market prices and policies as it may be used for biogas production. The assumption that corn fields can be found near biogas plants was not verified. This might also be explained by the small size of the study area and the small number of biogas plants.

The range of ROC values for the different land use classes can be explained by characteristics of rural land cover, e.g., settlement areas (0.97), orchard/garden (0.89), and forest (0.84) are well distinguished and thus have strong explanatory variables (e.g. population density, distance to villages, drained soil share, respectively), however, the explanatory variables are not similarly defining for one crop or the other and, therefore, yield lower accuracies with ROCs for most agricultural land between 0.7 and 0.8 (in Table 3-3). In many other studies, agriculture is, therefore, only one lump class (Mottet et al., 2006; Yang et al., 2012), whereas this study differentiates eleven agricultural land use classes including eight cropland classes. A possible improvement could be achieved if the land tenure system was included as a spatial variable. This variable could be used to better represent farmers' decisions as well as the influence of the market and policies.

A comparison of the model performances in 2013 and 2017 shows that the agricultural classes vary in time and that the performances differ, while they are more or less constant for non-agricultural classes. Usually, a slightly worse performance can be expected for temporal validation (Shu et al., 2014). This applies to winter rye, winter rape, and winter barley. But it has to be noted that some slight improvements for e.g. winter wheat and other cereals can be observed, indicating that the regression models fit the 2013 data moderately better. Since models are limited out at five explanatory variables it should not be neglected that if all significant variables are included better results can be achieved.

3.4.3. Value of landscape metrics for explaining land use patterns

Landscape metrics have been proven valuable in the context of our agricultural catchment. Hence, land patch structure and shape indicators are suitable to characterize and differentiate land use patterns, which is in agreement with the use of landscape

metrics in the context of urban land use change or land cover classification studies (Seto and Fragkias, 2005; Fichera et al., 2012). Our results indicate that the landscape metrics provide important complementary information to the more commonly used biophysical and socioeconomic variables. Due to their explanatory power, they may also be useful in other study areas. The derived regression models are suitable to predict land use patterns and the derived probability maps can be used to visualize competition among land use classes in space, by incorporating the R-G-B composites as a simple model of land use competition. To simulate future land use patterns, the regression models can be incorporated into an intergrated application of CLUE-S (Liu et al., 2017) and Markov chain or cellular automata models (Arsanjani et al., 2013). These models also account for non-spatial variables like policy and market changes to alter the shares of different crops and derive a corresponding land use pattern.

3.5. Conclusion

A set of spatially distributed variables from topography, soil properties, distance variables and population density, and landscape metrics are derived to accurately explain land use patterns in the Kielstau catchment. From these categories, 20 variables contribute to the logistic regression models to explain the land use pattern. In particular, the explanatory variables distance to protected areas, drained soil share, patch fractal dimension, and population density are most important to characterize the land use distribution in space. These variables are either linked to agriculture or the river course of the Kielstau, which are identified as the two main influences for land use distribution in the catchment.

The derived models are suitable to explain and predict land use patterns. Both probability maps and ROC values between 0.71 and 0.97 for spatial and temporal validation underline this for all land use classes except that corn is harder to predict (ROC = 0.68, 0.65 for validation in space and in time, respectively). Non-agricultural classes are explained with higher precision, whereas the models for cropland classes yield lower performances. This result is mainly attributed to the fact that agricultural fields are usually suitable for more than one crop. Moreover, non-agricultural and agricultural classes are well distinguished in space, whereas dominant cropland classes

compete mainly for the same land, so that modeling their distribution in space is particularly challenging. Competition between different classes can be explicitly and reasonably identified with probability maps and R-G-B composite maps of the main land use classes. The robustness of the models in space and in time indicates their potential for an inclusion in a combined modeling approach to produce land use patterns for future scenarios.

Chapter 4 Effects of land cover, topography, and soil on stream water quality at multiple spatial and seasonal scales in a German lowland catchment

Chaogui Lei *, Paul D. Wagner, Nicola Fohrer

Department of Hydrology and Water Resources Management, Institute for Natural Resource Conservation, Kiel University, Olshausenstr 75, 24118 Kiel, Germany

Correspondence author: Chaogui Lei (cglei@hydrology.uni-kiel.de)

Ecological Indicators 120(2021) 106940, https://doi.org/10.1016/j.ecolind.2020.106940
Received 15 June 2020 – Received in revised form 31 August 2020 – Accepted 7 September 2020 – Available online 25 September 2020

Abstract

The influence of catchment characteristics on water quality varies with space and time. Understanding the key factors influencing water quality is needed for effective land use and riparian management to protect river health. To this end, we quantified effects on stream water quality in summer and winter between 1992 and 2019 at multiple spatial scales in the upper Stör catchment, Germany. We applied multivariate statistical analyses on three scales: the catchment, riparian, and reach scale. Our results indicated that poorer water quality mostly occurred in winter and in steeper arable and pasture areas and in wetlands. Water quality was strongly affected by soil properties, land use composition (the areal shares of arable or pasture land respectively with slopes >2%, forest, and urban) and configuration. The spatial variation of the overall water quality was better explained at the larger scales (riparian and catchment) and in summer (73–78%). The most important variables differed among scales and for the different water quality variables. Forest and complex landscape patterns showed more negative correlations with degraded water quality at the reach scale when compared to larger scales. At larger scales, besides permeable and organic soils, steeper arable lands were most significant for nitrate-nitrogen (NO_3-N) and steeper pasture areas for phosphate-phosphorus (PO_4-P) pollution. The results of this study provide valuable insights for guiding sustainable and spatially specific land-water management of river catchments at different scales to improve stream water quality.

Keywords: Catchment characteristics; Stream water quality; Multivariate statistical analyses; Multiple scales

4.1. Introduction

Good water quality is indispensable for maintaining the stability of ecology and habitats, sustainable agriculture production as well as human health (Lu et al., 2015; Nguyen et al., 2015; Riseng et al., 2011). However, preserving water quality has been a major long-term challenge, due to extensive point source pollution (PS) due to anthropogenic factors and non-point source pollution (NPS) which is additionally influenced by climatic and environmental factors. Land use effects on water quality have often been investigated, e,g., in China by Shen et al. (2013) and in the US by Broussard and Turner (2009). However, the linkages between multiple catchment characteristics (including climate, soil, topography, land use, and anthropologic activities) and water quality have rarely been investigated at multiple spatial and temporal scales (Giri and Qiu, 2016; Lintern et al., 2018; Zhang et al., 2020). As water quality is essentially affected by different catchment characteristics, it is necessary to identify key impacts among the different attributes to facilitate sustainable watershed management.

Land use and hydrology are interdependent (Wagner et al., 2019; Wagner and Fohrer, 2019). The relationship between land use and water quality has been a research concern since the 1970s (Rimer et al., 1978). Early studies generally linked water quality to the simple descriptors of land use composition (e.g., areal percent of land use) within a watershed (Crosbie and Chow-Fraser, 1999; Donohue et al., 2006). Agriculture has previously been identified as one of the key nitrogen (N) and phosphorus (P) sources that contribute to water pollution. Urban land has negative impacts on water quality through impervious surfaces (i.e., streets, roof tops, and parking lots) that accelerate runoff processes and create additional routes of delivering NPS pollutants to rivers (Lee and Bang, 2000). Natural vegetation like forest can filter pollutant particles and reduce water pollution (Moreno-Mateos et al., 2008).

However, land use composition is only a lumped indicator of water quality; it does not contain any information of the structure of or spatial relationships in a landscape. It is evident that certain land use patterns, e.g., intensive riparian urbanization or pasture land uses, may magnify deliveries of N or P into streams (Moreno-Mateos et al., 2008; Tanaka et al., 2016). With the advancement of spatial analysis techniques (e.g., GIS),

landscape shape, configuration and interconnection can be assessed efficiently, e.g. by using land use classifications derived from remote sensing data. Landscape metrics have been recently included in the studies of landscape ecology and watershed hydrology (Amiri et al., 2018; Grafius et al., 2018). Aggregation (represented by e.g., contagion or cohesion indexes), diversity (e.g., Shannon's diversity index), and shape (e.g., area weighted shape index) variables of landscape patterns can be used to explicitly quantify main structures of the landscape at different spatial scales. Moreover, these variables have been proven to be correlated with water quality (Ding et al., 2016; Shi et al., 2017). Besides, new satellite data and GIS techniques enable the acquisition of land use data with a fine spatial resolution, e.g., land use proximity to rivers based on pixels (Walsh and Webb, 2014). Some studies have demonstrated that stream water quality was closely related to the proximity of land use to stream networks or monitoring sites. In addition, these spatially explicit land use metrics have been proven useful to explain stream physicochemical and ecological health (Ding et al., 2016; Peterson et al., 2011; Walsh and Kunapo, 2009).

So far, the influence of soil on water quality on the catchment scale has gained less attention when compared to the influence of land use on water quality. Nevertheless, there is a strong link between soil properties and water quality, e.g. significant negative correlations were found between sand content and electrical conductivity, and positive correlations have been observed between organic matter and phosphorus (Chardon and Schoumans, 2007; Redeker, 2011). Streams (ditches) characterized by peat soils have a higher concentration of P than those in mineral soils and rivers are susceptible to eutrophication in drained peat lands in German lowlands (Tiemeyer et al., 2009). The high organic matter content in the upper soil layer could trigger nitrification and denitrification processes under aerobic and anaerobic conditions, respectively (Pal et al., 2010). Soil water permeability affects soil quality and moisture, which consequently changes nutrients or organics inputs to groundwater and stream systems (Rodriguez-Galiano et al., 2014). Given that soil plays a complex role in pollutant transformation, emission or transport, it is highly valuable to understand how soil properties affect stream water quality.

The upper Stör catchment, with the main river Stör as the largest tributary of the

Elbe River in the federal state of Schlewig-Holstein, Germany, has been an important water supply area for living, fishery and farming. A variety of agriculture practices, e.g., livestock grazing, tillage, tile drainage, fertilization and pesticide application, are typically applied in this area. These activities might result in manure, fertilizer and insecticide residuals as well as fragile soil (Monaghan et al., 2007), which are important carriers of physicochemical and biochemical constituents of water quality, and which are transferred via surface runoff or subsurface drainage pathways into water bodies and ultimately deteriorate water quality (Monaghan et al., 2007; Tanaka et al., 2016; Tiemeyer et al., 2009). To improve agriculture productivity in the last century, amelioration measures, such as installation of tile drainages, straightening or canalizing of numerous tributaries, have been implemented, which resulted in water quality degradation by accelerating nutrients transport into streams (Koch et al., 2013; Schmalz et al., 2008; Schmalz and Fohrer, 2010). Additionally, this lowland catchment is characterized by dynamic interaction between near-surface groundwater and surface water, resulting in abundant groundwater recharge to the rivers. This interaction affects the release, transport and leaching of pollutants, and intensifies the risk of nutrient pollution both in surface water and groundwater (Schmalz et al., 2008; Venohr et al., 2005). In Germany groundwater is found to be a main pathway of total nitrogen (N) and phosphorus (P) (by about 50% and 20%, respectively) from diffuse sources (UBA, 2018). This catchment has been exposed to N and P pollution, particularly in winter, in the past three decades with varying pollution levels in space (Pott and Fohrer, 2017). Therefore, assessing the effects of land cover, topography, and soil on the seasonal dynamics of water quality is necessary to provide useful information for protecting water resources.

We hypothesize that catchment characteristics defined by topography, soil, and land use, and in particular landscape metrics are valuable to explain stream water quality at different spatial scales. Moreover, we attempt to identify important influencing factors for water quality using multiple regression which enables to assess the predictive power of factors, and to quantify the contribution of these factors to the overall variations of water quality with redundancy analysis (RDA) (Ding et al., 2016; Shi et al., 2017). The objectives of this study are to: (1) assess the spatial and seasonal

patterns of stream water quality; (2) identify the most important catchment characteristics that affect stream water quality in different seasons; (3) determine on which spatial scale catchment characteristics have the strongest impact on overall water quality variation.

4.2. Materials and methods

4.2.1. Study area

The Stör River, a main tributary of the Elbe River, flows through the lowlands of central Schlewig-Holstein in northern Germany (Figure 4-1). This study focuses on the upper Stör catchment as it is free of tidal influence. The upper Stör catchment has a total drainage area of 462 km^2. It is located in the high-latitude marine climatic zone and experiences mild summers (May-October) and wet winters (November-April) with a mean annual precipitation of 850 mm and an average temperature of 9.4°C from 1990 to 2019, according to weather stations Neumünster and Padenstedt (DWD, 2020) (Figure 4-2). The stream discharge gauged at the catchment outlet in Willenscharen shows seasonal variations with maximum values in winter and minimum values in summer (Figure 4-2). The high-flow months (December-March) account for 50% of the total annual stream flow. The topography is relatively flat, descending from 85 m and 55 m a.s.l. in the western and northeastern parts, respectively, to 20–30 m and to <10 m in the central and southern parts (Song et al., 2015). Sandy soils (Cambisol, Gley-Podsol, Podsol) are dominant in the catchment, along with Gley soils in the eastern part and peat soils along river depressions and near two natural wetlands (Pott, 2014). The land use in 2019 is dominated by arable land (36.1%) and pasture (31.3%), followed by forest (18.7%) and urban (12.8%). The main crops grown in the study area are corn, cereals (winter wheat, barley and rye), and rapeseed.

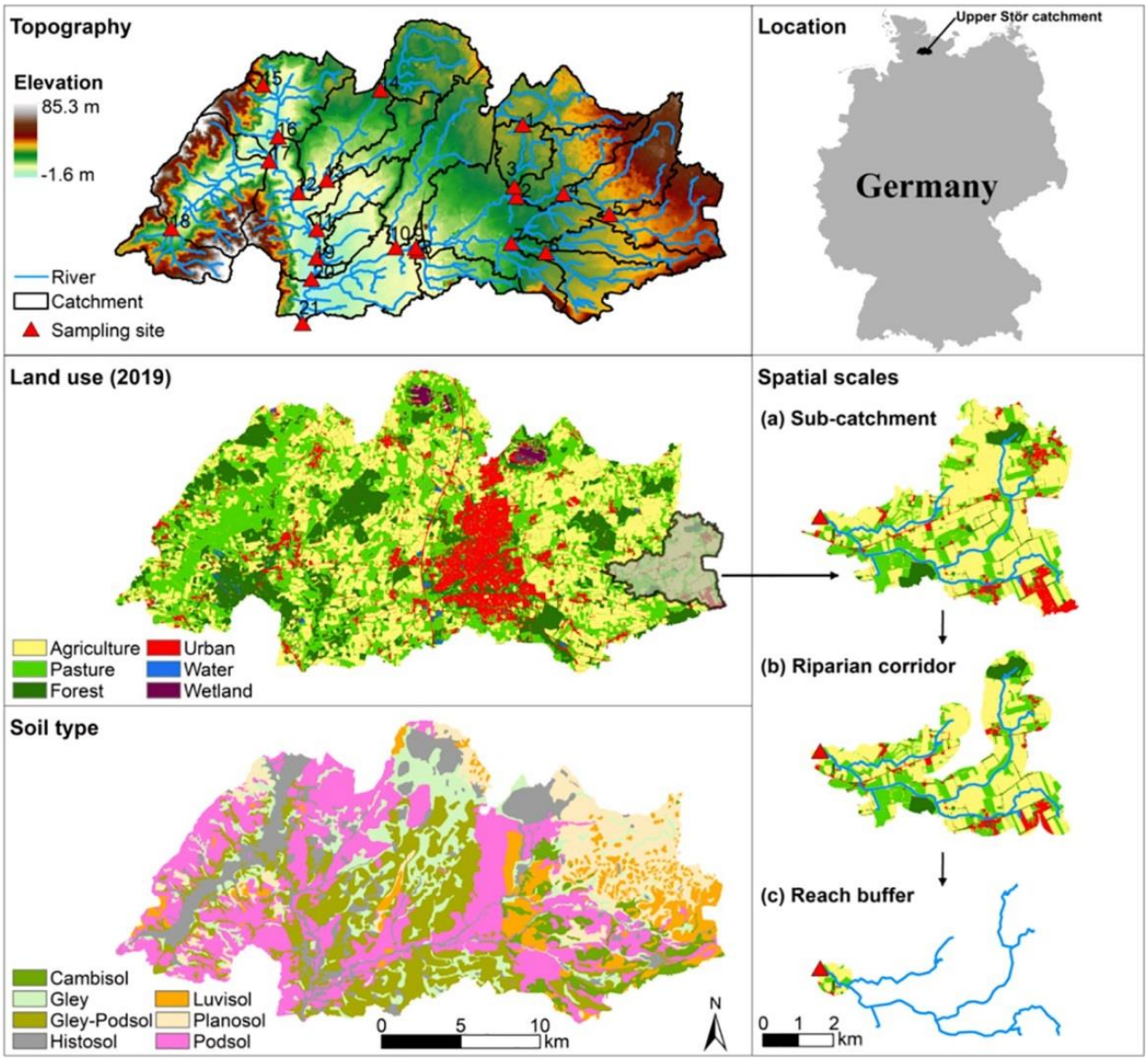

Figure 4-1. Topography, soil, and land use patterns in the upper Stör catchment, as well as the three spatial scales that are used for analysis: catchment, riparian, and reach.

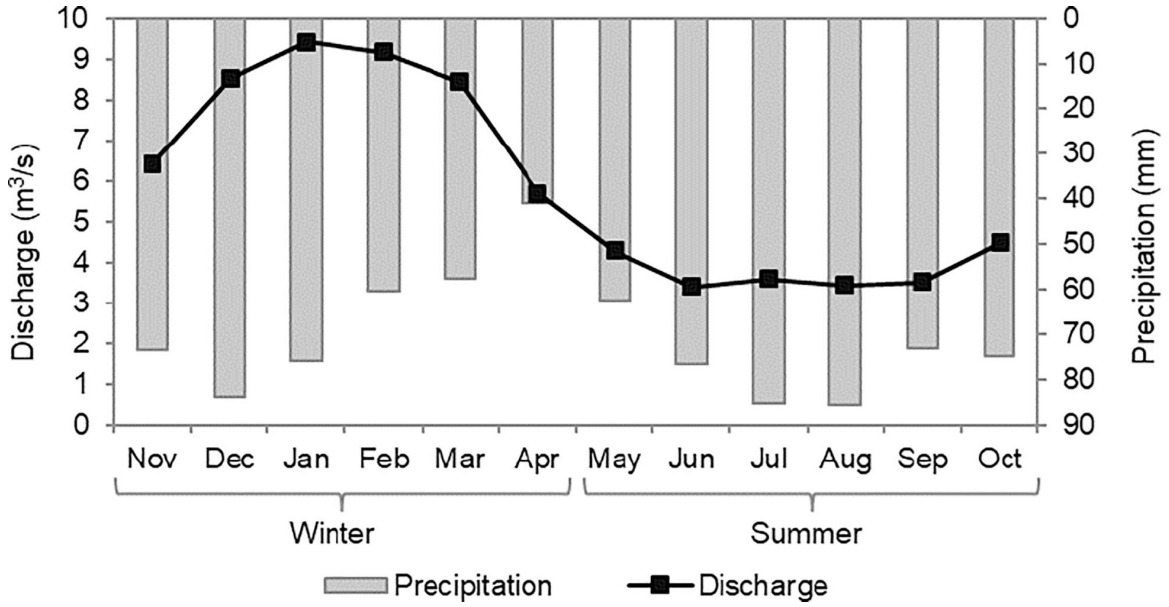

Figure 4-2. The monthly average precipitation (weather stations Neumünster and Padenstedt) and stream discharge (Willenscharen) in the upper Sto¨r catchment from 1990 to 2019 (DWD, 2020; LKN, 2020).

4.2.2. Water quality monitoring

The analysis is based on an exceptionally long spatially distributed data set spanning a time period of almost three decades. Water quality measurement campaigns have been conducted in the upper Stör catchment in three periods: 1992–1994, 2009–2011, and 2018–2019. Twenty-one sampling sites that gauge subbasins of the catchment were investigated, considering different land use as well as accessibility (Figure 4-1, Pott and Fohrer (2017)). Water samples were collected on a monthly basis from the central section of the stream. These water samples were analyzed for twelve water quality variables. Water samples from 1992 to1994 were collected and analyzed by Ripl et al. (1996). The samples of the other two campaigns were analyzed in the laboratory of the Department of Hydrology and Water Resources Management at Kiel University using the German standard procedure for water analysis (DEV) (Deutsche Einheitsverfahren, 1997). The respective concentration of chloride (Cl^-), sulphate (SO_4^{2-}), nitrate-nitrogen (NO_3-N) was determined ion chromatographically according to DEV D19. The concentration of ammonium-nitrogen (NH_4-N) was determined photometrically according to DEV E5, phosphate-phosphorus (PO_4-P) according to DEV D11, and total phosphorus (TP) according to DEV H36 and DEV D11. Total nitrogen (TN) was detected by chemiluminescence according to DEV H3, while organic

nitrogen (Org-N) was computed as the difference between TN and dissolved inorganic N (e.g., NO_3-N and NH_4-N,). All of the variables but TN and TP were all analyzed from the filtered water samples through the 0.45 µm celluloseacetate filter paper. Blank comparison analysis was performed for each measurement. Triplicate subsamples were set for paralleled analysis and concentration was determined by the arithmetic mean from the values of two subsamples with lowest difference (less than 10% for TP and TN; less than 5% for other variables). In addition, water temperature (WT), dissolved oxygen (DO), pH, and electrical conductivity (EC) were measured in the field using multi-parameter monitoring instrument (WTW Multiline, Germany). To depict seasonal variation, monthly water quality data were aggregated into summer (May-October) and winter (November-April) half year periods that correspond to low and high flow periods, respectively (Section 4.2.1).

4.2.3. Multi-scale environmental factors

Catchment characteristics from the three categories of topography, soil, and land use were used and shown in Table 4-1. Topographic variables include elevation, slope, and standard deviation of slope as measures of topography characteristics in this flat lowland study area. They were derived from a 5 m digital elevation model (LvermA, 2008).

Soil variables are based on the soil type map (Finnern, 1997) and were adapted from Pott and Fohrer (2017). Sand content was used as an indicator as the study area is dominated by sandy soils. The spatial heterogeneity of organic soil was also considered. Because the soil in this catchment is characterized by hydrologic soil groups A and B classified based on infiltration characteristics (Neilsen and Hjelmfelt, 1998), which are mainly permeable soils, we chose the areal ratio of soil group A to B as a measure of soil permeability and hydraulic conductivity (Brandes et al., 2005; Woltemade, 2010).

The land use information is available for all three measurement campaigns. The two earlier land use maps are based on Landsat 5 data (30 m resolution) from 1987 and 2010, which were adapted from Ripl et al. (1996) and Rathjens et al. (2014), respectively. For 2019, Sentinel- 2 satellite images with a 10 m resolution and randomly sampled ground truth data were used to prepare a supervised land use classification. The

following six land use classes (Figure 4-1) have been distinguished in all years: (1) pasture; (2) arable land; (3) forest; (4) urban; (5) wetland; and (6) water. Water and wetland covered a minor and mostly constant fraction and were therefore not considered in the statistical analyses of this research. The areal percentage of the different land use types was selected to indicate the land use composition. Shape, dominance, and diversity indices of the landscape pattern were chosen to characterize land use configuration (Liu et al., 2012; Shen et al., 2015). The hydrological flow length to monitoring sites and distance to rivers were calculated to assess the longitudinal and lateral distance of each land use class, respectively (Ding et al., 2016).

All the metrics were extracted at three spatial scales (Figure 4-1):

(1) catchment scale, comprising the sub-catchment upstream of the monitoring site and below the next upstream monitoring site;

(2) riparian scale, 500 m wide corridors on both sides of the stream extending from the monitoring site to the entire upstream sub-catchment (below the next upstream monitoring site);

(3) reach scale, the 500 m buffer section created with the geographical center being 500 m upstream the monitoring site.

The selected landscape metrics were obtained using FRAGSTATS 3.4 and catchment characteristics for the different scales were calculated in ArcGIS.

4.2.4. Statistical analysis

The normality of the distribution of the water quality variables was assessed with Kolmogorov–Smirnov tests. A log(x + 1) transformation of NH_4-N, TP and PO_4-P in winter and summer, and TN and NO_3-N in summer was applied to meet the assumption of normal distribution (indicated by $P > 0.05$).

To understand the relationship between catchment characteristics and water quality, we examined the influence of topography, soil, and land use (e.g., composition, configuration, and proximity to streams) on seasonal stream water quality at the reach, riparian and catchment scales, with the application of stepwise multiple linear regression (SMLR) and redundancy analyses (RDA). The relationship between predictors (i.e., catchment characteristics) and response (i.e., each water quality variable)

was analyzed by SMLR, during which only the significant ($p < 0.05$) predictors were kept (Dow et al., 2006). The predictive potential of the SMLR model was assessed by the adjusted determination coefficient (adjusted R^2). The relative importance of each single predictor on the response was measured by the standard partial regression coefficient (S.B). Higher values indicate that the predictor has more significant correlation with the response. To ensure predictors are non-collinear, the predictors with the variance inflation factor (VIF) > 2 were excluded from the SMLR models (Daoud, 2017). For each water quality variable, SMLR analyses were performed at the three different spatial scales and in different seasons and the candidate model with the highest adjusted R^2 was selected as final SMLR model for each scale. By scale comparison, the final SMLR model was considered as the best model for each water variable according to the highest adjusted R^2.

RDA was run at each scale to quantify the relationships between explanatory variables (i.e., predictors from the final SMLR models) and the variations in the overall water quality. The proportion of water quality variation explained by each single variable can be determined with the RDA analysis. The relationship between catchment characteristics and water quality variables could be explicitly reflected with ordination diagrams. A positive correlation is indicated if arrows of two variables point to the same direction, and vice versa. The angle between two arrows is inversely proportional to the degree of the correlations (Ding et al., 2016; Shi et al., 2017). The Monte Carlo permutation test (499 permutations under the reduced model) for each RDA run was performed to test if the RDA results were valid.

Table 4-1. The description of the metrics applied in this study.

Categories	Attributes	Name (abbreviation)	Unit	Description	Code at class level
Topography	Elevation & Slope	Mean elevation (ELEV)	m	The mean elevation for all 5 m grid cell	-
		Mean slope (SLOPE)	%	The mean slope for all 5 m grid cell	-
		Slope standard deviation (SLP_SD)	%	The standard deviation of slope for all 5m grid cell	-
Soil		Ratio of hydrologic soil group A to B (A/B)	-	The areal ratio of hydrologic soil group A to group B	-
	Main features	Sand content (SAND)	%	The percentage of sand content in the first soil layer	-
		Organic soil (ORGSOL)	%	The areal percentage of organic soil type	-
Land use	Composition	Land use percent (PLAND)	%	Areal Percentage of non-arable land use classes Areal Percentage of arable and pasture lands in slope >2%	FPLAND,WPLAND,UPLAND PPLANDS, APLANDS
	Configuration	Area-weighted mean shape index (AWMSI)	-	The sum of the mean shape index multiplied by the area weight of each patch type	
		Patch Cohesion Index (COHESION)	%	The physical connectedness of the corresponding patch type	
		Contagion Index (CONTAG)	%	The measure of the degree of aggregation tendency of different land use patch types	
		Shannon's Diversity Index (SHDI)	-	The number of different patch types and the proportional area distribution among patch types, indicating patch fragmentation and	
	Flow & distance	Flow length (FLOW)	m	Mean downstream distance along the flow path from all grid cells with certain land use class to the outlet of the catchment	PFLOW, AFLOW, FFLOW, UFLOW
		Distance to river (DISR)	m	Mean distance from all grid cells with one certain land use class to the river	PDISR, ADISR, FDISR, UDISR

4.3. Results

4.3.1. Spatial and seasonal variations in water quality

The spatial and seasonal distributions of stream water quality in the upper Stör catchment are shown in Figure 4-3 and Figure 4-4. The concentrations of DO, nitrogen (N) and phosphorus (P) variables were generally higher in winter than in summer, while pH, EC and Cl^- values were mostly higher in summer. Moreover, the seasonal concentration of water quality variables varied considerably in space. The lowest DO generally occurred in two subbasins in the North (subbasins 1 and 14, Figure 4-1) which are dominated by wetlands and have high redox potential, resulting in a consumption of oxygen. Higher EC and Cl^- occurred in the subbasins in which the city of Neumünster is located (subbasins 9 and 10). The most heavily-polluted streams in terms of TN and NO_3-N were in northwestern and southwestern parts (subbasins 16 and 18), in which rivers were mostly close to grazing and agricultural fields in steeper areas. The northern (subbasins 1 and 14) and northwestern areas (subbasin 16) had by far higher pollution of NH_4-N and TP than other areas, particularly in winter. These areas in addition to southwestern part (subbasin 18) also had the highest levels of PO_4-P and Org-N. In summary, water quality pollution was the highest in subbasins either characterized by wetlands or located in steeper areas deeply influenced by intensive farming or grazing activities. Relatively lower N and P values were generally found in the western lowlands of the central part which were mostly dominated by forest (subbasins 11, 13, and 19).

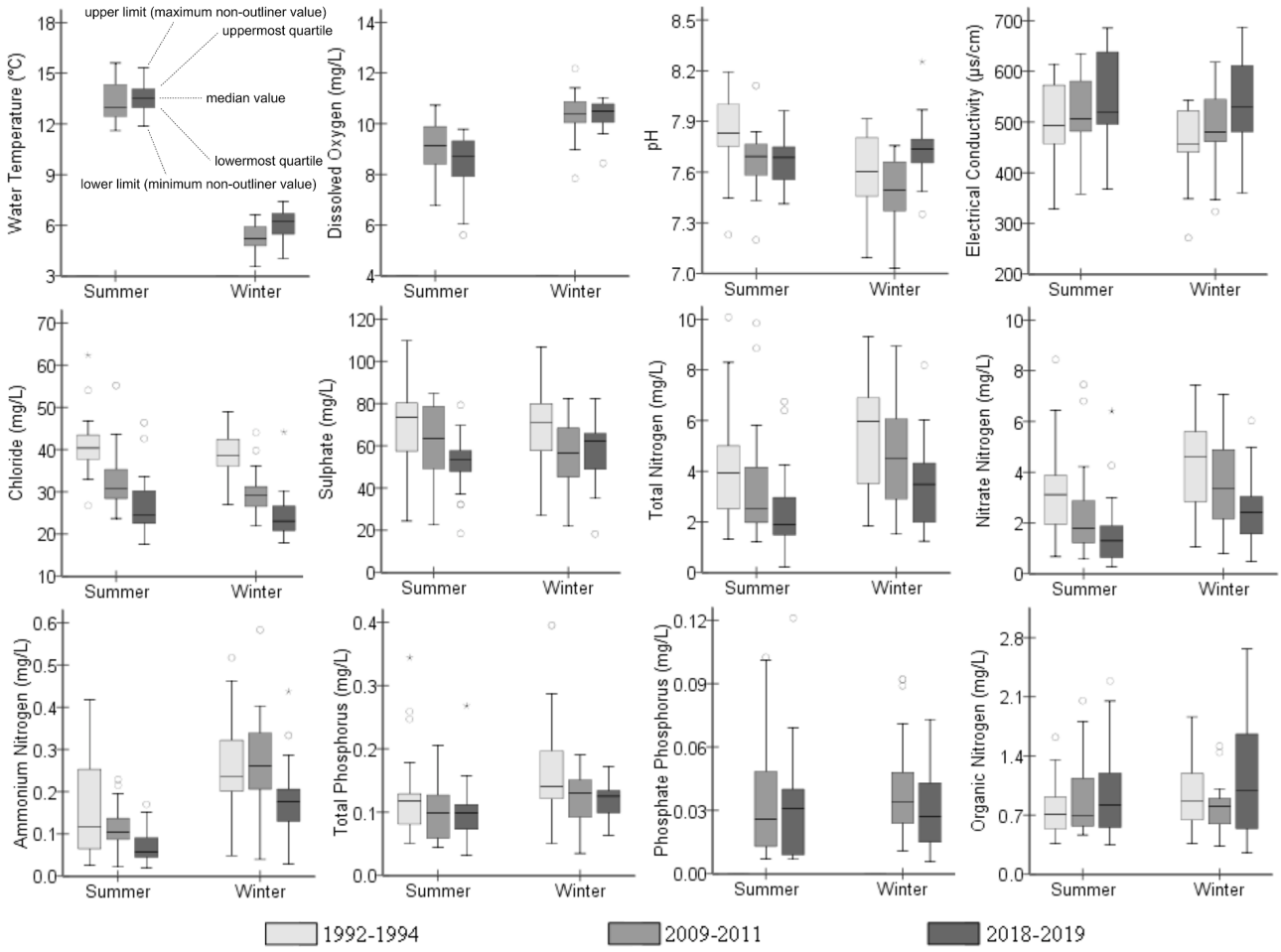

Figure 4-3. Comparison of the variability of water quality variables during summer and winter in the three respective periods of observation, 1992–1994, 2009–2011, and 2018–2019. The number of samples is 504 for 1992–1994, 504 for 2009–2011, and 252 for 2018–2019.

4.3.2. Differences of predictive capabilities and important predictors

The final SMLR models generally had a strong capability of predicting water quality variables (mostly, 0.5 < adjusted R^2 < 0.8, Table 4-2). They performed comparatively better at the (larger) riparian and catchment scales when compared to the reach scale (scales are shown in Figure 4-1). Only WT in summer and TP in winter were best predicted at the reach scale. In summer, the best models of pH, NH_4-N, TP, PO_4-P and Org-N were identified at the riparian scale, and those of DO, EC, Cl^-, SO_4^{2-}, TN and NO_3-N were identified at the catchment scale. In winter, WT, pH, TN, NH_4-N and PO_4-P had the best models at the riparian scale, whereas other variables of DO, EC, Cl^-, SO_4^{2-}, NO_3-N and Org-N obtained the best models at the catchment scale.

The most important predictors differed for the water quality variables and for the three spatial scales. At the reach scale, elevation (ELEV) was identified as the most

important predictor for WT, DO, and EC in summer. Moreover, areal weighted shape index (AWMSI) was most important for explaining chloride, whereas percentage of forest land (FPLAND) was determined as the most important factor for TN, NO_3-N, and TP. Looking at the riparian and catchment scale, the most important explanatory variable for water quality variables was often similar at both scales. The most significant impact for DO or pH was identified as the flow length of urban or arable land in winter, respectively. Cl^- was best predicted by the contagion index (CONTAG). TN and NO_3-N had the same most important predictors at the riparian and catchment scales, which are the areal ratio of hydrologic soil group A to B (A/B) and percentage of steeper arable land (APLANDS), respectively in summer and winter. EC and TP were most significantly affected by the predictor areal ratio of hydrologic soil groups (A/B), whereas NH_4-N was best predicted by the percentage of organic soil (ORGSOL) in winter. The most important predictors for SO_4^{2-} and Org-N were percentage of pasture with steeper slope (PPLANDS) and A/B. PO_4-P had complex scale impacts, which was best explained by sand content (- 0.5) at the riparian scale, and by ORGSOL (0.6, in summer) and PPLANDS (0.54, in winter) at the catchment scale.

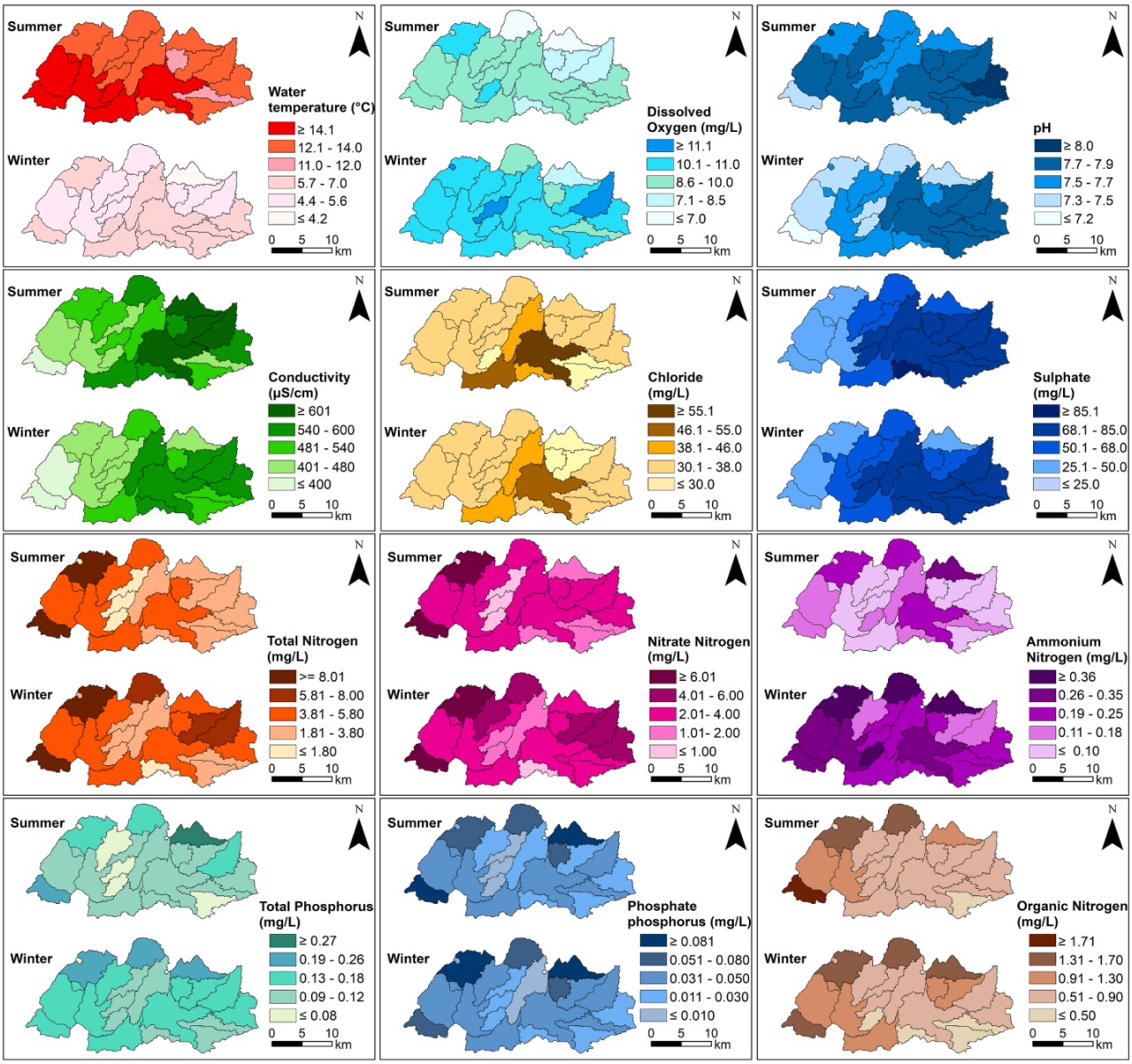

Figure 4-4. The spatial patterns of water quality variables during summer and winter seasons averaged for the periods of 1992–1994, 2009–2011, and 2018–2019.

4.3.3. The effects of catchment characteristics on water quality

The RDA results also indicated that more of the variation in overall water quality was explained by variables at larger scales and in summer as compared to the reach scale and winter (Table 4-3) At the reach scale, only 61% (summer) and 57.8% (winter) of the spatial variation in the overall water quality was explained, while this increased by 10 and 15 percentage points from the reach to the riparian and to the catchment scale, respectively. Hence, the processes affecting water quality are not limited to the reach scale. With regard to the two seasons, the average explanatory ability increased by 5 percentage points in summer as compared to winter.

Topography variables could explain more of the variation in water quality in summer (5.5-8.7%) than in winter (1.2-3.9%). This may be due to more convective rainfall events with higher rainfall intensity resulting in more surface runoff in July and August that transport more soil particles. In summer, SLOPE and SLP_SD played an important role in explaining spatial variation in water quality. In particular, they were strongly positively correlated with N nutrients and TP at the larger scales (Figure 4-5b and Figure 4-5c).

The effect of soil variables on water quality greatly depended on scale and season. ORGSOL was the controlling variable that explained the dominant part of variation in overall water quality (15.7%) at the reach scale in summer, whereas only <5% of the variation was explained at other scales. ORGSOL had significant and positive correlations with TN, NO_3-N, and NH_4-N (Figure 4-5). SAND was more explanatory at the reach scale than on larger scales in winter, and it was strongly and negatively correlated with N and P pollution. Unlike ORGSOL and SAND, A/B was more important along the river corridor, indicated by the explained variation of 15% at the riparian scale, which is more than twice of the variation explained at other scales. A/B was highly and positively correlated with TN, NO_3-N, TP, and Org-N, whereas negatively correlated with pH, EC and SO_4^{2-} (Figure 4-5).

Table 4-2. The predictive power (adjusted R^2) of the final models and the most important predictor for each water quality variable.

Parameters	Reach scale		Riparian scale		Catchment scale		Best model scale
	Important predictor	Adj.R^2	Important predictor	Adj.R^2	Important predictor	Adj.R^2	
Summer							
WT	**ELEV(-0.57)**	**0.62**	SLOPE (0.76)	0.61	SLOPE (0.82)	0.60	Reach
DO	ELEV(-0.58)	0.50	SAND (0.70)	0.67	**SHDI (-0.52)**	**0.71**	Catchment
pH	A/B (-0.47)	0.20	**UFLOW (0.38)**	**0.67**	FFLOW (0.39)	0.58	Riparian
EC	ELEV(0.46)	0.54	SAND (-0.62)	0.65	**UPLAND (0.53)**	**0.69**	Catchment
Cl^-	AWMSI (-0.46)	0.63	CONTAG (0.70)	0.75	**CONTAG (0.70)**	**0.79**	Catchment
SO_4^{2-}	ORGSOL (-0.48)	0.40	A/B (-0.38)	0.74	**PPLANDS (-0.30)**	**0.75**	Catchment
TN	FPLAND (-0.54)	0.66	A/B (0.47)	0.66	**A/B (0.58)**	**0.69**	Catchment
NO_3-N	FPLAND (-0.52)	0.62	A/B (0.46)	0.64	**A/B (0.56)**	**0.66**	Catchment
NH_4-N	ORGSOL (0.58)	0.32	**FDISR (0.46)**	**0.33**	UFLOW (-0.35)	0.31	Riparian
TP	FPLAND (-0.37)	0.43	**ORGSOL (0.37)**	**0.50**	APLANDS (0.56)	0.47	Riparian
PO_4-P	SAND (-0.69)	0.47	**SAND (-0.49)**	**0.64**	ORGSOL (0.60)	0.61	Riparian
Org-N	ORGSOL (0.65)	0.51	**PPLANDS (0.42)**	**0.61**	PPLANDS (0.51)	0.58	Riparian
Winter							
WT	APLANDS (-0.37)	0.12	**SAND (0.67)**	**0.43**	SAND (0.65)	0.41	Riparian
DO	UPLAND (-0.48)	0.21	UFLOW (0.35)	0.24	**UFLOW (0.45)**	**0.48**	Catchment
pH	ORGSOL (-0.56)	0.31	**AFLOW (0.47)**	**0.52**	AFLOW (0.40)	0.48	Riparian
EC	ELEV (0.41)	0.52	A/B (-0.51)	0.51	**A/B (-0.44)**	**0.57**	Catchment
Cl^-	AWMSI (-0.51)	0.51	CONTAG (0.75)	0.62	**CONTAG (0.62)**	**0.71**	Catchment
SO_4^{2-}	SAND (0.56)	0.42	PPLANDS (-0.46)	0.55	**A/B (-0.37)**	**0.59**	Catchment
TN	FPLAND (-0.48)	0.64	**APLANDS (0.51)**	**0.73**	APLANDS (0.71)	0.69	Riparian
NO_3-N	FPLAND (-0.58)	0.65	APLANDS (0.72)	0.67	**APLANDS (0.68)**	**0.71**	Catchment
NH_4-N	AFLOW (0.32)	0.26	**ORGSOL (0.47)**	**0.34**	ORGSOL (0.53)	0.27	Riparian
TP	**FPLAND (-0.36)**	**0.41**	A/B (0.45)	0.32	A/B (0.45)	0.36	Reach
PO_4-P	SAND (-0.70)	0.62	**SAND (-0.50)**	**0.70**	PPLANDS (0.54)	0.50	Riparian
Org-N	SAND (-0.65)	0.41	A/B (0.55)	0.57	**A/B (0.50)**	**0.57**	Catchment

Notes: WT – water temperature, DO – dissolved oxygen, EC – electrical conductivity, Cl^- – chloride, SO_4^{2-} – sulphate, TN – total nitrogen, NO_3-N – nitrate-nitrogen, NH_4-N – ammonium-nitrogen, TP – total phosphorus, PO_4-P – phosphate-phosphorus, Org-N – organic nitrogen; ElEV – elevation, A/B – areal ratio of hydrologic soil group A to B, AWMSI – Area-weighted mean shape index, ORGSOL – areal percentage of organic soil, FPLAND – areal percentage of forest land, SAND – sand content, APLANDS – areal percentage of arable land (slope >2%), UPLAND – areal percentage of urban, AFLOW – Flow length of arable land, CONTAG – ontagion Index , UFLOW – Flow length of urban area, FDISR – Distance of forest land to the rivers, PPLANDS – areal percentage of pasture (slope > 2%), SLOPE – the mean slope, SHDI – Shannon's Diversity Index, FFLOW – flow length of forest land; Adj.R^2 represents the adjusted R^2.

Table 4-3. Explained variations in water quality by important explanatory variables at different scales by redundancy analysis.

Season	Scales	Explained variation (%)						The first five most explanatory variables	pseudo-F	p Value
		Topography	Soil	Land use			Total explanation			
				Composition	Configuration	Proximity				
Summer	Reach	5.5	20.3	16.1	18.7	0.4	61	ORGSOL (15.7%), AWMSI (14.4%), FPLAND (9.2%), COHESINON (4.3%), ELEV (3.8%)	6.126	0.002
	Riparian	7.6	10.5	23.4	21.8	9.4	72.7	PPLANDS (20.5%), COHESION (16.9%), CONTAG (4.9%), SLP_SD (4.6%), A/B (4.5%)	6.547	0.002
	Catchment	8.7	11.9	28.6	21	8	78.2	PPLANDS (21%), CONTAG (16.7), A/B (6.7%), SLP_SD (5.6%), SAND (4%)	6.975	0.002
Winter	Reach	3.9	17.5	13.2	22.5	0.7	57.8	AWMSI (17%), SAND (14.2%), APLANDS (6.8%), COHESION (3.7%), PPLAND (3.5%)	4.848	0.002
	Riparian	1.2	23.8	11.5	19.5	10.2	66.2	CONTAG (19.1%), A/B (15.4%), APLANDS (7.7%), AFLOW (5.8%), SAND (4.7%)	6.295	0.002
	Catchment	2.9	11.8	16.2	33.1	8.6	72.6	CONTAG (20.8%), PPLANDS (13.8%), SHDI (8.9%), PFLOW (6.5%), SAND (4.6%)	7.068	0.002

Similar to topography, land use composition played a more important role in summer, particularly at larger scales, indicated by a 10 percentage point increase for explaining the variation in overall water quality compared to winter (Table 4-3). The influence of land use on water quality was scale-dependent. Pasture (in steeper areas) was the most significant variable at larger scales explaining >20% of the variation in water quality in summer, whereas it explained <5% of the variation at the reach scale. This tendency was evident in winter as well. Arable land (in steeper areas) slightly explained more of the variation at the riparian scale and in winter. Both land use types had pronounced positive correlations with TN and NO_3-N at larger scales (Figure 4-5b and c, e and f). Contrarily, forest percentage had much stronger effects at the reach scale as compared to other scales (Table 4-3 and Figure 4-5), and forest area was negatively correlated with TN, NO3-N, TP, and Org-N, while positively with DO (Figure 4-5a and d). Therefore, forest closer to the river may remedy nutrient pollution, which is in agreement with findings by Tran et al. (2010). There was no obvious scale dependence of urban area impact on water quality, but it showed a strong positive correlation with pH, EC and SO_4^{2-} (Figure 4-5).

Landscape patterns were an important factor that explained more of the variation in water quality at the catchment than at the reach or riparian scale. This is consistent with previous results that landscape metrics were more likely to correlate with water quality at large spatial scales (Bu et al., 2014; Shi et al., 2017). Nevertheless, the importance of the different variables differed with the scale. AWMSI explained more than 10 percentage points more of the variation in water quality at the reach scale than at larger scales. A high AWMSI value, which expresses a more complex patch shape, could considerably alleviate Cl^- , TN and NO_3-N contamination (Figure 4-5a and d), as complex shape coincides with forest areas. COHESION and CONTAG were more contributive at riparian and catchment scales. These variables show positive correlations with Cl^- , NO_3-N and TN (Figure 4-5).

Hydrological flow length and river distance showed higher explanatory power at the larger scales than at the reach scale during both seasons, with a decrease from >8% of explained variation in water quality to <1% from larger to reach scales (Table 4-3). Flow length of arable and pasture lands contributed the most towards the variation in

water quality in winter: 5.8% of the variation explained by AFLOW at riparian scale, and 6.5% by PFLOW at the catchment scale. With increasing scale, the respective negative correlation between AFLOW and N variables, PFLOW and TP, tended to intensify in winter. In summer, PDISR was more significant than other variables in affecting water quality. Particularly at the larger scales it was positively associated with WT and DO and negatively with TN, NO_3-N, and TP (Figure 4-5).

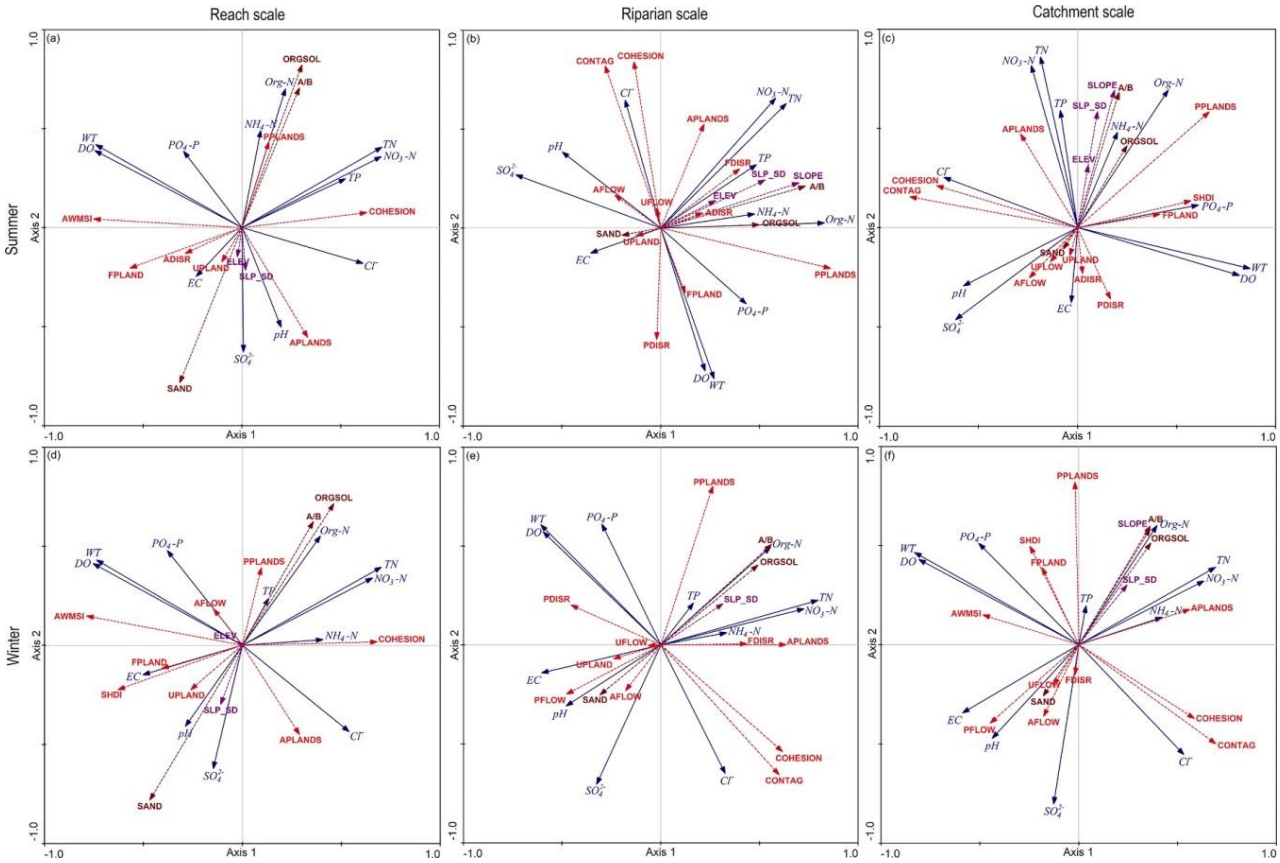

Figure 4-5. Biplots of stream water quality variables and explanatory variables at different spatial scales and seasons according to redundancy analysis (RDA).

4.4. Discussion

4.4.1. Water quality variations

The stream water quality exhibited significant seasonal variability, with more degraded water quality in winter as compared to summer. Seasonal variations of water quality have also been found in other studies, e.g., Poudel et al. (2013) found that nutrients of N and P varied considerably with different seasonal months in an agricultural catchment in the south central United States, and Wagner et al. (2018) observed explicit seasonal differences of various water quality variables in another rural

lowland catchment in Northern Germany. The seasonal changes of water quality can probably be linked to climatic seasonality and consequently to vegetation growth and farming schedules. The higher values of nutrients in winter may to some extent be explained by low interception and uptake of N and P by terrestrial plants and aquatic macrophytes in winter as well as fertilizer application in early spring (Alvarez-Cabria et al., 2016; Tisseuil et al., 2008).

The spatial pattern of water quality is generally determined by the heterogeneity of pollutant inputs, transport, reduction and dilution. The highest EC and Cl^- were measured in the city of Neumünster. This demonstrates that urban sewage carries high ionized matter and major ions (Daniel et al., 2002), urbanization and population density are typically responsible for the high level of chloride in surface water (Corsi et al., 2015; Scott et al., 2019). High concentrations of N and P in streams were found near two big wetlands (e.g., subbasins1 and 14) or in subbasins with steeper pasture or arable fields (e.g., subbasins16 and 18). This pattern is supported by the high redox potential in wetlands and the related substantial release of organic particles from the fertile topsoil. Additionally, both the excrements on pasture land and chemicals applied to farmland increase pollutant inputs, and the related transport might be intensified by a steeper slope (Yu et al., 2016).

4.4.2. Key variables for water quality prediction

Water quality in this region was best explained by soil property (viz. SAND, ORGSOL, A/B) and land use percent (Table 4-2). In the summer models, N and P variables were largely and positively correlated with areal ratio of hydrologic soil group A to group B (A/B) and percent of organic soil area (ORGSOL), and steeper arable (APLANDS) and pasture areas (PPLANDS), while negatively correlated with sand content (SAND) and proportion of forest land (FPLAND). The influence by soil is probably linked to the main soil type (sandy soil) and the large contribution of groundwater to stream flow (>50%) (Pott, 2014). More permeable soil (A/B) could result in a higher groundwater table and accelerate the nutrients recharging to stream (Rodriguez-Galiano et al., 2014). More organic soils could exacerbate the pollution of NH_4-N and P in summer (Table 4-2), because organic matter releases various P

components after mineralization particularly in warm summer (Chardon and Schoumans, 2007; Pott, 2014), and the ammonification process of generating NH_4^+ is favored by anaerobic organic soil condition (Reddy and Rao, 1983). Sandy soil has a higher rate of porosity and consequently lower water retention, leading to a lower absorption of contaminants (e.g., pesticides, metal ions and solutes). These properties in addition to the aerated structure and the deficient humus bound to sand particles are to an extent good for water quality in terms of DO, PO_4-P and Org-N pollution reduction (Andry et al., 2009; Zalidis et al., 2002). Agricultural activities on steeper slopes lead to an increase of TN, NO_3-N, and TP, due to the higher risk of fertilizers being transported to rivers. The loss of soil and water might be accelerated by the implementation of traditional tillage practices particularly in relatively steeper cultivated areas. The decreased application of phosphate fertilizer in Germany (Federal Statistical Office, 1991–2012) in addition to particulate phosphorus being strongly affected by soil erosion might obscure the impact of arable land (APLANDS) on P variables. Overgrazing could lead to undecomposed livestock excrements and accelerate soil loosening and erosion (Monaghan et al., 2007). The soil erosion and the transportation of chemical pollutants might be aggravated when cultivation or grazing practices occur in steeper areas. Subbasins 16 and 18 occupied high percentages of arable or pasture lands in the slope >2%. Particularly, rill erosion was sometimes observed in the fields without soil cover in subbasin 18. As a result, these two subbasins represented the highest potential of water quality contamination of N variables (which were highly influenced by steeper arable land, shown in Table 4-2 and Figure 4-5) and PO_4-P (which was influenced by steeper pasture, shown in Table 4-2 and Figure 4-5) within the catchment. More forest areas could reduce TN, NO_3-N and TP because the forest canopy could intercept and retain N and P loadings from the atmosphere as well as extenuate surface runoff (Matteo et al., 2006). Moreover, there is not any input of fertilizer or manure in forest areas compared to arable or pasture areas.

The roles of land use configuration and proximity are non-negligible influencing water quality levels. For example, higher SHDI value, depicted mainly by the diverse urban and agricultural land patches (Shi et al., 2017), could result in a decrease of DO in summer. Higher contagion index positively affected Cl^- level because it reflects well

physically connected agricultural landscape easily exposed to fertilizer and manure application, which might probably bring chloride residues to stream (Madsen et al., 2015). Our findings confirm the significant effects of landscape on chemical fluxes and hydrological processes (Shenet al., 2015). Last but not least, pH value (in winter) could increase due to long flow pathways of agricultural land use along which acidic compounds accumulated in soil particles during farming might be attenuated by surface runoff in winter. Higher level of DO appeared along with a higher urban flow distance (UFLOW), which corroborates the adverse impact of urban land use on ecosystem health (Zhou et al., 2012). Our results demonstrate that distance metrics of land use should be incorporated in the investigation of key NPS pollution processes because they represent the variations of surface runoff routing.

4.4.3. Effects of spatial and temporal scales

The RDA results revealed that water quality could be better explained at the catchment scale and in summer (Table 4-3) This suggests that water quality is more of a larger scale concern, which is in agreement with former findings that also found strongest correlations at the sub-catchment scale (Venohr et al., 2005a; Zhou et al., 2012). However, due to the differences of scale settings, of catchment characteristics and selected water quality variables, different results were found in other studies. Shi et al. (2017) found that the land use at the riparian buffer strip of 500 m contributed most towards water quality in wet season in the upper Dan River catchment (16,800 km^2) in China. To comprehensively depict riparian buffering effects, the relationships between different buffer strips and stream water quality should be further explored in the future. Chen et al. (2016) verified that TN, TP and chemical oxygen demand (COD) were dominantly affected by urban land in an urbanized catchment.

The SMLR results showed that the spatial-scale effectiveness differs among water quality variables. The scale impact for each separate variable showed seasonal consistency (Table 4-2). DO, EC, Cl^- , SO_4^{2-} , and NO_3-N were better explained by catchment characteristics in both seasons, because the major contaminants are induced by diffuse pollution processes on larger scales compared to the small buffers (Zhou et al., 2012). The anthropogenic activities mainly take place distant to rivers to ensure

health water quality. The lowland catchment has weak topographic gradients which only become more pronounced across larger scales, implying that their interactions with water quality normally lie at larger scales. Urban or population density is closely correlated with salt (e.g, constituents of Cl^-, SO_4^{2-} and EC) or organic content (e.g., DO) at the sub-watershed scale (Chen et al., 2016; Zhou et al., 2012). Beyond that, the widespread implementation of tile drainages (comprising 50% of the river length, adapted from Redeker (2011)) in the upper Stör catchment to sustain crop productivity might speed up water movement and thus increase entries of N or P to streams (Schmalz et al., 2008a; Williams et al., 2015). Although the major source of NH_4-N are the waste water treatment plants (Pott, 2014), a part of it could be still explained by riparian predictors. This is reasonable as moist peat soils prevailing on riversides are suitable for denitrification (Pal et al., 2010). Likewise, pH and PO_4-P were more accurately predicted at the riparian scale, which might be related to the frequent groundwater-fed ions recharge in the riparian zone, and associated riverine soil characteristics of being moist and fertile.

In addition, WT was better explained at the reach scale in summer or at riparian scale in winter, highlighting the dependence of water temperature dynamics on local processes (Ding et al., 2016). More of the variation in TP was explained by riparian-scale variables in summer, because riparian buffer strips functions as a filter of reducing contaminants and sediment from the surface (Gessner et al., 2009; Shen et al., 2015). However, TP was highly affected by forest (FPLAND) at the reach scale in winter, suggesting that the buffering effect of forest on TP is more sensitive at small spatial settings. The best model for Org-N varied from the riparian scale in summer to catchment in winter. Those differences might be related to the heavy grazing rates in summer (Di and Cameron, 2005), and intensive riverine groundwater-stream interrelation as well as strong nutrient dynamics in winter (Schmalz et al., 2008b).

4.4.4. Management insights

The upper Stör river catchment shows higher levels of N and P in winter and of pH, EC and Cl^- in summer, suggesting that there is a higher potential for eutrophication in winter and for inorganic pollution in summer. Management measures should be

targeted at these key water quality problems in the different seasons. Substantial groundwater contribution dominates the river discharge in this catchment, which has a significant impact on stream water quality. Peat soils are closely related to nutrient inputs in rivers. Groundwater regulation (i.e., improved subsurface drainages) and riparian conservation (i.e., buffer strips) would assist to reduce nutrient inputs in streams. Arable and pasture lands in steep areas significantly increase the risk of P and N pollution at larger scales. It is therefore essential to avoid overgrazing and traditional tillage practices particularly on slopes to control pollution effectively (Haas et al., 2017; Lam et al., 2011). Best management practices including proper fertilization and crop rotation would help to mitigate water quality deterioration (Haas et al., 2017). Forest strongly buffers N and P pollution at the reach scale. The conservation of nearer and wider vegetation buffers would be meaningful to maintain rivers at a health state. Strategies with respect to landscape structure might include increasing river buffer patch complexity and decreasing catchment-wide landscape connectivity to improve regional water quality. Proximity to rivers provided a process-mediated view of exploring water quality management measures. In the future, tile drainage and point pollution source (e.g., waste water plants) should be considered and included in a comprehensive watershed management of water quality.

4.5. Conclusion

This study revealed the impacts of catchment characteristics on stream water quality from multi-scale and multi-season perspectives, using a combined implementation of stepwise multiple linear regression analysis (SMLR) and redundancy analysis (RDA). Degraded water quality mostly occurred in streams surrounded by organic soil or arable and pasture fields with slightly steeper slopes and during winter. The SMLR results indicated that the method was capable of accurately predicting water quality variables with spatially distributed variables from soil, topography, and land use. The variation of overall water quality was better explained by the variables at the catchment scale than at the riparian or at the reach scale. In general, soil variables and land use composition and configuration are able to synergistically predict water quality more precisely than other explanatory variables. The explanatory ability of different

categories of catchment characteristics was also scale-and-season dependent. Topography and land use percent played an important role in explaining the spatial variation in overall water quality at the catchment scale and in summer, whereas soil properties contributed a major part towards the variation in water quality at the reach scale (summer) and the riparian scale (winter). The land use proximity to monitoring sites was identified to be more important in explaining the variations of water quality at the larger scales in both seasons. These differences suggested that catchment water quality management should take into account spatial and temporal scales and target key explanatory variables to improve water quality.

Chapter 5 Influences of land use changes on the dynamics of water quantity and quality in the German lowland catchment of the Stör

Chaogui Lei *, Paul D. Wagner, Nicola Fohrer

Department of Hydrology and Water Resources Management, Institute for Natural Resource Conservation, Kiel University, Olshausenstr. 75, 24118 Kiel, Germany.

Correspondence to: Chaogui Lei (cglei@hydrology.uni-kiel.de)

Journal of Hydrology and Earth System Science

Submitted 15 Sep 2021 ─ Under review 21 Sep 2021

Abstract

Understanding the impacts of land use changes (LUCC) on the dynamics of water quantity and quality is necessary to identify suitable mitigation measures that are needed for sustainable watershed management. Lowland catchments are characterized by a strong interaction of streamflow and near-surface groundwater that intensifies the risk of nutrient pollution. This study aims to reveal the relationship between long-term land use change and the water and nutrient balance in a typical lowland catchment in northern Germany. A hydrologic model (Soil and Water Assessment Tool, SWAT) and partial least squares regression (PLSR) were used to quantify the impacts of different land use types on the variations in actual evapotranspiration (ET), surface runoff (SQ), base flow (BF), and water yield (WYLD) as well as on sediment yield (SED), total phosphorus (TP) and total nitrogen (TN) loads. To this end, the model was calibrated and validated with daily streamflow data (30 years) as well as sediment and nutrient data from two water quality measurement campaigns (3 years in total). Three model runs over thirty years were performed using land use maps of 1987, 2010, and 2019, respectively. Land use changes between those years were used to explain the modeled changes in water quantity and quality on the subbasin scale applying PLSR. SWAT achieved a very good performance for daily streamflow values (calibration: NSE=0.79, KGE=0.88, PBIAS=0.3%; validation: NSE=0.79, KGE=0.87, PBIAS=7.2%), a satisfactory to very good performance for daily TN (calibration: NSE=0.64, KGE=0.71, PBIAS= -11.5%; validation: NSE=0.86, KGE=0.91, PBIAS=5%), a satisfactory performance for daily sediment load (NSE=0.54-0.65, KGE=0.58-0.59, PBIAS= -22.2%-12%), and an acceptable performance for daily TP (calibration: NSE=0.56, KGE=0.65, PBIAS= -4.7%; validation: NSE= 0.29, KGE= 0.22, PBIAS= -46.2%) in the Stör Catchment. The variations in ET, SQ, BF, WYLD, SED, TP, and TN could be explained to an extent of 61%-88% by changes in the area, shape, dominance, and aggregation of individual land use types. They were largely correlated with the major LUCC in the study area i.e. a decrease of arable land, and a respective increase of pasture and settlement. The change in the areal percentage of arable land positively affected the dynamics of SED, TP, TN and negatively affected BF, indicated by a Variable Influence on Projection (VIP) > 1.16 and large absolute regression coefficients

(RCs: 0.6-0.88 for SED, TP, TN; -1.65 for BF). The change in pasture area was negatively affecting SED, TP, and TN (RCs: -0.69 - -0.12, VIPs >1) while positively affecting ET (RC: 0.09, VIP: 0.92). The change in settlement percentage had a VIP of up to 1.17 for SQ and positively and significantly influenced it (RC: 1.16, p-value < 0.001). PLSR helped to identify the key contributions from individual land use changes on water quantity and quality dynamics. These provide a quantitative basis for targeting most influential land use changes to mitigate impacts on water quality in the future.

Keywords: SWAT; Partial least squares regression; Water quality; Landscape metrics; Variable Influence on Projection

5.1. Introduction

Good water quality and quantity are essential for enhancing ecological stability and diversity, and both of which play important roles in maintaining sustainable agricultural or economic development and human health (Antolini et al., 2020; Gleick, 2000; Lu et al., 2015; Singh et al., 2017; Srinivasan and Reddy, 2009). The dynamics of water quality and quantity at the catchment scale are mainly governed by a combination of climate and land use, as other catchment characteristics (e.g., topography, soil, and lithology) usually do not change on a short term (Farjad et al., 2017; Shuster et al., 2005; Wagner et al., 2018). Vice versa, hydrology affects land use as well (Wagner and Fohrer, 2019; Wagner and Waske, 2016). So far, many efforts have been made to study the influences of the change of land use area on water quality or water balance components (Kändler et al., 2017; Shrestha et al., 2018; Wagner et al., 2016). The effects on water quality have been a concern since the 1970s (Johnson et al., 1997). Land use patterns can alter surface roughness, evapotranspiration, soil infiltration, and the interaction between surface and subsurface water (Fiener et al., 2011; Wei et al., 2007). Consequently, the amount of water and the level of carried particles, chemicals, or metals transported can be promoted or hindered, altering water quantity and quality. The effects of land use changes on catchment water resources are manifold, e.g., urbanization results in a significant increase in surface runoff and water yield (Ayivi and Jha, 2018), expansion of farmland area poses increased risks to non-point source pollution of nitrogen (N) and phosphorus (P) as well as soil erosion (Hacisalihoglu, 2007; Jia et al., 2013; Rajaei et al., 2017; Roberts and Prince, 2010), whereas more semi-natural vegetation (e.g., forest, bushland, or grassland) increases the ability of filtering pollutants and intercepting rainfall thus reducing water pollution and streamflow (Moreno-Mateos et al., 2008; Yan et al., 2013). It is of great practical importance to identify key land use changes impacting water resources, in order to achieve an effective water and land use management in a particular catchment. Changes of both the composition and spatial structure of landscape can exert diverse influences on catchment hydrology and ecological systems (Allan, 2004; Ding et al., 2016; Haidary et al., 2013; Shawul et al., 2019). It is imperative to discriminate the effects of

different aspects of a certain land use class to target sustainable and comprehensive land and water management (Liu et al., 2012; Shi et al., 2013).

Earlier studies have generally measured relationships between land use transition and water quantity and quality, using the lumped indicators of landscape composition, e.g., land use proportion of the catchment area (Narain et al., 1998; Tong and Chen, 2002). However, composition indicators are rather coarse to depict the relationships, because they do not convey any details with respect to spatial settings of landscape patterns. Spatial configurations in landscapes, including the metrics of dominance, diversity, shape, cluster, and interconnection of land use patches, play a critical part in determining the energy and matter fluxes of e.g., solar radiation, temperature, evapotranspiration, runoff, nutrients, and sediments from the landscape ecology perspective (Amiri and Nakane, 2009; Forman, 1995; Lei et al., 2019; Wu and Lu, 2021). They therefore affect hydrological and ecological processes. With the availability of advanced spatial analysis (e.g., GIS) and remote sensing techniques (RS), various landscape metrics can be acquired efficiently for an overall assessment of landscape structure, based on classified land use maps from satellite data. Landscape metrics are sometimes more important as descriptors of water quality than composition metrics: Ding et al. (2016) found that water quality is more significantly affected by the configuration i.e. patch density (PD) or largest patch index (LPI) than by composition of the land use type in a low-order streams dominated catchment (drainage area: 35,340 km^2) in southeastern China. Gémesi et al. (2011) indicated that contagion, cohesion, and aggregation indices are more important than composition variables with regard to the variability in TN and TP in the Mississippi–Atchafalaya River watershed in USA. Recent studies on land use effects on water quantity mainly focus on land use percent, rarely on landscape metrics (Anand et al., 2018; Shrestha et al., 2018). However, metrics like landscape shape, dominance, or connectivity may play critical roles in altering the hydrological cycle, e.g., fragmented forest patches closely relate to the capacity of infiltration and interception of rainfall (Ghimire et al., 2017); hardness and straightness of land patches of farmland, urban, and natural land uses influence flow rates at different magnitudes and directions (Riitters, 2019; Shi et al., 2013); more concentrated grassland patches result in greater evapotranspiration (Yu et al., 2020).

Therefore, it is necessary to assess influences of changes in different aspects of a land use class to better understand their impact on water resources dynamics.

While land use changes and the associated changes in landscape metrics have a great potential of influencing hydrology, soil erosion or water quality dynamics at different spatial and seasonal scales (Haidary et al., 2013; Jones et al., 2001; Kändler et al., 2017), some landscape metrics have a high probability for collinearity. The collinear landscape metrics carry redundant information and are not independent predictor variables (Hargis et al., 1998). They can therefore result in biased or even misleading results when using conventional multivariate regression techniques like ordinary least-square regression, particularly in the case of a small number of observations (Shawul et al., 2019; Shi et al., 2013). Compared to ordinary multivariate statistical methods which present relatively low robustness dealing with multi-collinear variables, partial least squares regression analysis (PLSR) can overcome the limitation of multi-collinearity and achieve a robust performance by using techniques of multivariate statistical projection (Shi et al., 2013). The PLSR has widely been used to measure the "cause-effect" relationships between land use changes and water resource, based on the technique of projecting predicted and observed variables onto a new space and estimating the underlying structure between projected spaces (Ferreira et al., 2017; Shi et al., 2013; Yan et al., 2013).

The Stör River is the longest tributary of the Elbe River in the northernmost federal state of Germany, Schleswig-Holstein. Intensive agricultural activities (e.g., grazing, tillage, fertilizer, and pesticide application) are common in the catchment and increase the risk of water quality pollution (Monaghan et al., 2007). A variety of amelioration measures, e.g., tile drainage and straightening or canalizing of tributaries have been implemented in the past century to sustain agriculture productivity in lowlands. These activities brought about changes in the input and transport of nutrients and in hydrological fluxes. Meanwhile, the heterogeneity of the landscape pattern has been intensified due to artificial disturbances (Goldewijk and Ramankutty, 2004; Gu et al., 2007). We previously found significant relationships between land use patterns and water quality parameters at the landscape level in the upper Stör Catchment based on measurements (Lei et al., 2021). However, a modeling approach allows for

investigating the dynamic and quantitative effects of land use changes (composition and structure) measured by separate land use types on water quality and quantity, and it is necessary for developing effective and practicable strategies of improving water quality and controlling soil erosion (Pott, 2014; Ripl et al., 1996).

To identify the key land use changes controlling the spatial and temporal variations in water quantity and quality, relationships between landscape characteristics of each land use type and water quality (represented by sediment, TP and TN) and quantity (represented by evapotranspiration, surface runoff, base flow, and water yield) are explored at the subbasin scale in the upper Stör Catchment. To this end, the hydrologic model SWAT and partial least squares regression (PLSR) are employed. The study aims at (1) calibrating and validating a catchment model for streamflow, sediment, TP, and TN loads; (2) quantifying the changes of landscape characteristics and water quality and quantity variables at the subbasin scale; (3) investigating the relationships (depicted by the contribution and influence) between LUCC and water quality and quantity dynamics at the subbasin scale.

5.2. Materials and methods

5.2.1. Study area

The rural lowland catchment of the upper Stör is the focus of this study (Figure 5-1). It extends from the origin of the Stör River in Willingrade to the gauge in Willenscharen (Figure 5-1) and is free of tidal influence. The catchment has a drainage area of approximately 462 km², with a total length of the river network of about 221 km. Its temperate climate is characterized by an average annual precipitation of 850 mm and a mean temperature of 9.4 °C between 1990 and 2019, according to the records by weather stations Neumünster and Padenstedt (DWD, 2020a). The average daily streamflow measured at the catchment outlet in Willenscharen is 5.8 m^3 s^{-1} between 1990 and 2019, with low flows (mean value: 3.8 m^3 s^{-1}) in summer (May-October) and high flows (mean value: 7.9 m^3 s^{-1}) in winter (November-April) (LKN, 2020). Discharge occurring in the highest flow period (December-March) contributes most (around 50%) to the total annual amount of stream flow. The catchment is characterized by a flat topography, descending from nearly 60 m a.s.l. in the northeast and 85 m in the

western part towards 20 m in the center and to 5-10 m in the southern part. Sandy soil (Cambisol, Gley-Podsol, Podsol) dominates the catchment, particularly in the central lowland part, while some Gley soils are mainly distributed in the east and peat soils can be found in proximity to streams and near two major wetlands (Pott and Fohrer, 2017a). The catchment is dominated by rural land use composed of arable land (36.1%) and pasture (31.3%), followed by forest (18.7%), urban areas (12.8%), and a minor fraction of water and wetland as indicated by a land use map for 2019 (Lei et al., 2021). The main cultivated crops include winter cereals (wheat, barley, and rye), corn, and rapeseed.

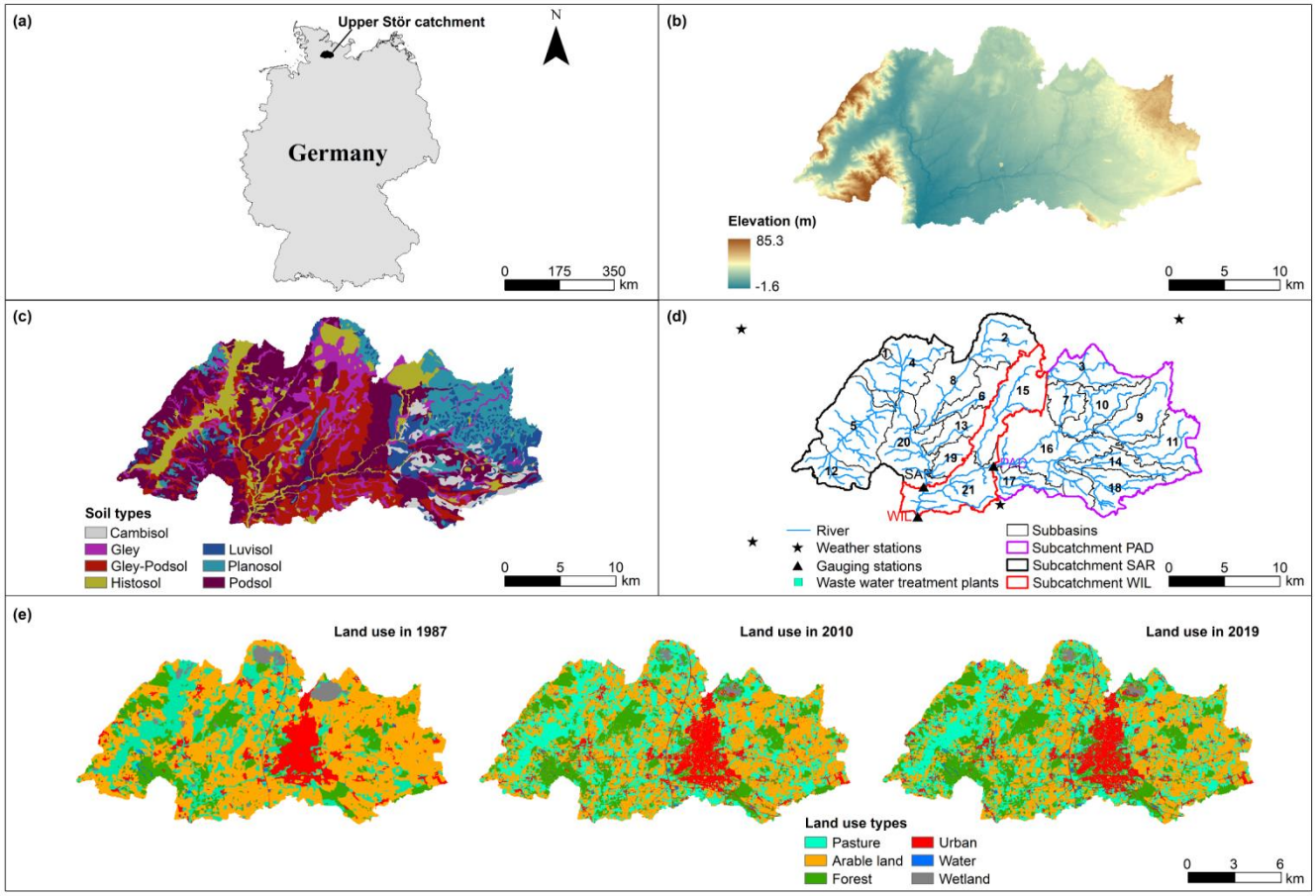

Figure 5-1. Characteristics of the study area: Location of the upper Stör Catchment (a), spatial distributions of topography (b) (LvermA, 2008) and soil types (c) (Finnern, 1997), of subbasins, weather and gauging stations, and waste water treatment plants (WWTPs) (d) (Pott, 2014), as well as land use maps (e) (Lei et al., 2021; Rathjens et al., 2014; Ripl et al., 1996).

5.2.2. Land use data and landscape metrics

Land use maps for 1987, 2010, and 2019 have been used to characterize changes in land use and landscape patterns. The earlier two maps (1987, 2010) have been adapted

from Ripl et al. (1996) and Rathjens et al. (2014), respectively, and are based on Landsat TM-5 image data at 30 m resolution. The land use map for 2019 has been derived from 10 m resolution Sentinel-2 satellite images (Lei et al. 2021). The land use types are categorized uniformly as: 1) arable land (winter cereals, corn, and winter rape, and other crops), 2) pasture (meadow, field grass, and rangeland); 3) forest (deciduous and coniferous forest); 4) urban (residential, commercial and industrial areas); 5) water (rivers, ponds, and lakes) and 6) wetland (Figure 5-1). Water and wetland are not considered for further analysis, as they comprise only minor and mostly constant percentages.

The area percentage of land use type (PLAND) has been used as a measure of land use composition. Configuration metrics include the largest patch index (LPI), area-weighted mean shape index (AWMSI), area-weighted mean contiguity index (CONTIGAW), aggregation index (AI), and interspersion juxtaposition index (IJI), considering the dominance, shape, and interconnection of landscape (Ding et al., 2016; Gémesi et al., 2011). Composition and configuration indices of pasture, arable land, forest and urban have been selected for subsequent analysis (Table 5-1) They have been derived with the help of the software FRAGSTATS 4.2. All indices and their changes are analyzed at subbasin scale.

Table 5-1. Description of the landscape metrics selected for the study.

Attributes	Metrics	Unit	Description	Abbreviation at class level	Note
Composition	Percentage of land use (PLAND)	%	Areal percentage of land use types	PLAND*a*, PLAND*p*, PLAND*f*, PLAND*u*	
Configuration	Largest patch index (LPI)	%	Percentage of the landscape composed of the largest patch	LPI*a*, LPI*p*, LPI*f*, LPI*u*	
	Area-weighted mean shape index (AWMSI)	-	The sum of the mean shape index multiplied by the area weight of each patch type involving the corresponding class	AWMSI*a*, AWMSI*p*, AWMSI*f*, AWMSI*u*	Metrics for land use type *a* (refers to arable land), *p* (refers to pasture), *f* (refers to forest), *u* (refers to urban)
	Aggregation index (AI)	%	Number of the same patch type being adjacent divided by the maximum number of adjacencies for the corresponding land use class	AI*a*, AI*p*, AI*f*, AI*u*	
	Area-weighted mean contiguity index (CONTIGAW)	-	Measure of the patch shape based on the sum of spatial connectedness multiplied by the area weight of the patch for a certain class	CONTIGAW*a*, CONTIGAW*p*, CONTIGAW*f*, CONTIGAW*u*	
	Interspersion juxtaposition index (IJI)	%	Measure of patch adjacency and interspersion or intermixing of patch types for a class	IJI*a*, IJI*p*, IJI*f*, IJI*u*	

5.2.3. Hydrologic and water quality modeling

5.2.3.1. SWAT model

The Soil and Water Assessment Tool (SWAT) is a process-based and semi-distributed eco-hydrological model with a continuous time step (Arnold et al., 1998). It is suitable for the simulation of streamflow, sediment, nutrients, and groundwater dynamics in catchments of different sizes (Aghsaei et al., 2020; Bieger et al., 2014; Haas et al., 2016; Tigabu et al., 2020). The computation of water routing, nutrient cycles and soil erosion is based on hydrologic response units (HRUs) characterized by the same land use, soil type, and slope in the same subbasin representing the spatial heterogeneity of the catchment (Arnold et al., 2013). The HRU-based calculations for the subbasins are routed through the rivers that connect the subbasins (Neitsch et al., 2011).

To accurately represent groundwater dynamics in this lowland catchment, we applied the enhanced SWAT model SWAT3s that is based on SWAT 2012 Rev. 582 (Pfannerstill et al., 2014). SWAT3s uses three groundwater aquifers and subdivides the original shallow aquifer from SWAT into a fast and a slow aquifer. SWAT3s was developed in the German lowland catchment of the Kielstau, where it better represented low flows and groundwater dynamics when compared to the original SWAT version (Pfannerstill et al., 2014). It was already successfully applied to the lowland catchment of the Treene proving its usefulness for modeling nutrients as well (Haas et al., 2017; Haas et al., 2016).

5.2.3.2. Model databases and setup

SWAT requires topography, soil, land use, hydro-meteorological input data. Topography data was obtained from a Digital Elevation Model (DEM) in 5 m resolution (LvermA, 2008) and used to delineate the watershed into 21 subbasins. Soil data and attributes for SWAT have been derived by Pott and Fohrer (2017b) from a soil type map (Finnern, 1997). The land use map for 2019 is used to build the model. Three-year crop rotations (winter wheat/winter wheat/corn; winter rape/winter wheat/corn; corn/corn/corn) are adapted from Oppelt et al. (2012) and implemented for the respective land use classes. Agriculture management schedules and fertilization (e.g.,

application rates of N, P fertilizers and manure at different crop growth stages) have been determined according to the actual guidelines of agriculture practices (KTBL, 1995 and 2008; Kühling, 2011; LWK, 1991 and 2011). From the DEM a four slope classes (<1%, 1-2%, 2-5% and >5%) are defined. Slope, soil, and land use classes were combined to obtain 3618 HRUs in the catchment. The HRUs were generated without excluding any HRUs by thresholds for land use, soil, or slope class percentages, to allow for a better spatial representation. To accurately represent lowland hydrology, drainage tiles were considered based on the estimated distribution of drained areas in the catchment (Venohr, 2000). We adapted drainage parameter values for DEP_IMP (1200 mm), DDRAIN (875 mm), TDRAIN (24 h), and GDRAIN (61 h) from a previous modeling study in the catchment (Pott and Fohrer, 2017b). Waste water treatment plants (WWTP) were implemented as point sources using data from monthly measurement campaigns in 2009 and 2010 and WWTP data vary with space and seasons (Pott, 2014). Daily values of temperature (max. and min), solar radiation, humidity, and wind speed are available from 1990 to 2019 for the climate station Padenstedt (DWD, 2020b). Precipitation data are available for four stations (DWD, 2020b) (Figure 5-1). Daily streamflow is measured at the gauges in Padenstedt (PAD), Sarlhusen (SAR) and Willenscharen (WIL) from 1990 to 2019 (LKN, 2020). Daily sediment and nutrient data have been obtained during two measurement campaigns between August 2009 and August 2011 and between October 2018 and November 2019 in Willenscharen. Daily mixed samples have been taken by an automatic and cooled sampler from a depth of 0.30 m above the river bed at the central section of the stream. They have been analyzed according to German standard procedure for water analysis (DEV) (Einheitsverfahren, 1997) in the laboratory of Department of Hydrology and Water Resources Management at Kiel University. Total suspended sediment concentration has been measured by filtering 1 l of water sample through 0.45 µm celluloseacetate filter paper and drying at 105ºC. The concentration of total phosphorus (TP) has been determined by spectrophotometry, according to DEV H36 and DEV D11, while total nitrogen (TN) has been measured by chemiluminescence detection according to DEV H3. Each measurement of TP or TN concentration from unfiltered samples has been performed based on a blank comparison analysis of distilled water

and triplicate analysis of subsamples. Their concentrations have been determined by the arithmetic mean values of any two subsamples with smallest measurement differences (less than <10%).

5.2.3.3. Model calibration and validation

A step-wise calibration approach has been applied for daily streamflow (1), sediment (2), TP (3), and TN (4) data. Streamflow was calibrated using a fifteen-year time period from 1990 to 1991 and from 2007 to 2019. The other available fifteen years (1992-2006) have been used for validation. This split of the observation data ensures an equal representation of dry, normal, and wet years in the calibration and validation period, according to the annual precipitation. First, data from the two upstream gauges Padenstedt (PAD) and Sarlhusen (SAR) have been used to calibrate parameters in the respective subcatchments (Figure 5-1). Then, the parameters for the area downstream of PAD and SAR and upstream of the outlet gauge Willenscharen (WIL) have been calibrated. Sediment, TP and TN loads have been calibrated for two hydrologic years (sediment: 30/10/2009-07/08/2011; TP, TN: 08/08/2009-10/08/2011) using a model with the land use map in 2010 and validated for one hydrologic year (19/10/2018-05/11/2019) using a model with the land use map in 2019, for the entire catchment based on the daily data from Willenscharen. The calibration has been performed based on 8000 (stream flow) and 5000 (sediment, TP, and TN loads) parameter sets generated using Latin Hypercube Sampling method (Soetaert and Petzoldt, 2010). For each parameter set a model run has been performed, allowing for a warm-up period of 4 years. From experiences with the SWAT model in the Stör Catchment (Pott and Fohrer, 2017b) and other German lowland catchments (i.e., Kielstau and Treene catchments) (Haas et al., 2016; Lam et al., 2012; Pfannerstill et al., 2014) as well as in relevant studies from other countries (Aghsaei et al., 2020; Boongaling et al., 2018), the parameters most likely to affect hydrological and water quality processes have been selected and their preliminary ranges have been defined (Table 5-2). The final ranges of selected parameters have been determined based on the sensitivity of parameters to model outputs as derived from 2000 trial runs following Guse et al. (2020) (Table 5-2). Calibration and validation have been carried out in R using the packages FME

(Soetaert and Petzoldt, 2010), hydroGOF (Zambrano-Bigiarini, 2020) and zoo (Zeileis and Grothendieck, 2005).

The performances for modeling streamflow and sediment, TP and TN loads have been assessed using Nash-Sutcliffe efficiency (NSE), Kling-Gupta Efficiency (KGE), and Percent Bias (PBIAS) as proposed in Guse et al. (2014) and Moriasi et al. (2007). For an accurate representation of all phases of flow hydrograph for water quality simulation periods, the additional signature measure RSR (Ratio of Root Mean Square Error to the Standard Deviation of the Observations) was used to calibrate the very high, high, middle, low, and very low periods (Haas et al., 2016; Zambrano-Bigiarini, 2020). For each of the three streamflow gauges, we pre-selected the parameter sets that yielded a KGE >0.75 for the streamflow calibration period. To particularly represent runoff dynamics during the periods of water quality measurements (Aug. 2009 - Aug. 2011 and Oct. 2018 - Nov. 2019) well, the mean of RSR for the five flow duration segments during these periods was assessed and the best 300 streamflow parameter sets indicated by a low RSR were selected. From these 300 sets, the final parameter set yielding the highest KGE in these periods was selected. For sediment, TP, and TN calibration the parameter set that yielded the highest NSE during the calibration period was selected to represent peak loads and their dynamics well.

Table 5-2. Parameters used to calibrate streamflow, sediment, total phosphorus and total nitrogen.

Parameters	**Definition**	**Calibrated range**			**Calibrated value**		
Parameters used to calibrate streamflow							
		WILL	SAR	PAD	WILL	SAR	PAD
r_SURLAG	Surface runoff lag coefficient	0.1-0.6	0.1-0.6	0.1-0.5	0.13	0.13	0.13
r_GWDELAY*fs*	Groundwater delay time – fast shallow aquifer (days)	48-85	40-80	65-100	83	42	71
r_ALPHABF*fsh*	Baseflow alpha factor – fast shallow aquifer (day^{-1})	0.17-0.38	0.18-0.38	0.05-0.22	0.18	0.26	0.08
r_RCHRG*ssh*	Aquifer percolation fraction – slow shallow aquifer	0.8-0.94	0.08-0.58	0.38-0.7	0.91	0.34	0.44
r_GWDELAY*ss*	Groundwater delay time – slow shallow aquifer (days)	68-105	58-100	80-120	80	92	87
r_ALPHABF*ssh*	Baseflow alpha factor – slow shallow aquifer (day^{-1})	0.0009-0.002	0.001-0.007	0.003-0.009	0.0019	0.0036	0.0064
r_RCHRG*dp*	Aquifer percolation fraction inactive deep aquifer	0.02-0.15	0.015-0.14	0.1-0.45	0.14	0.03	0.15
r_ESCO	Soil evaporation compensation factor	0.85-0.98	0.93-1	0.7-0.95	0.86	0.94	0.77
r_EPCO	Plant uptake compensation factor	0.01-0.025	0.05-0.22	0.1-0.35	0.02	0.06	0.23
as_CN2	Initial SCS runoff curve number for moisture condition II	-13 - -1	-12 - -1	-12 - -2	-5.64	-3.27	-4.89
as_SOL_AWC	Available water capacity of the soil layer (mm)	-0.06 - 0.02	-0.06 - -0.01	-0.04 - 0.03	-0.006	-0.020	0.001
m_SOL_K	Saturated hydraulic conductivity (mm h^{-1})	0.7-1.3	0.8-1.2	0.8-1.2	1.052	0.811	1.079
Parameters used to calibrate sediment							
r_ADJ_PKR	Peak rate adjustment factor for sediment routing in main channel	0.55-2			0.61		
r_CH_COV_1	Channel erodibility factor	0.1-0.5			0.41		
r_CH_COV_2	Channel cover factor	0.4-0.7			0.57		
r_USLE_P	USLE support practice factor	0.5-1			0.93		
m_SLSUBBSN	Average slope length (m)	0.8-1.08			0.88		
m_HRUSLP	Average slope stepness (m m^{-1})	0.95-1.28			1.1		
r_LAT_SED	Sediment concentration in lateral and groundwater flow (mg l^{-1})	55-140			110		
r_USLE_K	Soil erodibility (K) factor	0.06-0.2			0.09		
as_SOL_Z	Depth from soil surface to bottom of layer (mm)	-70-20			-65		
r_USLE_C	Minimum value of USLE C factor for land cover/plant	0.08-0.43 (cropland); 0.002-0.017 (pasture)			0.192 (cropland), 0.015 (pasture)		
Parameters used to calibrate total phosphorus							
r_P_UPDIS	Phosphorus uptake distribution parameter	30-100			73.61		
r_PPERCO	Phosphorus percolation coefficient	10-16			10.3		
r_PHOSKD	Phosphorus soil partitioning coefficient	115-190			181.14		
r_PSP	Phosphorus sorption coefficient	0.01-0.5			0.21		
r_ERORGP	Organic P enrichment ratio	0.8-4.8			2.38		
r_GWSOLP	Concentration of soluble phosphorus in groundwater contribution to stream flow from the subbasin	0.04-0.4			0.19		
r_SOL_SOLP	Soluble phosphorus concentration in the soil layer (mg kg^{-1})	30-90			32.1		
Parameters used to calibrate total nitrogen							
r_CMN	Rate factor for humus mineralization of active organic nitrogen	0.001-0.003			0.002		
r_RCN	Concentration of nitrogen in rainfall (mg l^{-1})	1.3-6			5		
r_CDN	Denitrification exponential rate coefficient	0.09-0.18			0.16		
r_N_UPDIS	Nitrogen uptake distribution parameter	20-90			69.05		
r_NPERCO	Nitrogen percolation coefficient	0.03-0.5			0.06		
r_SDNCO	Denitrification threshold water content	0.3-0.95			0.95		
r_HLIFENGW*fsh*	Half-life of nitrate in fast shallow aquifer (days)	30-125			52		
r_HLIFENGW*ssh*	Half-life of nitrate in slow aquifer (days)	250-480			454		
r_SHALLSTN*ssh*	Initial concentration of nitrate in slow aquifer (mg l^{-1})	30-85			37.41		

Note: for calibration, the parameter values were varied by replacing (r), multiplication (m) or addition/subtraction (as)

5.2.3.4. Model application

The model has been run for each of the three land use maps (in 1987, 2010, and 2019) from 1990 to 2019. As agriculture in 1987 was generally classified, it has been split as corn (12%), rapeseed (29%), and wheat (59%) randomly distributed in the catchment in SWAT model, according to the statistical data from Schleswig-Holstein Statistical Office (1992-2012). All other inputs i.e. DEM, soil data, weather data, waste water quality data, management practices, and fertilization have been kept constant, and the calibrated parameters have been adapted. Hence, each model run is performed under a different land use scenario defined by one of the three land use maps. The results from these model runs have been used to explore the influences of land use changes (LUCC)

on actual evapotranspiration (ET), surface runoff (SQ), base flow (BF), and water yield (WYLD) as well as on sediment (SED), TP, and TN loads. Based on the model results, the contributions of LUCC on changes in ET, SQ, BF, and WYLD as well as SED, TP, TN at the subbasin scale are evaluated, and key impacts from LUCC are identified.

5.2.4. Partial least squares regression

Combining the features of principal component and multiple linear regression analyses, partial least squares regression (PLSR) is a robust multivariate analysis method even when dealing with multi-collinear predictor variables. The principle of PLSR is to extract a few latent components from original predictor variables that carry as much variation as possible, and which are meanwhile most likely to predict the variation in the response variable. Detailed information on the underlying theory and algorithms of PLSR is available in Abdi (2010).

In this study, PLSR is used to reveal the contribution of changes in land use types on the variation in ET, SQ, BF, WYLD, SED, TP, and TN across three time steps (1987, 2010, and 2019). The predictor variables are the changes in area percent and landscape metrics of four main land use types (arable land, pasture, forest, and urban). The response variables include the respective changes in the mean annual values of ET, SQ, BF, WYLD and SED, TP, and TN loads at the subbasin scale between 1987, 2010, and 2019. PLSR models for all of these response variables were constructed. A cross-validation is performed with 50 random repetitions on 10 equal segments of the data set. It is used to determine the number of optimal components of the PLSR model to obtain a desirable balance between the explained variation in the response (R^2) and predictive power of the model (measured as cross-validated goodness of the prediction: Q^2). The cumulative predictive ability (cumulative goodness of prediction: Q^2_{cum}) and the cross-validated root mean squared error (RMSECV) as the difference between actual and predicted values, are determined for each model (Yan et al., 2013). The regression coefficients (RCs) signify the direction and extent of the effect of LUCC predictor variables. The variable importance for the projection (VIP) quantifies the importance of the predictors. By Wold's criterion, a predictor with VIP<0.8 is assessed as less important (Boongaling et al., 2018; Wold et al., 2001). To achieve model parsimony,

the following PLSR modeling procedures has been conducted: First, an initial simulation of PLSR is run using all predictors. Next, new PLSR models are run by iteratively excluding the predictor with small variable importance (VIP) until the modeling procedure resulted in acceptable variable importance or only two predictors remained. The number of components of candidate PLSR model was determined so that the Q2 cum is maximized (Shi et al., 2013).

All the PLSR analyses were performed with the R packages pls (Mevik et al., 2020) and mdatools (Kucheryavskiy, 2020).

5.3. Results and discussion

5.3.1. Calibration and validation of streamflow and water quality

The simulated and measured daily values of streamflow (Figure 5-2) and water quality (Figure 5-3) data are visually compared for the calibration and validation periods, and the statistical performance of the models is assessed (Table 5-3). The model obtains a NSE of 0.76-0.81 and a KGE of 0.82-0.85 for streamflow at the two upstream gauges Padenstedt and Sarlhusen, and a slightly higher NSE (calibration: 0.79, validation: 0.79) and KGE (calibration: 0.88, validation: 0.87) for streamflow at the outlet in Willenscharen. The PBIAS values are within the range of -2.2% - 10.6%. These values indicate a good to very good model performance for depicting daily streamflow in the catchment (Moriasi et al., 2007). Likewise, the model shows a nearly good to very good performance for daily TN load indicated by an NSE of 0.64 for calibration and of 0.86 for validation and by a KGE $\geq$ 0.71 (for calibration: 0.71; for validation: 0.91), while absolute values of PBIAS are below 15%. For sediment and TP the model shows a lower performance. Sediment achieves a satisfactory performance during calibration (NSE = 0.54, KGE = 0.58, PBIAS = 12%) and a good performance during the validation period (NSE = 0.65, KGE = 0.59, PBIAS = -22.2%). For TP the model obtains a satisfactory performance for calibration (NSE =0.56) but an unsatisfactory performance (NSE =0.29) for validation. The worse TP model performance may be due to the short and possibly different conditions during calibration and validation periods. Nevertheless, PBIAS for TP model is still within the acceptable performance range ($\pm 40 \leq$ PBIAS $< \pm 70$) (Moriasi et al., 2007). It should be

noted that the performance ranges from Moriasi et al. (2007) refer to a monthly time step, whereas we used a daily time step, a finer temporal scale, on which it is usually harder to achieve a good model representation. We therefore conclude that even for daily TP the model performance is acceptable, particularly with regard to the study purpose of analyzing long-term changes in the water and matter balance.

Overall, modeled and measured daily values show clear consistency in their dynamics (Figure 5-2 and 3). Differences appear for a few peak flows in winter or low flow periods in summer. As already indicated by the goodness of fit measures (Table 5-3), the modeled streamflow matches the measured values most of the time from 1990 to 2019. However, a few single flood peaks are underestimated in winter, e.g. on 27-28/Feb/2002, 5-6/Jan/2012, and 24-25/Dec/2014. This might be related to an insufficient representation of snow in the model, or deficiencies in single-event flood routing (Lam et al., 2012). The underestimation of peak streamflow in winter was also observed in other rural lowland catchments of Treene (Haas et al., 2016) and Kielstau (Lam et al., 2010) in northern Germany. Sediment loads are overestimated during the calibration period and slightly underestimated during the validation period mainly for a few peak values. The incorrect estimation might be due to the fact that river sediment load is also influenced by tile drains and bank erosion in lowland catchments (Kiesel et al., 2009), while SWAT takes into account sheet erosion. A few sediment peaks in early March 2010, mid-Jan 2011 and mid-Feb 2019 are underestimated but other peaks e.g. in Nov, Dec 2009, and Mar 2019 are very well depicted. A similar behavior can be observed for TP load during the calibration and validation periods, with slight overestimation of TP in summer (April - June of 2009 and 2019) and underestimation of a few peaks in winter (between November and March). TN is generally well represented, except for only a few underestimations of extreme peaks in winter (e.g., early March or November 2010, mid-March 2019). Overall, the underestimation of some peak loads of sediment, TP and TN might be attributed to the underestimation of corresponding peak flows.

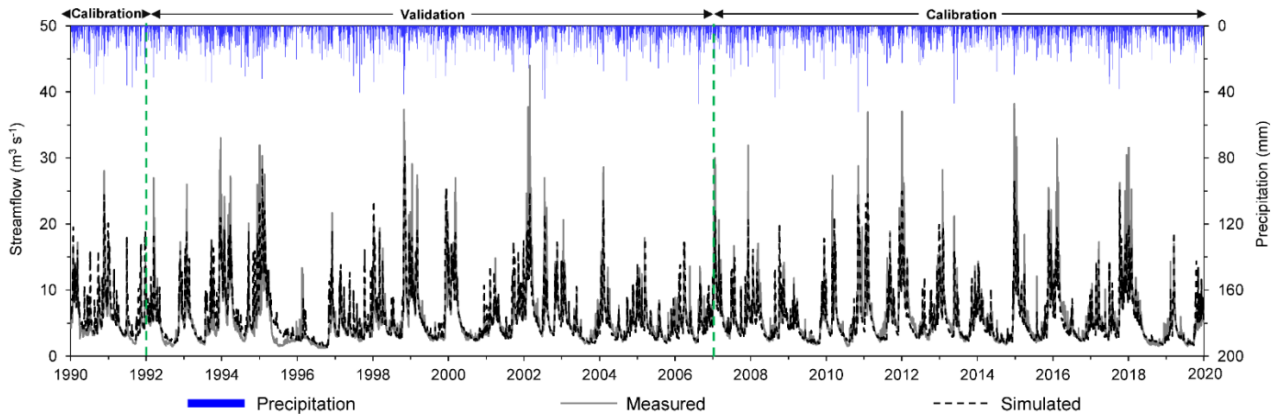

Figure 5-2. Comparison of measured and modeled daily streamflow during the calibration and validation periods in Willenscharen.

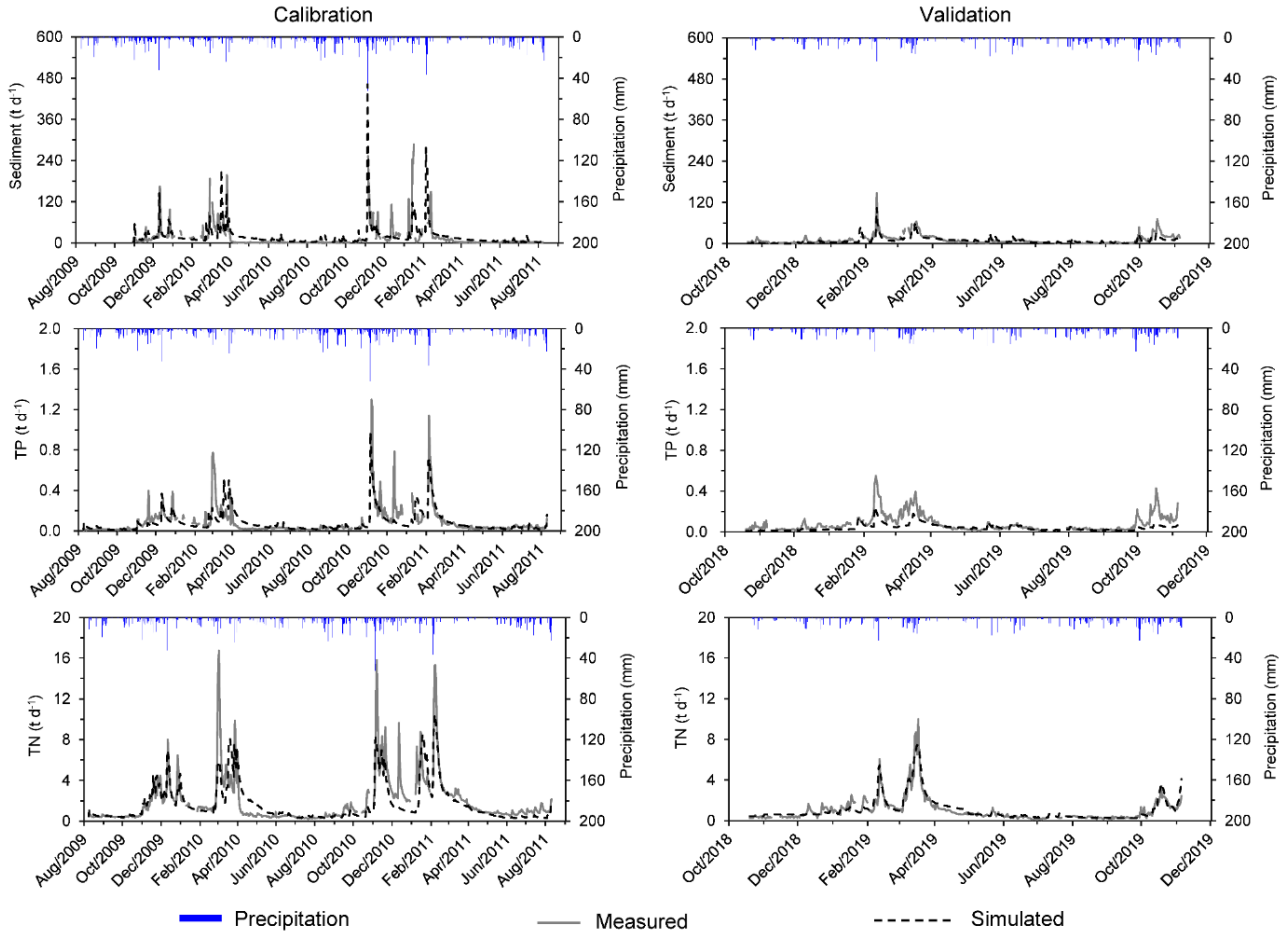

Figure 5-3. Comparisons between measured and modeled daily loads of sediment, total phosphorus (TP), and total nitrogen (TN), respectively for calibration (left) and validation (right) periods

Table 5-3. Performance metrics for the model calibration and validation.

Index	Calibration				Validation			
	Streamflow (PAD/SAR/WIL)	Sediment load	TP load	TN load	Streamflow (PAD/SAR/WIL)	Sediment yield	TP load	TN load
Period	1990-1991; 2007-2019	30/10/2009-7/8/2011	8/8/2009-10/8/2011	8/8/2009-10/8/2011	1992-2006	19/10/2018-5/11/2019	19/10/2018-5/11/2019	19/10/2018-5/11/2019
KGE	0.85/0.82/0.88	0.58	0.65	0.71	0.84/0.85/0.87	0.59	0.22	0.91
NSE	0.76/0.78/0.79	0.54	0.56	0.64	0.81/0.81/0.79	0.65	0.29	0.86
PBIAS (%)	5.6/-2.2/0.3	12	-4.7	-11.5	0.7/10.6/7.2	-22.2	-46.2	5

5.3.2. Characteristics of land use change

Land use changes between 1987 and 2019 vary across the catchment (Figure 5-4). This is indicated by the individual dynamics in the four main land use types of arable land, pasture, forest, and settlement area. Arable land has been decreasing and primarily replaced by pasture (by 16.2% of the catchment, dark cyan in Figure 5-4). The decrease of arable land is more pronounced in the northeast (e.g., subbasins 3 and 9-11) than in the northwestern part (e.g., subbasins 2, 4, 6, 8) where pasture was sometimes converted to arable land (dark pink, Figure 5-4). Conversely, pasture shows an increasing trend over the period of observation. The increase is stronger in the east as compared to the west of the catchment (Figure 5-4 and 5). The change of pasture is in part associated with the stream restoration including stabilizing river shore and increasing riparian vegetation (Dickhaut, 2005; Gessner et al., 2010). Besides, agricultural grasses may have been included in the pasture class due to the classification approach. Forest also shows an increasing trend as indicated by green colors in Figure 5-4, with a strong increase in the lowlands of the middle (subbasins 6 and 13) and southern parts (subbasin 17, Figure 5-5). Urban area has expanded mainly around the city of Neumünster (subbasin 15 and 17) (Figure 5-5).

In addition, the subbasin-scale land use metrics varied substantially between 1987, 2010, and 2019 (Figure 5-6). The mean area percent (PLAND) per subbasin declined for arable land (PLAND*a*) by 16% and 3% during the periods of 1987-2010 and 2010-2019, respectively. In contrast, subbasin-averaged pasture (PLAND*p*) increased for the period of 1987-2010 by 12% but decreased slightly from 2010 to 2019 by 0.8%. Both forest (PLAND*f*) and urban (PLAND*u*) areas have steadily increased from 1987 over

2010 to 2019. Similar trends are found in the metrics of the percentage of largest patch index (LPI) and the interspersion juxtaposition index (IJI). The subbasin average of LPI for arable land has decreased by 20% from 1987 to 2019, whereas the LPIs of other land use types shows a slight and stable increase. The IJI of arable land displays an overall slight increase from 1987 to 2019, while the IJI values of other land uses have steadily and notably increased (with a net increase up to over 20%). Both the area-weighted mean contiguity (CONTIGAW) and aggregation (AI) of each land use type have decreased over time, whereas the area-weighted mean shape index (AWMSI) has continuously and slightly increased. Despite similar changing directions of the land use patterns in the periods of 1987-2010 and 2010-2019, land use has been subject to more alterations in the former period than in the latter. Additionally, CONTIGAW, AI, and IJI of arable land exhibited opposite trends in the two periods, with a decrease from 1987 to 2010, and a slight increase from 2010 to 2019.

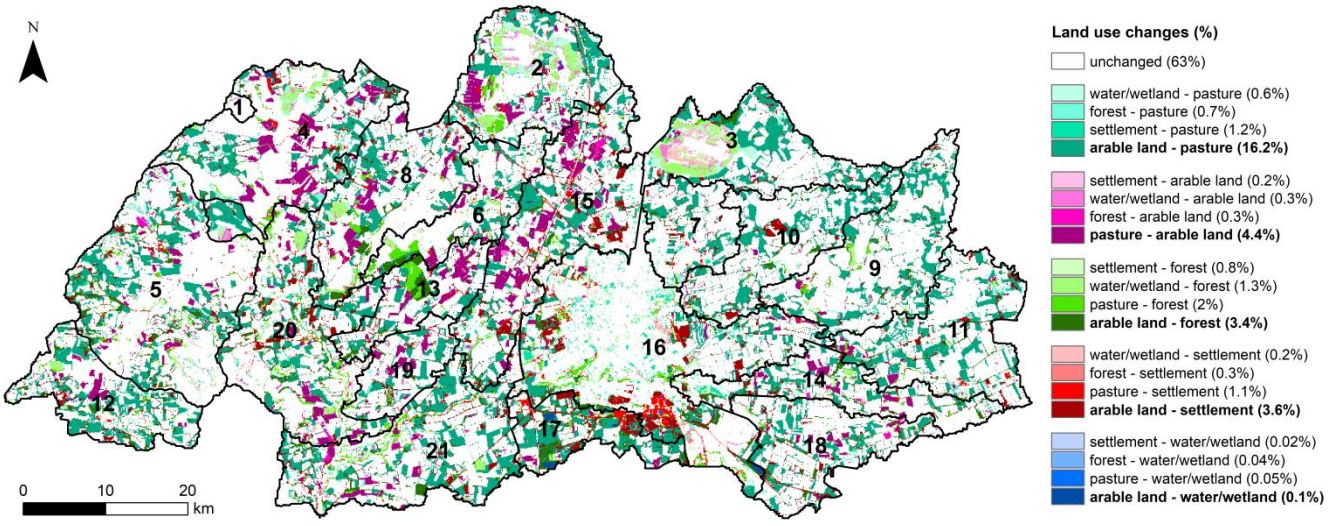

Figure 5-4. Spatial distribution of land use changes between 1987 and 2019 in the Stör Catchment. Individual land use change types are marked by different colors. The percentage of each change type calculated as percentage of the catchment area is given in the parentheses. The strongest change is marked in bold.

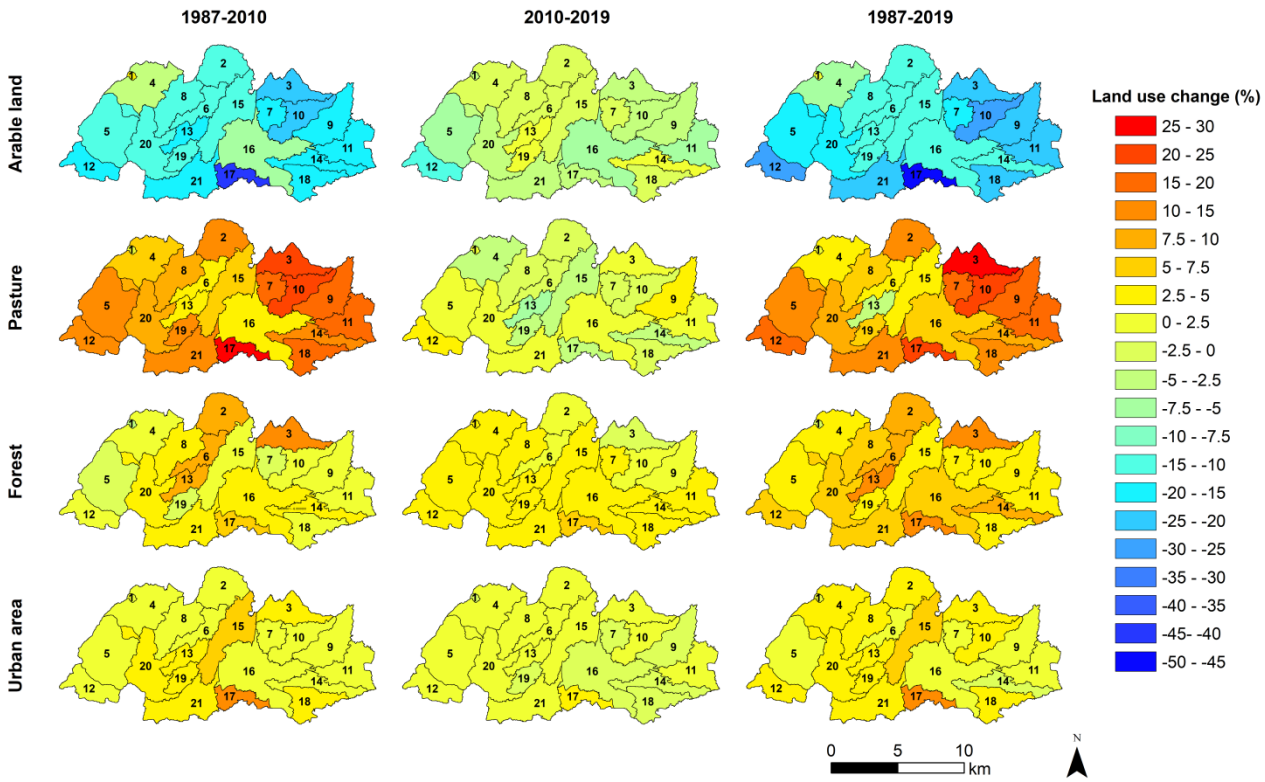

Figure 5-5. Spatial distribution patterns of the change of each land use type between 1987, 2010, and 2019.

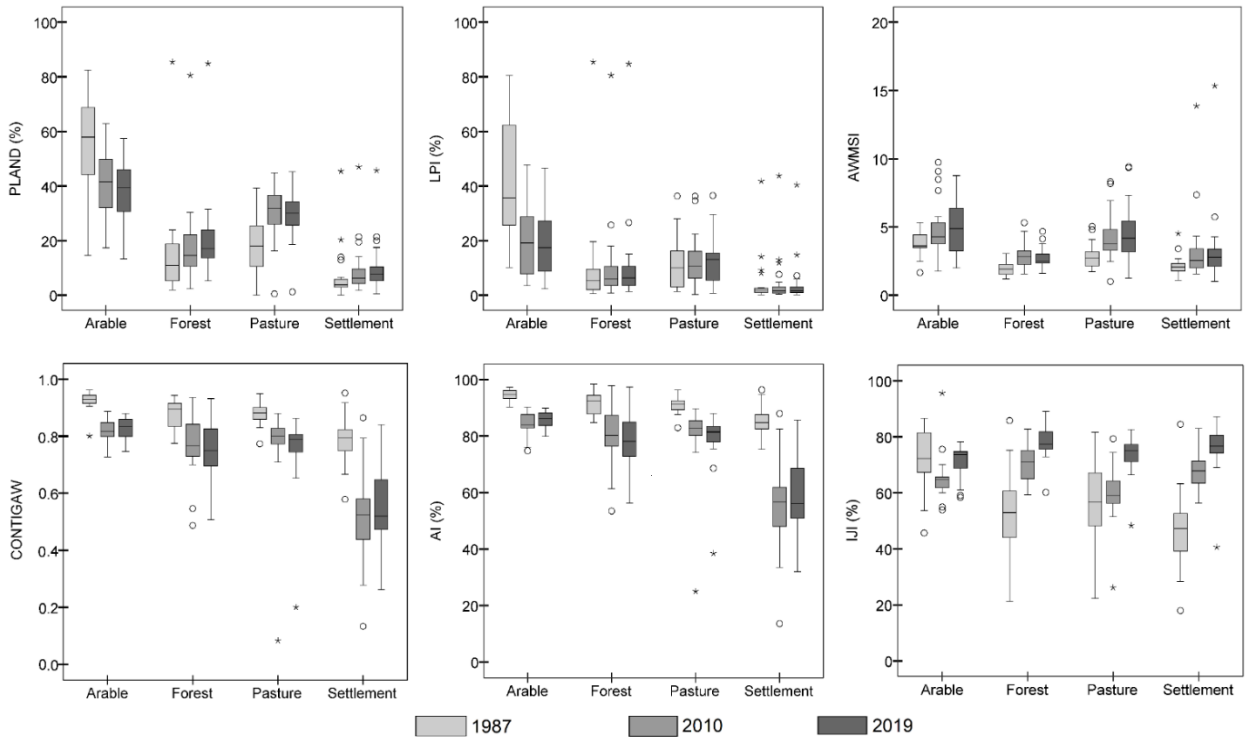

Figure 5-6. Changes of land use metrics between 1987, 2010, and 2019 in the Stör Catchment.

5.3.3. Differences of changes in water quantity and quality

Using the results from the three different model runs based on three land use maps of 1987, 2010, and 2019, we calculated changes in water quantity and quality. The spatial distribution of the variations in modeled subbasin-scale actual evapotranspiration (ET), surface runoff (SQ), base flow (BF), water yield (WYLD), and loads of sediment (SED), total phosphorus (TP), and total nitrogen (TN) between 1987, 2010, and 2019 are shown in Figure 5-7. ET and SQ are mostly characterized by increases of up to 10.8 mm and 11.4 mm, respectively from 1987 to 2019, with slight decreases by up to 3.8 mm in several subbasins between 2010 and 2019. The most significant increase in ET occurs in subbasins which show a larger increase in forest from 1987 to 2019, such as subbasins 8, 12 and 17 (Figure 5-5). SQ shows a stronger increase in the middle-western subbasins which experienced larger expansion of urban (Figure 5-5), with the strongest increase of SQ occurring in subbasins 15 and 17 that experienced the largest increase of urban area between 1987 and 2019. This might be attributed to the increased surface sealing (Anand et al., 2018; Sood et al., 2021). Contrarily, BF and WYLD have decreased by up to 20 mm and 13 mm, respectively in most subbasins in the periods 1987-2010 and 1987-2019, with slight increases between 2010 and 2019. The loads of SED, TP, and TN show notable decreasing trends from 1987 to 2019. Pronounced reductions of SED (7.8-18.2 t km^{-2}) occur in the relatively steeper northeastern corner (e.g., subbasins 3, 9-10) and the southwestern corner (e.g., subbasins 5 and 12) and subbasin 17, while the decrease is weaker in the mid-west. Overall, the changes in TP and TN loads show a weak decrease in the (mid) west and more pronounced decreases in the east and steeper southwest of the catchment (Figure 5-7). The most pronounced net decrease of TP and TN loads are observed in subbasins 12 and 17, corresponding to the largest decrease of arable land percentage (50% in subbasin 17, 30% in subbasin 12) between 1987 and 2019. The single subbasin that has experienced a slight increase of sediment or TP load is subbasin 1, which is characterized by the least reduction of arable land and minor decrease of forest. The most significant decrease in nutrients and sediment has occurred in subbasins which have experienced notable increases of pasture or forest and a decrease of arable land, e.g., subbasins 12 and 17 (Figure 5-5). Overall, variations in surface runoff, sediment,

TP, and TN are depicted by spatially explicit patterns on the subbasin scale. It is necessary to consider this spatial heterogeneity, when establishing management measures in order to improve water quality.

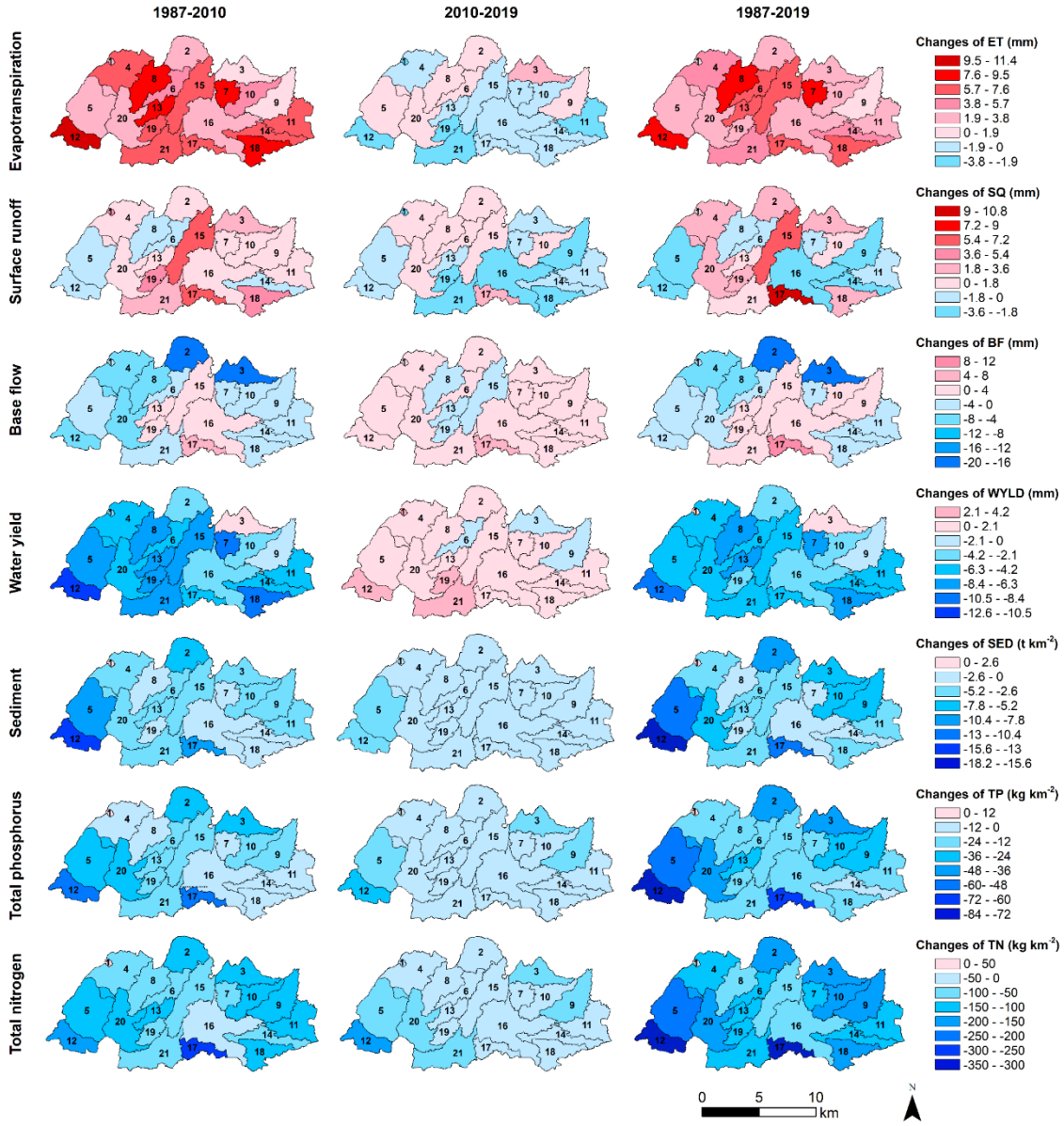

Figure 5-7. Spatial distribution of variations in water quantity and water quality variables during the periods of 1987-2010, 2010-2019, and 1987-2019 at subbasin scale.

5.3.4. Influences of changes in land use metrics on water quantity and quality

5.3.4.1. Contributions of LUCC to variations in water quantity and quality

A summary of the PLSR models separately constructed for ET, SQ, BF, WYLD, SED, TP and TN, is provided in Table 5-4. The prediction plots for the seven variables by applying the PLSR models are shown in Figure 5-8. The changes in water quantity

and quality could be reasonably explained by the constructed PLSR models ($0.61<R2<0.88$, $0.57<Q2<0.85$, Table 5-4). The comparison of the actual and predicted values (in Figure 5-8) illustrates the accuracy of the model calibration and cross-validation. For the ET and WYLD models, the percentage of unexplained variation decreases with increasing number of components, whereas the prediction error of cross-validated observations (indicated by cross-validated root mean squared error, RMSECV) is minimal with one or two components, respectively. This indicates that adding more components does not improve the correlation with the residuals of the response variables (Onderka et al., 2012). Overall, 60.5% and 68.3% of the variations in the changes in ET and WYLD can be explained by the first component and the first two components, respectively. Adding other components does not strongly increase the cumulative explained variations (only by +4.2-5.4%) in ET and WYLD changes from 1987 to 2019 (Table 5-4). For SQ, two components are extracted for the PLSR model, with 58.9% of variation is explained on the first component and cumulative explained variations increase to 81.3% when adding the second component. For all other variables, the minimum RMSECV is achieved with models using five components. For base flow, 37.4% of the variation in the dynamics is explained by the first component, cumulatively 64.2% adding the second component, and ultimately 87.7% with a consecutive addition of third, fourth, and fifth component. For the changes in loads of sediment, TP, and TN, the first component of the models always explains the majority of the variation (43.7-63%, Table 5-4). With all water quality variables together, approximately 75% of the variation is accurately explained on average.

Approximately 70-80% of the variations in water quantity and quality dynamics were explained by LUCC, underlining the importance of LUCC on catchment water resources. Better explanations (over 81%) of SQ and BF by LUCC confirmed the significant influences of landscape heterogeneity on surface runoff and groundwater dynamics (Kändler et al., 2017; Xu et al., 2020b; Zhang and Schilling, 2006). Only a quarter of the variations in sediment, TP, or TN cannot be interpreted by LUCC, which demonstrates that rural landscape patterns are essentially important in controlling nutrients pollution. The minor unexplained fraction may be attributed to potential changes in waste water treatment which sometimes remained constant in our modeling

approach. Lower explanation of TP may be additionally due to the lower SWAT model performance for TP, the susceptibility of P to soil or geomorphology properties (Maranguit et al., 2017; Noe et al., 2013). More than 60% of the variations in ET and WYLD are explained by LUCC. The unexplained fraction may be attributed to the different contributions from specific crops (included in SWAT) and the lumped agriculture land use class as well as the compensating effect of subbasins (Wagner et al., 2013).

Table 5-4. Summary of the PLSR models of evapotranspiration (ET), surface runoff (SQ), base flow (BF), water yield (WYLD), sediment yield (SED), total phosphorus load (TP) and total nitrogen load (TN) at subbasin scale**.**

Response	R^2	Q^2	Component	Explained variability in *Y* (%)	Cumulative explained variability in *Y* (%)	RMSECV	Q^2_{cum}
ET	0.61	0.57	**1**	60.5	60.5	2.32 (mm)	0.568
			2	2.4	62.9	2.35 (mm)	0.558
			3	1.2	64.1	2.44 (mm)	0.524
			4	0.2	64.3	2.41 (mm)	0.535
			5	0.4	64.7	2.41 (mm)	0.534
SQ	0.81	0.78	**1**	58.9	58.9	1.70 (mm)	0.561
			2	22.4	81.3	1.20 (mm)	0.783
BF	0.88	0.85	**1**	37.4	37.4	4.61 (mm)	0.230
			2	26.8	64.2	3.92 (mm)	0.442
			3	9.7	73.9	3.15 (mm)	0.640
			4	8.8	82.7	2.59 (mm)	0.757
			5	5.0	87.7	2.05 (mm)	0.847
WYLD	0.68	0.61	**1**	64.6	64.6	2.43 (mm)	0.611
			2	3.7	68.3	2.43 (mm)	0.614
			3	0.9	69.2	2.46 (mm)	0.602
			4	0.4	69.6	2.47 (mm)	0.598
			5	0.4	70.0	2.49 (mm)	0.592
SED	0.77	0.67	**1**	43.7	43.7	2.76 (t km^{-2})	0.382
			2	19.2	62.9	2.50 (t km^{-2})	0.493
			3	11.1	74.0	2.13 (t km^{-2})	0.630
			4	1.6	75.6	2.08 (t km^{-2})	0.650
			5	1.0	76.6	2.03 (t km^{-2})	0.667
TP	0.76	0.65	**1**	51.5	51.5	12.03 (kg km^{-2})	0.468
			2	10.7	62.2	11.14 (kg km^{-2})	0.544
			3	10.4	72.6	10.32 (kg km^{-2})	0.608
			4	3.0	75.6	9.80 (kg km^{-2})	0.647
			5	0.7	76.3	9.71 (kg km^{-2})	0.653
TN	0.73	0.68	**1**	63.0	63.0	43.04 (kg km^{-2})	0.597
			2	5.8	68.8	40.56 (kg km^{-2})	0.643
			3	3.1	72.1	39.20 (kg km^{-2})	0.666
			4	0.5	72.6	38.90 (kg km^{-2})	0.671
			5	0.7	73.3	38.51 (kg km^{-2})	0.678

Note: R^2 indicates the goodness of fit of the model; Q^2 indicates the cross-validated goodness of prediction; RMSECV indicates cross-validated root mean squared error; Q^2_{cum} indicates the cumulative cross-validated goodness of predication over all the selected PLSR components; the components selected for each model are highlighted in bold.

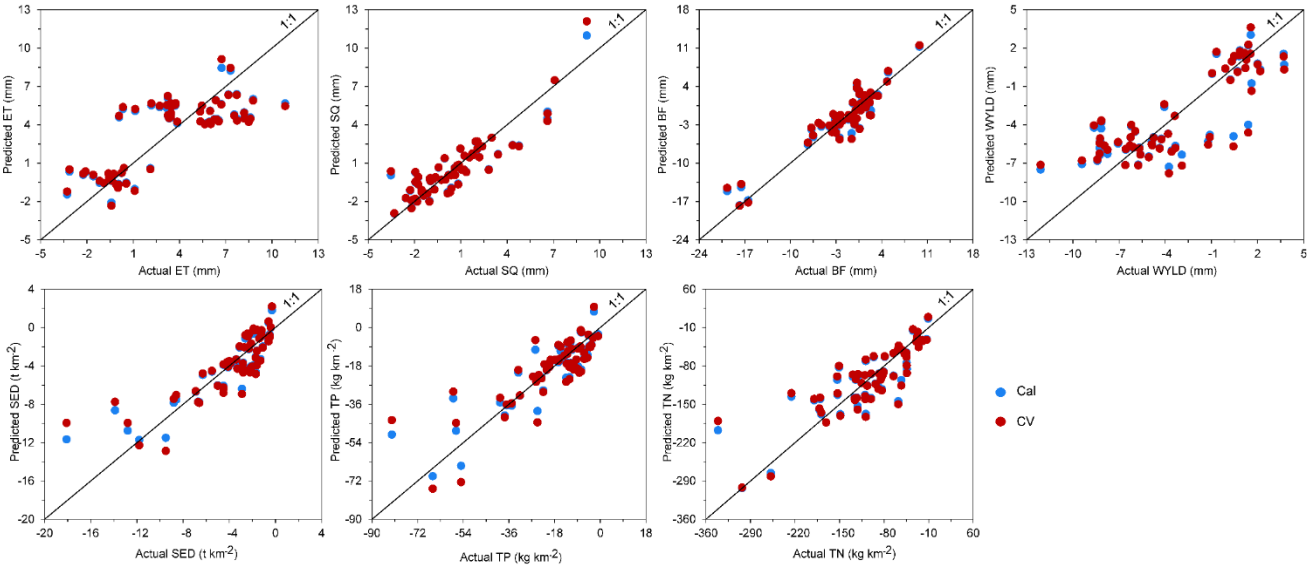

Figure 5-8. Comparison of subbasin-scale changes in evapotranspiration (ET), surface runoff (SQ), base flow (BF), water yield (WYLD), sediment (SED), total phosphorus (TP), and total nitrogen (TN) as derived from the SWAT model and the predicted values from the PLSR models. The changes were obtained based on land use changes between 1987 and 2010, 2010 and 2019, and between 1987 and 2019, respectively. Cal indicates calibration. CV indicates cross validation.

5.3.4.2. Effects of LUCC predictors on water quantity and quality

According to the PLSR results, each category of the landscape indices including percentage (PLAND), largest patch (LPI), shape (AWMSI), contiguity (CONTIGAW), aggregation (AI), or interspersion (IJI), plays an essential role in influencing as least one water quantity or quality variable (Table 5-5). The effects on the changes in ET, SQ, BF, WYLD, SED, TP, and TN are measured using weights, regression coefficients (RCs), and VIP values in the PLSR models. VIPs for predictors included into the models are greater than 0.8. For the ET model, the highest VIPs are obtained in predictors AIa and CONTIGAW*a* (VIP = 1.25, RCs = -0.122), followed by PLAND*a* (VIP = 1.037, RC = -0.101) and AI*u* (VIP = 1.03, RC = -0.1). ET tends to decrease with larger aggregation (AIa) and contiguity (CONTIGAW*a*) indices, and arable land percent (PLAND*a*) (negative RCs), whereas it increases with more pasture (PLAND*p*) (positive RC). In the case of surface runoff, the first and second components of the model are dominated by PLAND*u* on the positive side, with minor positive effect from PLAND*a* on the second component (Table 5-5). The urban area percent (PLAND*u*) obtains largest VIP of 1.173, and are identified as most important influencing the change in surface runoff. Surface runoff increases with an increase in arable (PLAND*a*)

and urban areas (PLAND*u*) (RCs=0.403, 1.161, respectively). For base flow, in addition to arable land, pasture plays a key role in explaining its variation. Arable land (PLAND*a*), pasture (PLAND*p*) percent and area-weighted shape index of pasture (AWMSI*p*) obtain the largest VIPs of 1.259, 1.03, and 1.063, respectively. All show negative correlations with base flow. AI*a* and CONTIGAM*a* are important predictors for water yield with large VIPs of 1.226 and 1.218, respectively. Their higher values result in an increase of water yield. For sediment, TP or TN models, the selected components are dominated by areal percentages of arable land and pasture, in addition to the landscape metrics of arable land. The models obtain the largest regression coefficients or VIPs for PLAND*a*, LPI*a*, or PLAND*p*. They have VIPs of 1.0113-1.173 for sediment, 1.089-1.305 for TP, 1.005-1.232 for TN, respectively. Inferred by the RCs, an increase in sediment, TP, or TN occurs with increasing arable land (RCs: 0.602-0.884), while a decrease may occur with higher percentage of arable land in largest patches (LPI*a*) (RCs: -0.74 - -0.225), or with more pasture area (RCs: -0.693 - -0.122).

LPI*a*, AI*a* and CONTIGAW*a* are the most important landscape structure indicators affecting water quantity or quality (VIP ≥1 most of the time, Table 5-5). AIa and CONTIGAW*a* have positive impacts on WYLD while negative impacts on ET. By definition, AI*a* and CONTIGAW*a* would increase, respectively, when arable landscape patches are more clumped and contiguous (Shi et al., 2013; Uuemaa et al., 2009). Clumped and connected agriculture patches with fewer edges have reduced more infiltration of runoff, compared to small scattered patches (Boongaling et al., 2018), thus resulting in the increase of water yield amount in the catchment. Our results also corroborate with Ayivi and Jha (2018) who reported that increased water yield and base flow occur with increasing cohesive and aggregated agriculture. Negative impacts on ET may be explained by the interactive changes between arable and pasture, i.e., arable land has been increased at the cost of losing pasture, and vice versa. The negative effect of AWMSI*p* on base flow implies that the coarse grass landscape has a higher capacity of absorbing and intercepting rainfall thereby resulting in lower base flow. Though landscape metrics are more often used to explain water quantity than quality variables (Table 5-5), the negative influences of LPI*a* on sediment and nutrients, and positive

influences of AWMSI*a* on sediment and TP cannot be overlooked. This is in agreement with previous findings that scattered and complicated agriculture patches are susceptible to soil erosion and thus water quality deterioration (Nafi'Shehab et al., 2021; Yan et al., 2013).

The change in the percentage of arable land is most responsible for water quantity and quality dynamics, with VIP values greater than 1 for all response variables but WYLD. This may be explained by the fact that the decrease in arable land is the strongest. The negative correlations between PLANDa and evapotranspiration (ET) and base flow (BF) imply that conversion of arable land to e.g., pasture or forest would result in increased ET and BF, due to higher capability of plant evapotranspiration and slower water transmission, which is in agreement with previous findings that perennial vegetation is more likely to increase ET (Li et al., 2017a; Peel et al., 2010) and the decrease in agriculture leads to increased annual base flow (Basuki et al., 2019). Changes of the percentage of arable land positively influence SQ, WYLD, SED TP, and TN loads. Less runoff interception by crops and additional runoff routes resulting from implementation of tillage practices (e.g., tractor road) can result in increased surface runoff (SQ). The lower ET amount of crops compared to pasture and forest is in part responsible for the increase in WYLD. Soil erosion might be accelerated due to uncovered and fragile soil by tillage practices implemented in cultivated areas as well as the increased surface runoff. N and P pollution is prone to occur in arable areas, which have a high risk of generating nutrient pollutants from excessive fertilizer or manure and eroded soil particles. The positive relationships between arable land percent and SQ, WYLD, SED TP, and TN loads are found in other studies as well (Mirghaed et al., 2018; Sood et al., 2021; Wagner et al., 2013; Wang et al., 2019). Pasture shows a positive influence on ET and negative influences on sediment, TP, and TN. This also illustrates that more grassland (or rangeland) would increase plant evapotranspiration process. Pasture can improve water quality due to reduced soil erosion and nutrient transportation rate, as well as the high uptake and infiltration of nutrients by vegetation cover (Ding et al., 2016; Hatano et al., 2005; Li et al., 2008).

By applying the quantitative results that the increases in arable or pasture areas most significantly intensify or reduce the risk of soil erosion and nutrient pollution,

respectively, individual subbasins can be identified as nutrient pollution "source" or "sink". Based on these results, it is possible to develop a set of more targeted strategies to effectively control diffuse pollution at a spatial scale. At the same time, best management practices such as proper fertilization, abate of traditional tillage, crop rotation, vegetation buffer, are important to improve water quality in rural catchments (Haas et al., 2017; Pott and Fohrer, 2017a). Urban expansion is most important influencing surface runoff, the increase in urban area percent results in an increase of it (regression coefficient value > 1.16, Table 5-5). Similar results have been found, e.g., by Shi et al. (2007) who discovered that increased urbanized land led to increased runoff, by increasing peak flood runoff and decreasing runoff confluence time, in a typical urbanized region (Shenzhen) in China. It is therefore necessary to increase the frequency of measuring runoff, sediment and nutrient, particularly during the course of storm flood events in settlement area. Unlike previous findings (Wang et al., 2018; Yan et al., 2013), forest properties have not exerted significant influences, probably due to only minor temporal changes in some landscape metrics, e.g., area percent (PLAND), dominance (LPI), and shape (AWMSI) of forest (Figure 5-6).

Table 5-5. Regression coefficients (RCs), VIP and weight values of each PLSR model.

Predictors	ET			SQ				BF							WYLD			
	RC	VIP	W*[1]	RC	VIP	W*[1]	W*[2]	RC	VIP	W*[1]	W*[2]	W* [3]	W* [4]	W* [5]	RC	VIP	W*[1]	W*[2]
PLAND*a*	-0.101	**1.037**	-0.017	0.403	0.790	-0.048	*0.189*	-1.654	**1.259**	-0.001	*-0.128*	*-0.135*	*-0.208*	*-0.201*	0.043	0.882	0.017	-0.042
PLAND*p*	0.089	0.918	0.015					-1.474	**1.030**	-0.034	0.024	*-0.117*	*-0.304*	*-0.256*	0.011	0.866	-0.015	0.072
PLAND*f*								-0.575	0.915	-0.035	-0.074	-0.072	-0.045	0.092				
PLAND*u*	0.080	0.818	0.013	1.161	**1.173**	0.090	*0.173*											
LPI*a*	-0.088	0.906	-0.015															
AWMSI*p*								-0.143	**1.063**	-0.052	-0.058	0.059	0.093	-0.013				
AWMSIf	0.085	0.870	0.014												-0.039	0.837	-0.016	0.041
AI*a*	-0.122	**1.254**	-0.020												0.187	**1.226**	0.024	0.025
AI*P*	-0.094	0.961	-0.016												0.100	0.924	0.018	-0.009
AI*u*	-0.100	**1.030**	-0.017												0.212	**1.068**	0.020	0.058
CONTIGAW*a*	-0.122	**1.251**	-0.020												0.184	**1.218**	0.024	0.024
CONTIGAW*P*	-0.087	0.891	-0.015												0.112	0.880	0.018	0.004
CONTIGAW*u*	-0.094	0.959	-0.016					0.281	0.805	0.040	0.029	-0.078	0.064	0.011	0.198	**1.007**	0.019	0.054
IJI*a*								0.038	0.859	0.040	0.024	0.098	*-0.142*	-0.091				

Predictors	SED							TP							TN						
	RC	VIP	W*[1]	W*[2]	W*[3]	W*[4]	W*[5]	RC	VIP	W*[1]	W*[2]	W*[3]	W*[4]	W*[5]	RC	VIP	W*[1]	W*[2]	W*[3]	W*[4]	W*[5]
PLAND*a*	0.602	**1.165**	0.027	0.038	*0.106*	0.037	0.040	0.755	**1.305**	0.029	0.031	*0.117*	*0.142*	0.059	0.884	**1.232**	0.033	*0.103*	*0.133*	*0.166*	*0.333*
PLAND*p*	-0.693	**1.173**	-0.026	-0.022	*-0.124*	-0.096	-0.099	-0.499	**1.089**	-0.025	-0.007	-0.099	-0.074	0.002	-0.122	**1.005**	-0.030	-0.054	-0.049	0.031	*0.324*
PLAND*u*	0.013	0.908	-0.022	-0.033	0.020	0.097	*0.116*	-0.045	**1.038**	-0.025	-0.033	0.005	0.057	*0.137*	0.028	**1.013**	-0.024	-0.032	0.052	*0.197*	0.093
PLAND*f*								-0.009	0.821	-0.016	-0.053	0.061	0.047	0.004							
LPI*a*	-0.632	**1.113**	0.015	-0.095	*-0.117*	-0.037	-0.070	-0.740	**1.205**	0.017	-0.064	-0.208	-0.091	-0.057	-0.225	0.945	0.023	-0.054	*-0.209*	0.028	0.019
LPI*p*	0.397	0.819	-0.009	0.075	0.086	-0.043	0.020														
AWMSI*a*	0.472	0.902	0.007	*0.103*	-0.017	0.073	0.080	0.492	0.817	0.008	0.087	0.020	0.093	0.085							
AWMSI*p*	-0.445	**1.087**	-0.023	-0.077	-0.050	-0.022	*0.107*	-0.152	0.872	-0.019	-0.031	-0.057	*0.127*	-0.001							
CONTIGAWa	0.039	0.877	0.023	-0.001	-0.042	-0.024	0.075	0.079	0.864	0.021	-0.027	-0.013	0.015	0.069	0.114	0.840	0.022	-0.072	0.037	0.019	0.077
AIa	-0.053	0.876	0.022	-0.006	-0.055	-0.039	0.041	0.008	0.856	0.021	-0.030	-0.025	0.000	0.052	-0.034	0.833	0.022	-0.081	0.015	-0.024	-0.038

Note: VIP values greater than 1 were marked in bold; the absolute weights greater than 0.1 were marked in Italic.

5.4. Conclusion

In this study the separate contributions of changes in land use on the dynamics of seven water quantity and quality variables, i.e., actual evapotranspiration (ET), surface runoff (SQ), base flow (BF), water yield (WYLD), sediment (SED), total phosphorus (TP), and total nitrogen (TN) loads have been quantified by applying an integrated approach of hydrological modeling (SWAT) and partial least squares regression (PLSR). The influences of the changes in individual landscape metrics on variations in water quantity and quality have been measured and identified using a scenario analysis for three different land use maps of the past.

With an exceptional data set that covers land use changes and three water quality campaigns over a period of three decades, a hydrologic model was set up and showed reasonable performance on the daily time scale. The results of the scenario analysis indicate that the dynamics of all water quantity and quality variables are largely explained (61-68% of the variations in ET and WYLD; 75-88% of the variations in other water quantity and quality variables) by land use changes (LUCC) between 1987 and 2019. Landscape metrics show a stronger effect on water quantity than on water quality. Moreover, water quantity and quality variables are most influenced by arable land change. The percentage (PLANDa), contiguity (CONTIGAWa), and aggregation (AIa) of arable land are identified as primary landscape metrics controlling the variations in BF, ET and WYLD. Greater percentages of settlement area and arable land may significantly accelerate runoff processes. Land planners and decision makers probably need to control land use patterns in runoff-sensitive areas to minimize negative impacts. Sediment, TP, and TN loads are closely associated with pasture and arable land. The expansion of arable land (PLANDa) may exacerbate soil erosion and P and N pollution. The arable land in large and aggregated (LPIa) or simpler shape (AWMSIa) patches can help to mitigate soil erosion and water quality deterioration. The results indicate that the smaller changes in forest did not exert significant influence on water quantity and quality.

The approach applied in this study identifies the important influences of land use changes on water quantity and quality, which are helpful for formulating an informed

and targeted plan with regard to land and water resource management. This approach is applicable to other catchments to predict both the water quality and hydrological responses to land use changes with the help of time-sequenced land use data.

Chapter 6 General discussion and conclusion

6.1. General discussion of research questions

Fresh water resources face a globally growing pressure, due to the rising water demands of a growing world population and improved living standards as well as the increasing human activities on river or lake systems. A major stress originates from land use change. Land use patterns are shaped by a range of spatially distributed catchment characteristics. The land use pattern greatly influences hydrological and water quality processes in catchments. Germany is characterized by an intensification of agricultural land use classes and nutrient pollution. The situation is critical in Northern Germany, due to the intensified agricultural landscape and related management practices of improving agriculture productivity in the lowland environment (Pott and Fohrer, 2017b; Schmalz et al., 2008a). As a result of the heterogeneity in land use distribution and transformation, water quality and quantity display pronounced spatial and temporal dynamics (Guse et al., 2015b; Lam et al., 2012). It is necessary to identify land use patterns and their explanatory variables to answer the first research question:

- Which variables typically affect land use patterns in rural lowland catchments of Northern Germany?

Variable impact

The logistic regression analysis results indicated that the spatial pattern of each land use class was determined by a composite of spatially distributed variables including topography, soil, socioeconomic and landscape indices for the Kielstau catchment. The semi-natural land use classes were likely to appear in areas with relatively higher topography. Soil property (like the clay, silt, sand or rock content of the first soil layer) mainly accounted for the distribution of different crops. The probability for winter wheat and barley, the major cereals in the catchment, increased with an increase of silt content. Grassland was more likely to be near the nature reserves, the Kielstau River and Lake Winderatt. Population density is a determinant for urban areas (Yue et al 201). Croplands tended to be distributed in land patches in simpler shape with a larger extent, because agricultural fields usually have straight edges and

large areas due to artificial reconstruction (Riitters, 2019). The drained soil share affected the appearance probability of seven land use classes. The probabilities for urban areas, garden or orchard decreased with an increase in the areal percent of drained soil, while the probability for pasture and field beans increased. These findings are in agreement with the purpose of exporting excess soil water by tile drainages in lowland areas to sustain agriculture activities (Schmalz and Fohrer, 2010). The variables distance to protected areas, drained soil share, and fractal dimension were assessed as the most important variables for explaining the distribution of land use classes. These variables relate to the key catchment characteristics of a rural landscape with a flood plain near the rivers. Topography variables were less important for rural land use patterns.

Prediction of land use patterns

By using the explanatory variables, the spatial relationships between different land use classes can be assessed with R-G-B composites of probability maps for them. No strong competition was observed between urban areas, grassland/pasture, and croplands, which illustrated that non-agricultural and agricultural classes are well distinguishable in space due to little exposure to population pressure in this rural environment. The major crops including winter wheat, winter rape, corn and winter barley compete for the same areas, indicating the high suitability for different crops. This result is supported by the prevailing implementation of crop rotations between dominant crops. Kandziora et al. (2014) reported that the commonly implemented crop rotation practices in Kielstau catchment consist of mixtures of rapeseed and cereals, of corn and cereals, or of corn, cereal, and rapeseed. This illustrates the simultaneous suitability of fields for winter cereals, corn and winter rape. The derived probability maps can be used to reasonably interpret the spatial distribution of different land use classes in the rural catchment.

The results are generally supported by findings from previous studies. Qureshi et al. (2013) also found that grassland rather than cropland was in vicinity to streams to maintain a good stream water quality. Spatial factors determining the locations of agriculture are linked to soil fertility and distance to markets (Mottet et al., 2006; Piquer-Rodríguez et al., 2018). Inkoom et al. (2018) and Fernandes et al. (2011)

demonstrated that patch shape index (perimeter-area ratio) is able to depict the spatial characteristics of landscape and modification gradients of natural land use. Hence, landscape metrics are useful to predict the presence of one certain land use class and applicable to land use modeling (Yang et al., 2014). They can provide important supplementary information to commonly used explanatory variables. Other studies may identify different important explanatory variables using a dataset with a coarser spatial resolution or in a catchment with different features.

The revealed complex interconnections of land use and other catchment characteristics in a changing rural environment have a potential impact on water quality. It is important to identify the key factors at different spatial scales that influence water quality to answer the second question.

- How does water quality evolve seasonally and spatially and how do land use and other catchment characteristics influence water quality at different spatial and season scales?

The major economic activity in the upper Stör catchment is agriculture. We analyzed the variabilities of water quality parameters between summer and winter, and at each outlet of twenty-one sub-catchments with spatially-varying soil, topography, and land use. Heterogeneity of land cover characteristics alter surface roughness, albedo and other properties of the catchment. In turn, the changes of catchment properties will cause hydrological processes and water quality to alter (Pratt and Chang, 2012; Yan et al., 2013). This study reveals the manifold variabilities of water quality in space and season under the influences of heterogeneous catchment characteristics.

Seasonal variability

Aggregating the monthly measurements into average values for summer (May to October) and winter (November to April), we find that stream water quality exhibits distinct seasonal differences. Nitrogen (N) and phosphorus (P) have higher levels in winter as compared to summer. This is primarily attributed to the lower interception and uptake of N and P by the less vegetation cover in winter, and the fertilization practices which take place in early spring (Pott and Fohrer, 2017b). Higher concentrations of electrical conductivity and chloride generally occur in summer than

winter. The lower level of dissolved oxygen in summer can be explained by the higher temperature.

Seasonal variations of stream water quality corroborated with previous findings. Poudel et al. (2013) indicated that N and P parameters had quite different concentrations in different seasons in an agriculture dominated catchment in the southern United States. Wagner et al. (2018) observed seasonally varying values of various nutrients in the lowland rural catchment of Kielstau in Germany. The seasonal distribution of water quality is probably related to the seasonal differences of flow regime and precipitation, and vegetation growth as well as the agricultural management schedules.

Spatial variability

The spatial variability of water quality results from the heterogeneity in the generation, delivery, mitigation and dilution of pollutants. In this study, highest values of electrical conductivity and chloride are observed near the biggest city (Neumunster) of the Stör catchment, likely due to higher release of ionized matter and major ions from effluents from urban waste water plants. Higher levels of N and P occur in proximity to either two major peat wetlands or relatively steeper fields affected by intensive agriculture or grazing activities. High redox potential in wetlands and abundant organic matters in peat soils explain the accumulation of nutrients to some extent. N and P may be retained in agricultural field at the excess of the fertilizer or manure amount demanded for crop growth and subsequently transported to streams (Yu et al., 2016). Moreover, the transportation or leaching process may be intensified by accelerated surface runoff occurring on a steeper slope (Ziegler et al., 2006). Low levels of N and P nutrients occur in middle west of the Stör catchment which is dominated by forest.

Key impacts

Among the different environmental variables, we found that dominant soil properties and land use area percent play the biggest part in explaining the overall variations in stream water quality. The nitrogen and phosphorus parameters are highly and positively influenced by the hydrologic property of soil (represented by the areal

ratio of hydrologic soil group A to group B, A/B) and areal percent of organic soil types, and more importantly, by the extent of steeper arable or grazing areas. However, a wider coverage of forest or sand content (in the first soil layer) may result in a reduction of nutrients, indicating that they are beneficial for improving stream water quality. The cause-effect findings highlight the principal features of a "lowland" and "rural" catchment. They demonstrated the significant effects of the prevailing soil (sandy soil) and land use (agriculture) on water quality in the catchment. The indice A/B measures the permeability of soil and a higher value of it results in the shallower groundwater table typical for lowland catchment, which consequently increase the nutrients recharge from groundwater to stream flow (Pott, 2014). Peat soils, mainly distributed along the streams and around the wetlands, are fertile and rich in humus matter, which can easily leach P components after mineralization in particular in summers (Chardon and Schoumans, 2007; Redeker, 2011). The higher percent of agriculture results in the water quality pollution in terms of TN, NO_3-N and TP. The risks of nutrient pollution may be intensified when farming activities (like cultivation and grazing) occur in steeper fields. The results illustrated that in order to keep a good status of stream water, it is necessary to give up the intensive grazing or traditional tillage on steeper areas, thus avoiding soil erosion (e.g., rill erosion) and eutrophication problems which are caused by abundant nutrient inputs (Buck et al., 2004; Wilson et al., 2014; Yu et al., 2016). This study revealed that landscape configuration and proximity play unneglectable roles in affecting dissolved oxygen, chloride, and nitrogen. A higher value of area weighted land shape index (representing a more complex shape of landscape) could help alleviate the pollution of chloride, TN, and NO_3-N, as is mainly depicted by forest. Positive correlations were found between the connectedness of landscape (measured by cohesive and contagious index) and chloride, TN, and NO_3-N. This is because the physically connected agriculture patches may increase transporting the residuals of fertilizer or pesticide which carry chloride or nitrogen chemicals into streams (Ding et al., 2016; Lee et al., 2009). Moreover, nitrogen inputs to streams may be decreased with further flow distance of agriculture. Lower levels of TP are more probable when grazing activities are located further away from streams. These findings confirm that landscape metrics have significant influences on chemical fluxes and

hydrological processes (Shen et al., 2015). The structure and proximity of land use should be incorporated in future research of investigating the key landscape characteristics of influencing nonpoint source pollution processes.

Scale effect

Redundancy analysis results revealed that the overall variations in water quality are better predicted by environmental factors at the sub-catchment scale than at smaller scales. This is confirmed in some previous studies that indicated that strongest correlations lie at the sub-catchment scale (Venohr et al., 2005b; Zhou et al., 2012). However, different findings have been observed in other catchments. Shi et al. (2017) reported that the 500 m riparian buffer is most contributive towards explaining water quality variations in a larger catchment (Dan river catchment: 16,800 km^2) in China. Zhou et al. (2012) indicated that diffuse pollution processes on the wider spatial scale are responsible for the major contaminants compared to those on smaller scales. Chen et al. (2016) found population density would result in worse pollution of salt and organic chemicals within the sub-catchments. The lowland landscape is characterized by small topography gradients and their effects are not strong until gradients become slightly more pronounced across the larger region and trigger its interactions with water quality. In addition to the effects of widespread agriculture landscape, the prevalent installation of agriculture tile drainages may favor the collection of nutrient residuals from agriculture fields across larger areas and the increase of N and P entries to streams (Williams et al., 2015). In summary, the reasons why sub-catchment environmental factors significantly influence the dynamics of water quality are primarily linked to the major features of the catchment, including prevailing agriculture and associated management practices as well as the installation of tile drainage in lowlands. In future studies of sustainable catchment management, it is necessary to address water resources and catchment characteristics on the most influential scale. Studies on the cause-effect of surrounding environments and water quality should be dedicated to the investigation of multiple scale effects. The effectiveness of riparian buffering effects shed light on the need of a comprehensive investigation of spatial buffer settings to address water quality

problems. However, a further investigation of different buffer strip widths, in particular smaller than the 500 m buffer used here, may provide more detailed insights.

- A hydrologic model was set up to represent the dynamics of water quantity and quality and to allow for a more detailed analysis of land use impacts on water quantity and quality to answer research question 3: How do water quality and quantity dynamically respond to the changes of each land use class and landscape indices at subbasin scale?

Model performance

A hydrologic model (SWAT) has been successfully constructed and applied to the calibration and validation of daily streamflow (30 years), sediment, TP, and TN (3 years) in the Stör catchment during 1990-2019. According to model performance statistics (Moriasi et al., 2007), the model achieved a very good performance for depicting daily streamflow at two upstream gauges (i.e., Padenstedt and Sarlhusen) and the outlet gauge (Willenscharen) of the catchment. The modeled streamflow is in agreement with the observed values most of the time. Differences are mainly represented by the underestimation of a few peak flows in winter. Haas et al. (2016) and Lam et al. (2010) also observed an underestimation of peak values with SWAT models in other lowland catchments in northern Germany. This might be due to the deficient performance of modeling single-event flood routing (Lam et al., 2012) and snow events (Myers et al., 2021) in the model. The model also shows a nearly good to good performance for representing daily TN loads within the three years of campaign measurements. Sediment is represented by the model with a satisfactory to good performance. TP gains a comparatively lower performance, which is however still satisfactory during the calibration period. The lower performances for TP may be attributed to short time series observations and different conditions during calibration and validation periods. A model study of a longer time series of daily water quality data is needed to improve model accuracy in the future. The underestimation of peak values in sediment, TP, and TN in winter is probably related to the underestimation of corresponding peak runoff values. In summary, the model reasonably represents the dynamics of streamflow and nutrients in the studied lowland catchment.

Land use changes

Between 1987 and 2019, agriculture, pasture (grassland), forest, and settlement area experienced different changes across the Stör catchment The main change of land use is the decrease of arable land while three other land use classes increase, particularly pasture land. Agriculture is mainly converted to pasture, with a pronounced reduction of it in northeast compared to northwestern part of the catchment. The lower decrease of agriculture in the northwest is partly due to the concurrent occurrence of the pasture areas being replaced by agriculture in that region. The changes between agriculture and pasture may be influenced by the "river renaturation" project that was recently initiated to stabilize the river shore and increase the riparian vegetation aiming to restore the main river segments to a nearly natural state as much as possible (Dickhaut, 2005; Gessner et al., 2010). The increase of forest occurs in the middle lowland part in which subbasins are already dominated by forest. The growth of natural landscape is in agreement with the incentive of landscape renaturation measures that are carried out in recent years. The settlement areas are unevenly scattered in space with the largest area in the subbasins influenced by the major city of Neumünster. The slight expansion of urbanization mainly occurs around the city of Neumünster. Temporally, land use percent exhibits similar changing trends between the periods of 1987-2010 and 2010-2019. Land use experienced more marked changes during the earlier period 1987-2010 than the latter period. Our results indicate that the landscape metrics dominance, shape, aggregation, and connectedness exhibit the evident changing trends in time, in addition to the change of areal percent of each land use class.

Dynamics in water quantity and quality

Modeling the dynamics of major components of water balance and nutrients under different land use scenarios (1987, 2010, and 2019), we find that the subbasin-scale variables of actual evapotranspiration (ET), surface runoff (SQ), baseflow (BF), water yield (WYLD), sediment (SED), total nitrogen (TN), and total phosphorus (TP) loads show distinct temporal and spatial variabilities. ET and SQ experience the respective increase in the majority of subbasins between 1987 and 2019. The largest increase of ET occurs in subbasins corresponding to larger increase of forest. This result agrees

with the general understanding that forest is associated with higher evapotranspiration due to the larger leaf area and denser vegetation cover (Oishi et al., 2010). At the subbasin scale, although the change magnitude of surface runoff is moderate, a pronounced increase of surface runoff still occurs in the mid-western part which is in proximity to Neumünster and influenced by urban expansion. The increase of surface runoff is mainly attributed to the increased impervious cover. Surface runoff exhibited stronger dynamics during period 1987-2010 than during period 2010 -2019. Moreover, the annual base flow and water yield have decreased during the period 1987-2010, while they increased in most of the subbasins between 2010 and 2019. Notable reductions are found in the annual average loads of suspended sediment, TP, and TN. The stronger decrease of sediment occurs in the southwestern and northeastern parts with relatively steeper slope. The increase of vegetation may reduce soil erosion, since natural vegetation can stabilize soil structure and intercept soil particles compared to agriculture land use (Yan et al., 2013). Driven by land use changes, TP is depicted by spatially explicit patterns which are similar to surface runoff change. This corroborate with the prevailing view that the P is largely immobile and its loss is mainly triggered by surface runoff (Smith et al., 2015). The most pronounced reduction of TP and TN occurred in subbasins affected by a decrease of cropland and increases of pasture and forest.

In summary, water quality and quantity dynamics show consistency to land use changes in time and space. Sediment and nutrient dynamics demonstrated that stream water quality is improved over time, probably due to the decrease of agricultural areas and strict rules of agriculture management practices, whereas other semi-natural land use classes increased.

Influences of land use composition and configuration

Based on the SWAT modeled results of dynamics in water quality and quantity components, the effects of individual land use class changes on each component were distinguished applying a partial least squares regression (PLSR) analysis (Abdi, 2010). Therefore, an approach integrating SWAT model with PLSR method was used to gain new insights on the influences of land use changes on water quality and quantity.

In this section, we analyze the contributions of land use changes on the spatial and temporal variability of water quality and quantity. Further, we investigate the main effects of separate land use indices on seven variables of water quality and quantity. Results showed that the modeled changes of seven main water resources variables can be reasonably explained by the land use indices through the PLSR models. Compared to other variables, the respective variation of SQ, SED or TN load are better explained by LUCC. This demonstrates that the LUCC of rural landscape significantly alter the surface runoff and related water quality process (Kändler et al., 2017; Xu et al., 2020b). However, other variables still have more than 2/3 of their individual variations accurately explained by the changes of land use composition and configuration indices. The explanations may be additionally affected by the efficiency of the SWAT model, the differences between specific crops (represented in SWAT) and the simple lumped class of agriculture (PLSR). Nevertheless, the higher contributions of LUCC indicate that there are strong associations between land use change and water quality and quantity.

Among all the landscape metrics, arable land percent is the most influential in altering water resources. This is because the land use change is dominated by the decrease of arable land. A reduction of arable land may result in a decrease of ET and BF, as the decreased area is mainly converted to pasture or forest with more plant evapotranspiration and slower water transmission (Li et al., 2017a; Peel et al., 2010). The increase of ET is prone to be caused by the growth of more perennial vegetation. Basuki et al. (2019) demonstrated that the decrease of agriculture resulted in the increase of base flow. It was found that the increase of arable land is the main factor responsible for the increase of SED, TP, or TN loads, which is in agreement with previous studies (Bu et al., 2014; Shi et al., 2017; Zhou et al., 2012). Soils are more susceptible to erosion and loss problems in cultivated areas, in which the tillage practices probably cause loosen and fragile soil structure and influence surface runoff processes (Klik and Rosner, 2020; Turtola et al., 2007). The area percent of pasture is found to be positively correlated with ET while negative with WYLD, SED, TP, and TN. This finding confirms that increased grassland (or rangeland) may increase ET whereas it may decrease of WYLD (Hu et al., 2009; Li et al., 2017b). Moreover, Ding

et al. (2016) and Li et al. (2008) illustrated that the increase of pasture may improve water quality, since grass vegetation can take up and filter more nutrients and reduce soil and water loss. Urban expansion has the greatest impact on the increase of surface runoff. Shi et al. (2007) revealed that the increase of urban (impervious) areas would result in elevated flooding peaks and decreased runoff confluence time.

The landscape metrics of arable land strongly affect water quality and quantity. The larger values of aggregation (AI*a*) or contiguity (CONTIGAW*a*) for arable land cause higher WYLD and lower ET. This can be in part explained by the fact that the clumped and contiguous agriculture land patches with fewer edges have lower infiltration of runoff than small scattered land patches, thus leading to more water yield remained in the catchment (Boongaling et al., 2018). The main land use change pattern (i.e., interactive changes between agriculture and pasture) can partly explain the negative influences of contiguity and aggregation degree of agriculture on ET. AI*a* and CONTIGAW*a* showed negative influences on sediment, TP and TN. Nafi'Shehab et al. (2021) and Yan et al. (2013) reported that the agriculture is more likely to cause soil erosion and thus water quality pollution when it is of more scattered and disaggregated land patches.

In this study, the variability of water quality and quantity are largely correlated with the major LUCC in the subbasins. The subbasin scale serves as the unit of the relationships between water resources and LUCC. Our results illustrated that it is meaningful to propose more targeted strategies to effectively reduce diffuse pollution at this spatial scale.

6.2. General conclusion

This PhD thesis provides a comprehensive understanding and new information about rural landscape patterns and their relationships with hydrology in two rural lowland catchments in Northern Germany. In general, key catchment characteristics for predicting a rural landscape have been identified and their effects on spatio-temporal dynamics of water resources have been analyzed. The “cause-effect” relationships were assessed using major features of rural catchments across different spatial and temporal scales. The following key findings and achievements can be deduced from this work:

(1) Land use patterns can be reasonably explained by spatially explicit catchment characteristics. These patterns as well as soil properties strongly affected seasonal water quality.
(2) Water quality pollution by sediment, TP, and TN has been generally improved in Willenscharen (outlet of Stör catchment) over time.
(3) Land use effects on water quality vary with spatial scale settings, which was more significant at larger scale (i.e., subbasin scale).
(4) Disentangling complex effects of the land use composition and configuration is essential, as their changes can accurately predict the dynamics of water quantity and quality.
(5) It is valuable to identify the key factors and spatial scales that influence water resources. The study allows for an attribution of causality of environmental factors and water resources with a hydrological model.

This thesis contributes to the investigation of water quality and land use within a time span of 30 years in rural lowlands applying combined approaches of multivariate analyses and hydrological modeling. It improves our understanding of the interactions between a changing environment and land use, and their influences on dynamics of water quantity and quality. The approaches covered in the thesis are applicable to other areas. The work shows that monitoring water quality and land use at high spatial and temporal resolution is essential to investigate their interplay and provide comprehensive insights for effective catchment management of land and water resources.

6.3. Outlook

The complex landscape characteristics of rural lowland catchments in Germany impose various influences on hydrological process and water quality. This research addressed water quality and quantity changes in response to varying land use and other catchment characteristics in the Stör catchment. Our results revealed that the spatial and overall variations in water quality are more related to environmental factors at larger scale (subbasin scale). However, the effective spatial scale differs with different water quality parameters. Therefore, multiple scale studies are worth more efforts and future water quality management should consider the spatial-scale effectiveness. The water

quality and quantity dynamics were found to be mainly explained by the changes of arable land and pasture. However, the arable land is a lumped land use class. Therefore, the cause-effect effects can provide only general insights into management. To facilitate a more detailed and targeted management plan, the influences of individual crops should be separated in future study and further investigations on land use and water quality data are needed. To come up with effective and sustainable catchment management, scientific research outputs are still required. Detailed investigation of the influences of land use changes on water quality and quantity dynamics, by considering the composition and configuration of each land use class, multiple spatial scales, and temporal and spatial variations in water resources and land use, is needed to be furthered. The future research could be directed towards an integrated hydrological and land use modeling. A combined analysis of water quality and quantity by making use of longer time series of high-resolution measured data is necessary.

References

Abbaspour, K.C. et al., 2015. A continental-scale hydrology and water quality model for Europe: Calibration and uncertainty of a high-resolution large-scale SWAT model. Journal of Hydrology, 524: 733-752.

Abdi, H., 2010. Partial least squares regression and projection on latent structure regression (PLS Regression). Wiley interdisciplinary reviews: computational statistics, 2(1): 97-106.

Aghsaei, H., Dinan, N.M., Moridi, A., Asadolahi, Z., Delavar, M., Fohrer, N., Wagner, P.D., 2020. Effects of dynamic land use/land cover change on water resources and sediment yield in the Anzali wetland catchment, Gilan, Iran. Science of the Total Environment, 712: 136449

Ahearn, D.S. et al., 2005. Land use and land cover influence on water quality in the last free-flowing river draining the western Sierra Nevada, California. Journal of Hydrology, 313(3-4): 234-247.

Al-Awadhi, T., Mansour, S., 2015. Spatial Assessment of Water Quantity Stress in Sultanate of Oman Provinces: A GIS Based Analysis of Water Resources Variability. Journal of Geographic Information System, 7(06): 565.

Alberti M, 2005. The effects of urban patterns on ecosystem function. International Regional Science Review, 28(2): 168–192.

Alberto, W.D. et al., 2001. Pattern recognition techniques for the evaluation of spatial and temporal variations in water quality. a case study:: Suquía River Basin (Córdoba–Argentina). Water research, 35(12): 2881-2894.

Allan, J.D., 2004. Landscapes and riverscapes: the influence of land use on stream ecosystems. Annu. Rev. Ecol. Evol. Syst., 35: 257-284.

Álvarez-Cabria, M., Barquín, J., Peñas, F.J., 2016. Modelling the spatial and seasonal variability of water quality for entire river networks: relationships with natural and anthropogenic factors. Sci. Total Environ. 545, 152–162.

Amin, M.M., Veith, T.L., Shortle, J.S., Karsten, H.D., Kleinman, P.J., 2020. Addressing the spatial disconnect between national-scale total maximum daily loads and localized land management decisions. Journal of Environmental Quality, 49(3): 613.

Amiri, B. J., Fohrer, N., Cullmann, J., Hörmann, G., Müller, F., & Adamowski, J., 2016. Regionalization of tank model using landscape metrics of catchments. Water Resources Management, 30(14), 5065-5085.

Amiri, B.J., Junfeng, G., Fohrer, N., Mueller, F., Adamowski, J., 2018. Regionalizing flood magnitudes using landscape structural patterns of catchments. Water Resour. Manage. 32, 2385–2403.

Amiri, B.J., Nakane, K., 2009. Modeling the linkage between river water quality and landscape metrics in the Chugoku district of Japan. Water resources management, 23(5): 931-956.

Anand, J., Gosain, A.K., Khosa, R., 2018. Prediction of land use changes based on Land Change Modeler and attribution of changes in the water balance of Ganga basin to land use change using the SWAT model. Science of the total environment, 644: 503-519.

Andry, H., Yamamoto, T., Irie, T., Moritani, S., Inoue, M., Fujiyama, H., 2009. Water retention, hydraulic conductivity of hydrophilic polymers in sandy soil as affected by temperature and water quality. J. Hydrol. 373, 177–183.

Antolini, F. et al., 2020. Flood risk reduction from agricultural best management practices. JAWRA Journal of the American Water Resources Association, 56(1): 161-179.

Aquilué N, De Cáceres M, Fortin M J et al., 2017. A spatial allocation procedure to model land-use/land-cover changes: Accounting for occurrence and spread processes. Ecological Modelling, 344: 73–86.

Aredo, M.R., Hatiye, S.D., Pingale, S.M., 2021. Impact of land use/land cover change on stream flow in the Shaya catchment of Ethiopia using the MIKE SHE model. Arabian Journal of Geosciences, 14(2): 1-15.

Arnold, J., Kiniry, J., Srinivasan, R., Williams, J., Haney, E., Neitsch, S., 2013. SWAT 2012 input/output documentation, Texas Water Resources Institute.

Arnold, J.G., Srinivasan, R., Muttiah, R.S., Williams, J.R., 1998. Large area hydrologic modeling and assessment part I: model development 1. JAWRA Journal of the American Water Resources Association, 34(1): 73-89.

Arsanjani J J, Helbich M, Kainz W et al., 2013. Integration of logistic regression, Markov chain and cellular automata models to simulate urban expansion. International Journal of Applied Earth Observation and Geoinformation, 21: 265–275.

Astuti, I.S., Sahoo, K., Milewski, A., Mishra, D.R., 2019. Impact of land use land cover (LULC) change on surface runoff in an increasingly urbanized tropical watershed. Water Resources Management, 33(12): 4087-4103.

Ayivi, F., Jha, M.K., 2018. Estimation of water balance and water yield in the Reedy Fork-Buffalo Creek Watershed in North Carolina using SWAT. International Soil and Water Conservation Research, 6(3): 203-213.

Bai, X., Shen, W., Wang, P., Chen, X., He, Y., 2020. Response of Non-point Source Pollution Loads to Land Use Change under Different Precipitation Scenarios from a Future Perspective. Water Resources Management, 34(13): 3987-4002.

Baker, T.J., Miller, S.N., 2013. Using the Soil and Water Assessment Tool (SWAT) to assess land use impact on water resources in an East African watershed. Journal of hydrology, 486: 100-111.

Barceló, D., Sabater, S., 2010. Water quality and assessment under scarcity. Prospects and challenges in Mediterranean watersheds. Journal of hydrology (Amsterdam), 383(1-2).

Basisgewässernetz des Landes Schleswig-Holstein für das Einzugsgebiet der Treene bis Treia. (Arc-View- Shape), Flintbek.

Basuki, T.M., Nugrahanto, E.B., Pramono, I.B., Wijaya, W.W., 2019. Baseflow and lowflow of catchments covered by various old teak forest areas. Journal of Degraded and Mining Lands Management, 6(2): 1609.

Baumann M, Kuemmerle T, Elbakidze M et al., 2011. Patterns and drivers of post-socialist farmland abandonment in Western Ukraine. Land Use Policy, 28(3): 552–562.

Becker, H.T., Kristina 2017. Sustainable Development in Germany - Indicator Report 2016. Federal Statistical Office (Destatis), p. 152.

Betts, R.A., Falloon, P.D., Goldewijk, K.K., Ramankutty, N., 2007. Biogeophysical effects of land use on climate: Model simulations of radiative forcing and large-scale temperature change. Agricultural and forest meteorology, 142(2-4): 216-233.

BGR, 1999. BUK 200, Bodenubersichtskarte 1 : 200 000 . Bundesanstalt für Geowissenschaften und Rohstoffe: CC.1518 Flensburg, Hannover.

Bhaduri, A. et al., 2016. Achieving sustainable development goals from a water perspective. Frontiers in Environmental Science, 4: 64.

Bicknell, B. R., Imhoff, J. C., Kittle, J. L., Jobes, T. H., Donigian, A. S., Johanson, R., 2001. Hydrological simulation program-Fortran: HSPF version 12 user's manual AQUA TERRA Consultants.

Bieger, K., Hörmann, G., Fohrer, N., 2014. Simulation of streamflow and sediment with the soil and water assessment tool in a data scarce catchment in the three gorges region, China. Journal of environmental quality, 43(1): 37-45.

Bin, L., Xu, K., Xu, X., Lian, J., Ma, C., 2018. Development of a landscape indicator to evaluate the effect of landscape pattern on surface runoff in the Haihe River Basin. Journal of hydrology, 566: 546-557.

Blöschl, G. et al., 2019. Twenty-three unsolved problems in hydrology (UPH)–a community perspective. Hydrological sciences journal, 64(10): 1141-1158.

Bonan G B, DeFries R S, Coe M T et al., 2012. Land use and climate. In: Land Change Science. Dordrecht: Springer, 301–314.

Boongaling, C.G.K., Faustino-Eslava, D.V., Lansigan, F.P., 2018. Modeling land use change impacts on hydrology and the use of landscape metrics as tools for watershed management: The case of an ungauged catchment in the Philippines. Land use policy, 72: 116-128.

Bormann, F., Likens, G., Eaton, J., 1969. Biotic regulation of particulate and solution losses from a forest ecosystem. BioScience, 19(7): 600-610.

Borrelli, P. et al., 2017. An assessment of the global impact of 21st century land use change on soil erosion. Nature communications, 8(1): 1-13.

Brandes, D., Hoffmann, J.G., Mangarillo, J.T., 2005. Base flow recession rates, low flows, and hydrologic features of small watersheds in PENNSYLVANIA, USA 1. JAWRA J. Am. Water Resour. Assoc. 41, 1177–1186.

Brandes, E., McNunn, G.S., Schulte, L.A., Bonner, I.J., Muth, D.J., Babcock, B.A., Sharma, B. and Heaton, E.A., 2016. Subfield profitability analysis reveals an economic case for cropland diversification. Environmental Research Letters, 11(1), p.014009.

Broussard, W., Turner, R.E., 2009. A century of changing land-use and water-quality relationships in the continental US. Front. Ecol. Environ. 7, 302–307.

Bu, H., Meng, W., Zhang, Y., Wan, J., 2014. Relationships between land use patterns and water quality in the Taizi River basin, China. Ecol. Ind. 41, 187–197.

Buck, O., Niyogi, D.K., Townsend, C.R., 2004. Scale-dependence of land use effects on water quality of streams in agricultural catchments. Environmental pollution, 130(2): 287-299.

Carlson, T.N., Arthur, S.T., 2000. The impact of land use—land cover changes due to urbanization on surface microclimate and hydrology: a satellite perspective. Global and planetary change, 25(1-2): 49-65.

Chan, K.M., Vu, T.T., 2017. A landscape ecological perspective of the impacts of urbanization on urban green spaces in the Klang Valley. Applied Geography, 85: 89-100.

Chang, Y., Hou, K., Li, X., Zhang, Y., Chen, P., 2018. Review of land use and land cover change research progress, IOP Conference Series: Earth and Environmental Science. IOP Publishing, pp. 012087.

Chardon, W., Schoumans, O., 2007. Soil texture effects on the transport of phosphorus from agricultural land in river deltas of Northern Belgium, The Netherlands and North-West Germany. Soil Use Manag. 23, 16–24.

Chen, Q., Mei, K., Dahlgren, R.A., Wang, T., Gong, J., Zhang, M., 2016. Impacts of land use and population density on seasonal surface water quality using a modified geographically weighted regression. Science of the total environment, 572: 450-466.

Corsi, S.R., De Cicco, L.A., Lutz, M.A., Hirsch, R.M., 2015. River chloride trends in snow- affected urban watersheds: increasing concentrations outpace urban growth rate and are common among all seasons. Sci. Total Environ. 508, 488–497.

Crosbie, B., Chow-Fraser, P., 1999. Percentage land use in the watershed determines the water and sediment quality of 22 marshes in the Great Lakes basin. Can. J. Fish. Aquat. Sci. 56, 1781–1791.

Daniel, M.H., Montebelo, A.A., Bernardes, M.C., Ometto, J.P., De Camargo, P.B., Krusche, A.V., Ballester, M.V., Victoria, R.L., Martinelli, L.A., 2002. Effects of urban sewage on dissolved oxygen, dissolved inorganic and organic carbon, and electrical conductivity of small streams along a gradient of urbanization in the Piracicaba river basin. Water Air Soil Pollut. 136, 189–206.

Daoud, J.I., 2017. Multicollinearity and regression analysis. In: Journal of Physics: Conference Series (vol. 949, No. 1, p. 012009). IOP Publishing.

DeFries, R., Eshleman, K.N., 2004. Land-use change and hydrologic processes: a major focus for the future. Hydrological processes, 18(11): 2183-2186.

Deng, J.S., Wang, K., Hong, Y., Qi, J.G., 2009. Spatio-temporal dynamics and evolution of land use change and landscape pattern in response to rapid urbanization. Landscape and urban planning, 92(3-4): 187-198.

Deng, X., Huang, J., Rozelle, S., Uchida, E., 2010. Economic growth and the expansion of urban land in China. Urban studies, 47(4): 813-843.

Deutsche Einheitsverfahren, 1997. Selected Methods of Water Analysis, Bd. I, II. VEB Gustav Fisher, Jena (in German).

Di, H., Cameron, K., 2005. Reducing environmental impacts of agriculture by using a fine particle suspension nitrification inhibitor to decrease nitrate leaching from grazed pastures. Agric. Ecosyst. Environ. 109, 202–212.

Dickhaut, W., 2005. Fließgewässerrenaturierung Heute–Forschung zu Effizienz und Umsetzungspraxis–Abschlussbericht. Hochschule für angewandte.

Ding, J., Jiang, Y., Liu, Q., Hou, Z., Liao, J., Fu, L., Peng, Q., 2016. Influences of the land use pattern on water quality in low-order streams of the Dongjiang River basin, China: a multi-scale analysis. Science of the total environment, 551: 205-216.

Dissart J C, Vollet D, 2011. Landscapes and territory-specific economic bases. Land Use Policy, 28(3): 563–573.

Dodds, W.K., Oakes, R.M., 2008. Headwater influences on downstream water quality. Environmental management, 41(3): 367-377.

Donmez, C., Sari, O., Berberoglu, S., Cilek, A., Satir, O., Volk, M., 2020. Improving the Applicability of the SWAT Model to Simulate Flow and Nitrate Dynamics in a Flat Data-Scarce Agricultural Region in the Mediterranean. Water, 12(12): 3479.

Donohue, I., McGarrigle, M.L., Mills, P., 2006. Linking catchment characteristics and water chemistry with the ecological status of Irish rivers. Water Res. 40, 91–98.

Dow, C.L., Arscott, D.B., Newbold, J.D., 2006. Relating major ions and nutrients to watershed conditions across a mixed-use, water-supply watershed. J. North Am. Benthol. Soc. 25, 887–911.

DWD, 2009. Weather and Climate Data from the German Weather Service., Offenbach, Station Flensburg 1957–2006 and Station Meierwik, 1993–2008, 1993–2008 ed, Offenbach.

DWD, 2020. Deutscher Wetterdienst. Precipitation data 1990–2019, Climate stations

DWD, 2020a. Deutscher Wetterdienst. Climate data 1990–2019, Climate station Pony Padenstedt. https://opendata.dwd.de/climate_environment/CDC/. Accessed in July 2020.

DWD, 2020b. Deutscher Wetterdienst. Precipitation data 1990–2019, Precipitation stations Haale, Padenstedt, Nettelsee and Itzehoe, Climate data 1990-2019, Climate station Pony Padenstedt. https://opendata.dwd.de/climate_environment/CDC/. Accessed in July 2020.

EEA, 2005. Source apportionment of nitrogen and phosphorus inputs into the aquatic environment. EEA Report No. 7/ 2005. European Environment Agency, Copenhagen, 48 pp.

Ehlers, E., 2016. From HDP to IHDP: Evolution of the International Human Dimensions of Global Environmental Change Programme (1996–2014), Handbook on Sustainability Transition and Sustainable Peace. Springer, pp. 359-376.

Einheitsverfahren, D., 1997. Selected Methods of Water Analysis, Bd. I, II. VEB Gustav Fisher, Jena (in German).

Elfert, S., Bormann, H., 2010. Simulated impact of past and possible future land use changes on the hydrological response of the Northern German lowland 'Hunte'catchment. Journal of Hydrology, 383(3-4): 245-255.

El-Kawy O A, Rød J, Ismail H et al., 2011. Land use and land cover change detection in the western Nile delta of Egypt using remote sensing data. Applied Geography, 31(2): 483–494.

Etter A, McAlpine C, Wilson K et al., 2006. Regional patterns of agricultural land use and deforestation in Co- lombia. Agriculture, ecosystems & environment, 114(2–4): 369–386.

Fan, M., Shibata, H., 2015. Simulation of watershed hydrology and stream water quality under land use and climate change scenarios in Teshio River watershed, northern Japan. Ecological Indicators, 50: 79-89.

Farjad, B., Pooyandeh, M., Gupta, A., Motamedi, M., Marceau, D., 2017. Modelling interactions between land use, climate, and hydrology along with stakeholders' negotiation for water resources management. Sustainability, 9(11): 2022.

Federal Statistical Office., 1991-2012. Statistisches Jahrbuch für die Bundesrepublik Deutschland. Statistisches Bundesamt.

Feranec J, Jaffrain G, Soukup T et al., 2010. Determining changes and flows in European landscapes 1990–2000 using CORINE land cover data. Applied Geography, 30(1): 19–35.

Fernandes, A.C.P., de Oliveira Martins, L.M., Pacheco, F.A.L., Fernandes, L.F.S., 2021. The consequences for stream water quality of long-term changes in landscape patterns: Implications for land use management and policies. Land Use Policy, 109: 105679.

Fernandes, M.R., Aguiar, F.C., Ferreira, M.T., 2011. Assessing riparian vegetation structure and the influence of land use using landscape metrics and geostatistical tools. Landscape and Urban Planning, 99(2): 166-177.

Ferreira, A., Fernandes, L.S., Cortes, R., Pacheco, F., 2017. Assessing anthropogenic impacts on riverine ecosystems using nested partial least squares regression. Science of the Total Environment, 583: 466-477.

Fichera C R, Modica G, Pollino M, 2012. Land Cover classification and change-detection analysis using multi-temporal remote sensed imagery and landscape metrics. European Journal of Remote Sensing, 45(1): 1–18.

Fiener, P., Auerswald, K., Van Oost, K., 2011. Spatio-temporal patterns in land use and management affecting surface runoff response of agricultural catchments—A review. Earth-Science Reviews, 106(1-2): 92-104.

Finnern, J., 1997. Böden und Leitbodengesellschaften des Störeinzugsgebietes in Schleswig-Holstein: Vergesellschaftung und Stoffaustragsprognose (K, Ca, Mg) mittels GIS. Schriftenreihe des Instituts für Pflanzenernährung und Bodenkunde der Universität Kiel, Kiel.

Fischer, J., Hartel, T., Kuemmerle, T., 2012. Conservation policy in traditional farming landscapes. Conservation letters, 5(3): 167-175.

Fitzpatrick, M., Long, D., Pijanowski, B., 2007. Exploring the effects of urban and agricultural land use on surface water chemistry, across a regional watershed, using multivariate statistics. Applied Geochemistry, 22(8): 1825-1840.

Fohrer N. , Schmalz B., 2012. Das UNESCO Ökohydrologie-Referenzprojekt Kielstau-Einzugsgebiet–nachhaltiges Wasserressourcenmanagement und Ausbildung im ländlichen Raum (in German). Hydrologie und Wasserbewirtschaftung 56(4): 160–168.

Fohrer, N., Dietrich, A., Kolychalow, O., Ulrich, U., 2014. Assessment of the environmental fate of the herbicides flufenacet and metazachlor with the SWAT model. Journal of environmental quality, 43(1), 75-85.

Fohrer, N., Haverkamp, S., & Frede, H. G. (2005). Assessment of the effects of land use patterns on hydrologic landscape functions: development of sustainable land use concepts for low mountain range areas. Hydrological Processes: An International Journal, 19(3), 659-672.

Fohrer, N., Schmalz, B., Tavares, F., Golon, J., 2007. Modelling the landscape water balance of mesoscale lowland catchments considering agricultural drainage systems. Hydrologie und Wasserbewirtschaftung/Hydrology and Water Resources Management-Germany, 51(4): 164-169.

Foley, J.A., DeFries, R., Asner, G.P., Barford, C., Bonan, G., Carpenter, S.R., Chapin, F.S., Coe, M.T., Daily, G.C., Gibbs, H.K., 2005. Global consequences of land use. science, 309(5734): 570-574.

Forman R T, Godron M, 1981. Patches and structural components for a landscape ecology. BioScience, 31(10): 733–740.

Forman, R.T., 1995. Some general principles of landscape and regional ecology. Landscape ecology, 10(3): 133-142.

Fuchs, S., Weber, T., Wander, R., Toshovski, S., Kittlaus, S., Reid, L., Bach, M., Klement, L., Hillenbrand, T., Tettenborn, F., 2017. Effizienz von Maßnahmen zur Reduktion von Stoffeinträgen. Endbericht. UBA-Texte, 5: 2017.

Galpern, P., Gavin, M.P., 2020. Assessing the potential to increase landscape complexity in Canadian Prairie croplands: a multi-scale analysis of land use pattern. Frontiers in Environmental Science, 8: 31.

Gao, J., Xiong, Z., Zhang, J., Zhang, W., Mba, F.O., 2009. Phosphorus removal from water of eutrophic Lake Donghu by five submerged macrophytes. Desalination, 242(1-3): 193-204.

Gémesi, Z., Downing, J.A., Cruse, R.M., Anderson, P.F., 2011. Effects of watershed configuration and composition on downstream lake water quality. Journal of environmental quality, 40(2): 517-527.

Gerrish, J., Peterson, P., Morrow, R., 1995. Distance cattle travel to water affects pasture utilization rate. American Forage and Grassland Council.

Gessner, J., Spratte, S., Kirschbaum, F., 2010. Störe für die Stör–Wem hilft ein lebendes Fossil. Steinburger Jahrbuch, 54: 247-273.

Getachew, H.E., Melesse, A.M., 2012. The impact of land use change on the hydrology of the Angereb Watershed, Ethiopia. International Journal of Water Sciences, 1(6).

Ghimire, C.P., Bruijnzeel, L.A., Lubczynski, M.W., Ravelona, M., Zwartendijk, B.W., van Meerveld, H.I., 2017. Measurement and modeling of rainfall interception by two differently aged secondary forests in upland eastern Madagascar. Journal of hydrology, 545: 212-225.

Giri, S., Qiu, Z., 2016. Understanding the relationship of land uses and water quality in Twenty First Century: a review. J. Environ. Manage. 173, 41–48.

Gleick, P.H., 2000. A look at twenty-first century water resources development. Water international, 25(1): 127-138.

Goldewijk, K.K., Ramankutty, N., 2004. Land cover change over the last three centuries due to human activities: The availability of new global data sets. GeoJournal, 61(4): 335-344.

Golon J, 2009. Enviromental Effects of varied Energe Crop Cultivation Scenarios on a Lowland Catchment in Northern Germany A SWAT Approach,Thesis (Master), Ecology Centre. Kiel University.

Gong, X., Bian, J., Wang, Y., Jia, Z., Wan, H., 2019. Evaluating and Predicting the Effects of Land Use Changes on Water Quality Using SWAT and CA–Markov Models. Water Resources Management, 33(14): 4923-4938.

Grafius, D.R., Corstanje, R., Harris, J.A., 2018. Linking ecosystem services, urban form and green space configuration using multivariate landscape metric analysis. Landscape Ecol. 33, 557–573.

Gu, D., Zhang, Y., Fu, J., Zhang, X., 2007. The landscape pattern characteristics of coastal wetlands in Jiaozhou Bay under the impact of human activities. Environmental Monitoring and Assessment, 124(1): 361-370.

Gu, X., Zhang, Q., Li, J., Chen, D., Singh, V.P., Zhang, Y., Liu, J., Shen, Z., Yu, H., 2020. Impacts of anthropogenic warming and uneven regional socio-economic development on global river flood risk. Journal of Hydrology, 590: 125262.

Gumindoga, W., Rientjes, T., Haile, A., Dube, T., 2014. Predicting streamflow for land cover changes in the Upper Gilgel Abay River Basin, Ethiopia: A TOPMODEL based approach. Physics and Chemistry of the Earth, Parts A/B/C, 76: 3-15.

Guse, B., Kail, J., Radinger, J., Schröder, M., Kiesel, J., Hering, D., Wolter, C., Fohrer, N., 2015a. Eco-hydrologic model cascades: Simulating land use and climate change impacts on hydrology, hydraulics and habitats for fish and macroinvertebrates. Science of the Total Environment, 533: 542-556.

Guse, B., Kiesel, J., Pfannerstill, M., Fohrer, N., 2020. Assessing parameter identifiability for multiple performance criteria to constrain model parameters. Hydrological Sciences Journal, 65(7): 1158-1172.

Guse, B., Pfannerstill, M., Fohrer, N., 2015b. Dynamic modelling of land use change impacts on nitrate loads in rivers. Environmental Processes, 2(4): 575-592.

Guse, B., Reusser, D.E., Fohrer, N., 2014. How to improve the representation of hydrological processes in SWAT for a lowland catchment–temporal analysis of parameter sensitivity and model performance. Hydrological processes, 28(4): 2651-2670.

Haas, M.B., Guse, B., Fohrer, N., 2017. Assessing the impacts of Best Management Practices on nitrate pollution in an agricultural dominated lowland catchment considering environmental protection versus economic development. Journal of environmental management, 196: 347-364.

Haas, M.B., Guse, B., Pfannerstill, M., Fohrer, N., 2016. A joined multi-metric calibration of river discharge and nitrate loads with different performance measures. Journal of Hydrology, 536: 534-545.

Haberl, H., Erb, K.H., Krausmann, F., Gaube, V., Bondeau, A., Plutzar, C., Gingrich, S., Lucht, W., Fischer-Kowalski, M., 2007. Quantifying and mapping the human appropriation of net primary production in earth's terrestrial ecosystems. Proceedings of the National Academy of Sciences, 104(31): 12942-12947.

Hacisalihoglu, S., 2007. Determination of soil erosion in a steep hill slope with different land-use types: a case study in Mertesdorf (Ruwertal/Germany). Journal of Environmental Biology, 28(2): 433.

Haidary, A., Amiri, B.J., Adamowski, J., Fohrer, N., Nakane, K., 2013. Assessing the impacts of four land use types on the water quality of wetlands in Japan. Water Resources Management, 27(7): 2217-2229.

Hakimdavar, R., Hubbard, A., Policelli, F., Pickens, A., Hansen, M., Fatoyinbo, T., Lagomasino, D., Pahlevan, N., Unninayar, S., Kavvada, A., 2020. Monitoring water-related ecosystems with earth observation data in support of Sustainable Development Goal (SDG) 6 reporting. Remote Sensing, 12(10): 1634.

Hargis, C.D., Bissonette, J.A., David, J.L., 1998. The behavior of landscape metrics commonly used in the study of habitat fragmentation. Landscape ecology, 13(3): 167-186.

Harrel, R.C., Dorris, T.C., 1968. Stream order, morphometry, physico-chemical conditions, and community structure of benthic macroinvertebrates in an intermittent stream system. American Midland Naturalist: 220-251.

Hatano, R., Nagumo, T., Hata, H., Kuramochi, K., 2005. Impact of nitrogen cycling on stream water quality in a basin associated with forest, grassland, and animal husbandry, Hokkaido, Japan. Ecological Engineering, 24(5): 509-515.

Hesse, C., Krysanova, V., Päzolt, J., Hattermann, F.F., 2008. Eco-hydrological modelling in a highly regulated lowland catchment to find measures for improving water quality. Ecological Modelling, 218(1-2): 135-148.

Hijmans, R.J., van Etten, J., Cheng, J., Mattiuzzi, M., Sumner, M., Greenberg, J.A., Lamigueiro, O.P., Bevan, A., Racine, E.B., Shortridge, A., 2016. Package 'raster': Geographic data analysis and modeling. R version 2.5–8.

Hirt, U., Venohr, M., Kreins, P., Behrendt, H., 2008. Modelling nutrient emissions and the impact of nutrient reduction measures in the Weser river basin, Germany. Water Science and Technology, 58(11): 2251-2258.

Hu, Z., Yu, G., Zhou, Y., Sun, X., Li, Y., Shi, P., Wang, Y., Song, X., Zheng, Z., Zhang, L., 2009. Partitioning of evapotranspiration and its controls in four grassland ecosystems: Application of a two-source model. Agricultural and Forest Meteorology, 149(9): 1410-1420.

Huang, T., Yu, D., Cao, Q., Qiao, J., 2019. Impacts of meteorological factors and land use pattern on hydrological elements in a semi-arid basin. Science of the Total Environment, 690: 932-943.

Inkoom, J.N., Frank, S., Greve, K., Walz, U., Fürst, C., 2018. Suitability of different landscape metrics for the assessments of patchy landscapes in West Africa. Ecological Indicators, 85: 117-127.

Jia, H., Yao, H., Shaw, L.Y., 2013. Advances in LID BMPs research and practice for urban runoff control in China. Frontiers of Environmental Science & Engineering, 7(5): 709-720.

Johnson, L., Richards, C., Host, G., Arthur, J., 1997. Landscape influences on water chemistry in Midwestern stream ecosystems. Freshwater biology, 37(1): 193-208.

Jones, K.B., Neale, A.C., Nash, M.S., Van Remortel, R.D., Wickham, J.D., Riitters, K.H., O'neill, R.V., 2001. Predicting nutrient and sediment loadings to streams from landscape metrics: a multiple watershed study from the United States Mid-Atlantic Region. Landscape Ecology, 16(4): 301-312.

Kändler, M., Blechinger, K., Seidler, C., Pavlů, V., Šanda, M., Dostál, T., Krása, J., Vitvar, T., Štich, M., 2017. Impact of land use on water quality in the upper Nisa catchment in the Czech Republic and in Germany. Science of the Total Environment, 586: 1316-1325.

Kandziora, M., Dörnhöfer, K., Oppelt, N.M., Müller, F., 2014. Detecting land use and land cover changes in Northern German agricultural landscapes to assess ecosystem service dynamics. Landscape Online, 35: 1-24.

Karen, G., Patrick, W., 2021. Performance evaluation of spatially distributed, CN-based rainfall-runoff model configurations for implementation in spatial land use optimization analyses. Journal of Hydrology: 126872.

Kay, D., McDonald, A., Stapleton, C., Wyer, M., Fewtrell, L., 2006. Europe: a challenging new framework for water quality, Proceedings of the Institution of Civil Engineers-Civil Engineering. Thomas Telford Ltd, pp. 58-64.

Kiesel, J., Schmalz, B., Fohrer, N., 2009. SEPAL–a simple GIS-based tool to estimate sediment pathways in lowland catchments. Advances in Geosciences, 21: 25-32.

King-Okumu, C., Jillo, B., Kinyanjui, J., Jarso, I., 2018. Devolving water governance in the Kenyan Arid Lands: from top-down drought and flood emergency response to locally driven water resource development planning. International Journal of Water Resources Development, 34(4): 675-697.

Kirkby, M., Beven, K., 1979. A physically based, variable contributing area model of basin hydrology. Hydrological Sciences Journal, 24(1): 43-69.

Kirschke, S., Häger, A., Kirschke, D., Völker, J., 2019. Agricultural nitrogen pollution of freshwater in Germany. The governance of sustaining a complex problem. Water, 11(12): 2450.

Klik, A., Rosner, J., 2020. Long-term experience with conservation tillage practices in Austria: Impacts on soil erosion processes. Soil and Tillage Research, 203: 104669.

Koch, S., Bauwe, A., Lennartz, B., 2013. Application of the SWAT model for a tile-drained lowland catchment in North-Eastern Germany on subbasin scale. Water Resources Management, 27(3): 791-805.

Kok, K., Veldkamp, A., 2001. Evaluating impact of spatial scales on land use pattern analysis in Central America. Agriculture, Ecosystems & Environment, 85(1–3): 205–221.

Korzoun, V., 1978. World water balance and water resources of the earth.

Krause, S., Bronstert, A., Zehe, E., 2007. Groundwater–surface water interactions in a North German lowland floodplain–implications for the river discharge dynamics and riparian water balance. Journal of hydrology, 347(3-4): 404-417.

KTBL, 1995 and 2008. Kuratorium für Technik und Bauwesen in der Landwirtschaft. Betriebsplanung Landwirtschaft 1995/1996 and 2008/2009. 14.Ed and 21. Ed. Darmstadt: KTBL.

Kucheryavskiy, S., 2020. mdatools–R package for chemometrics. Chemometrics and Intelligent Laboratory Systems, 198: 103937.

Kühling, I., 2011. Modellierung und räumliche Analyse der Phosphateintragspfade im Einzugsgebiet eines norddeutschen Tieflandbaches. Master thesis, Christian-Albrechts-University Kiel.

Kuo, C.-W., Brierley, G.J., 2013. The influence of landscape configuration upon patterns of sediment storage in a highly connected river system. Geomorphology, 180: 255-266.

Kupfer, J.A., 2012. Landscape ecology and biogeography: rethinking landscape metrics in a post-FRAGSTATS landscape. Progress in physical geography, 36(3): 400-420.

Lam, Q., Schmalz, B., Fohrer, N., 2010. Modelling point and diffuse source pollution of nitrate in a rural lowland catchment using the SWAT model. Agricultural Water Management, 97(2): 317-325.

Lam, Q., Schmalz, B., Fohrer, N., 2012. Assessing the spatial and temporal variations of water quality in lowland areas, Northern Germany. Journal of Hydrology, 438: 137-147.

Lam, Q.D., Schmalz, B., Fohrer, N., 2011. The impact of agricultural Best Management Practices on water quality in a North German lowland catchment. Environ. Monit. Assess. 183, 351–379.

Lambin, E.F., Meyfroidt, P., 2011. Global land use change, economic globalization, and the looming land scarcity. Proceedings of the National Academy of Sciences, 108(9): 3465–3472.

Lambin, E.F., Turner, B.L., Geist, H.J., Agbola, S.B., Angelsen, A., Bruce, J.W., Coomes, O.T., Dirzo, R., Fischer, G., Folke, C., George, P., 2001. The causes of land-use and land-cover change: Moving beyond the myths. Global environmental change, 11(4): 261–269.

Lane, S., Reaney, S., Heathwaite, A.L., 2009. Representation of landscape hydrological connectivity using a topographically driven surface flow index. Water Resources Research, 45(8).

LANU, 2003. LANDESAMT FÜR NATUR UND UMWELT SCHLESWIG-HOLSTEIN: Ausschnitt aus dem Basisgewässernetz des Landes Schleswig-Holstein für das Einzugsgebiet der Treene bis Treia. (Arc-View-Shape), Flintbek.

Lawrence, D., D'Odorico, P., Diekmann, L., DeLonge, M., Das, R., Eaton, J., 2007. Ecological feedbacks following deforestation create the potential for a catastrophic ecosystem shift in tropical dry forest. Proceedings of the National Academy of Sciences, 104(52): 20696-20701.

Lee, J.H., Bang, K.W., 2000. Characterization of urban stormwater runoff. Water Res. 34, 1773–1780.

Lee, S.-W., Hwang, S.-J., Lee, S.-B., Hwang, H.-S., Sung, H.-C., 2009. Landscape ecological approach to the relationships of land use patterns in watersheds to water quality characteristics. Landscape and Urban Planning, 92(2): 80-89.

Lei, C., Wagner, P.D., Fohrer, N., 2019. Identifying the most important spatially distributed variables for explaining land use patterns in a rural lowland catchment in Germany. Journal of Geographical Sciences, 29(11): 1788-1806.

Lei, C., Wagner, P.D., Fohrer, N., 2021. Effects of land cover, topography, and soil on stream water quality at multiple spatial and seasonal scales in a German lowland catchment. Ecological Indicators, 120: 106940.

Li, C., Cai, Y., Tan, Q., Wang, X., Li, C., Liu, Q., Chen, D., 2021a. An integrated simulation-optimization modeling system for water resources management under coupled impacts of climate and land use variabilities with priority in ecological protection. Advances in Water Resources, 154: 103986.

Li, G., Zhang, F., Jing, Y., Liu, Y., Sun, G., 2017a. Response of evapotranspiration to changes in land use and land cover and climate in China during 2001–2013. Science of the Total Environment, 596: 256-265.

Li, J., Liu, D., Wang, T., Li, Y., Wang, S., Yang, Y., Wang, X., Guo, H., Peng, S., Ding, J., Shen, M., 2017b. Grassland restoration reduces water yield in the headstream region of Yangtze River. Scientific reports, 7(1): 1-9.

Li, K., Chi, G., Wang, L., Xie, Y., Wang, X., Fan, Z., 2018. Identifying the critical riparian buffer zone with the strongest linkage between landscape characteristics and surface water quality. Ecological Indicators, 93: 741-752.

Li, L., Gou, M., Wang, N., Ma, W., Xiao, W., Liu, C., La, L., 2021b. Landscape configuration mediates hydrology and nonpoint source pollution under climate change and agricultural expansion. Ecological Indicators, 129: 107959.

Li, S., Gu, S., Liu, W., Han, H., Zhang, Q., 2008. Water quality in relation to land use and land cover in the upper Han River Basin, China. Catena, 75(2): 216-222.

Li, X., Yeh, A. G. O., 2002. Neural-network-based cellular automata for simulating multiple land use changes using GIS. International Journal of Geographical Information Science 16(4): 323–343.

Liang, X., Lettenmaier, D. P., Wood, E. F., Burges, S. J., 1994. A simple hydrologically based model of land surface water and energy fluxes for general circulation models. Journal of Geophysical Research: Atmospheres, 99(D7), 14415-14428.

Lintern, A., Webb, J., Ryu, D., Liu, S., Bende-Michl, U., Waters, D., Leahy, P., Wilson, P., Western, A., 2018. Key factors influencing differences in stream water quality across space. Wiley Interdiscip. Rev.: Water 5, e1260.

Liu, G., Jin, Q., Li, J., Li, L., He, C., Huang, Y., Yao, Y., 2017. Policy factors impact analysis based on remote sensing data and the CLUE-S model in the Lijiang River Basin, China. Catena, 158: 286–297.

Liu, J., Zhang, Z., Xu, X., Kuang, W., Zhou, W., Zhang, S., Li, R., Yan, C., Yu, D., Wu, S., Jiang, N., 2010. Spatial patterns and driving forces of land use change in China during the early 21st century. Journal of Geographical Sciences, 20(4): 483–494.

Liu, W., Zhang, Q., Liu, G., 2012. Influences of watershed landscape composition and configuration on lake-water quality in the Yangtze River basin of China. Hydrological Processes, 26(4): 570-578.

LKN, 2020. Landesbetrieb für Küstenschutz, Nationalpark und Meeresschutz Schleswig-Holstein. Discharge data from gauges Padenstedt, Sarlhusen and Willenscharen.

Loliyana, V.D., Patel, P.L., 2020. A physics based distributed integrated hydrological model in prediction of water balance of a semi-arid catchment in India. Environmental Modelling & Software, 127: 104677.

Long, H., Qu, Y., 2018. Land use transitions and land management: A mutual feedback perspective. Land Use Policy, 74: 111–120.

Lu, Y., Song, S., Wang, R., Liu, Z., Meng, J., Sweetman, A.J., Jenkins, A., Ferrier, R.C., Li, H., Luo, W., 2015. Impacts of soil and water pollution on food safety and health risks in China. Environment international, 77: 5-15.

Luo, C., Li, Z., Liu, H., Li, H., Wan, R., Pan, J., Chen, X., 2020. Differences in the responses of flow and nutrient load to isolated and coupled future climate and land use changes. Journal of environmental management, 256: 109918.

LVA, 1992-2004. DEM 25 m Grid Size, DEM 5 m Grid Size Derived from Topographic Maps 1 : 5 000 and Map of Schleswig-Holstein. Land survey office Schleswig-Holstein: Kiel.

LVA, 2013, 2016. ATKIS-Digitale Orthophotos (DOP) with a ground resolution of 20 cm. Land Survey Office Schleswig-Holstein.

LVA, 2016. ATKIS- Digitales Basis-Landschaftsmodell (Basis-DLM). Land Survey Office Schleswig-Holstein: Kiel.

LvermA, 2008. Digitales Geländenmodell (ATKIS-DGM LiDAR). Gitterweite 5 x 5 m.

LVERMA-SH, Vermessungs-und Katasterverwaltung Schleswig-Holstein, 2004. Automatisierte Liegenscha-ftskarte (ALK).

LWK, 1991 and 2011. Landwirtschaftskammer Schleswig-Holstein. Richtwerte für die Düngung 1991 and 2011. 13 Ed and 21 Ed . Rendsburg: LWK.

Madsen, H.T., Søgaard, E.G., Muff, J., 2015. Study of degradation intermediates formed during electrochemical oxidation of pesticide residue 2, 6-dichlorobenzamide (BAM) in chloride medium at boron doped diamond (BDD) and platinum anodes. Chemosphere 120, 756–763.

Maranguit, D., Guillaume, T., Kuzyakov, Y., 2017. Land-use change affects phosphorus fractions in highly weathered tropical soils. Catena, 149: 385-393.

Mas, J.F., Kolb, M., Paegelow, M., Olmedo, M.T.C., Houet, T., 2014. Inductive pattern-based land use/cover change models: A comparison of four software packages. Environmental Modelling & Software, 51: 94–111.

Matteo, M., Randhir, T., Bloniarz, D., 2006. Watershed-scale impacts of forest buffers on water quality and runoff in urbanizing environment. J. Water Resour. Plann. Manage. 132, 144–152.

Mehdi, B., Lehner, B., Gombault, C., Michaud, A., Beaudin, I., Sottile, M.F., Blondlot, A., 2015. Simulated impacts of climate change and agricultural land use change on surface water quality with and without adaptation management strategies. Agriculture, Ecosystems & Environment, 213: 47-60.

Mehdi, B., Lehner, B., Ludwig, R., 2018. Modelling crop land use change derived from influencing factors selected and ranked by farmers in North temperate agricultural regions. Science of The Total Environment, 631: 407–420.

Meneses, B.M., Reis, R., Vale, M., Saraiva, R., 2015. Land use and land cover changes in Zêzere watershed (Portugal)—Water quality implications. Science of the Total Environment, 527: 439-447.

Mevik, B.-H., Wehrens, R., Liland, K.H., 2020. pls: Partial least squares and principal component regression. R package version, 2(3).

Mirghaed, F.A., Souri, B., Mohammadzadeh, M., Salmanmahiny, A., Mirkarimi, S.H., 2018. Evaluation of the relationship between soil erosion and landscape metrics across Gorgan Watershed in northern Iran. Environmental monitoring and assessment, 190(11): 1-14.

Mitsuda Y, Ito S, 2011. A review of spatial-explicit factors determining spatial distribution of land use/land-use change. Landscape and Ecological Engineering, 7(1): 117–125.

Molina-Navarro, E., Trolle, D., Martínez-Pérez, S., Sastre-Merlín, A., Jeppesen, E., 2014. Hydrological and water quality impact assessment of a Mediterranean limno-reservoir under climate change and land use management scenarios. Journal of Hydrology, 509: 354-366.

Monaghan, R.M., Wilcock, R.J., Smith, L.C., Tikkisetty, B., Thorrold, B.S., Costall, D., 2007. Linkages between land management activities and water quality in an intensively farmed catchment in southern New Zealand. Agriculture, ecosystems & environment, 118(1-4), 211-222.

Moreno-Mateos, D., Mander, Ü., Comín, F.A., Pedrocchi, C., Uuemaa, E., 2008. Relationships between landscape pattern, wetland characteristics, and water quality in agricultural catchments. Journal of environmental quality, 37(6): 2170-2180.

Moriasi, D.N., Arnold, J.G., Van Liew, M.W., Bingner, R.L., Harmel, R.D., Veith, T.L., 2007. Model evaluation guidelines for systematic quantification of accuracy in watershed simulations. Transactions of the ASABE, 50(3): 885-900.

Motamedi, R., Azari, M., Monsefi, R., 2019. Relationship between landscape metrics and sediment yield in some watersheds of Golestan Province. Watershed Engineering and Management, 11(4): 955-971.

Mottet, A., Ladet, S., Coqué, N., Gibon, A., 2006. Agricultural land-use change and its drivers in mountain landscapes: A case study in the Pyrenees. Agriculture, ecosystems & environment, 114(2-4): 296-310.

Mueller, N.D., Gerber, J.S., Johnston, M., Ray, D.K., Ramankutty, N., Foley, J.A., 2012. Closing yield gaps through nutrient and water management. Nature, 490(7419): 254-257.

Müller, D., Kuemmerle, T., Rusu, M., Griffiths, P., 2009. Lost in transition: Determinants of post-socialist cropland abandonment in Romania. Journal of Land Use Science, 4(1/2): 109–129.

Mustard, J.F., Defries, R.S., Fisher, T., Moran, E., 2012. Land-use and land-cover change pathways and impacts, Land change science. Springer, 411-429.

Mutlu, E., 2019. Evaluation of spatio-temporal variations in water quality of Zerveli stream (northern Turkey) based on water quality index and multivariate statistical analyses. Environmental monitoring and assessment, 191(6): 1-14.

Myers, D.T., Ficklin, D.L., Robeson, S.M., 2021. Incorporating rain-on-snow into the SWAT model results in more accurate simulations of hydrologic extremes. Journal of Hydrology, 126972.

Nafi'Shehab, Z., Jamil, N.R., Aris, A.Z., Shafie, N.S., 2021. Spatial variation impact of landscape patterns and land use on water quality across an urbanized watershed in Bentong, Malaysia. Ecological Indicators, 122: 107254.

Narain, P., Singh, R., Sindhwal, N., Joshie, P., 1998. Water balance and water use efficiency of different land uses in western Himalayan valley region. Agricultural Water Management, 37(3): 225-240.

Neilsen, R.D., Hjelmfelt, A.T., 1998. Hydrologic soil group assignment. Proc. Water Resour. Eng. 1297–1302.

Neitsch, S.L., Arnold, J.G., Kiniry, J.R., Williams, J.R., 2011. Soil and water assessment tool theoretical documentation version 2009, Texas Water Resources Institute.

Neupane, R. P., Kumar, S., 2015. Estimating the effects of potential climate and land use changes on hydrologic processes of a large agriculture dominated watershed. Journal of Hydrology, 529: 418–429.

Nguyen, H.H. et al., 2019. Comparison of the alternative models SOURCE and SWAT for predicting catchment streamflow, sediment and nutrient loads under the effect of land use changes. Science of The Total Environment, 662: 254-265.

Nguyen, H.H., Venohr, M., 2021. Harmonized assessment of nutrient pollution from urban systems including losses from sewer exfiltration: a case study in Germany. Environmental Science and Pollution Research: 1-16.

Nguyen, T.H.T., Boets, P., Lock, K., Ambarita, M.N.D., Forio, M.A.E., Sasha, P., Dominguez-Granda, L.E., Hoang, T.H.T., Everaert, G., Goethals, P.L., 2015. Habitat suitability of the invasive water hyacinth and its relation to water quality and macroinvertebrate diversity in a tropical reservoir. Limnologica 52, 67–74.

Ni, X., Parajuli, P.B., Ouyang, Y., Dash, P., Siegert, C., 2021. Assessing land use change impact on stream discharge and stream water quality in an agricultural watershed. Catena, 198: 105055.

Noe, G.B., Hupp, C.R., Rybicki, N.B., 2013. Hydrogeomorphology influences soil nitrogen and phosphorus mineralization in floodplain wetlands. Ecosystems, 16(1): 75-94.

Office, F.S., 1992-2012. Statistisches Jahrbuch für die Bundesrepublik Deutschland. Wiesbaden, Statistisches Bundesamt.

Oishi, A.C., Oren, R., Novick, K.A., Palmroth, S., Katul, G.G., 2010. Interannual invariability of forest evapotranspiration and its consequence to water flow downstream. Ecosystems, 13(3): 421-436.

Oñate-Valdivieso, F., Sendra, J. B., 2010. Application of GIS and remote sensing techniques in generation of land use scenarios for hydrological modeling. Journal of Hydrology, 395(3/4): 256–263.

Onderka, M., Wrede, S., Rodný, M., Pfister, L., Hoffmann, L., Krein, A., 2012. Hydrogeologic and landscape controls of dissolved inorganic nitrogen (DIN) and dissolved silica (DSi) fluxes in heterogeneous catchments. Journal of Hydrology, 450: 36-47.

Oppelt, N., Rathjens, H., Dörnhöfer, K., 2012. Integration of land cover data into the open source model SWAT, Proceedings of the First Sentinel-2 Preparatory Symposium held on, pp. 23-27.

Pal, L., Stres, B., Danevčič, T., Leskovec, S. and Mandic-Mulec, I., 2010. Transformations of mineral nitrogen applied to peat soil during sequential oxic/anoxic cycling. Soil Biology and Biochemistry, 42(8), 1338-1346.

Parris, K., 2011. Impact of agriculture on water pollution in OECD countries: recent trends and future prospects. International journal of water resources development, 27(1): 33-52.

Pašakarnis, G., Morley, D., Malienė, V., 2013. Rural development and challenges establishing sustainable land use in Eastern European countries. Land use policy, 30(1): 703-710.

Pearce, J., Ferrier, S., 2000. Evaluating the predictive performance of habitat models developed using logistic re- gression. Ecological Modelling, 133(3): 225–245.

Peel, M.C., McMahon, T.A., Finlayson, B.L., 2010. Vegetation impact on mean annual evapotranspiration at a global catchment scale. Water Resources Research, 46(9).

Peng, S., Li, S., 2021. Scale relationship between landscape pattern and water quality in different pollution source areas: A case study of the Fuxian Lake watershed, China. Ecological Indicators, 121: 107136.

Pereda, O., Acuña, V., von Schiller, D., Sabater, S., Elosegi, A., 2019. Immediate and legacy effects of urban pollution on river ecosystem functioning: A mesocosm experiment. Ecotoxicology and environmental safety, 169: 960-970.

Peterson, E.E., Sheldon, F., Darnell, R., Bunn, S.E., Harch, B.D., 2011. A comparison of spatially explicit landscape representation methods and their relationship to stream condition. Freshwater Biology, 56(3): 590-610.

Pfannerstill, M., Guse, B., Fohrer, N., 2014. A multi-storage groundwater concept for the SWAT model to emphasize nonlinear groundwater dynamics in lowland catchments. Hydrological processes, 28(22): 5599-5612.

Pidwirny, M., 2006. "The Hydrologic Cycle". Fundamentals of Physical Geography, 2nd Edition.

Piquer-Rodríguez, M., Butsic, V., Gärtner, P., Macchi, L., Baumann, M., Pizarro, G.G., Volante, J.N., Gasparri, I.N. and Kuemmerle, T., 2018. Drivers of agricultural land-use change in the Argentine Pampas and Chaco regions. Applied geography, 91, 111-122.

Pontius Jr, R. G., Huffaker, D., Denman, K., 2004. Useful techniques of validation for spatially explicit land-change models. Ecological modelling, 179(4), 445-461.

Pontius Jr, R. G., Schneider, L. C., 2001. Land-cover change model validation by an ROC method for the Ipswich watershed, Massachusetts, USA. Agriculture, ecosystems & environment, 85(1-3), 239-248.

Pott, C.A., 2014. Integrated monitoring, assessment and modeling of nitrogen and phosphorus pollution in a lowland catchment in Germany: a long-term study on water quality, Christian-Albrechts Universität Kiel.

Pott, C.A., Fohrer, N., 2017a. Best management practices to reduce nitrate pollution in a rural watershed in Germany. Revista Ambiente & Água, 12(6): 888-901.

Pott, C.A., Fohrer, N., 2017b. Hydrological modeling in a rural catchment in Germany. Applied Research & Agrotechnology, 10(1): 07-16.

Poudel, D., Lee, T., Srinivasan, R., Abbaspour, K., Jeong, C., 2013. Assessment of seasonal and spatial variation of surface water quality, identification of factors associated with water quality variability, and the modeling of critical nonpoint source pollution areas in an agricultural watershed. Journal of Soil and Water Conservation, 68(3): 155-171.

Pratt, B., Chang, H., 2012. Effects of land cover, topography, and built structure on seasonal water quality at multiple spatial scales. Journal of hazardous materials, 209: 48-58.

Prusty, R.M., Das, A., Patra, K.C., 2021. Impact of Land Use and Land Cover Change on Streamflow of Upper Baitarani River Basin Using SWAT, Water Management and Water Governance. Springer, pp. 227-242.

Qasim, M., Hubacek, K., Termansen, M., Khan, A., 2011. Spatial and temporal dynamics of land use pattern in District Swat, Hindu Kush Himalayan region of Pakistan. Applied Geography, 31(2): 820-828.

Qi, J., Li, S., Bourque, C.P.-A., Xing, Z., Meng, F.-R., 2018. Developing a decision support tool for assessing land use change and BMPs in ungauged watersheds based on decision rules provided by SWAT simulation. Hydrology and Earth System Sciences, 22(7): 3789-3806.

Qureshi, M.E., Hanjra, M.A., Ward, J., 2013. Impact of water scarcity in Australia on global food security in an era of climate change. Food Policy, 38: 136-145.

Rajaei, F., Sari, A.E., Salmanmahiny, A., Delavar, M., Bavani, A.R.M., Srinivasan, R., 2017. Surface drainage nitrate loading estimate from agriculture fields and its relationship with landscape metrics in Tajan watershed. Paddy and Water Environment, 15(3): 541-552.

Ramachandran, R.M., Roy, P.S., Chakravarthi, V., Sanjay, J., Joshi, P.K., 2018. Long-term land use and land cover changes (1920–2015) in Eastern Ghats, India: Pattern of dynamics and challenges in plant species conservation. Ecological Indicators, 85: 21-36.

Rathjens, H., Dörnhöfer, K., Oppelt, N., 2014. IRSeL—An approach to enhance continuity and accuracy of remotely sensed land cover data. International journal of applied earth observation and geoinformation, 31: 1-12.

Reddy, K., Rao, P., 1983. Nitrogen and phosphorus fluxes from a flooded organic soil. Soil Sci. 136, 300–307.

Redeker, M., 2011. Impact of wastewater treatment plants on the stream water quality in the upper Stör catchment. Masterarbeit in der Abteilung Hydrologie und Wasserwirtschaft der CAU Kiel.

Refshaard, J., Storm, B., 1995. MIKE SHE. Computer models of watershed hydrology.: 809-846.

Ren, W., Zhong, Y., Meligrana, J., Anderson, B., Watt, W.E., Chen, J., Leung, H. L., 2003. Urbanization, land use, and water quality in Shanghai: 1947–1996. Environment international, 29(5): 649-659.

Riedel W, Polensky R, 1987. Umweltatlas für den Landesteil Schleswig. Forschungsprojekt des Institutes für Regionale Forschung und Information im Deutschen Grenzverein e.V. in Zusammenarbeit mit der Zentralstelle für Landeskunde des Schleswig-Holsteinischen Heimatbundes.

Riitters, K., 2019. Pattern metrics for a transdisciplinary landscape ecology. Springer.

Rimer, A.E., Nissen, J.A., Reynolds, D.E., 1978. Characterization and impact of stormwater runoff from various land cover types. J. (Water Pollut. Control Federation) 252–264.

Ripl, W., Hildmann, C., 2000. Dissolved load transported by rivers as an indicator of landscape sustainability. Ecological Engineering, 14(4): 373-387.

Ripl, W., Janssen, T., Hildmann, C., Otto, I., 1996. Entwicklung eines Land-Gewässer Bewirtschaftungskonzeptes zur Senkung von Stoffverlusten an Gewässer (Stör-Projekt I und II). Forschungsbericht, TU Berlin.

Risal, A., Parajuli, P.B., Dash, P., Ouyang, Y., Linhoss, A., 2020. Sensitivity of hydrology and water quality to variation in land use and land cover data. Agricultural Water Management, 241: 106366.

Riseng, C., Wiley, M., Black, R., Munn, M., 2011. Impacts of agricultural land use on biological integrity: a causal analysis. Ecol. Appl. 21, 3128–3146.

Roberts, A.D., 2016. The effects of current landscape configuration on streamflow within selected small watersheds of the Atlanta metropolitan region. Journal of Hydrology: Regional Studies, 5: 276-292.

Roberts, A.D., Prince, S.D., 2010. Effects of urban and non-urban land cover on nitrogen and phosphorus runoff to Chesapeake Bay. Ecological indicators, 10(2): 459-474.

Rodriguez-Galiano, V., Mendes, M.P., Garcia-Soldado, M.J., Chica-Olmo, M., Ribeiro, L., 2014. Predictive modeling of groundwater nitrate pollution using Random Forest and multisource variables related to intrinsic and specific vulnerability: a case study in an agricultural setting (Southern Spain). Sci. Total Environ. 476, 189–206.

Rounsevell, M., Annetts, J., Audsley, E., Mayr, T., Reginster, I., 2003. Modelling the spatial distribution of agricultural land use at the regional scale. Agriculture, Ecosystems & Environment, 95(2-3): 465-479.

Rounsevell, M.D., Pedroli, B., Erb, K.-H., Gramberger, M., Busck, A.G., Haberl, H., Kristensen, S., Kuemmerle, T., Lavorel, S., Lindner, M., 2012. Challenges for land system science. Land use policy, 29(4): 899-910.

Sabater, S., Bregoli, F., Acuña, V., Barceló, D., Elosegi, A., Ginebreda, A., Marcé, R., Muñoz, I., Sabater-Liesa, L., Ferreira, V., 2018. Effects of human-driven water stress on river ecosystems: a meta-analysis. Scientific reports, 8(1): 1-11.

Sabzi, H.Z., Moreno, H.A., Fovargue, R., Xue, X., Hong, Y., Neeson, T.M., 2019. Comparison of projected water availability and demand reveals future hotspots of water stress in the Red River basin, USA. Journal of Hydrology: Regional Studies, 26: 100638.

Schmalz, B., Bieger, K., Fohrer, N., 2008a. A method to assess instream water quality–the role of nitrogen entries in a North German rural lowland catchment. Adv. Geosci. 18, 37–41.

Schmalz, B., Fohrer, N., 2009. Comparing model sensitivities of different landscapes using the ecohydrological SWAT model. Advances in Geosciences, 21: 91-98.

Schmalz, B., Fohrer, N., 2010. Ecohydrological research in the German lowland catchment Kielstau. IAHS Publ. 336, 115–120.

Schmalz, B., Tavares, F., Fohrer, N., 2008b. Modelling hydrological processes in mesoscale lowland river basins with SWAT—capabilities and challenges. Hydrological sciences journal, 53(5): 989-1000.

Schoumans, O., Chardon, W., Bechmann, M., Gascuel-Odoux, C., Hofman, G., Kronvang, B., Rubæk, G., Ulén, B., Dorioz, J.-M., 2014. Mitigation options to reduce phosphorus losses from the agricultural sector and improve surface water quality: a review. Science of the Total Environment, 468: 1255-1266.

Scott, R., Goulden, T., Letman, M., Hayward, J., Jamieson, R., 2019. Long-term evaluation of the impact of urbanization on chloride levels in lakes in a temperate region. J. Environ. Manage. 244, 285–293.

Searchinger, T.D., Wirsenius, S., Beringer, T., Dumas, P., 2018. Assessing the efficiency of changes in land use for mitigating climate change. Nature, 564(7735): 249-253.

Semwal, R.L., Nautiyal, S., Sen, K., Rana, U., Maikhuri, R., Rao, K., Saxena, K., 2004. Patterns and ecological implications of agricultural land-use changes: a case study from central Himalaya, India. Agriculture, Ecosystems & Environment, 102(1): 81-92.

Seto, K. C., Fragkias, M., 2005. Quantifying spatiotemporal patterns of urban land-use change in four cities of China with time series landscape metrics. Landscape Ecology, 20(7): 871–888.

Shawul, A.A., Chakma, S., Melesse, A.M., 2019. The response of water balance components to land cover change based on hydrologic modeling and partial least squares regression (PLSR) analysis in the Upper Awash Basin. Journal of Hydrology: Regional Studies, 26: 100640.

Shen, Z., Chen, L., Hong, Q., Qiu, J., Xie, H., Liu, R., 2013. Assessment of nitrogen and phosphorus loads and causal factors from different land use and soil types in the Three Gorges Reservoir Area. Sci. Total Environ. 454, 383–392.

Shen, Z., Hou, X., Li, W., Aini, G., Chen, L., Gong, Y., 2015. Impact of landscape pattern at multiple spatial scales on water quality: a case study in a typical urbanised watershed in China. Ecol. Ind. 48, 417–427.

Shi, P., Zhang, Y., Li, Z., Li, P., Xu, G., 2017. Influence of land use and land cover patterns on seasonal water quality at multi-spatial scales. Catena 151, 182–190.

Shi, P.J., Yuan, Y., Zheng, J., Wang, J.A., Ge, Y., Qiu, G.Y., 2007. The effect of land use/cover change on surface runoff in Shenzhen region, China. Catena, 69(1): 31-35.

Shi, Z., Ai, L., Li, X., Huang, X., Wu, G., Liao, W., 2013. Partial least-squares regression for linking land-cover patterns to soil erosion and sediment yield in watersheds. Journal of Hydrology, 498: 165-176.

Shiklomanov, I.A., 1991. The world's water resources, Proceedings of the international symposium to commemorate, pp. 93-126.

Shrestha, S., Bhatta, B., Shrestha, M., Shrestha, P.K., 2018. Integrated assessment of the climate and landuse change impact on hydrology and water quality in the Songkhram River Basin, Thailand. Science of the Total Environment, 643: 1610-1622.

Shu, B., Zhang, H., Li, Y., Qu, Y., Chen, L., 2014. Spatiotemporal variation analysis of driving forces of urban land spatial expansion using logistic regression: A case study of port towns in Taicang City, China. Habitat international, 43: 181-190.

Shuster, W.D., Bonta, J., Thurston, H., Warnemuende, E., Smith, D., 2005. Impacts of impervious surface on watershed hydrology: A review. Urban Water Journal, 2(4): 263-275.

Silverman B W, 1981. Using kernel density estimates to investigate multimodality. Journal of the Royal Statistical Society. Series B (Methodological), 97–99.

Sing, T., Sander, O., Beerenwinkel, N., Lengauer, T., 2005. ROCR: visualizing classifier performance in R. Bioinformatics, 21(20): 3940-3941.

Singh, H., Singh, D., Singh, S.K., Shukla, D., 2017. Assessment of river water quality and ecological diversity through multivariate statistical techniques, and earth observation dataset of rivers Ghaghara and Gandak, India. International Journal of River Basin Management, 15(3): 347-360.

Siriwardena, L., Finlayson, B., McMahon, T., 2006. The impact of land use change on catchment hydrology in large catchments: The Comet River, Central Queensland, Australia. Journal of Hydrology, 326(1-4): 199-214.

Smith, D.R., King, K.W., Johnson, L., Francesconi, W., Richards, P., Baker, D., Sharpley, A.N., 2015. Surface runoff and tile drainage transport of phosphorus in the midwestern United States. Journal of Environmental Quality, 44(2): 495-502.

Soetaert, K., Petzoldt, T., 2010. Inverse modelling, sensitivity and Monte Carlo analysis in R using package FME. Journal of statistical software, 33(3): 1-28.

Song, S., Schmalz, B., Fohrer, N., 2015. Simulation, quantification and comparison of in-channel and floodplain sediment processes in a lowland area–A case study of the Upper Stör catchment in northern Germany. Ecological indicators, 57: 118-127.

Sood, A., Ghosh, S., Upadhyay, P., 2021. Impact of land cover change on surface runoff. Advances in Remote Sensing for Natural Resource Monitoring: 150-169.

Sood, A., Smakhtin, V., 2015. Global hydrological models: a review. Hydrological Sciences Journal, 60(4): 549-565.

Srinivasan, J.T., Reddy, V.R., 2009. Impact of irrigation water quality on human health: A case study in India. Ecological Economics, 68(11): 2800-2807.

Srivastava, A., Kumari, N., Maza, M., 2020. Hydrological response to agricultural land use heterogeneity using variable infiltration capacity model. Water Resources Management, 34(12): 3779-3794.

Statistikamt Nord, 2013, 2015. Bevölkerung der Gemeinden in Schleswig-Holstein 2. Quartal 2013; Bevölkerungsentwicklung in den Gemeinden Schleswig-Holsteins 2015.

StiftungNaturschutz, 2016. Flächenmanagement Kreis SL-Stiftung Naturschutz Schleswig-Holstein. http://www.stiftungsland.de/.

Strehmel, A., Schmalz, B., Fohrer, N., 2016. Evaluation of land use, land management and soil conservation strategies to reduce non-point source pollution loads in the three gorges region, China. Environmental management, 58(5): 906-921.

Suh, M.S., Lee, D.K., 2004. Impacts of land use/cover changes on surface climate over east Asia for extreme climate cases using RegCM2. Journal of Geophysical Research: Atmospheres, 109(D2).

Suliman, A.H.A., Jajarmizadeh, M., Harun, S., Darus, I.Z.M., 2015. Comparison of semi-distributed, GIS-based hydrological models for the prediction of streamflow in a large catchment. Water resources management, 29(9): 3095-3110.

Ta, P., Tetzlaff, B., Trepel, M., Wendland, F., 2020. Implementing a Statewide Deficit Analysis for Inland Surface Waters According to the Water Framework Directive—An Exemplary Application on Phosphorus Pollution in Schleswig-Holstein (Northern Germany). Water, 12(5): 1365.

Tanaka, M.O., de Souza, A.L.T., Moschini, L.E., de Oliveira, A.K., 2016. Influence of watershed land use and riparian characteristics on biological indicators of stream water quality in southeastern Brazil. Agriculture, Ecosystems & Environment, 216: 333-339.

Tarhule, A., 2017. The future of water: Prospects and challenges for water management in the 21st century, Competition for Water Resources. Elsevier, pp. 442-454.

Tibaijuka, A., 2003. Water and sanitation in the world's cities: local action for global goals. United Nations Human Settlement Programme UN-HABITAT/WWF/18/03, Provision for Water and Sanitation in Cities. Earthscan Publishers.

Tiemeyer, B., Kahle, P., Lennartz, B., 2009. Phosphorus losses from an artificially drained rural lowland catchment in North-Eastern Germany. Agricultural Water Management, 96(4): 677-690.

Tigabu, T.B., Wagner, P.D., Hörmann, G., Fohrer, N., 2020. Modeling the spatio-temporal flow dynamics of groundwater-surface water interactions of the Lake Tana Basin, Upper Blue Nile, Ethiopia. Hydrology Research, 51(6): 1537-1559.

Tisseuil, C., Wade, A.J., Tudesque, L., Lek, S., 2008. Modeling the stream water nitrate dynamics in a 60,000-km 2 European catchment, the Garonne, Southwest France. J. Environ. Qual. 37, 2155–2169.

Tong, S.T., Chen, W., 2002. Modeling the relationship between land use and surface water quality. Journal of environmental management, 66(4): 377-393.

Tong, S.T., Sun, Y., Ranatunga, T., He, J., Yang, Y.J., 2012. Predicting plausible impacts of sets of climate and land use change scenarios on water resources. Applied Geography, 32(2): 477-489.

Tran, C.P., Bode, R.W., Smith, A.J., Kleppel, G.S., 2010. Land-use proximity as a basis for assessing stream water quality in New York State (USA). Ecol. Ind. 10 (3), 727–733.

Tsani, S., Koundouri, P., Akinsete, E., 2020. Resource management and sustainable development: A review of the European water policies in accordance with the United Nations' Sustainable Development Goals. Environmental Science & Policy, 114: 570-579.

Tu, J., 2011. Spatially varying relationships between land use and water quality across an urbanization gradient explored by geographically weighted regression. Applied Geography, 31(1): 376-392.

Turtola, E., Alakukku, L., Uusitalo, R., Kaseva, A., 2007. Surface runoff, subsurface drainflow and soil erosion as affected by tillage in a clayey Finnish soil. Agricultural and Food Science, 16(4): 332-351.

UBA, 2018. Water Resource Management in Germany: Part 2 – Water quality.

UBA, G.E.A., 2018. Water Resource Management in Germany. Fundamentals, pressures, measures. Dessau-Roßlau. Texte.

Ulrich, U., Hörmann, G., Unger, M., Pfannerstill, M., Steinmann, F., Fohrer, N., 2018. Lentic small water bodies: Variability of pesticide transport and transformation patterns. Science of the Total Environment, 618: 26-38.

Urrutia, A.L., González-González, C., Van Cauwelaert, E.M., Rosell, J.A., Barrios, L.G., Benítez, M., 2020. Landscape heterogeneity of peasant-managed agricultural matrices. Agriculture, Ecosystems & Environment, 292: 106797.

Uuemaa, E., Antrop, M., Roosaare, J., Marja, R., Mander, Ü., 2009. Landscape metrics and indices: an overview of their use in landscape research. Living reviews in landscape research, 3(1): 1-28.

van Meijl, H., Van Rheenen, T., Tabeau, A., Eickhout, B., 2006. The impact of different policy environments on agricultural land use in Europe. Agriculture, Ecosystems & Environment, 114(1): 21-38.

Van Nieuwenhuyse, B.H., Antoine, M., Wyseure, G., Govers, G., 2011. Pattern-process relationships in surface hydrology: hydrological connectivity expressed in landscape metrics. Hydrological Processes, 25(24): 3760-3773.

Velthof, G.L., Lesschen, J., Webb, J., Pietrzak, S., Miatkowski, Z., Pinto, M., Kros, J., Oenema, O., 2014. The impact of the Nitrates Directive on nitrogen emissions from agriculture in the EU-27 during 2000–2008. Science of the Total Environment, 468: 1225-1233.

Venohr, M., 2000. Einträge und Abbau von Nährstoffen in Fließgewässern der oberen Stör. Diplomarbeit im Fach Geographie, Christian-Albrechts-Universität Kiel.

Venohr, M., Behrendt, H., Kluge, W., 2005a. The effects of different input data and their spatial resolution on the results obtained from a conceptual nutrient emissions model: The River Stör case study. Hydrological Processes: An International Journal, 19(18): 3501-3515.

Venohr, M., Donohue, I., Fogelberg, S., Arheimer, B., Irvine, K., Behrendt, H., 2005b. Nitrogen retention in a river system and the effects of river morphology and lakes. Water Science and Technology, 51(3-4): 19-29.

Verburg, P.H., Van Eck, J.R.R., de Nijs, T.C., Dijst, M.J., Schot, P., 2004. Determinants of land-use change patterns in the Netherlands. Environment and Planning B: Planning and Design, 31(1): 125-150.

Vleeshouwers, L., Verhagen, A., 2002. Carbon emission and sequestration by agricultural land use: a model study for Europe. Global change biology, 8(6): 519-530.

Volk, M., Liersch, S., Schmidt, G., 2009. Towards the implementation of the European Water Framework Directive?: Lessons learned from water quality simulations in an agricultural watershed. Land use policy, 26(3): 580-588.

von Falkenhayn, L., Rechkemmer, A., Young, O.R., 2011. The international human dimensions programme on global environmental change–taking stock and moving forward, Coping with Global Environmental Change, Disasters and Security. Springer, pp. 1221-1233.

Von Schiller, D., Martí, E., Riera, J.L., Ribot, M., Marks, J.C., Sabater, F., 2008. Influence of land use on stream ecosystem function in a Mediterranean catchment. Freshwater Biology, 53(12): 2600-2612.

Wagner, P., Kumar, S., Schneider, K., 2013. An assessment of land use change impacts on the water resources of the Mula and Mutha Rivers catchment upstream of Pune, India. Hydrology and Earth System Sciences, 17(6): 2233-2246.

Wagner, P.D., Bhallamudi, S.M., Narasimhan, B., Kantakumar, L.N., Sudheer, K., Kumar, S., Schneider, K., Fiener, P., 2016. Dynamic integration of land use changes in a hydrologic assessment of a rapidly developing Indian catchment. Science of the Total Environment, 539: 153-164.

Wagner, P.D., Bhallamudi, S.M., Narasimhan, B., Kumar, S., Fohrer, N., Fiener, P., 2019. Comparing the effects of dynamic versus static representations of land use change in hydrologic impact assessments. Environmental Modelling & Software, 122: 103987.

Wagner, P.D., Fohrer, N., 2019. Gaining prediction accuracy in land use modeling by integrating modeled hydrologic variables. Environmental Modelling & Software, 115: 155-163.

Wagner, P.D., Hoermann, G., Schmalz, B., Fohrer, N., 2018. Characterisation of the water and nutrient balance in the rural lowland catchment of the Kielstau. Hydrologie und Wasserbewirtschaftung, 62(3): 145-158.

Wagner, P.D., Reichenau, T.G., Kumar, S., Schneider, K., 2015. Development of a new downscaling method for hydrologic assessment of climate change impacts in data scarce regions and its application in the Western Ghats, India. Regional environmental change, 15(3): 435-447.

Wagner, P.D., Waske, B., 2016. Importance of spatially distributed hydrologic variables for land use change model- ing. Environmental Modelling & Software, 83: 245–254.

Walsh, C.J., Kunapo, J., 2009. The importance of upland flow paths in determining urban effects on stream ecosystems. J. North Am. Benthol. Soc. 28, 977–990.

Walsh, C.J., Webb, J.A., 2014. Spatial weighting of land use and temporal weighting of antecedent discharge improves prediction of stream condition. Landscape Ecol. 29, 1171–1185.

Wang, Q., Xu, Y., Xu, Y., Wu, L., Wang, Y., Han, L., 2018. Spatial hydrological responses to land use and land cover changes in a typical catchment of the Yangtze River Delta region. Catena, 170: 305-315.

Wang, W., Wu, X., Yin, C., Xie, X., 2019. Nutrition loss through surface runoff from slope lands and its implications for agricultural management. Agricultural Water Management, 212: 226-231.

Watts, G., Battarbee, R.W., Bloomfield, J.P., Crossman, J., Daccache, A., Durance, I., Elliott, J.A., Garner, G., Hannaford, J., Hannah, D.M., 2015. Climate change and water in the UK–past changes and future prospects. Progress in Physical Geography, 39(1): 6-28.

Wei, W., Chen, L., Fu, B., Huang, Z., Wu, D., Gui, L., 2007. The effect of land uses and rainfall regimes on runoff and soil erosion in the semi-arid loess hilly area, China. Journal of hydrology, 335(3-4): 247-258.

Weng, Q., 2001. Modeling urban growth effects on surface runoff with the integration of remote sensing and GIS. Environmental management, 28(6): 737-748.

Werners, S., Ludwig, F., 2012. Water resources in Europe in the context of vulnerability.

WFD, 2000. Water Framework Directive. Journal reference OJL, 327: 1-73.

Wigmosta, M. S., Vail, L. W., Lettenmaier, D. P., 1994. A distributed hydrology-vegetation model for complex terrain. Water resources research, 30(6), 1665-1679.

Wijesiri, B., Deilami, K., Goonetilleke, A., 2018. Evaluating the relationship between temporal changes in land use and resulting water quality. Environmental pollution, 234: 480-486.

Williams, M., King, K., Fausey, N., 2015. Drainage water management effects on tile discharge and water quality. Agricultural water management, 148: 43-51.

Wilson, G.L., Dalzell, B.J., Mulla, D.J., Dogwiler, T., Porter, P.M., 2014. Estimating water quality effects of conservation practices and grazing land use scenarios. Journal of Soil and Water Conservation, 69(4): 330-342.

Winsemius, H.C., Aerts, J.C., Van Beek, L.P., Bierkens, M.F., Bouwman, A., Jongman, B., Kwadijk, J.C., Ligtvoet, W., Lucas, P.L., Van Vuuren, D.P., 2016. Global drivers of future river flood risk. Nature Climate Change, 6(4): 381-385.

Wold, S., Sjöström, M., Eriksson, L., 2001. PLS-regression: a basic tool of chemometrics. Chemometrics and intelligent laboratory systems, 58(2): 109-130.

Woltemade, C.J., 2010. Impact of residential soil disturbance on infiltration rate and stormwater runoff 1. JAWRA J. Am. Water Resour. Assoc. 46, 700–711.

Wu, J., Lu, J., 2021. Spatial scale effects of landscape metrics on stream water quality and their seasonal changes. Water Research: 116811.

Wu, J., Shen, W., Sun, W., Tueller, P.T., 2002. Empirical patterns of the effects of changing scale on landscape metrics. Landscape ecology, 17(8): 761-782.

Wu, M., Demissie, Y., Yan, E., 2012. Simulated impact of future biofuel production on water quality and water cycle dynamics in the Upper Mississippi river basin. Biomass and Bioenergy, 41: 44-56.

Wu, N., Schmalz, B., Fohrer, N., 2011. Distribution of phytoplankton in a German lowland river in relation to environmental factors. Journal of Plankton Research, 33(5): 807-820.

Wu, X., Hu, Y., He, H.S., Bu, R., Onsted, J., Xi, F., 2009. Performance evaluation of the SLEUTH model in the Shenyang metropolitan area of northeastern China. Environmental modeling & assessment, 14(2): 221-230.

Xie, K., Liu, P., Zhang, J., Libera, D.A., Wang, G., Li, Z., Wang, D., 2020. Verification of a new spatial distribution function of soil water storage capacity using conceptual and SWAT models. Journal of Hydrologic Engineering, 25(3): 04020001.

Xu, C., Rahman, M., Haase, D., Wu, Y., Su, M., Pauleit, S., 2020a. Surface runoff in urban areas: The role of residential cover and urban growth form. Journal of Cleaner Production, 262: 121421.

Xu, S., Li, S.-L., Zhong, J., Li, C., 2020b. Spatial scale effects of the variable relationships between landscape pattern and water quality: Example from an agricultural karst river basin, Southwestern China. Agriculture, Ecosystems & Environment, 300: 106999.

Yan, B., Fang, N., Zhang, P., Shi, Z., 2013. Impacts of land use change on watershed streamflow and sediment yield: An assessment using hydrologic modelling and partial least squares regression. Journal of Hydrology, 484: 26-37.

Yan, Q., Bian, Z., Zhang, P., 2011. Spatialization of population density based on residential spots density. Geography and Geoinformatics, 27: 95-98. (in Chinese)

Yang, X., Zheng, X.-Q., Chen, R., 2014. A land use change model: Integrating landscape pattern indexes and Markov-CA. Ecological Modelling, 283: 1-7.

Yang, X., Zheng, X.-Q., Lv, L.-N., 2012. A spatiotemporal model of land use change based on ant colony optimization, Markov chain and cellular automata. Ecological Modelling, 233: 11-19.

Yu, D., Li, X., Cao, Q., Hao, R., Qiao, J., 2020. Impacts of climate variability and landscape pattern change on evapotranspiration in a grassland landscape mosaic. Hydrological Processes, 34(4): 1035-1051.

Yu, S., Xu, Z., Wu, W., Zuo, D., 2016. Effect of land use types on stream water quality under seasonal variation and topographic characteristics in the Wei River basin, China. Ecological Indicators, 60: 202-212.

Yue, W., Liu, Y., Fan, P., 2013. Measuring urban sprawl and its drivers in large Chinese cities: The case of Hangzhou. Land use policy, 31: 358-370.

Zalidis, G., Stamatiadis, S., Takavakoglou, V., Eskridge, K., Misopolinos, N., 2002. Impacts of agricultural practices on soil and water quality in the Mediterranean region and proposed assessment methodology. Agriculture, Ecosystems & Environment, 88(2): 137-146.

Zambrano-Bigiarini, M., 2020. Package 'hydroGOF'. Goodness-of-fit Functions for Comparison of Simulated and Observed.

Zebisch, M., Grothmann, T., Schroeter, D., Hasse, C., Fritsch, U., Cramer, W., 2005. Climate change in Germany. vulnerability and adaption of climate sensitive sectors; Klimawandel in Deutschland. Vulnerabilität und Anpassungsstrategien klimasensitiver Systeme.

Zeileis, A., Grothendieck, G., 2005. zoo: S3 infrastructure for regular and irregular time series. arXiv preprint math/0505527.

Zhang, J., Li, S., Jiang, C., 2020. Effects of land use on water quality in a River Basin (Daning) of the Three Gorges Reservoir Area, China: Watershed versus riparian zone. Ecol. Ind. 113, 106226.

Zhang, N., Luo, Y.-J., Chen, X.-Y., Li, Q., Jing, Y.-C., Wang, X., Feng, C.-H., 2018. Understanding the effects of composition and configuration of land covers on surface runoff in a highly urbanized area. Ecological Engineering, 125: 11-25.

Zhang, P., Liu, Y., Pan, Y., Yu, Z., 2013. Land use pattern optimization based on CLUE-S and SWAT models for agricultural non-point source pollution control. Mathematical and Computer Modelling, 58(3-4): 588-595.

Zhang, Y.-K., Schilling, K., 2006. Increasing streamflow and baseflow in Mississippi River since the 1940 s: Effect of land use change. Journal of Hydrology, 324(1-4): 412-422.

Zhao, Q., Wen, Z., Chen, S., Ding, S., Zhang, M., 2020. Quantifying land use/land cover and landscape pattern changes and impacts on ecosystem services. International journal of environmental research and public health, 17(1): 126.

Zhou, T., Wu, J., Peng, S., 2012. Assessing the effects of landscape pattern on river water quality at multiple scales: a case study of the Dongjiang River watershed, China. Ecological Indicators, 23: 166-175.

Zhou, Z., Li, J., 2015. The correlation analysis on the landscape pattern index and hydrological processes in the Yanhe watershed, China. Journal of Hydrology, 524: 417-426.

Ziegler, A.D., Tran, L.T., Giambelluca, T.W., Sidle, R.C., Sutherland, R.A., Nullet, M.A., Vien, T.D., 2006. Effective slope lengths for buffering hillslope surface runoff in fragmented landscapes in northern Vietnam. Forest Ecology and Management, 224(1-2): 104-118.

Zou, Y., Duan, X., Xue, Z., Mingju, E., Sun, M., Lu, X., Jiang, M., Yu, X., 2018. Water use conflict between wetland and agriculture. Journal of environmental management, 224: 140-146.

Acknowledgments

This dissertation is result of substantial field trips in the State of Schleswig-Holstein, Germany. Approximately 3,000 water samples were collected in the upper Stör catchment and considerable laboratory analyses were carried out. The hybrid of multiple multivariate analyses and SWAT model were applied. Many people have contributed to the completion of my dissertation in achievement of field and lab work or computer work or other ways.

My sincere gratitude shall go to Prof. Dr. Nicola Fohrer for her professional supervision and support in different ways. Firstly, I shall thank her for offering me the opportunity of pursing my PhD in the department of Hydrology and Water Resources. Secondly, thank her for the academic guidance and support in this interested research topic. Last but not least, I deeply appreciate that you always showed great kindness and generous support in my study and life. I would also like thank my second supervisor Dr. Paul Wagner for all the selfless favors he did for my PhD project. He is always patient, tolerant and friendly. The dissertation will not be completed without Paul's considerable technical supports and advice. Paul you made such a huge contribution to my PhD project work. Besides research work, I also learnt a lot from Dr. Paul Wagner in other ways. My words are not enough here to express my gratitude for all what you did to help with my PhD project. I will keep in mind the favors you both did for me forever.

I also thank our colleagues Dr. Björn Guse, Dr. Tibebe Tigabu, and Nariman Mahmoodi for sharing their experience or tips on hdrological modeling work. Dr. Björn Guse provided useful suggestion on parameter calibration for modeling hydrology. Dr. Tibebe Tigabu and Nariman Mahmoodi gave useful advice on small questions during the modeling of streamflow.

I would like to thank Bettina Hollmann, Falko Torreck, Monika Westphal, and Imke Meyer for guidance and help with field work and lab analysis. I particularly thank Jia Yuan, Anne-Kathrin Wendell, Henrike Risch, Lisa Jensen, Marian Scheffler, Josephiene Theresa Loeck, Tanja Boehlke for their support with the huge field and lab work. I am grateful to Cristiano Andre Pott for collecting water quality data of 2009-

2011. I shall thank Mrs. Sperlich, who allowed the installation of the automatic sampler near her house.

Thanks go to Georg Hörmann who helped me with computer or software installation issues. I appreciate favors that Dr. Uta Ulrich and Dr. Daniel Rosado did for me. Dr. Uta Ulrich provided friendly support in mapping land use in Kielstau catchment. Dr. Daniel Rosado supported me in IGCS scholarship project.

Very nice to meet Chinese colleagues Prof. Naicheng Wu, Prof. Yu Zeng, Prof. Chao Wang, Dr. Lichun Xie, Dr. Bing Li, Dr. Yueming Qu, Xiuming Sun. Thank you all for the company and support. And I am lucky to have Xiuming around whenever I need help. I also thank every member of the hydrology team for providing all kinds of supports to me during my study.

I would like to highly acknowledge the China Scholarship Council (CSC) for funding my doctoral study grant. Without the CSC scholarship, I may not have a chance to study abroad. I deeply appreciate the support from my motherland.

I am pleased to show my gratitude to Prof. Dr. Balaji Narasimhan for accepting me as IGCS scholar at the Indian Institute of Technology Madras (IITM). I am thankful to the IGCS team of German side for the funding support for the online IGCS exchange.

Lots of supports came from my family and friends back in China. Thanks to my parents, sister and brother for their unconditional love and support. Thank my parents for raising us happily and healthily. Thank my father for his good education and encouragement as always. Thank my sister and brother for keeping parents company when I am not around. I am also grateful to have a few best friends who always support me wherever I am!

I forward my gratitude to my former supervisor Prof. Dr. Youpeng Xu (Nanjing University, China) who led me to hydrology and water resources. Thank you for selfless help and encouragement! I was really happy to join in this big and warm hydrology family led by you. I would also like to say thanks to Dr. Song Song who recommended me to the current hydrology family in Kiel, Germany. Without you, I may miss the chance of joining the current team and knowing so many new lovely colleagues. Thank you so much! I thank all other former colleagues for the time we spent together.

Annex

Table 1. Four monthly in-situ measured water quality parameters of 21 sampling points in the Stör catchment in 2018-2019.

Date	Sampling Point	WT (°C)	EC (µs/cm)	DO (mg/l)	pH
18/10/2018	1	12.6	705	5.92	7.70
19/11/2018	1	5.0	762	9.76	8.02
16/12/2018	1	1.0	817	12.07	8.40
17/1/2019	1	2.1	646	10.34	7.42
18/2/2019	1	4.0	500	8.47	7.04
18/3/2019	1	5.1	400	9.33	7.40
18/4/2019	1	7.1	541	7.89	7.25
20/5/2019	1	16.5	500	4.30	7.60
17/6/2019	1	16.4	599	6.21	7.45
18/7/2019	1	14.6	733	NA	7.45
19/8/2019	1	15.9	659	NA	7.20
19/9/2019	1	9.0	715	7.75	7.78
18/10/2019	1	12.6	491	4.99	7.02
18/10/2018	2	11.9	650	5.79	7.40
19/11/2018	2	6.4	678	7.80	7.78
16/12/2018	2	3.5	680	10.85	9.27
17/1/2019	2	2.9	749	11.82	7.72
18/2/2019	2	5.9	708	10.29	7.77
18/3/2019	2	5.5	556	11.09	7.57
18/4/2019	2	8.7	671	9.25	7.70
20/5/2019	2	13.2	560	7.48	7.70
17/6/2019	2	14.3	634	7.56	7.65
18/7/2019	2	12.5	663	NA	7.81
19/8/2019	2	13.8	652	7.62	7.76
19/9/2019	2	9.9	669	8.27	7.77
18/10/2019	2	12.5	616	8.83	7.70
18/10/2018	3	12.3	652	7.14	7.66
19/11/2018	3	5.8	668	8.85	7.92
16/12/2018	3	2.2	716	12.50	8.53
17/1/2019	3	2.1	639	12.53	7.71
18/2/2019	3	4.8	535	10.42	7.30
18/3/2019	3	5.2	359	10.56	7.50
18/4/2019	3	7.5	585	9.54	7.66
20/5/2019	3	12.9	620	7.80	7.80
17/6/2019	3	14.2	606	8.09	7.77
18/7/2019	3	12.3	634	NA	7.94
19/8/2019	3	14.5	624	6.78	7.75
19/9/2019	3	9.5	641	9.77	8.20
18/10/2019	3	12.3	504	7.12	7.32
18/10/2018	4	12.5	682	5.78	7.38

19/11/2018	4	5.7	710	8.30	7.73
16/12/2018	4	2.6	722	11.45	8.72
17/1/2019	4	2.2	772	12.77	7.57
18/2/2019	4	5.3	700	10.80	7.74
18/3/2019	4	5.5	536	11.35	7.37
18/4/2019	4	8.3	679	10.02	7.65
20/5/2019	4	13.5	560	7.84	7.71
17/6/2019	4	14.5	668	8.01	7.68
18/7/2019	4	12.9	685	NA	7.70
19/8/2019	4	14.5	665	7.95	7.80
19/9/2019	4	9.9	704	7.62	7.62
18/10/2019	4	12.6	611	9.31	7.72
18/10/2018	5	12.2	657	7.96	7.63
19/11/2018	5	5.2	683	10.93	7.93
16/12/2018	5	2.0	690	13.19	11.25
17/1/2019	5	2.4	661	11.77	7.73
18/2/2019	5	6.2	662	9.81	7.55
18/3/2019	5	5.9	556	9.92	7.40
18/4/2019	5	9.1	643	10.05	7.67
20/5/2019	5	13.6	635	8.34	7.73
17/6/2019	5	16.0	634	8.22	7.68
18/7/2019	5	14.7	655	9.67	7.87
19/8/2019	5	14.3	656	9.18	7.77
19/9/2019	5	9.8	715	7.66	7.67
18/10/2019	5	12.4	659	7.40	7.59
18/10/2018	6	11.3	512	6.90	7.41
19/11/2018	6	7.3	512	9.51	7.88
16/12/2018	6	4.9	511	11.58	8.29
17/1/2019	6	5.1	506	11.50	7.76
18/2/2019	6	7.2	506	10.00	7.43
18/3/2019	6	7.0	503	10.05	7.52
18/4/2019	6	9.6	508	10.25	7.78
20/5/2019	6	12.3	510	9.49	7.94
17/6/2019	6	14.7	512	8.94	7.79
18/7/2019	6	14.3	512	9.11	7.86
19/8/2019	6	13.0	504	9.40	7.84
19/9/2019	6	11.2	510	9.00	7.76
18/10/2019	6	11.7	496	8.84	7.66
18/10/2018	7	11.4	495	6.41	7.46
19/11/2018	7	7.6	501	8.16	7.82
16/12/2018	7	5.2	504	10.85	8.88
17/1/2019	7	5.1	493	10.65	7.70
18/2/2019	7	7.9	493	8.98	7.62
18/3/2019	7	6.8	486	9.42	7.62
18/4/2019	7	9.4	500	10.63	7.85
20/5/2019	7	12.0	490	8.27	7.82

17/6/2019	7	13.1	498	8.69	7.79
18/7/2019	7	12.3	503	8.94	7.88
19/8/2019	7	12.3	497	9.00	7.81
19/9/2019	7	10.3	490	8.75	7.73
18/10/2019	7	11.6	488	7.85	7.65
18/10/2018	8	12.8	578	4.32	7.12
19/11/2018	8	7.0	594	4.82	7.33
16/12/2018	8	3.8	620	10.10	8.82
17/1/2019	8	3.7	576	11.87	7.65
18/2/2019	8	7.1	557	9.99	7.50
18/3/2019	8	6.3	500	9.55	7.54
18/4/2019	8	9.8	572	11.31	7.56
20/5/2019	8	13.2	587	7.41	7.45
17/6/2019	8	15.5	548	7.77	7.59
18/7/2019	8	14.9	599	7.94	7.59
19/8/2019	8	14.4	601	7.97	7.58
19/9/2019	8	11.3	587	8.00	7.57
18/10/2019	8	12.9	533	7.38	7.49
18/10/2018	9	13.4	726	8.37	7.71
19/11/2018	9	8.4	702	9.27	7.59
16/12/2018	9	4.3	675	11.83	8.26
17/1/2019	9	4.3	655	11.89	7.73
18/2/2019	9	7.3	649	10.50	7.72
18/3/2019	9	6.2	511	10.92	7.51
18/4/2019	9	10.6	641	11.40	7.96
20/5/2019	9	14.9	664	9.47	7.86
17/6/2019	9	16.8	644	8.99	7.83
18/7/2019	9	15.7	697	9.80	8.01
19/8/2019	9	15.4	666	9.38	7.94
19/9/2019	9	12.3	715	9.92	8.09
18/10/2019	9	13.1	596	8.57	7.70
18/10/2018	10	12.5	553	6.50	7.31
19/11/2018	10	7.6	548	9.03	7.57
16/12/2018	10	3.5	613	12.33	8.16
17/1/2019	10	3.8	626	12.80	7.80
18/2/2019	10	6.7	604	10.85	7.69
18/3/2019	10	6.2	535	10.65	7.42
18/4/2019	10	10.0	582	10.54	7.74
20/5/2019	10	13.8	575	8.80	7.75
17/6/2019	10	15.8	569	9.07	7.79
18/7/2019	10	15.1	552	9.00	7.80
19/8/2019	10	14.3	539	8.95	7.75
19/9/2019	10	11.3	561	9.14	7.78
18/10/2019	10	12.9	522	8.87	7.64
18/10/2018	11	11.9	485	6.76	7.75
19/11/2018	11	6.5	504	8.78	7.45

17/12/2018	11	3.7	522	11.19	8.48
18/1/2019	11	3.3	534	12.81	7.59
18/2/2019	11	5.6	505	11.02	7.51
18/3/2019	11	5.9	412	10.55	7.53
18/4/2019	11	9.1	512	11.83	7.58
20/5/2019	11	14.6	500	9.44	7.66
17/6/2019	11	16.1	505	9.85	7.68
18/7/2019	11	14.9	506	9.16	7.70
19/8/2019	11	14.7	495	8.49	7.63
19/9/2019	11	10.9	496	8.86	7.70
18/10/2019	11	12.9	503	8.57	7.35
18/10/2018	12	12.5	508	7.53	7.47
19/11/2018	12	6.0	511	9.50	7.48
17/12/2018	12	3.4	533	11.73	7.94
18/1/2019	12	6.3	553	11.18	7.61
18/2/2019	12	5.5	531	11.95	7.71
18/3/2019	12	6.1	425	9.25	7.41
18/4/2019	12	8.2	528	11.25	7.52
20/5/2019	12	13.8	517	9.73	7.60
17/6/2019	12	15.1	503	8.75	7.77
18/7/2019	12	15.1	478	10.02	7.84
19/8/2019	12	14.4	525	8.81	7.84
19/9/2019	12	10.5	528	11.48	7.97
18/10/2019	12	12.4	516	7.49	7.44
18/10/2018	13	12.7	498	4.79	7.23
19/11/2018	13	5.7	524	7.54	7.01
17/12/2018	13	2.7	568	11.61	8.65
18/1/2019	13	6.1	580	11.26	7.60
18/2/2019	13	4.8	536	12.03	7.63
18/3/2019	13	6.0	440	9.03	7.43
18/4/2019	13	8.2	537	11.47	7.60
20/5/2019	13	13.5	507	9.14	7.48
17/6/2019	13	15.2	500	8.47	7.63
18/7/2019	13	14.5	465	9.20	7.64
19/8/2019	13	14.5	532	7.64	7.67
19/9/2019	13	10.4	509	9.36	7.66
18/10/2019	13	12.5	491	6.76	7.39
18/10/2018	14	12.4	682	4.04	7.34
19/11/2018	14	5.8	688	6.54	7.49
17/12/2018	14	2.9	691	9.01	8.13
18/1/2019	14	6.0	660	9.26	7.27
18/2/2019	14	4.6	610	9.71	7.40
18/3/2019	14	5.7	431	7.63	7.16
18/4/2019	14	7.8	633	8.51	7.46
20/5/2019	14	13.9	644	5.01	7.37
17/6/2019	14	14.6	604	5.72	7.49

18/7/2019	14	13.4	637	7.22	7.51
19/8/2019	14	14.6	660	4.82	7.43
19/9/2019	14	10.3	692	6.83	7.53
18/10/2019	14	12.5	616	6.12	7.15
18/10/2018	15	11.7	414	8.05	7.64
19/11/2018	15	7.0	409	8.33	7.57
17/12/2018	15	3.9	404	11.85	8.46
18/1/2019	15	5.9	362	NA	7.68
18/2/2019	15	6.6	364	11.93	7.82
18/3/2019	15	6.5	220	9.52	7.50
18/4/2019	15	11.1	403	10.92	7.51
20/5/2019	15	12.5	414	10.17	7.82
17/6/2019	15	14.0	406	9.26	8.05
18/7/2019	15	13.8	399	10.12	8.10
19/8/2019	15	13.9	418	9.31	8.04
19/9/2019	15	11.0	422	10.90	8.12
18/10/2019	15	12.6	393	3.94	7.34
18/10/2018	16	13.5	579	11.41	7.76
19/11/2018	16	7.8	523	10.25	7.61
17/12/2018	16	5.2	529	10.17	8.59
18/1/2019	16	6.2	480	9.46	7.36
18/2/2019	16	5.0	486	10.77	7.52
18/3/2019	16	5.6	342	8.41	7.25
18/4/2019	16	7.8	523	12.53	7.62
20/5/2019	16	14.0	508	11.11	7.77
17/6/2019	16	15.2	504	9.18	7.67
18/7/2019	16	14.0	481	11.32	7.81
19/8/2019	16	14.1	510	5.78	7.32
19/9/2019	16	10.0	536	9.89	7.62
18/10/2019	16	12.3	440	6.70	6.94
18/10/2018	17	13.4	396	9.02	7.46
19/11/2018	17	6.4	422	9.70	7.54
17/12/2018	17	3.7	449	11.35	8.81
18/1/2019	17	5.8	433	10.60	7.48
18/2/2019	17	4.6	409	11.81	7.68
18/3/2019	17	5.4	310	8.97	7.39
18/4/2019	17	8.8	440	10.88	7.55
20/5/2019	17	15.8	436	8.92	7.67
17/6/2019	17	17.6	427	8.93	7.78
18/7/2019	17	16.5	419	9.61	7.81
19/8/2019	17	15.8	430	7.98	7.65
19/9/2019	17	10.8	435	9.91	7.71
18/10/2019	17	13.3	410	7.77	7.08
18/10/2018	18	12.7	376	8.07	7.77
19/11/2018	18	7.3	379	8.68	7.16
17/12/2018	18	5.5	375	10.12	8.08

18/1/2019	18	6.4	375	NA	7.25
18/2/2019	18	7.0	388	10.86	7.55
18/3/2019	18	6.9	286	7.89	6.74
18/4/2019	18	11.5	387	12.53	7.33
20/5/2019	18	15.3	372	9.88	7.70
17/6/2019	18	16.0	365	7.76	7.26
18/7/2019	18	14.6	351	9.40	7.32
19/8/2019	18	14.8	367	7.41	7.15
19/9/2019	18	11.0	375	9.86	7.28
18/10/2019	18	12.9	367	5.02	6.75
18/10/2018	19	12.1	432	8.42	7.33
19/11/2018	19	7.0	440	9.29	7.28
17/12/2018	19	4.9	470	10.36	8.68
18/1/2019	19	6.7	515	10.14	7.44
18/2/2019	19	5.6	478	10.92	7.58
18/3/2019	19	6.6	435	8.03	7.17
18/4/2019	19	8.9	493	11.58	7.45
20/5/2019	19	14.3	458	10.02	7.59
17/6/2019	19	15.7	487	9.10	7.62
18/7/2019	19	14.5	436	10.59	7.74
19/8/2019	19	14.5	486	8.66	7.53
19/9/2019	19	10.2	463	9.96	7.53
18/10/2019	19	12.4	492	5.72	7.07
18/10/2018	20	13.4	467	9.11	7.54
19/11/2018	20	5.6	478	10.25	7.54
17/12/2018	20	3.4	495	11.67	8.79
18/1/2019	20	6.2	482	NA	7.67
18/2/2019	20	6.0	467	11.54	7.70
18/3/2019	20	6.0	363	8.67	7.22
18/4/2019	20	10.2	502	11.31	7.73
20/5/2019	20	16.3	479	9.46	7.79
17/6/2019	20	17.4	452	8.65	7.73
18/7/2019	20	16.3	464	9.82	7.82
19/8/2019	20	15.9	481	7.82	7.68
19/9/2019	20	11.7	500	10.46	7.79
18/10/2019	20	12.7	445	6.97	7.24
18/10/2018	21_N	13.4	603	9.18	7.83
19/11/2018	21_N	5.9	589	10.01	7.56
17/12/2018	21_N	3.4	579	11.70	8.53
18/1/2019	21_N	6.3	537	NA	7.61
18/2/2019	21_N	6.8	545	11.60	7.81
18/3/2019	21_N	6.6	424	8.41	7.34
18/4/2019	21_N	11.4	584	11.77	7.80
20/5/2019	21_N	16.0	587	9.41	7.92
17/6/2019	21_N	17.6	577	8.49	7.86
18/7/2019	21_N	16.8	569	9.93	7.92

19/8/2019	21_N	16.0	582	8.92	7.93
19/9/2019	21_N	11.9	617	10.50	7.97
18/10/2019	21_N	12.9	516	6.17	7.52
18/10/2018	21_O	13.5	603	8.99	7.75
19/11/2018	21_O	5.9	590	9.95	7.67
17/12/2018	21_O	3.7	573	11.52	8.58
18/1/2019	21_O	6.6	540	NA	7.57
18/2/2019	21_O	6.8	544	11.55	7.74
18/3/2019	21_O	6.4	434	8.60	7.48
18/4/2019	21_O	10.8	617	11.50	7.82
20/5/2019	21_O	16.1	588	9.66	7.91
17/6/2019	21_O	17.3	561	8.42	7.87
18/7/2019	21_O	16.5	565	10.05	7.99
19/8/2019	21_O	16.4	570	8.78	7.87
19/9/2019	21_O	12.0	617	10.64	7.99
18/10/2019	21_O	12.8	517	5.99	7.51

Note: 21_N refers to the site of sampler in 2018-2019; 21_O refers to the old site of sampler in 2009-2011.

Table 2. Monthly nutrient parameters of 21 sampling points in the Stör catchment in 2018-2019.

Date	Sampling Point	NH_4-N(mg/l)	NO_3-N(mg/l)	TN(mg/l)	PO_4-P(mg/l)	TP(mg/l)	TSS(mg/l)
18/10/2018	1	0.015	0.384	2.870	0.023	0.067	3
19/11/2018	1	0.024	0.672	1.200	0.044	0.067	NA
16/12/2018	1	0.534	2.140	3.940	0.060	0.133	NA
17/1/2019	1	0.657	3.818	7.380	0.084	0.160	2.5
18/2/2019	1	0.239	2.679	5.730	0.068	0.133	4.2
18/3/2019	1	0.164	4.066	3.590	0.083	0.152	4.9
18/4/2019	1	0.101	1.062	2.190	0.070	0.157	2.5
20/5/2019	1	0.067	0.293	1.900	0.069	0.135	6.2
17/6/2019	1	0.519	1.051	2.750	0.300	0.466	2.6
18/7/2019	1	0.024	0.032	0.270	0.041	0.087	1.1
19/8/2019	1	0.255	0.028	2.340	0.233	0.701	0.7
19/9/2019	1	0.024	0.436	1.180	0.060	0.152	10.5
18/10/2019	1	0.348	3.035	6.350	0.166	0.306	2.8
18/10/2018	2	0.019	0.949	0.840	0.017	0.054	4.8
19/11/2018	2	0.057	0.713	1.340	0.017	0.053	1.4
16/12/2018	2	0.093	1.217	1.480	0.014	0.215	0.4
17/1/2019	2	0.213	5.582	8.910	0.041	0.172	0.4
18/2/2019	2	0.124	6.554	6.020	0.026	0.117	14.1
18/3/2019	2	0.113	8.257	6.250	0.093	0.167	7.2
18/4/2019	2	0.026	1.455	1.920	0.011	0.074	7.2
20/5/2019	2	0.029	0.993	1.200	0.012	0.049	5.3
17/6/2019	2	0.118	3.500	5.680	0.082	0.221	1.8
18/7/2019	2	0.033	0.959	1.500	0.019	0.055	1.7

19/8/2019	2	0.039	1.599	2.460	0.061	0.160	3
19/9/2019	2	0.029	0.997	1.620	0.019	0.075	1
18/10/2019	2	0.054	6.582	9.570	0.120	0.239	2
18/10/2018	3	0.010	1.336	1.670	0.017	0.039	1.9
19/11/2018	3	0.057	1.676	3.270	0.024	0.044	14.5
16/12/2018	3	0.220	1.823	4.010	0.026	0.099	1.1
17/1/2019	3	0.304	4.465	6.990	0.066	0.148	NA
18/2/2019	3	0.143	3.155	4.580	0.054	0.115	NA
18/3/2019	3	0.162	3.840	3.290	0.071	0.161	1.8
18/4/2019	3	0.049	1.707	3.180	0.051	0.107	6.7
20/5/2019	3	0.029	2.619	2.200	0.032	0.075	3.4
17/6/2019	3	0.191	1.719	3.450	0.161	0.287	6.1
18/7/2019	3	0.046	1.980	3.020	0.038	0.073	3.2
19/8/2019	3	0.040	1.098	2.660	0.073	0.143	2.6
19/9/2019	3	0.019	1.525	2.830	0.036	0.069	1.7
18/10/2019	3	0.175	2.975	6.300	0.134	0.202	2.1
18/10/2018	4	0.022	1.007	3.110	0.006	0.124	1.7
19/11/2018	4	0.050	0.966	0.920	0.007	0.103	0.9
16/12/2018	4	0.148	0.926	1.520	0.013	0.127	6.1
17/1/2019	4	0.402	10.193	8.890	0.091	0.224	7.7
18/2/2019	4	0.158	7.361	3.960	0.040	0.127	5
18/3/2019	4	0.117	8.261	5.550	0.095	0.168	5
18/4/2019	4	0.031	2.059	2.540	0.011	0.099	5.6
20/5/2019	4	0.060	1.255	1.910	0.013	0.083	5.9
17/6/2019	4	0.117	3.175	5.540	0.143	0.298	5
18/7/2019	4	0.043	0.842	1.360	0.012	0.069	7
19/8/2019	4	0.036	1.684	2.710	0.140	0.253	3.7
19/9/2019	4	0.039	0.895	1.320	0.014	0.120	3.8
18/10/2019	4	0.057	6.145	9.400	0.134	0.252	4.7
18/10/2018	5	0.029	1.612	1.460	0.019	0.133	3.4
19/11/2018	5	0.022	0.528	1.580	0.017	0.085	3.6
16/12/2018	5	0.092	1.364	1.760	0.010	0.098	6.5
17/1/2019	5	0.646	3.144	4.040	0.015	0.177	14.2
18/2/2019	5	0.089	2.787	3.810	0.010	0.102	7.6
18/3/2019	5	0.187	8.235	7.920	0.077	0.153	5.3
18/4/2019	5	0.027	1.815	3.310	0.012	0.170	5.3
20/5/2019	5	0.033	1.704	1.610	0.015	0.073	3.5
17/6/2019	5	0.080	1.785	2.900	0.026	0.137	6.6
18/7/2019	5	0.019	0.488	0.920	0.012	0.056	4.5
19/8/2019	5	0.024	0.368	0.550	0.011	0.088	5.5
19/9/2019	5	0.114	0.449	0.560	0.017	0.119	11.9
18/10/2019	5	0.178	3.999	5.790	0.031	0.199	3.4
18/10/2018	6	0.034	0.773	2.470	0.018	0.082	3.4
19/11/2018	6	0.042	0.405	1.060	0.024	0.053	3.3
16/12/2018	6	0.097	0.761	1.670	0.020	0.083	4.4
17/1/2019	6	0.215	1.074	1.040	0.019	0.104	10

18/2/2019	6	0.305	1.056	1.540	0.025	0.108	9.2
18/3/2019	6	0.302	1.921	1.890	0.037	0.067	5
18/4/2019	6	0.110	1.014	1.400	0.022	0.096	0.4
20/5/2019	6	0.134	1.093	1.150	0.032	0.086	0.4
17/6/2019	6	0.165	0.877	1.590	0.037	0.143	1.3
18/7/2019	6	0.084	0.480	1.300	0.032	0.099	4.8
19/8/2019	6	0.066	0.902	1.380	0.030	0.088	2.9
19/9/2019	6	0.063	0.862	1.130	0.028	0.095	1.5
18/10/2019	6	0.227	1.100	2.160	0.035	0.108	2.4
18/10/2018	7	0.024	0.868	1.490	0.027	0.094	2.8
19/11/2018	7	0.028	1.095	1.170	0.028	0.063	3
16/12/2018	7	0.084	1.006	1.320	0.022	0.131	4.1
17/1/2019	7	0.303	0.892	2.420	0.027	0.184	1.5
18/2/2019	7	0.233	1.352	2.180	0.027	0.137	3.5
18/3/2019	7	0.433	1.830	2.520	0.046	0.098	6.2
18/4/2019	7	0.041	1.039	1.700	0.024	0.115	3.7
20/5/2019	7	0.086	1.312	1.230	0.040	0.118	0.6
17/6/2019	7	0.135	1.005	1.650	0.044	0.136	0.6
18/7/2019	7	0.057	0.900	1.580	0.038	0.093	3
19/8/2019	7	0.064	1.273	1.360	0.038	0.103	10
19/9/2019	7	0.055	0.988	1.730	0.033	0.128	5
18/10/2019	7	0.228	1.133	2.380	0.048	0.141	1.8
18/10/2018	8	0.042	0.427	2.180	0.007	0.024	2.7
19/11/2018	8	0.402	0.201	1.080	0.003	0.058	4.3
16/12/2018	8	0.334	0.460	1.340	0.000	0.071	2.7
17/1/2019	8	0.147	0.283	1.630	0.007	0.270	2.7
18/2/2019	8	0.133	0.486	1.220	0.007	0.057	1.2
18/3/2019	8	0.188	1.057	1.390	0.011	0.130	5.8
18/4/2019	8	0.034	0.455	0.770	0.001	0.071	2
20/5/2019	8	0.127	0.677	1.120	0.008	0.130	0.4
17/6/2019	8	0.118	0.359	1.220	0.011	0.084	3.7
18/7/2019	8	0.113	0.793	1.600	0.008	0.046	3.7
19/8/2019	8	0.114	0.756	3.380	0.010	0.088	2.5
19/9/2019	8	0.097	0.822	1.730	0.009	0.066	34.5
18/10/2019	8	0.282	0.488	2.100	0.019	0.131	3.4
18/10/2018	9	0.042	1.046	1.260	0.011	0.088	3.7
19/11/2018	9	0.219	0.942	1.770	0.031	0.079	8.5
16/12/2018	9	0.234	1.183	1.730	0.000	0.164	62.4
17/1/2019	9	0.289	2.349	3.460	0.024	0.274	3.9
18/2/2019	9	0.205	2.335	3.070	0.025	0.150	3.3
18/3/2019	9	0.149	4.219	4.440	0.048	0.265	4.2
18/4/2019	9	0.039	0.725	1.730	0.009	0.097	3.4
20/5/2019	9	0.127	0.686	1.140	0.036	0.129	8.5
17/6/2019	9	0.224	1.550	2.820	0.062	0.163	3
18/7/2019	9	0.081	0.684	1.430	0.056	0.122	1.1
19/8/2019	9	0.067	0.908	1.440	0.043	0.152	1.1

19/9/2019	9	0.024	0.889	1.550	0.034	0.150	6.7
18/10/2019	9	0.129	3.826	6.200	0.075	0.194	40.8
18/10/2018	10	0.009	1.905	1.300	0.004	0.014	5.7
19/11/2018	10	0.031	1.452	1.740	0.008	0.047	8
16/12/2018	10	0.133	1.234	1.350	0.008	0.077	3.3
17/1/2019	10	0.149	0.965	2.000	0.005	0.103	5.1
18/2/2019	10	0.141	1.513	1.090	0.006	0.111	2.1
18/3/2019	10	0.178	3.151	3.120	0.021	0.124	2.1
18/4/2019	10	0.048	1.088	1.880	0.009	0.065	1.6
20/5/2019	10	0.037	1.168	1.670	0.011	0.057	7.9
17/6/2019	10	0.035	0.889	1.640	0.012	0.084	8.8
18/7/2019	10	0.037	1.360	2.200	0.007	0.039	0.7
19/8/2019	10	0.034	1.126	1.930	0.007	0.059	0.4
19/9/2019	10	0.030	1.336	1.180	0.011	0.075	0.4
18/10/2019	10	0.065	1.215	2.300	0.008	0.056	4.3
18/10/2018	11	0.035	0.450	2.580	0.006	0.018	8.5
19/11/2018	11	0.057	0.343	0.780	0.002	0.024	10.6
17/12/2018	11	0.176	0.571	1.380	0.000	0.086	9.6
18/1/2019	11	0.206	1.238	3.390	0.006	0.123	4
18/2/2019	11	0.179	1.985	2.140	0.005	0.083	3.8
18/3/2019	11	0.118	5.144	4.740	0.052	0.117	4.6
18/4/2019	11	0.046	0.727	0.430	0.008	0.078	3.4
20/5/2019	11	0.035	0.457	0.570	0.007	0.056	1.8
17/6/2019	11	0.051	0.765	1.550	0.006	0.075	3.2
18/7/2019	11	0.037	0.429	0.720	0.006	0.036	7.2
19/8/2019	11	0.049	0.459	0.570	0.011	0.080	1.2
19/9/2019	11	0.045	0.499	0.710	0.007	0.065	1.6
18/10/2019	11	0.075	3.400	4.980	0.005	0.090	1.6
18/10/2018	12	0.008	2.535	0.800	0.003	0.029	6.6
19/11/2018	12	0.039	1.531	2.560	0.005	0.051	7.8
17/12/2018	12	0.093	2.354	2.350	0.000	0.130	12.2
18/1/2019	12	0.105	3.611	5.020	0.021	0.065	14.8
18/2/2019	12	0.117	4.164	3.530	0.025	0.090	5.7
18/3/2019	12	0.141	1.556	4.380	0.010	0.170	3.3
18/4/2019	12	0.047	3.253	3.070	0.022	0.092	1.3
20/5/2019	12	0.013	2.606	3.790	0.012	0.085	3.6
17/6/2019	12	0.055	1.516	3.670	0.013	0.126	5.3
18/7/2019	12	0.029	2.194	3.150	0.005	0.053	1.8
19/8/2019	12	0.031	2.254	3.050	0.006	0.077	6.2
19/9/2019	12	0.020	2.267	3.320	0.010	0.065	1.8
18/10/2019	12	0.057	3.497	5.850	0.048	0.120	4.8
18/10/2018	13	0.004	NA	2.050	0.004	0.026	4.8
19/11/2018	13	0.045	0.166	0.620	0.004	0.038	8.4
17/12/2018	13	0.119	0.732	1.270	0.000	0.072	4.8
18/1/2019	13	0.113	1.916	4.070	0.009	0.114	5.4
18/2/2019	13	0.109	2.579	1.890	0.006	0.071	10.4

18/3/2019	13	0.127	2.489	4.790	0.025	0.113	4.1
18/4/2019	13	0.056	0.818	1.330	0.010	0.066	5.1
20/5/2019	13	0.070	0.638	0.910	0.012	0.061	3.6
17/6/2019	13	0.091	0.610	1.330	0.013	0.092	4
18/7/2019	13	0.051	0.459	0.550	0.004	0.053	7.5
19/8/2019	13	0.050	0.437	0.470	0.012	0.076	2.2
19/9/2019	13	0.043	0.273	0.540	0.008	0.072	4.3
18/10/2019	13	0.069	1.546	3.370	0.026	0.128	1.6
18/10/2018	14	0.017	1.289	0.380	0.010	0.055	1.7
19/11/2018	14	0.092	2.219	4.060	0.024	0.077	1.7
17/12/2018	14	0.224	2.242	3.860	0.020	0.147	2.4
18/1/2019	14	0.185	5.444	6.660	0.077	0.183	7.9
18/2/2019	14	0.195	5.421	6.890	0.048	0.091	7
18/3/2019	14	0.141	5.421	8.750	0.121	0.198	11.7
18/4/2019	14	0.115	4.051	5.860	0.034	0.102	3.8
20/5/2019	14	0.107	3.468	4.910	0.039	0.109	3.5
17/6/2019	14	0.090	3.368	5.320	0.063	0.145	3.4
18/7/2019	14	0.070	3.025	4.510	0.030	0.084	5.1
19/8/2019	14	0.058	3.143	4.390	0.038	0.105	2.9
19/9/2019	14	0.048	3.725	5.980	0.040	0.099	3.2
18/10/2019	14	0.105	4.547	7.820	0.099	0.192	6
18/10/2018	15	0.005	0.253	0.610	0.008	0.021	0.7
19/11/2018	15	0.014	0.132	0.530	0.008	0.023	3
17/12/2018	15	0.024	0.459	0.600	0.000	0.064	3
18/1/2019	15	0.028	7.384	6.340	0.005	0.062	3.9
18/2/2019	15	0.040	0.844	1.360	0.000	0.080	6.5
18/3/2019	15	0.040	2.902	2.980	0.008	0.071	2.7
18/4/2019	15	0.025	0.184	0.110	0.015	0.081	18.1
20/5/2019	15	0.021	0.195	0.100	0.012	0.060	3
17/6/2019	15	0.023	0.225	0.260	0.009	0.130	2.5
18/7/2019	15	0.020	0.293	0.260	0.007	0.047	0.9
19/8/2019	15	0.019	0.262	0.170	0.007	0.076	3.1
19/9/2019	15	0.027	0.262	0.120	0.016	0.070	0.3
18/10/2019	15	0.042	11.035	10.970	0.016	0.062	2.3
18/10/2018	16	0.048	3.932	6.460	0.018	0.040	4.8
19/11/2018	16	0.289	2.467	5.840	0.026	0.057	9.6
17/12/2018	16	0.497	4.256	6.590	0.035	0.134	NA
18/1/2019	16	0.704	4.334	8.180	0.125	0.248	NA
18/2/2019	16	0.494	1.757	4.870	0.061	0.150	2.3
18/3/2019	16	0.377	4.268	4.210	0.157	0.212	2.1
18/4/2019	16	0.259	4.615	4.230	0.031	0.087	21.6
20/5/2019	16	0.031	3.523	7.500	0.023	0.058	15.8
17/6/2019	16	0.473	4.212	7.750	0.088	0.148	7.2
18/7/2019	16	0.013	5.504	7.050	0.030	0.060	18.6
19/8/2019	16	0.171	4.002	4.520	0.094	0.139	39.8
19/9/2019	16	0.281	4.419	7.210	0.037	0.108	6.2

18/10/2019	16	0.377	5.286	9.300	0.125	0.234	9.8
18/10/2018	17	0.041	2.020	2.730	0.019	0.035	9.8
19/11/2018	17	0.145	1.056	3.830	0.021	0.057	5.6
17/12/2018	17	0.288	3.023	3.590	0.022	0.157	0.7
18/1/2019	17	0.321	5.307	6.360	0.027	0.148	1.5
18/2/2019	17	0.257	2.860	3.880	0.023	0.107	1.5
18/3/2019	17	0.215	2.764	5.180	0.078	0.194	4.7
18/4/2019	17	0.060	3.201	4.670	0.018	0.088	3.8
20/5/2019	17	0.106	2.899	3.750	0.023	0.072	2.6
17/6/2019	17	0.252	2.171	4.070	0.052	0.142	7
18/7/2019	17	0.028	2.330	3.210	0.034	0.093	3.1
19/8/2019	17	0.065	2.072	3.690	0.063	0.137	2.3
19/9/2019	17	0.045	2.316	3.570	0.028	0.082	0.1
18/10/2019	17	0.220	3.037	5.150	0.065	0.158	1.4
18/10/2018	18	0.066	4.968	7.090	0.038	0.060	5.7
19/11/2018	18	0.111	6.002	8.140	0.043	0.077	3.3
17/12/2018	18	0.205	6.605	8.720	0.043	0.117	9.2
18/1/2019	18	0.402	6.620	7.720	0.073	0.183	2.3
18/2/2019	18	0.323	6.471	7.810	0.042	0.106	3.5
18/3/2019	18	0.230	4.144	6.830	0.168	0.239	3.5
18/4/2019	18	0.047	6.328	9.880	0.027	0.147	NA
20/5/2019	18	0.170	6.859	4.950	0.043	0.164	10.4
17/6/2019	18	0.312	5.412	7.880	0.078	0.167	6.4
18/7/2019	18	0.086	7.748	9.000	0.073	0.134	11.9
19/8/2019	18	0.138	6.269	4.660	0.119	0.190	3.3
19/9/2019	18	0.081	7.228	6.420	0.064	0.119	2
18/10/2019	18	0.167	5.243	9.810	0.149	0.234	1.1
18/10/2018	19	0.013	0.443	1.180	0.009	0.010	1.7
19/11/2018	19	0.246	0.452	1.210	0.009	0.066	4
17/12/2018	19	0.536	0.300	1.330	0.012	0.120	1.9
18/1/2019	19	0.339	1.139	1.510	0.011	0.135	10.9
18/2/2019	19	0.390	1.303	2.300	0.017	0.086	0.2
18/3/2019	19	0.294	2.146	2.290	0.026	0.126	2
18/4/2019	19	0.192	0.534	1.260	0.010	0.060	2
20/5/2019	19	0.152	0.449	0.430	0.008	0.048	3
17/6/2019	19	0.152	0.564	1.800	0.010	0.058	3.5
18/7/2019	19	0.009	0.566	0.680	0.006	0.030	3.7
19/8/2019	19	0.012	0.315	0.630	0.004	0.028	0
19/9/2019	19	0.010	0.545	0.430	0.004	0.019	12.6
18/10/2019	19	0.027	1.193	1.950	0.008	0.029	10.7
18/10/2018	20	0.051	2.258	3.210	0.019	0.080	2.7
19/11/2018	20	0.179	2.280	3.320	0.019	0.072	1.9
17/12/2018	20	0.253	2.927	3.710	0.022	0.128	3.4
18/1/2019	20	0.279	2.941	6.000	0.025	0.172	1.5
18/2/2019	20	0.198	3.032	3.270	0.034	0.118	6
18/3/2019	20	0.194	3.427	5.690	0.062	0.164	1.7

18/4/2019	20	0.035	2.564	4.110	0.019	0.108	10.9
20/5/2019	20	0.060	2.202	1.140	0.017	0.080	10.9
17/6/2019	20	0.170	1.697	3.230	0.029	0.119	7.9
18/7/2019	20	0.060	1.551	3.770	0.028	0.098	8.8
19/8/2019	20	0.036	2.041	3.070	0.033	0.124	7.5
19/9/2019	20	0.049	1.578	3.400	0.021	0.086	8.6
18/10/2019	20	0.140	3.063	5.540	0.058	0.137	6.4
18/10/2018	21_N	0.009	1.213	2.180	0.016	0.089	2.9
19/11/2018	21_N	0.128	1.266	2.290	0.019	0.034	1.5
17/12/2018	21_N	0.203	2.195	1.800	0.020	0.144	0.2
18/1/2019	21_N	0.232	1.699	3.260	0.020	0.169	0.5
18/2/2019	21_N	0.182	2.502	4.070	0.031	0.141	1.5
18/3/2019	21_N	0.156	3.283	4.030	0.052	0.158	9.9
18/4/2019	21_N	0.019	2.011	2.900	0.012	0.113	5
20/5/2019	21_N	0.030	0.876	1.520	0.017	0.089	4.7
17/6/2019	21_N	0.113	1.517	2.940	0.037	0.140	4.7
18/7/2019	21_N	0.029	1.568	2.580	0.040	0.107	5.6
19/8/2019	21_N	0.015	1.267	2.240	0.039	0.123	14.8
19/9/2019	21_N	0.019	1.115	2.260	0.027	0.120	8.2
18/10/2019	21_N	0.095	3.666	5.810	0.068	0.161	5.8
18/10/2018	21_O	0.017	1.672	2.130	0.016	0.067	5.1
19/11/2018	21_O	0.141	1.289	2.300	0.022	0.086	3.8
17/12/2018	21_O	0.227	2.025	2.880	0.025	0.155	4.5
18/1/2019	21_O	0.226	3.273	2.430	0.020	0.157	4.1
18/2/2019	21_O	0.187	1.117	3.690	0.030	0.141	5.2
18/3/2019	21_O	0.153	3.002	3.160	0.051	0.162	3.4
18/4/2019	21_O	0.023	1.983	2.980	0.012	0.111	10
20/5/2019	21_O	0.027	1.491	1.700	0.017	0.080	8.5
17/6/2019	21_O	0.106	1.641	2.120	0.044	0.140	3.5
18/7/2019	21_O	0.039	1.511	2.750	0.040	0.156	3.5
19/8/2019	21_O	0.016	1.391	1.910	0.039	0.121	7.9
19/9/2019	21_O	0.019	1.453	1.950	0.028	0.094	12.9
18/10/2019	21_O	0.101	3.627	4.100	0.059	0.195	9.6

Note: 21_N refers to the site of sampler in 2018-2019; 21_O refers to the old site of sampler in 2009-2011.

Table 3. Daily measurements of water quality parameters in Willenscharen in 2018-2019.

Date	NH_4-N(mg/l)	NO_3-N(mg/l)	TN (mg/l)	PO_4-P(mg/l)	TP (mg/l)	TSS (mg/l)
09/10/2018	0.004	1.924	2.310	0.018	0.105	NA
19/10/2018	0.041	1.117	1.870	0.013	0.176	36.9
20/10/2018	0.015	1.290	2.000	0.009	0.195	28.8
21/10/2018	0.035	1.311	2.000	0.010	0.193	26.6
22/10/2018	0.012	1.285	2.020	0.008	0.242	34.5
23/10/2018	0.020	1.502	2.670	0.016	0.263	46.3
24/10/2018	0.039	1.711	2.670	0.014	0.126	20.2
25/10/2018	0.014	1.411	2.190	0.009	0.356	16.7
26/10/2018	0.021	1.253	2.210	0.010	0.191	34.8

27/10/2018	0.027	1.095	1.270	0.013	0.416	85.0
28/10/2018	0.020	1.558	2.220	0.016	0.253	75.5
29/10/2018	0.323	1.638	2.290	0.032	0.293	39.5
30/10/2018	0.073	1.555	1.570	0.029	0.303	45.0
31/10/2018	0.095	1.233	2.830	0.026	0.221	39.0
01/11/2018	0.072	1.258	2.410	0.019	0.211	36.5
02/11/2018	0.040	1.407	1.450	0.005	0.286	40.0
03/11/2018	0.047	1.511	1.930	0.007	0.250	30.5
04/11/2018	0.086	1.717	2.950	0.012	0.612	42.5
05/11/2018	0.045	1.432	1.840	0.007	0.242	30.0
06/11/2018	0.039	1.334	2.260	0.010	0.723	34.5
07/11/2018	0.048	1.465	2.200	0.013	0.301	11.0
08/11/2018	NA	NA	NA	NA	NA	NA
09/11/2018	NA	NA	NA	NA	NA	NA
10/11/2018	NA	NA	NA	NA	NA	NA
11/11/2018	NA	NA	NA	NA	NA	NA
12/11/2018	NA	NA	NA	NA	NA	NA
13/11/2018	NA	NA	NA	NA	NA	NA
14/11/2018	NA	NA	NA	NA	NA	NA
15/11/2018	0.112	1.889	2.230	0.017	0.172	16.8
16/11/2018	0.056	1.630	3.330	0.020	0.168	15.5
17/11/2018	0.035	1.718	2.050	0.018	0.139	12.8
18/11/2018	0.064	1.522	2.500	0.016	0.162	14.2
19/11/2018	0.025	1.896	2.470	0.022	0.158	12.8
20/11/2018	0.038	1.810	2.500	0.024	0.208	17.0
21/11/2018	0.039	1.259	2.010	0.020	0.168	17.7
22/11/2018	0.031	1.582	2.140	0.017	0.210	17.8
23/11/2018	0.035	1.836	2.640	0.011	0.145	10.8
24/11/2018	0.032	1.730	2.340	0.011	0.135	10.1
25/11/2018	0.031	1.878	2.750	0.010	0.128	9.2
26/11/2018	0.033	1.933	2.830	0.014	0.147	12.6
27/11/2018	0.044	1.756	1.950	0.013	0.137	12.3
28/11/2018	0.049	1.838	2.520	0.012	0.151	10.4
29/11/2018	0.018	1.792	2.820	0.012	0.157	33.9
30/11/2018	0.019	1.833	1.690	0.011	0.148	10.1
01/12/2018	0.017	1.815	2.630	0.009	0.135	12.5
02/12/2018	0.025	1.748	1.930	0.008	0.038	15.0
03/12/2018	0.009	1.445	2.640	0.011	0.141	17.4
04/12/2018	0.023	1.946	2.380	0.018	0.165	17.8
05/12/2018	0.029	1.727	2.410	0.026	0.145	10.3
06/12/2018	0.009	1.814	2.950	0.012	0.111	8.6
07/12/2018	0.013	2.088	2.210	0.009	0.155	12.9
08/12/2018	0.046	2.414	1.950	0.015	0.231	38.5
09/12/2018	0.100	3.298	2.290	0.018	0.234	55.7
10/12/2018	0.051	3.186	4.260	0.020	0.333	38.9
11/12/2018	0.058	1.953	4.090	0.020	0.172	19.6
12/12/2018	0.089	2.222	3.490	0.012	0.102	18.5
13/12/2018	0.028	2.492	3.420	0.011	0.186	19.6
14/12/2018	0.019	2.248	2.930	0.010	0.111	14.1
15/12/2018	0.024	2.299	3.100	0.008	0.116	14.8
16/12/2018	0.030	1.967	3.100	0.008	0.178	13.6
17/12/2018	0.033	2.121	2.620	0.006	0.182	12.3
18/12/2018	0.014	2.085	1.160	0.005	0.117	11.1
19/12/2018	0.028	1.525	2.980	0.006	0.151	13.2

20/12/2018	0.015	2.018	2.590	0.005	0.156	33.6
21/12/2018	0.015	1.959	2.180	0.007	0.184	45.5
22/12/2018	0.079	3.067	4.170	0.011	0.193	41.0
23/12/2018	0.043	3.077	2.930	0.006	0.216	25.3
24/12/2018	0.068	3.460	3.120	0.007	0.191	17.9
25/12/2018	0.041	3.148	3.820	0.008	0.152	15.3
26/12/2018	0.055	2.723	4.150	0.009	0.169	14.3
27/12/2018	0.027	2.164	3.560	0.008	0.166	14.8
28/12/2018	0.023	2.443	2.880	0.008	0.156	16.6
29/12/2018	0.030	1.496	2.810	0.009	0.198	24.7
30/12/2018	0.048	NA	3.650	0.007	0.000	21.0
31/12/2018	0.044	2.682	3.490	0.018	0.000	16.9
01/01/2019	0.023	2.576	2.440	0.017	0.160	15.9
02/01/2019	0.069	2.781	3.500	0.021	0.148	16.9
03/01/2019	0.060	2.308	3.380	0.017	0.199	21.1
04/01/2019	0.024	2.161	2.980	0.014	0.144	16.0
05/01/2019	0.037	1.728	2.220	0.017	0.141	15.6
06/01/2019	0.024	2.156	2.980	0.027	0.124	12.6
07/01/2019	0.026	1.999	1.850	0.025	0.128	16.2
08/01/2019	0.058	2.572	3.570	0.029	0.145	24.9
09/01/2019	0.073	2.735	3.240	0.027	0.126	13.0
10/01/2019	0.041	2.384	3.650	0.023	0.123	13.3
11/01/2019	0.036	2.448	3.270	0.021	0.136	14.7
12/01/2019	0.032	2.358	3.240	0.022	0.136	17.4
13/01/2019	0.052	2.616	3.710	0.022	0.160	22.7
14/01/2019	0.078	2.600	4.380	0.026	0.157	20.3
15/01/2019	0.044	2.203	2.360	0.023	0.149	24.4
16/01/2019	0.077	2.465	2.760	0.023	0.198	20.3
17/01/2019	0.016	2.145	5.180	0.040	0.184	31.5
18/01/2019	0.025	3.406	4.510	0.039	0.166	23.5
19/01/2019	0.023	3.715	4.410	0.039	0.217	34.4
20/01/2019	0.051	2.712	4.840	0.035	0.199	30.5
21/01/2019	NA	NA	NA	NA	NA	NA
22/01/2019	NA	NA	NA	NA	NA	NA
23/01/2019	NA	NA	NA	NA	NA	NA
24/01/2019	NA	NA	NA	NA	NA	NA
25/01/2019	NA	NA	NA	NA	NA	NA
26/01/2019	0.031	2.252	3.210	0.016	0.444	NA
27/01/2019	0.013	2.860	3.930	0.055	0.346	48.6
28/01/2019	0.015	3.796	4.960	0.051	0.247	39.4
29/01/2019	0.019	4.113	5.200	0.044	0.210	35.3
30/01/2019	0.028	3.589	4.820	0.039	0.252	52.0
31/01/2019	0.028	3.692	4.640	0.043	0.295	46.0
01/02/2019	NA	NA	NA	NA	NA	NA
02/02/2019	0.048	2.679	2.740	0.024	0.240	39.6
03/02/2019	0.076	2.666	3.190	0.029	0.185	29.9
04/02/2019	0.090	2.460	2.590	0.027	0.233	31.8
05/02/2019	0.094	2.415	2.860	0.026	0.232	32.4
06/02/2019	0.135	2.429	3.340	0.026	0.264	36.1
07/02/2019	0.044	1.664	4.190	0.034	0.240	69.7
08/02/2019	0.065	4.107	3.660	0.031	0.229	35.3
09/02/2019	0.070	4.146	2.690	0.028	0.330	37.0
10/02/2019	0.053	2.812	3.620	0.038	0.695	56.6
11/02/2019	0.122	4.530	4.920	0.044	0.447	119.9

12/02/2019	0.112	5.219	4.330	0.033	0.559	59.1
13/02/2019	0.105	4.257	5.490	0.028	0.573	43.5
14/02/2019	0.095	4.123	4.920	0.025	0.595	47.3
15/02/2019	0.103	3.794	4.320	0.022	0.664	51.6
16/02/2019	0.091	2.763	2.840	0.020	0.377	42.8
17/02/2019	0.105	3.252	4.040	0.026	0.432	45.4
18/02/2019	0.029	2.945	3.320	0.020	0.362	44.5
19/02/2019	0.049	1.769	2.760	0.019	0.413	38.1
20/02/2019	0.053	1.320	3.700	0.022	0.228	40.4
21/02/2019	0.119	2.251	3.730	0.020	0.364	42.9
22/02/2019	0.101	2.112	3.510	0.018	0.307	39.1
23/02/2019	0.065	1.857	3.710	0.014	0.417	42.4
24/02/2019	0.075	2.277	3.560	0.012	0.450	29.6
25/02/2019	0.082	2.326	2.720	0.011	0.318	43.4
26/02/2019	0.093	1.895	3.280	0.010	0.271	40.3
27/02/2019	0.049	2.268	3.150	0.008	0.316	37.7
28/02/2019	0.042	1.824	3.140	0.007	0.326	35.3
01/03/2019	0.048	2.221	2.960	0.005	0.232	32.8
02/03/2019	0.055	1.592	3.400	0.002	0.216	32.4
03/03/2019	0.084	2.199	2.320	0.005	0.359	55.3
04/03/2019	0.138	1.987	3.550	0.010	0.415	97.9
05/03/2019	0.146	2.557	4.800	0.024	0.382	63.9
06/03/2019	0.001	3.053	3.800	0.025	0.248	55.3
07/03/2019	0.008	3.542	3.980	0.030	0.256	72.7
08/03/2019	0.033	3.757	5.690	0.043	0.351	86.1
09/03/2019	0.040	3.843	5.880	0.037	0.293	81.2
10/03/2019	0.046	3.658	6.440	0.036	0.348	53.2
11/03/2019	0.063	3.868	3.900	0.035	0.319	43.4
12/03/2019	0.075	3.352	4.950	0.029	0.207	34.4
13/03/2019	0.065	3.352	4.950	0.027	0.305	64.9
14/03/2019	0.058	4.684	6.310	0.030	0.247	59.0
15/03/2019	0.033	4.682	6.630	0.022	0.211	40.1
16/03/2019	0.053	4.083	5.640	0.038	0.226	51.3
17/03/2019	0.053	4.111	6.800	0.045	0.220	43.8
18/03/2019	0.070	4.052	4.600	0.046	0.273	34.6
19/03/2019	0.078	3.780	3.490	0.047	0.238	36.9
20/03/2019	0.036	3.818	3.820	0.033	0.195	43.9
21/03/2019	0.050	3.116	3.670	0.029	0.168	31.1
22/03/2019	0.069	3.066	4.140	0.029	0.348	30.9
23/03/2019	0.055	2.858	2.850	0.024	0.241	30.9
24/03/2019	0.046	2.568	3.950	0.022	0.325	34.1
25/03/2019	0.056	2.662	3.380	0.025	0.333	37.1
26/03/2019	0.059	2.619	3.400	0.023	0.234	38.4
27/03/2019	0.045	2.622	4.140	0.029	0.242	34.1
28/03/2019	0.046	2.694	3.410	0.031	0.210	37.0
29/03/2019	0.038	2.583	2.810	0.024	0.207	42.7
30/03/2019	0.027	1.978	2.700	0.022	0.273	40.2
31/03/2019	0.040	1.889	3.130	0.019	0.299	46.2
01/04/2019	0.033	2.237	2.400	0.020	0.334	47.6
02/04/2019	0.028	2.407	3.790	0.018	0.230	45.2
03/04/2019	0.040	2.362	3.240	0.016	0.202	43.1
04/04/2019	0.035	1.991	2.670	0.015	0.240	38.5
05/04/2019	0.024	2.084	2.720	0.015	0.205	38.9
06/04/2019	0.023	1.584	2.780	0.017	0.229	36.6

07/04/2019	0.022	1.462	2.830	0.017	0.242	38.9
08/04/2019	0.015	1.912	2.900	0.014	0.174	34.9
09/04/2019	0.039	2.145	3.050	0.017	0.178	34.4
10/04/2019	0.020	2.118	2.950	0.012	0.167	25.2
11/04/2019	0.017	1.448	2.720	0.010	0.160	27.1
12/04/2019	0.011	1.404	3.020	0.011	0.135	23.0
13/04/2019	0.010	1.949	3.020	0.012	0.172	20.5
14/04/2019	0.008	1.881	2.920	0.012	0.118	18.7
15/04/2019	0.001	1.755	2.720	0.011	0.117	19.8
16/04/2019	0.004	1.754	2.560	0.011	0.137	20.1
17/04/2019	0.001	1.670	2.490	0.010	0.120	21.1
18/04/2019	0.039	1.716	2.420	0.013	0.142	20.6
19/04/2019	0.031	1.588	2.400	0.012	0.102	24.4
20/04/2019	0.021	1.507	2.270	0.011	0.072	19.4
21/04/2019	0.044	1.516	2.260	0.010	0.135	20.0
22/04/2019	0.015	1.385	2.160	0.010	0.112	20.4
23/04/2019	0.011	1.494	2.320	0.010	0.090	34.2
24/04/2019	0.008	1.328	2.060	0.010	0.105	25.6
25/04/2019	0.007	1.110	2.200	0.010	0.137	23.0
26/04/2019	0.013	1.246	2.240	0.011	0.163	20.6
27/04/2019	0.011	1.262	2.450	0.013	0.109	25.6
28/04/2019	0.075	1.468	2.270	0.021	0.097	16.5
29/04/2019	0.045	1.794	2.740	0.015	0.119	17.9
30/04/2019	0.045	1.677	2.130	0.014	0.105	18.0
01/05/2019	0.078	1.860	2.500	0.016	0.110	17.9
02/05/2019	0.046	1.973	2.740	0.015	0.099	14.3
03/05/2019	0.031	1.816	2.660	0.014	0.083	11.2
04/05/2019	0.022	1.861	2.630	0.013	0.076	10.9
05/05/2019	0.028	1.824	2.600	0.014	0.089	11.4
06/05/2019	0.018	1.713	2.600	0.012	0.090	11.6
07/05/2019	0.022	1.682	2.340	0.012	0.072	12.0
08/05/2019	0.069	NA	1.900	0.017	0.078	13.3
09/05/2019	0.091	1.537	2.520	0.025	0.077	15.2
10/05/2019	0.067	1.733	2.340	0.018	0.081	15.8
11/05/2019	0.044	1.525	2.500	0.015	0.080	12.4
12/05/2019	0.040	1.294	2.140	0.006	0.065	12.9
13/05/2019	0.045	1.407	1.870	0.012	0.047	11.8
14/05/2019	0.033	1.456	1.630	0.005	0.069	11.9
15/05/2019	0.039	1.360	2.210	0.007	0.077	10.4
16/05/2019	0.043	1.585	2.210	0.006	0.094	10.8
17/05/2019	0.024	1.558	2.520	0.006	0.087	11.8
18/05/2019	0.031	1.317	2.300	0.006	0.116	9.8
19/05/2019	0.055	1.279	1.950	0.007	0.100	10.5
20/05/2019	0.048	1.218	2.110	0.006	0.107	10.5
21/05/2019	0.138	1.014	2.800	0.012	0.363	63.4
22/05/2019	0.194	1.621	2.510	0.017	0.181	25.9
23/05/2019	0.073	1.642	2.600	0.013	0.203	23.6
24/05/2019	0.053	1.557	2.900	0.008	0.177	21.2
25/05/2019	0.055	1.591	1.670	0.007	0.148	22.8
26/05/2019	0.048	1.662	2.470	0.007	0.143	28.8
27/05/2019	0.073	1.682	2.370	0.017	0.087	26.0
28/05/2019	0.052	1.707	1.810	0.020	0.115	21.5
29/05/2019	0.080	1.672	1.960	0.024	0.102	17.8
30/05/2019	0.048	1.578	2.600	0.021	0.106	19.0

31/05/2019	0.054	1.249	2.120	0.020	0.096	19.6
01/06/2019	0.038	1.080	1.420	0.013	0.113	20.0
02/06/2019	0.017	0.949	1.740	0.010	0.113	21.1
03/06/2019	0.040	1.033	1.690	0.013	0.200	20.4
04/06/2019	0.099	1.091	2.900	0.006	0.143	20.7
05/06/2019	0.009	0.733	1.650	0.008	0.172	27.9
06/06/2019	0.013	1.021	1.660	0.006	0.140	22.8
07/06/2019	0.050	1.062	1.340	0.019	0.209	18.3
08/06/2019	0.053	1.148	1.810	0.018	0.192	20.9
09/06/2019	0.039	1.250	1.280	0.017	0.209	11.8
10/06/2019	0.046	1.088	1.600	0.021	0.273	29.8
11/06/2019	0.063	1.233	1.800	0.022	0.252	37.8
12/06/2019	0.054	1.192	1.680	0.022	0.233	38.9
13/06/2019	0.052	1.193	0.690	0.021	0.210	31.5
14/06/2019	0.037	0.973	1.370	0.016	0.285	37.4
15/06/2019	0.060	1.157	1.280	0.018	0.239	40.0
16/06/2019	0.060	1.325	1.260	0.031	0.295	39.7
17/06/2019	0.065	0.626	1.670	0.029	0.219	32.6
18/06/2019	0.096	0.606	1.220	0.019	0.205	34.6
19/06/2019	0.072	0.605	1.550	0.015	0.183	47.3
20/06/2019	0.053	0.754	1.350	0.016	0.144	23.8
21/06/2019	0.037	0.833	1.460	0.013	0.142	24.0
22/06/2019	0.032	0.613	1.360	0.010	0.187	29.9
23/06/2019	0.031	0.639	1.110	0.008	0.180	27.6
24/06/2019	0.033	0.440	1.120	0.011	0.249	31.1
25/06/2019	0.090	0.453	0.940	0.005	0.184	37.9
26/06/2019	0.027	0.446	0.570	0.010	0.216	33.3
27/06/2019	0.080	0.586	0.720	0.016	0.252	29.8
28/06/2019	0.057	0.441	0.770	0.011	0.234	25.9
29/06/2019	0.037	0.234	0.650	0.008	0.236	26.9
30/06/2019	0.034	0.196	0.650	0.006	0.148	26.2
01/07/2019	0.053	0.359	0.730	0.007	0.138	30.1
02/07/2019	0.045	0.425	0.750	0.008	0.137	30.0
03/07/2019	0.034	0.544	1.300	0.007	0.119	24.8
04/07/2019	0.018	0.540	0.750	0.006	0.194	18.4
05/07/2019	0.027	0.558	1.290	0.005	0.102	19.7
06/07/2019	0.023	0.847	1.450	0.008	0.091	15.8
07/07/2019	0.019	0.896	1.210	0.008	0.091	15.3
08/07/2019	0.031	1.437	1.420	0.036	0.086	1.6
09/07/2019	NA	NA	NA	NA	NA	NA
10/07/2019	NA	NA	NA	NA	NA	NA
11/07/2019	NA	NA	NA	NA	NA	NA
12/07/2019	NA	NA	NA	NA	NA	NA
13/07/2019	NA	NA	NA	NA	NA	NA
14/07/2019	NA	NA	NA	NA	NA	NA
15/07/2019	NA	NA	NA	NA	NA	NA
16/07/2019	NA	NA	NA	NA	NA	NA
17/07/2019	NA	NA	NA	NA	NA	NA
18/07/2019	0.018	1.690	2.340	0.042	0.100	7.6
19/07/2019	0.015	1.576	2.130	0.039	0.102	8.8
20/07/2019	0.008	1.471	1.700	0.031	0.095	9.8
21/07/2019	0.006	0.934	1.840	0.025	0.128	7.7
22/07/2019	0.010	1.208	1.970	0.021	0.122	12.1
23/07/2019	NA	NA	NA	NA	NA	NA

24/07/2019	NA	NA	NA	NA	NA	NA
25/07/2019	NA	NA	NA	NA	NA	NA
26/07/2019	NA	NA	NA	NA	NA	NA
27/07/2019	NA	NA	NA	NA	NA	NA
28/07/2019	NA	NA	NA	NA	NA	NA
29/07/2019	NA	NA	NA	NA	NA	NA
30/07/2019	0.079	1.119	1.870	0.036	0.169	33.7
31/07/2019	0.097	1.204	2.170	0.041	0.186	6.5
01/08/2019	0.069	1.566	2.350	0.048	0.216	5.5
02/08/2019	0.044	1.615	2.570	0.053	0.244	6.9
03/08/2019	0.078	1.556	2.140	0.049	0.245	6.7
04/08/2019	0.030	1.606	2.490	0.044	0.219	5.7
05/08/2019	0.041	1.604	2.430	0.045	0.148	8.1
06/08/2019	0.018	1.525	2.040	0.042	0.251	12.0
07/08/2019	0.023	1.521	2.260	0.037	0.130	17.4
08/08/2019	0.039	1.428	2.140	0.042	0.124	10.3
09/08/2019	0.039	1.053	1.830	0.044	0.119	9.9
10/08/2019	0.046	1.068	1.990	0.051	0.210	9.2
11/08/2019	0.039	1.058	1.960	0.047	0.107	11.5
12/08/2019	0.031	0.619	1.940	0.048	0.180	7.7
13/08/2019	0.027	1.096	1.760	0.048	0.171	7.2
14/08/2019	0.024	1.292	2.130	0.042	0.189	8.6
15/08/2019	0.050	1.442	2.490	0.046	0.201	9.9
16/08/2019	0.034	1.079	2.010	0.045	0.204	10.5
17/08/2019	0.014	1.478	2.260	0.040	0.131	13.2
18/08/2019	0.021	1.474	2.190	0.040	0.135	13.6
19/08/2019	0.034	1.507	1.730	0.042	0.196	9.5
20/08/2019	0.023	1.536	1.820	0.045	0.101	12.2
21/08/2019	0.043	1.544	2.110	0.044	0.138	10.7
22/08/2019	0.014	1.503	0.780	0.036	0.110	11.1
23/08/2019	0.015	1.042	2.330	0.038	0.111	11.0
24/08/2019	0.029	1.375	1.880	0.034	0.124	10.5
25/08/2019	0.008	1.279	2.000	0.034	0.123	9.0
26/08/2019	0.017	1.291	1.840	0.031	0.124	9.4
27/08/2019	0.011	1.276	1.560	0.028	0.120	9.0
28/08/2019	0.014	1.356	0.930	0.024	0.119	10.8
29/08/2019	0.032	1.292	1.770	0.030	0.174	13.0
30/08/2019	0.029	1.292	1.960	0.026	0.129	8.6
31/08/2019	0.015	1.271	2.080	0.024	0.192	12.2
01/09/2019	0.022	1.302	1.900	0.026	0.108	14.5
02/09/2019	0.017	1.324	1.110	0.022	0.116	14.2
03/09/2019	0.027	1.218	1.640	0.025	0.167	13.8
04/09/2019	0.030	1.380	0.690	0.025	0.113	15.2
05/09/2019	0.040	1.479	2.500	0.029	0.119	15.8
06/09/2019	0.041	1.468	1.140	0.037	0.121	12.8
07/09/2019	0.042	1.465	2.180	0.034	0.156	9.7
08/09/2019	0.015	NA	2.290	0.031	0.100	4.7
09/09/2019	0.028	2.467	1.800	0.033	0.104	13.8
10/09/2019	0.029	1.197	1.660	0.036	0.099	23.5
11/09/2019	0.025	1.431	1.750	0.027	0.102	19.5
12/09/2019	0.024	1.475	2.050	0.032	0.119	23.5
13/09/2019	0.018	1.478	2.440	0.026	0.236	6.7
14/09/2019	0.023	1.438	2.120	0.028	0.280	10.4
15/09/2019	0.027	1.191	2.380	0.025	0.181	7.5

16/09/2019	0.021	1.213	1.660	0.024	0.160	9.8
17/09/2019	0.016	1.387	1.930	0.023	0.144	8.2
18/09/2019	0.015	1.258	2.130	0.024	0.149	8.2
19/09/2019	0.015	1.272	2.050	0.027	0.105	11.4
20/09/2019	0.026	1.191	1.550	0.030	0.106	14.6
21/09/2019	0.015	1.464	1.920	0.024	0.139	11.0
22/09/2019	0.019	1.578	1.810	0.028	0.141	9.6
23/09/2019	0.027	0.970	1.730	0.029	0.177	10.4
24/09/2019	0.026	0.778	1.620	0.032	0.117	13.4
25/09/2019	0.030	0.641	1.700	0.025	0.264	17.6
26/09/2019	0.069	1.379	2.470	0.029	0.162	19.5
27/09/2019	0.047	1.467	1.760	0.034	0.297	42.1
28/09/2019	0.065	1.503	2.470	0.033	0.199	24.5
29/09/2019	0.085	1.557	1.170	0.048	0.324	40.4
30/09/2019	0.105	1.841	3.230	0.070	0.537	115.4
01/10/2019	0.126	2.394	2.050	0.071	0.414	16.0
02/10/2019	0.087	2.695	1.490	0.065	0.368	61.3
03/10/2019	0.060	2.284	4.220	0.058	0.355	59.8
04/10/2019	0.053	1.957	1.680	0.048	0.384	48.3
05/10/2019	0.057	1.711	0.920	0.046	0.244	48.6
06/10/2019	0.064	1.897	2.550	0.038	0.254	32.3
07/10/2019	0.082	1.962	3.140	0.037	0.218	25.4
08/10/2019	0.059	1.435	2.020	0.040	0.244	46.7
09/10/2019	0.062	1.795	2.550	0.034	0.289	36.2
10/10/2019	0.038	1.951	1.560	0.033	0.273	35.9
11/10/2019	0.038	1.824	2.810	0.033	0.231	33.5
12/10/2019	0.045	1.652	3.160	0.042	0.622	97.2
13/10/2019	0.049	2.529	4.130	0.045	0.359	78.1
14/10/2019	0.043	2.015	4.860	0.047	0.436	82.4
15/10/2019	0.026	2.144	3.700	0.044	0.534	69.9
16/10/2019	0.019	2.546	3.710	0.040	0.528	144.6
17/10/2019	0.050	2.329	3.860	0.054	0.724	93.5
18/10/2019	0.019	3.427	5.860	0.049	0.580	76.3
19/10/2019	0.023	3.478	3.840	0.058	0.493	65.3
20/10/2019	0.024	3.531	4.730	0.057	0.337	50.2
21/10/2019	0.023	3.108	4.790	0.049	0.249	49.6
22/10/2019	0.024	2.900	4.740	0.046	0.377	48.6
23/10/2019	0.024	2.800	4.750	0.042	0.301	46.3
24/10/2019	0.027	2.379	4.420	0.040	0.378	52.7
25/10/2019	0.034	2.539	4.140	0.038	0.372	49.3
26/10/2019	0.044	2.053	3.360	0.037	0.323	54.9
27/10/2019	0.040	2.303	3.640	0.034	0.419	50.9
28/10/2019	0.011	2.190	3.390	0.035	0.306	49.1
29/10/2019	0.010	2.338	3.700	0.036	0.241	58.9
30/10/2019	0.012	2.052	3.250	0.033	0.506	78.3
31/10/2019	0.015	2.326	3.680	0.024	0.377	41.9
01/11/2019	0.033	2.306	3.330	0.022	0.308	42.8
02/11/2019	0.040	2.227	3.470	0.028	0.293	42.8
03/11/2019	0.049	2.349	3.620	0.031	0.278	49.1
04/11/2019	0.044	2.398	3.700	0.036	0.293	55.0
05/11/2019	0.133	2.393	4.230	0.049	0.484	52.3

Declaration

I, Chaogui Lei, hereby declare that the dissertation submitted, entitled “Analysis of land use changes and water resources in lowland catchments of Northern Germany” was written independently by me. The content and design of this thesis, apart from the supervisor’s guidance, is my own work. The thesis has not been submitted either partially or wholly as a part of a doctoral degree to another examining body and is my first and only doctoral procedure. Chapter 3 and 4 of the thesis have been published in peer-reviewed journals and chapter 5 is currently under review. This work has been prepared respecting the Rules of Good Scientific Practice of the German Research Foundation. I have not been deprived of an academic degree.

Kiel, September-2021

Chaogui Lei

Chaogui Lei